Development of Controlled Release Drug Delivery Systems

By
Ming Li, M.Sc.

A Dissertation
Submitted to the Graduate Studies
in Partial Fulfillment of the Requirement
for the Degree
Doctor of Philosophy

McMaster University

DEVELOPMENT OF CONTROLLED RELEASE DRUG DELIVERY SYSTEMS

DOCTOR OF PHILOSOPHY (2002) **McMaster University**

(Chemistry) **Hamilton, Ontario**

TITLE:	**Development of Controlled Release Drug Delivery Systems**
AUTHOR:	**Ming Li, M. Sc. (McMaster University)**
SUPERVISOR:	**Professor: François M. Winnik**
COSUPERVISORS:	**Professors: Harald D. Stöver and Shiping Zhu**
NUMBER OF PAGES:	**xxi, 213**

Abstract

The newly emerged biotechnology of liposome-based drug delivery has drawn great interest in research and pharmaceuticals. Liposomes are potential candidates to carry highly toxic drugs to target cells in order to minimize the damage to normal cells and side effects. In the past two decades, extensive work has improved the stability of phospholipid liposomes in physiological fluids as drug carriers.

My research on developing controlled release drug delivery systems started with the synthesis of a highly reliable anchor for water-soluble polymers, which will serve as an anchor with a high affinity towards lipid bilayers and can be monitored by fluorescence. A new family of hydrophobic building block, namely cholesterol and fluorescence groups, was prepared and characterization. The conformation study suggests that intramolecular hydrogen bonds form via the amide proton of these compounds in methanol-d3 and DMSO-d6. Furthermore, an efficient synthetic route was developed to synthesize the corresponding pyrenylbutyl cholesterol lysine derivative.

These functional hydrophobic building blocks were successfully attached to water-soluble polymers such as poly(*N*-isopropylacrylamide). Solution properties of the modified polymers were investigated by fluorescence, time-resolved fluorescence, and dynamic light scattering. The cholesterol bearing PNIPAM exhibited the lower critical solution temperature (LCST), which was close to that of the precursor polymer. The polymers formed micellar aggregates

in water via inter or/and intrapolymeric associations, which depended on the polymer architecture and solution temperature.

Interaction of phospholipid and nonphospholipid liposomes with these thermoresponsive polymers was followed in order to develop controlled release systems based on cholesterol-bearing poly(*N*-isopropylacrylamide) coated liposomes. The strong interaction between the polymer and liposomes was found via fluorescence and gel-filtration chromatography measurement. As expected, the cholesterol-bearing polymers remained on the liposome surfaces as increasing temperature up to 60°C. In contrast, above the LCST of PNIPAM, octadecyl group modified PNIPAM escaped from liposome surfaces and left liposome unprotected. Interesting results were also found in the study of temperature controlled release and target fusion of these polymers coated liposomes.

In addition, controlled release systems based on hybrid polymeric nanoparticles formed by self-assembled cholesterol-bearing pullulan and poly(*N*-isopropylacrylamide) (PNIPAM) were studied. The hybrid nanoparticles further proved that cholesterol was a reliable anchor, which remained in hydrophobic microdomains of the hybrid nanoparticles in the studied temperature range from 20 to 45°C. In comparison, octadecyl group modified PNIPAM escaped from hybrid nanoparticles at the temperature above the LCST of PNIPAM.

Finally, these hydrophobic building blocks were attached to polysaccharide, hyaluronan (HA), to develop targeting delivery systems. Synthesis, characterization, solution properties of cholesterol bearing HA and interaction of the polymer with liposomes were conducted. The highly reliable

liposomes as site-specific carriers were developed by coating the cholesterol-bearing hyaluronan onto liposomes.

Acknowledgements

I would like to express my sincere appreciation to my supervisor, Professor. François M. Winnik, for the opportunity to complete this dissertation and for her continued support and constructive guidance throughout my graduate studies. To my co-supervisors, Professor Harald D. Stöver and Professor Shiping Zhu, for their encouragement, guidance and support, especially their comments and assistance regarding the thesis after Professor F. M. Winnik left McMaster University.

I am very grateful to my committee member, Professor John Brennan for his suggestion and advice.

I thank my colleagues in Professor Winnik's group: Alla Polozova, Sudarshi Regismond, Ester Goh, Roger Liu, Celine, Gangadhara & Jayanthi, Masanobu Mizusaki, Jean-Francois Stumbe, Markus Brune, Akiko Yamazaki, Peiyun Jiang, Shalini Nigam, Jing Zheng, Kim Gracie and Xingping Qiu. It has always been a pleasure to work with all of you!

I wish to give a special thank you to Wenhui Li, who is more than a friend and sister, thanks for everything! To Randy Frank and Frank LaRonde, for reading and helping me with my writing. To my graduate fellows: Jeff Downey, Janevieve Jones, Daryl Vanbesien, Guodong Zheng, Anna Shulkin, Lisa Croll and Mukarram Ali, thank you for making a wonderful "polymer floor" section.

I am very grateful to Professor William Leigh, for his valuable advice and providing time-resolved fluorescence instrument. To Professor John Brennan and Professor Vettai S. Ananthanarayanan, for their generosity in providing

instruments. I would like to thank Dr. Don Hughes (NMR) and Yew-Meng Heng (Electron Microscope) for their technical assistance. Special thanks to Tania Pointe, who conducted viscosity measurement. To Tracy Morkin and Kulwinder Flora for their assistance during the experiments in their labs.

Thanks to Professor Jacques Barbier, for his suggestion and supervision of the thesis process. Thank you, also, Carol Dada and the secretaries in the Chemistry Department, for their kindness and enthusiasm.

I am indebted to my parents, uncle, aunt and my daughter for their support, especially, my mom who offered countless hours of help taking care my daughter whenever I needed it. I also thank my husband, Liang, for his love, understanding and encouragement, without which I would not have been able to complete this work.

Table of Contents

List of Figures

Figure 5.4. Changes as a function of lipid concentration in the ratio of pyrene monomer intensity (I_{Mo}/I_M) of PNIPAM-Pybucho in the absence (I_{Mo}) and presence (I_M) of CPC bearing liposomes at 25°C, λ_{ex} = 346 nm, polymer concentration 0.05 g/L. (a) NPL, (b) DMPC.

Figure 5.5. Ratio I_1/I_3 of 20K-P_M88 in the presence of liposomes as a function of concentration ratio of lipid to polymer at 25°C, λ_{ex} = 346 nm, [20K-P_M88] = 0.05 g/L.

Figure 5.6. DSC traces of p-DMPC liposomes and p-DMPC/polymer mixtures, polymer concentration 0.1 g/L, the ratio of lipid to polymer from top to bottom: 10, 20, 30. (a) 240K-P_B177/p-DMPC, (b) 240K-N72-P_B325/p-DMPC, (3) 20K-P_M88/p-DMPC (10, 30).

Figure 5.7. DSC traces of nonphospholipid liposomes (NPL) and NPL/polymer mixtures, polymer concentration 0.3 g/L, the ratio of lipid to polymer from top to bottom in order of increasing: (a) 240K-P_B177/NPL, 10, 20, 30. (b) 240K-N72-P_B325/NPL, 10, 20. (C) 20K-P_M88/NPL, 10, 30.

Figure 5.8. Ratio of I_E/I_M for 20K-P_M88 in the presence of liposomes as a function of temperature, λ_{ex} = 346 nm, [20K-P_M88] 0.05 g/L, full signals are heating scan, empty signals are cooling scan.

Figure 5.9. Ratio I_E/I_M of 20K-P_M88 in water as a function of temperature, λ_{ex} = 346 nm, [20K-P_M88] = 0.05 and 0,1 g/L, full signals are heating scan, empty signals are cooling scan.

Figure 5.10. DSC traces of 20K-P_M88 in water, [20K-P_M88]= 0.92 g/L, from bottom to top: 1st heating, 1st cooling, 2nd heating and 2nd cooling.

Figure 5.11. Ratio I_1/I_3 of 20K-P_M88 in the presence of liposomes as a function of temperature, λ_{ex} = 346 nm, [20K-P_M88] = 0.05 g/L, lipid to polymer concentration ratios were 10, 20, 25, respectively. Full signals are heating scan and empty signals are cooling scan.

Figure 5.12. Ratio I_{Py}/I_{Np} of 240K-N72-P_B325 in the presence of liposomes as a function of temperature, λ_{ex} = 290 nm, [240K-N72-P_B325] = 0.05 g/L, lipid to polymer concentration ratio were 5, 10, 20, respectively, full signals are heating scan and empty signals are cooling scan. (a) Fluorescence emission intensities of 240K-N72-P_B325/NPL mixtures as a function of temperature, I_{Np}: naphthalene emission intensity, I_{Py}: pyrene emission intensity, concentration ratio of lipid to polymer: 10 or 20.

Figure 5.13. Ratio I_{Py}/I_{Np} of mixed singly labeled polymers: 20K-P_M88/240K-N74 in the presence of NPL as a function of temperature, λ_{ex} = 290 nm, [20K-P_M88] = 0.045 g/L, [240K-N74] = 0.055 g/L. lipid to polymer ratios were 10 and

List of schemes

List of Tables

Abbreviations

tBOC	tert-butoxylcarbonyl
CBZ	benzyloxylcarbonyl
ChoPybu	*N*α-[4-(1-pyrenyl)butyl]amide-*L*-lysine-[6-(3β-cholesteryl)urethane]-1-hexylamide-ε-amine hydrochloride (5e)
CPC	cetylpyridinum chloride monohydrate
CHP	cholesterol-bearing pullulan
DCC	dicyclohexylcarbodiimide
DDAB	Didodeceyldioctadecylammonium bromide (DDAB)
DMPC	dimyristoylphosphatidylcholine
DSC	differential scan microcalorimetry
DSL	dynamic light scattering
HA	hyaluronic acid
IR	infrared spectroscopy
LCST	lower critical solution temperature
NASI	*N*-acryloxysuccinimide
NMR	nuclear magnetic resonance
Np	naphthalene
Npcho	*N*α-[6-(3β-cholesteryl)urethane]-1-hexylurea-*L*-lysine-{*N*-[1-(1-naphthyl)ethyl]}amide-*ε*-amine hydrochloride (compound 5c)
NPL	nonphospholipid liposomes
NRET	nonradiative energy transfer
NSI	*N*-hydroxysuccinimide
PNIPAM	poly(*N*-isopropylacrylamide)
POPC	palmitoyloleoylglycerophosphocholine
POPS	palmitoyloleoylglycerophosphoserine
Py	pyrene
Pybucho	*N*α-[6-(3β-cholesteryl)urethane]-1-hexylurea-*L*-lysine-*N*-[4-(1-pyrenyl)butyl]amide-ε-amine hydrochloride (5b)
Pymecho	*N*α-[6-(3β-cholesteryl)urethane]-1-hexylurea-*L*-lysine-[*N*-(1-pyrenyl)methyl]amide-ε-amine hydrochloride (5a)
Pycho	Pymecho + Pybucho
TFA	trifluoroacetic acid
UV	ultraviolet spectroscopy

Chapter 1

Introduction

In the past decades liposomes have drawn great attention because of their potential applications as delivery systems for drugs, vitamins and cosmetic materials.[1] The unique quality of liposomes is that they enable water-soluble and water insoluble materials to be used together in a formulation without surfactants or other emulsifiers. One believes that liposomes can be designed to meet many applications by varying contents, sizes and surface charge of lipid, and methods of preparation.

However, one important drawback of liposomes as drug delivery carrier is that they are unstable in physiological fluids such as plasma and lymph which limits many applications. Two principal techniques have been employed to enhance the liposome stability and to improve the drug internalization. One involves crosslinked phospholipid molecules as an impermeable lipid vesicle (polymerized phospholipid liposomes).[2] The other involves surfaces modification of phospholipid liposomes (PL) with water-soluble polymers. Major improvements to reduce the uptake of liposomes have been achieved by modifying the surfaces of liposomes with specifically-designed water-soluble polymers such as poly(ethyleneglycol)[3] (PEG), poly (*N*-isopropylacrylamide)[4] (PNIPAM) and polysaccharides.[5] Stabilized liposomes have sufficient time to reach and interact with target cells. The modification of liposomes with hydrophobic substituents bearing water-soluble polymers is one of the promising approaches for developing new highly

efficient drug delivery systems with the characteristics of increased circulation time and fast response to external stimuli.

An important development in the design of new functional water-soluble polymers concerns the choice of a reliable hydrophobic substitutent. In most cases, straight alkyl chains with length from 12 to 18 carbons are used due to the ready attachment of these groups to polymer backbones. However, Winnik and her coworkers[6] found that octadecane-substituted poly(*N*-isopropylacrylamide) bound to fluid bilayers can dynamically exchange with the unbound polymers, which caused a major population of liposomes to become unprotected at the temperature above the phase transition of liposomes or above the lower critical solution temperature of the polymers, in case the phase transition of liposomes was suppressed. To overcome this problem, cholesterol was chosen to serve as a hydrophobic anchor since cholesterol is well known to possess a high affinity to lipid bilayers.

1. 1. Hydrophobic Building Block

Cholesterol (Figure 1.1) has amphipathic structure with a polar hydroxyl head group at C-3 and a nonpolar hydrocarbon body (steroid nucleus and hydrocarbon side chain at C-17) about as long as a 16-carbon fatty acid in its extended form. Its characteristic structure is the steroid nucleus consisting of four fused hydrocarbon rings. The steroid nucleus is almost planar and relatively rigid and the fused rings cannot be rotated around C-C bounds.

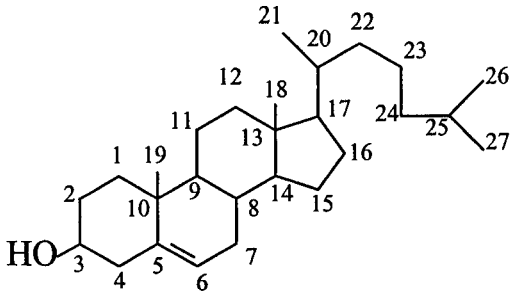

Figure. 1.1. Structure of cholesterol

Sunamoto and coworkers[5] pioneered using cholesteryl substituent as hydrophobic side chain and prepared cholesterol-bearing pullulans, which formed monodispersed nanoparticles in water. These nanoparticles were colloidally stable since the cholesterol-bearing pullulans bound to the liposome membranes demonstrated the architecture of cholesteryl substituents inserted within the bilayers. Very stable complexes were built between polymer and liposomes. Cholesteryl moieties were also attached to biofunctional headgroups such as antiinflammatory drugs via either oligo-(*L*-lactic acid)$_n$ or oligo-(ethylene oxide)$_n$ oligomers to generate cholesterol-bearing oligomers.[7] The cholesterol-bearing oligomers could further self-assemble into liquid crystals and can be expected to control cellular response to ordered surfaces, and to mediate interactions between implants and cells. Cholesterol-bearing poly(allylamine) could form complexes with bile salt (amphipathic steroids) by self-aggregation in water. This property was expected to reduce the cholesterol level in the blood (preventing atherosclerosis) via lowering intestinal bile salt concentration.[8]

In this dissertation, a new class of cholesteryl and fluorophore lysine derivatives was synthesized, which can play double roles as hydrophobic microdomains and anchor

groups by linking to water-soluble polymers. On the one hand, they can be detected and monitored by fluorescence spectroscopy.

1. 2. Luminescence Fundamentals

Luminescence is the process in which a molecule in an electronically excited state returns to a ground state by emitting a photon.[9] Absorption of light ($h\nu$) from the visible or ultraviolet region of the spectrum may promote the molecule into excited electronic states. The characteristics of the molecular electronic states are well illustrated by Jablonski energy-level diagrams.[10]

1. 2. 1. Excimer Formation

An excimer is an excited state complex that is formed between two identical species, one of them is in the excited state and the other in the ground state.[11] Pyrene is one of the most commonly used hydrophobic probes and is an excellent excimer probe for investigation of amphiphilic macromolecule properties. Pyrene excimer may be associated in an electronically excited state and dissociated in its ground state. The emission of pyrene excimer arises from a 'sandwich structure' of two pyrene molecules, in which one pyrene molecule sits on top of the other with the molecular planes being partially or totally overlapping.[12] If two pyrene molecules are separated sufficiently far away when light is absorbed, then the excitation will be localized on one of the molecules and the excited pyrene will give rise to monomer emission. In solutions, the excimer formation is a diffusion-controlled process. However, if pyrene molecules are incorporated into polymer backbones in which their mobility is severally limited, so that

the rate of diffusion is small compared with the fluorescence rate constant; then only pyrene molecules in close proximity can form excimers. This excimer formed by an excited pyrene associating with a ground state pyrene is referred to dynamic excimer. There are also instances where an excimer-like emission is observed, but pyrene moieties are preassociated together when light is absorbed; which is referred as static excimer. Under normal condition, the distinction between static and dynamic excimer is that the growth emission of a dynamic excimer can be observed in a time-resolved fluorescence measurement, but not for static excimer. This distinction between static and dynamic excimer can also be observed in absorption and excitation spectra. Pyrene excimer fluorescence has been extensively used in the study of the conformational change of macromolecules in solution, gel and solid.[13]

1. 2. 2. Nonradiative Energy Transfer

Nonradiative energy transfer (NRET) originates from dipole-dipole interactions between an energy donor in its singlet excited state (^1D *) and an energy acceptor in its ground state (^1A).[10] It can be represented by

$$^1D^* + {}^1A \rightarrow {}^1D + {}^1A^* \qquad (1)$$

The photophysical process of NRET requires that the absorption spectrum of the acceptor molecule must overlap with the emission of the donor, the intervening medium must be transparent to the light emitted and the fluorescent quantum yield of the donor molecule must be high. The theory of NRET was quantitatively developed by Förster. The probability of a nonradiative transfer of excitation energy from one chromophore to another has a sixth power dependence on the distance as shown in equation 2[14]

$$E = R_0^6/(R_0^6 + R^6) \qquad (2)$$

where E is the energy transfer efficiency, R is the donor/acceptor separation distance and R_0 is the energy transfer donor and acceptor separation distance for which half of the excitation energy is transferred (E = 0.5), defined by

$$R_0^6 = [900(\ln 10)\, \kappa^2\, \Phi_D^0]/(128\, \pi^5 n^4\, N) \int \lambda^4\, I(\lambda)\, \varepsilon(\lambda)\, d\lambda \qquad (3)$$

where κ^2 is a function of the mutual orientation of the donor and the acceptor, Φ_D^0 is the emission quantum yield of the donor in the absence of the acceptors, n is the solvent refractive index, and N is Avogadro's number. $\int I(\lambda)d\lambda$ is the normalized fluorescence emission intensity, $\varepsilon(\lambda)$ is the absorption coefficient of the acceptor at the wavelength λ.

The energy transfer efficiency is a well-defined function of the distance between a donor and an acceptor, which is used as a molecular 'ruler" to identify the distance ranging from 10 to 100 Å depending on the pair of chromophores.

1. 2. 3. Fluorescence Lifetime

Fluorescence lifetime (τ) represents the average amount of time a fluorophore probe remains in the excited state, and the radiative fluorescence lifetime is defined as the reciprocal of the radiative transition probability K_{FM} (in S^{-1}).[12] K_{FM} is equal to the Einstein A coefficient summed over the complete fluorescence spectrum as shown in equation 4

$$1/\tau = K_{FM} = A_{u\,0\rightarrow 1} = \sum A_{u\,0\rightarrow 1m} \qquad (4)$$

The fluorescence lifetime can reveal the frequency of collision encounters of the probe with quenching agents, the rate of energy transfer, and the rate of excited state reactions. Two methods are used for the measurement of fluorescence lifetime. They are

modulation method the sample is excited with sinusoidally modulated light. The phase shift and demodulation of the emission, relative to the incident light, is used to calculate the lifetime. In the pulse method the sample is excited with a brief pulse of light and the time-dependent decay of fluorescence intensity is measured.

Pulse lifetime measurements require quantification of the time-resolved decay of the fluorescence intensity F(t). The decay is generally fitted to a sum of exponentials, i.e.

$$F(t) = \sum \alpha_i \, e^{-t/\tau i} \qquad (5)$$

where α_i is a preexponential factor representing the fractional contribution to the time-resolved decay of the component with a lifetime τ_i. Many methods have been proposed for estimation of the impulse response function F(t) from the measured decay curve R(t) and the lamp profile L(t). R(t) is given by the convolution of the lamp pulse with the impulse response of the sample[10], i.e.

$$R(t) = \int_0^t L(t') \, F(t-t') \, dt' \qquad (6)$$

The least-squares method seems to provide the most reliable results. The basis of the least-squares method is the calculation of the expected value of the decay curve R(t) using assumed values of α_i and τ_I and the measured time-profile of the lamp pulse. The calculated values $R_c(t)$ are compared with the observed values R(t). α_i and τ_i are varied until the best fit is obtained. A reduced chi-squared (χ^2) is calculated from the weighted residuals and measures how good the estimates were. A good fit is indicated by a residual of χ^2 close to unity, meanwhile, the autocorrelation function of the residuals and the residuals between experimental and fitted curves are also criteria to measure the estimation. The precise nature of the fluorescence decay can reveal details about the interactions of a given fluorophore with its environment. For example, multiple decay

constants can be a result of a fluorophore being in several different environments, or a result of excited state processes.

1. 3. Poly(*N*-isopropylacrylamide)

Poly(*N*-isopropylacrylamide) (PNIPAM) and its copolymers have attracted much attention in both areas of academic and industry because of their unique solution properties.[15] PNIPAM with both hydrophobic and hydrophilic segments tends to lead a schizophrenic behavior and to cause unique solution properties, especially in water. The polymer is soluble in cold water with an extended coil conformation and aggregates into globular form when heated above its lower critical solution temperature (ca. 32°C). The phase separation process is rapid, reversible and readily controlled by changing temperature. The physical property of the amphiphilic PNIPAM copolymers depends on their chemical composition and the relative ratio of hydrophobic to hydrophilic moieties. The hydrophobic groups may be in polymer backbones or as side chains. These polymers form intra- or/and interpolymeric micelles in aqueous solutions and hydrophobic groups form the cores of micelles, which are solvated by hydrophilic polymeric chains extending around these cores to minimize interfacial tension.[16] The unique physical properties of these polymer systems lead them to be utilized in controlled drug release delivery systems[14c], chemical separations,[17] sensors,[18] coatings, rheology modifiers,[19] personal care products, food additives and enhancers for oil recovery.[20]

Ringsdorf and Winnik have reported copolymers bearing fluorescent pyrene labels next to hydrophobic octadecyl groups (PNIPAM-C18Py).[4a] The fluorescent spectra of the polymers were characterized by a large pyrene excimer emission. The ratio

of excimer emission intensity to monomer emission intensity (I_E/I_M) was shown to be insensitive to changes in polymer concentration, indicating that the overall polymeric microdomains did not change once a required minimum polymer concentration has been reached.

In this thesis, the cholesteryl and fluorephore lysine derivatives were attached to poly(*N*-isopropylacrylamide) as a hydrophobic building block. The degree of hydrophobic substitution was varied and the solution properties of modified polymers were investigated.

1. 4. Hyaluranon

Hyaluranon (HA) is naturally occurred polysaccharide with the repeating disaccharide units of *N*-acetylglucosamine and glucuronic acid.[21] It is synthesized at cell surfaces without a protein core precursor and is then released into the extracellular matrix. Some hyaluranon molecules appear to remain attached to the cell surfaces, where they participate in interaction with surrounding matrix molecules. Others are bound to the cell surfaces via specific receptors.[22] In addition, HA is a major contributor to biomechanical properties of tissues and helps control tissue hydration and water transport.

The biocompatibility, non-immunogenicity and viscoelastic properties of HA make it an ideal building block for tissue engineering.[23] The applications of HA in medicine have created considerable interest in chemical modification of HA.[24] The modified HAs without losing their natural biocompatibility and physical properties satisfy to new medical applications. For instance, the attachment of a hydrophobic side

chains to the carboxylate group of HA decreases water solubility and, therefore increases tissue residence time.[25] Such pendant groups could also be drugs or proteins as hyaluranon-drug adducts for controlled delivery and as hyaluranon-protein adducts for biomaterials and cell substrates.[26]

Furthermore, HA has specific natural receptors in human body such as CD44 and RAHMM.[22a] These two HA binding proteins are overexpressed in some types of tumor cells, e.g. breast cancer cells. Thus HA coated liposomes are able to deliver drugs to these cells with high levels of CD44 or/and RAHMM. In gene therapy, DNA is considered as a prodrug for the synthesis of a therapeutic protein in cells, which could be introduced into the cell nuclei by an appropriate carrier.

In this study, HA has been chemically modified by cholesteryl and fluorophore lysine derivatives. The cholesterol-bearing HAs formed micelles in aqueous solutions, which were disrupted in the presence of liposomes. The resulting HA coated liposome complexes are expected to become highly reliable targeting delivery systems for gene therapy or delivery diagnostic agents to targeting sites.

1. 5. Liposomes

Amphiphilic lipids can form three types of aggregates in aqueous solutions, namely micelles, bilayers and liposomes depending on the nature of lipids and precise condition.[27] A liposome is a closed vesicle as shown in Figure 1.2, in which the lipid bilayer folds back on itself to form a hollow sphere. By forming vesicles, bilayer sheets lose their hydrophobic edge regions to achieve maximal stability in their aqueous

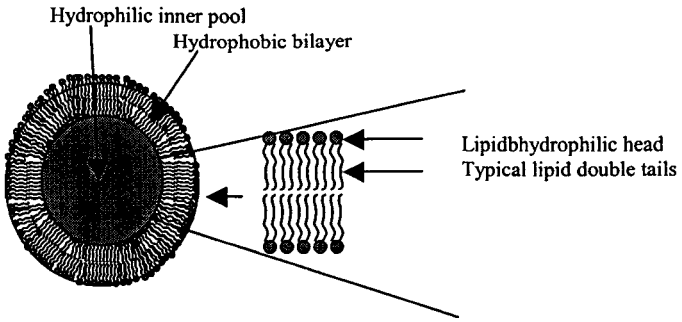

Figure 1.2. Illustration of liposome

environment. These bilayer vesicles enclose water and create a separate aqueous compartment in their inner pool.

Membrane stability and vesicle sizes are important properties of liposomes. The membrane stability is determined by lipid compositions, while the sizes of the liposomes ranged from 25 nm to several microns in diameter are governed by the method of preparation. Liposomes can be made of either phospholipids such as phosphatidylcholine (PC), so-called phospholipid liposomes (PL) or synthetic nonionic surfactants, such as single- or double- tailed ether (or ester) derivatives of polyglycerol (or polyoxyethylene), so-called nonphospholipid liposomes (NPL) or "Niosomes"[1e]. The value of liposomes as model membrane systems derives from the fact that liposome membranes can be constructed from natural constituents, which are in principle identical to the lipid portion of natural cell membranes. Because of the structural similarity with cellular membranes, liposomes are able to interact with cells. Various types of interactions were discovered, such as endocytosis, fusion and transfer or exchange of phospholipids. Each of the interactions can release liposome contents and has a special effect in liposomes as delivery systems. The first liposome-based product was a cosmetic product that appeared

in the market in 1986. Recently, liposomes have been explored as controlled carriers for drugs, nutrients and medical image agents.

In lipid bilayers, the molecules appear to be aligned with the glycerol backbone approximately perpendicular to the plane of the membrane, and the phosphocholine headgroup in a straight line roughly parallel with the membrane surface. This conformation would be expected to reduce the distance between positive and negative charges within the phospholipid molecule. The hydrocarbon chains tilt relatively to the plane of the membrane in order to fill the extra space created by the headgroups and bring the chains of adjacent molecules into close proximity to maximize Van der Waals and other non-covalent interactions. The lipid membranes undergo the transition from gel to liquid crystal phase (T_c) as the temperature increased. T_c is an important physical property of liposomes, since the phase behavior determines other properties of liposome membranes such as permeability, fusion, aggregation, and protein binding. All properties can markedly affect the stability and behavior of liposomes in biological systems. In fact, the transition involves two steps, a main transition and a pretransition. In the main transition, the fatty acid chains tend to adopt gauche configurations other than the all-trans straight chain conformation, thus expanding the area occupied by the chains and decreasing the bilayer thickness. The pretransition in which a change in headgroup orientation may occur is usually a few degrees lower than the main transition. The translation of fatty acid chains in the direction normal to lipid bilayer surface is strictly limited, but it is allowed within the plane of the membrane. The lateral translation becomes much faster at increasing temperature above T_c.

1. 6. Research Objectives

The objectives of this thesis are to develop reliable controlled release carriers based on water-soluble polymer modified liposomes, which will have enough lifespan in vivo in order to efficiently deliver drugs to targeting sites. The objectives can be broken down in four sections. The first aim is to synthesize and to characterize a reliable anchor, which will incorporate into lipid bilayers with a high affinity, and can be detected and monitored by fluorescence. The second target is to attach the labeling anchor (hydrophobic building blocks) to water-soluble polymers and to understand the polymer behavior in water. The third aim is to coat polymers on liposome surfaces and to study the interaction and properties of polymer-liposome complexes. Final aim is to apply this anchor in extended systems to further prove the new hydrophobic building blocks as reliable anchors. Two systems are evaluated detail: (1) controlled release systems based on hybrid polymeric nanoparticles formed by cholesterol bearing pullulan and poly(N-isopropylamide); (2) targeting delivery systems based on cholesterol bearing hyaluranon coated liposomes.

1. 7. Organization of Dissertation

The content of thesis is presented in the order of synthesis and characterization of hydrophobic building blocks; the water-soluble polymers modified by hydrophobic building block and the solution properties of related polymers; the interaction of polymers with liposomes; and the properties of the polymer coated liposomes. Then an extended system of hybrid polymeric nanoparticles was studied to further identify cholesterol as a reliable anchor.

Chapter 1 briefly reviews literature of polymer modified liposomes, and approaches used in this thesis.

Chapter 2 summarizes the synthetic method for a new kind of hydrophobic building block from water-soluble polymers. Three cholesteryl and fluorophore lysine derivatives were synthesized by parallel methods. The conformation of the compounds was studied by temperature and concentration-dependent NMR, COSY, and ROESY experiments. Furthermore, an efficient synthetic route was developed to synthesize pyrenylbutyl substituted cholesteryl lysine derivative.

In Chapter 3, the syntheses of reactive poly(*N*-isopropylacrylamide) and cholesterol bearing poly(*N*-isopropylacrylamide) are presented. Lower critical solution temperature (LCST) of different polymers was determined. Polymeric micellar aggregates and the conformation of the polymers in water were investigated.

Chapter 4 illustrated the experimental results of inter- and intramolecular associations of cholesterol bearing poly(*N*-isopropylacrylamide). The chapter is focused on the effect of temperature, sample preparation, and polymer architecture on the polymeric associations.

Chapter 5 described the controlled release systems based on thermosensitve polymer coated liposomes. Cholesterol bearing poly(*N*-isopropylacrylamide) coated phospholipid and nonphospholipid liposomes were prepared. The interaction of polymers and liposomes was investigated and the effect of temperature, polymer architecture and liposome types on the interaction were studied as well. The strong interaction between the polymer and liposomes was evidenced by fluorescence and gel-filtration chromatography measurement.

In Chapter 6, temperature-controlled release and target fusion of thermo sensitive polymers coated by liposomes were reported. The effect of polymer architecture and lipid types was studied. Interesting results were found in the results of temperature-controlled release and target fusion on these controlled release carriers. As expected, the polymers bearing cholesterol anchor remained on the liposomes surfaces as temperature increased up to 60°C.

Chapter 7 presented the development of controlled release carriers based on hybrid polymeric nanoparticles, which are generated by cholesterol bearing pullulan (CHP, Akiyoshi's lab) and cholesterol bearing poly(*N*-isopropylacrylamide). The interaction of two polymers was studied. The sizes of nanoparticles and the effect of temperature and molecular weight of poly(*N*-isopropylacrylamide) on the sizes of nanoparticles were investigated. The polymer nanoparticles further proved that cholesterol was a reliable anchor, which remained in hydrophobic microdomains of the hybrid nanoparticles in the studied temperature range from 20 to 45°C. In contrast, above the low critical solution temperature of PNIPAMs, octadecyl group modified PNIPAMs escaped from hybrid nanoparticles.

Chapter 8 presents the development of target delivery systems based on hyaluranon coated liposomes. Chemical modification of hyaluranon (HA) is introduced. Micellar structure, aggregation of these micelles and secondary structure of the modified HA were studied. Interaction of cholesterol bearing HA with liposomes and the stability of the modified liposomes in physiological fluid was studied as well. The highly reliable liposomes as site-specific carriers were developed by coating the cholesterol-bearing hyaluronan onto liposomes.

Chapter 2

Synthesis and Characterization of Fluorescent Cholesterol-bearing Lysine Derivatives: Novel Hydrophobic Building Blocks for Water-soluble Polymers

Abstract

Three lysine derivatives bearing a cholesteryl group and either pyrene or naphthalene were prepared starting from N-ε-Boc-N-α-CBZ-L-lysine, 1-hexylisocyanato-6-(3β-cholesteryl)-urethane, 1-(pyrenyl)-methylamine, 4-[1-(pyrenyl)-butylamine, and N-1-(1-naphthyl)-ethylamine. Temperature- and concentration-dependent NMR data together with COSY experiments provide the evidence for intramolecular hydrogen bond involving the amide proton of these compounds dissolved in methanol-d_3 or DMSO-d_6. In addition, an efficient synthetic route is developed to prepare cholesteryl lysine derivative with pyrenylbutyl substitutents.

2.1. Introduction

Supermolecular assembly based on the controlled association of hydrophobically modified (HM) polymers in water has led to new methodologies for the design of functional macromolecules.[28] These polymers consist usually of a water-soluble main chain carrying a small number of hydrophobic groups.[29] The hydrophobic substituents associate and form hydrophobic domains with several transient cross-links connecting the polymer chains.[30] The hydrophobic domains can serve as solubilizing media for organic compounds, such as lipophilic drugs, or they can act as 'anchor' groups within lipid bilayers.[2] Hence amphiphilic polymers have attracted considerable interest as drug delivery vehicles.[31] An important issue in the design of amphiphilic polymers concerns the choice of a suitable hydrophobic substituent. In most cases straight alkyl chains ranging in length from 12 to 17 carbons are selected, in view of the relative ease of attachment of these groups to polymer backbones. Sunamoto and coworkers pioneered the use of cholesterol substituents as polymer modifiers.[32] They prepared cholesterol-bearing pullulan, which formed monodispersed nanoparticles in water consisting of several pullulan chains linked together by associated cholesteryl groups. When placed in the presence of liposomes, the modified pullulan bound to the liposome membrane and the cholesteryl substituents were inserted within the bilayers.[33]

We report here the preparation of a new class of hydrophobic modifiers, which performed a double role when linked to water-soluble polymers. On the one hand, they formed hydrophobic microdomains and served as anchor groups and can be detected and monitored by fluorescence spectroscopy, a powerful technique in the study of amphiphilic polymers[11a] and the interaction of polymers with liposomes.[34] Three different compounds starting from a protected lysine were prepared (scheme 2.1). To use

lysine as the backbone of compounds was driven by the following design considerations: first, the compounds must possess a primary amine group, which is easily converted to polymerizable acrylamide by a Schotten-Bauman reaction or linked to polymers carrying reactive groups, such as a *N*-hydroxysuccinimide moiety; second, the cholesteryl group and the fluorescent dye, while remaining in close proximity when linked to a macromolecule, are kept spatially apart, so as not to preclude the insertion of the cholesterol within a lipid bilayer. The preparation and spectroscopic characterization of these compounds is reported here together with a study by ^{1}H NMR spectroscopy of their conformation in solution.

2. 2. Experimental Section.

General procedures All melting points are uncorrected; reagent grade solvents were used without further purification. Toluene was dried over 4Å molecular sieves. Tetrahydrofuran (THF) was distilled from sodium/benzophenone before use. The other solvents were obtained from Caledon Lab. Ltd. or BDH and used as received unless described otherwise. *N*ε-t-Boc-*N*α-CBZ-*L*-lysine dicyclohexylammonium salt, 1,3-dicyclohexylcarbodiimide (DCC), and 3β-hydroxy-Δ^5-cholestene (or cholesterol) were purchased from Sigma Chemical Co. *N*-hydroxysuccinimide (NSI), 1-pyrenemethylamine hydrochloride, 4-(1-pyrenyl)butyric acid, *N*-[1-(1-naphthyl)ethyl]amine 1, 6-hexyldiisocyanate, 1, 4-cyclohexadiene and palladium-on charcoal catalyst (10%) were obtained from Aldrich Chemical Co. 4-(1-pyrenyl)butylamine hydrochloride was prepared from 4-(1-pyrenyl)-butyric acid as previously described.[35] 1-hexylisocyanato-6-cholesterylurethane was obtained by

reaction of 1, 6-hexyldiisocyanate and cholesterol following a reported procedure.[36] ^{1}H NMR spectra were recorded with Bruker AC-200 or DRX-500 spectrometers. Using $CDCl_3$, CD_3OD, CD_3OH or DMSO-d_6 as a solvent. FTIR spectra were obtained with a Bio-Rad FTS-40 FTIR spectrometer; samples were prepared as KBr pellets. Melting points were measured with Fisher-Johns Melting Point Apparatus, using glass slides as sample holder. Mass spectra were recorded on either a Finnigan 4500 (Chemical Ionization) or a Micromass Quattro LC (Electrospray) mass spectrometer. Thin layer chromatography was performed on silica gel 60F plates. UV spectra were measured with a Hewlett Packard 8425A photodiode array spectrometer.

2. 2. 1. *N*ε-*t*-Boc-*N*α-CBZ-*L*-lysine-[*N*-1-pyrenemethylamide) (2a) A solution of 1-pyrenemethylamine hydrochloride (0.7 g, 2.6 mmol) in 20 mL of DMF was added to a solution of *N*ε-*t*-Boc-Nα-CBZ-*L*-lysine dicyclohexylammonium salt (2 g, 3.56 mmol) and *N*-hydroxysuccinimide (0.4 g, 3.56 mmol) in 20 mL of methylene chloride. 1,3-dicyclohexylcarbodiimide (DCC, 2.96 g, 4.3 mmol) was added at once into the stirred mixture. The reaction mixture was stirred for 2 days at room temperature. Methylene chloride (50 mL) was added to the mixture, which was stirred for an additional 30 min. The residual solid was removed by filtration. The filtrate was concentrated by evaporation to remove methylene chloride and further distilled under high vacuum to remove DMF yielding a gray solid. Final product was dissolved in methylene chloride (500mL), washed with water, aqueous citric acid (10%), aqueous Na_2CO_3 (5%) and water sequentially. The product was dried completely at oven. Evaporation solvent yielded crude 2a, which was recrystallized from ethyl acetate (1.8 g, 90%); ^{1}H NMR

($CDCl_3$, ppm) 7.90-8.20 (m, 9H aromatic protons of pyrene), 7.33 (s, 5H, aromatic protons of CH_2Ph), 6.52 (s, 1H, NH of pyrenylmethylamine), 5.45 (s, α-NH of lysine), 5.14 (d, 2H, CH_2Ph), 4.98 (d, CH_2 of pyrene), 4.50 (s, ε-NH of lysine), 4.19 (m 1H, H_2 of lysine), 2.98-3.17 (m, H_6 of lysine), 1.87-1.04 (m H_3-H_5 of lysine) 1.398 (s, CH_3 of t-butyl); IR (KBr, cm^{-1}): 3327, 3280 (NH), 2930, 2852 (CH), 1691.6, 1628, 1533.4 (amide band), 1449, 1364 (CH_3), 891, 846.6 (pyrene CH out of plane), 642.

2. 2. 2. *N*ε-*t*-Boc-*N*α-CBZ-*L*-lysine-*N*-[4-(1-pyrenyl)butylamide] (2b) Compound 2b was prepared following the same procedure as used for compound 2a, but starting with 4-(1-pyrenyl)butylamine) hydrochloride (1.16 g, 3.86 mmol); ^1H NMR ($CDCl_3$, ppm). 7.99-8.23 (m, 9H aromatic protons of pyrene), 7.32 (m, 5H, aromatic protons of CH_2Ph), 6.14 (s, 1H, NH of pyrenylbutylamide), 5.49 (s, 2H, CH_2Ph), 5.40 (s, α-NH of lysine), 4.52 (s, ε-NH of lysine), 4.19 (m, 1H, H_2 of lysine), 2.99-3.62 (m, H_6 of lysine and 1, 4-CH_2 of pyrene), 1.96-1.03 (m H_3-H_5 of lysine and 2, 3-CH_2 of pyrene) 1.40 (s, CH_3 of t-BOC). IR (KBr, cm^{-1}): 3327 (NH), 2930 & 2852 (CH), 1691, 1627, 1574, 1533 (amide band), 1450 & 1365, 1312, 1245, 1170, 892, 844 (Pyrene C-H out of plane), 642.

2. 2. 3. *N*ε-*t*-Boc-*N*α-CBZ-*L*-lysine-*N*-[1-(1-naphthyl)ethylamide] (2c) Compound 2c was prepared by following the same procedure as for 2a, starting with 1-(1-naphthyl)ethylamine (1.52 g, 8.9 mmol); ^1H NMR ($CDCl_3$, ppm): 8.019-7.467 (m, aromatic proton of naphthalene), 7.298 (s, aromatic proton of CH_2Ph), 6.521 (d, NH of naphthaleneamine), 5.859 (s, methine of naphthylethylene), 5.49 (d, α-NH), 5.05 (s, $\underline{CH_2}$ph), 4.56 (d, ε-NH), 4.07 (m, H_2 of lysine), 3.05 (s, H_6 of lysine), 1.89-1.14 (m, H_3-

H_5 of lysine), 1.40 (s, t-BOC). IR (KBr): 3300, 2932, 2855, 1688, 1638, 1553, 1269, 1247, 1174, 799, 777.

2. 2. 4. *N*ε-*t*-Boc-*N*α-amine -*L*-lysine-(*N*-1-pyrenyl-methyl)amide (3a) A suspension of palladium on charcoal (4.0 g, 10%) in absolute ethanol containing 2a (1.8, 3.22 mmol) was purged with nitrogen at 25°C for 15 min. 1,4-cyclohexadiene (5 mL) was injected into the suspension. The resulting mixture was stirred for 2 days. The Pd/C was removed from the mixture by filtration. It was washed thoroughly with ethanol. The combined filtrate was concentrated in *vacuo*, yielding an oil material that was recrystallized from absolute ethanol/petroleum ether (1/4, v/v); 1.2 g, 72%; Mp. 118-120 °C. ^{1}H NMR ($CDCl_3$, ppm) 7.90-8.20 (m, 9H aromatic protons of pyrene), 6.52 (s, NH of pyrenylmethylamine), 5.45 (s, α-NH), 5.05 (d, CH_2 of pyrenylmethylamine), 4.45 (d, ε-NH), 4.19 (m 2H, H_2 of lysine), 3.17 (m, H_6 of lysine), 1.87-1.04 (m H_3-H_5 of lysine) 1.398 (s, CH_3 of t-butyl); FTIR (KBr cm^{-1}): 3327(NH), 2929, 2851(CH), 1690, 1627.7, 1534.4 (C=O of amide), 1449, 1365(CH_3), 844.7(pyrene), 641; MS/EI, *m/e* 460 (MH^+), calcd. for $C_{28}H_{33}N_3O_3$: 459.

2. 2. 5. *N*ε-*t*Boc-*N*α-amine-*L*-lysine-*N*-[4-(1-pyrenyl)butyl]amide (3b) Compound 3b was prepared by the same procedure as 3a, starting with 2b (3.50 mmol); ^{1}H NMR ($CDCl_3$, ppm): 7.988-8.230 (m, 9H aromatic protons of pyrene), 6.138 (s, 1H, NH of pyrenylbutylamide), 4.45(s, ε-NH of lysine), 4.19 (m 1H, H_2 of lysine), 3.050-3.451 (m, H_6 of lysine and 1, 4-CH_2 of pyrene), 1.87-1.04 (m, H_3-H_5 of lysine and 2, 3-CH_2 of pyrene), 1.398 (s, CH_3 of t-BOC); FTIR (KBr cm^{-1}): 3327 (NH), 2930 & 2852 (CH),

1691, 1627, 1574, 1533, (C=O of amide), 1450 & 1365, 1312, 1245, 1170, 844 (pyrene CH out of plane), 642.

2. 2. 6. *N*ε-*t*Boc-*N*α-amine-*L*-lysine-[*N*-1-(1-naphthyl)ethylamide] (3c) Compound 3c was prepared by a procedure analogous to the preparation of 3a, starting with 2c (8.0 mmol); yielding: 83%; ^{1}H NMR ($CDCl_3$, ppm): 8.07-7.43 (m, 7H, aromatic protons of naphthalene), 6.52 (s, NH), 5.88 (s, methine of naphthylethylene), 4.55 (d, ε-NH), 4.10 (m, H_2 of lysine), 3.05 (d, H_6 of lysine), 2.14-1.06 (m, H_3 -H_5 of lysine), 1.40 (s, t-BOC); IR (KBr cm^{-1}): 3329 (NH), 2932, 2854 (CH), 1699, 1652, 1558, 1540, 1456, 1366, 1247, 1172, 801 and 779 (naphthalene CH out of plane); MS/ES, m/e: 400 (MH^+) ; calcld. for $C_{23}H_{33}O_3N_3$ 399.

2. 2. 7. *N*ε-*t*-Boc-*N*α-[6-(3β-cholesteryl)urethane]-1-hexylurea-*L*-lysine-*N*-(1-pyrenyl)methylamide (4a) A solution of 3a (1 g 2.12 mmol) and 1-hexylisocyanato-6(-3-β-cholesteryl)-urethane (1.0 g, 1.8 mmol) in dry toluene (20 mL) was stirred at 35 °C for 24 hrs. The solvent was removed in *vacuo*. The residue was dissolved in methylene chloride (150 mL). It was washed with water, 0.1 N HCl, and brine, consecutively. The organic layer evaporated to yield an oil material, and it was recrystallized from a mixture of ethyl acetate/absolute ethanol (1/1, v/v). 1.4 g, 68% yield; ^{1}H NMR ($CDCl_3$, ppm): 7.90-8.20 (m, 9H aromatic protons of pyrene), 5.32 (s, H_6 of cholesterol), 5.05 (d, CH_2 of pyrene), 4.45 (s, 1H, H_3 of cholesterol), 4.12 (m 1H, H_2 of lysine), 3.46 (m, $\underline{CH_2}$NHCOO), 3.27 (m, $\underline{CH_2}$NHCONH), 3.13 (m, H_6 of lysine), 2.02-0.84 (m, H_3-H_5 of lysine, H of cholesterol) 1.40 (s, CH_3 of t-butyl), 0.64 (s, 18-CH_3 of cholesterol); IR (KBr

cm^{-1}): 3329 (NH), 2932, 2854 (CH), 1694, 1629, 1554 (amide), 1450, 1378 (CH_3), 1250, 1137 (C-C-OCO of Cholesterol), 845 (pyrene), 642.

2. 2. 8. *Nε-t*-Boc-*Nα*-[6-(3β-cholesteryl)urethane]-1-hexylurea-*L*-lysine-*N*-[4-(1-pyrenyl)butyl]amide (4b) Compound 4b was prepared by the procedure employed to prepare 4a. Started with 3b (1.25 g, 2.49 mmol). The crude product was purified by chromatograph on silica gel eluted first with EtOAc/hexane (1:2, v/v), then with $CHCl_3$/MeOH (2/1 v/v); 2.1 g, 79%; ^1H NMR ($CDCl_3$, ppm): 7.979-8.207 (m, 9H, aromatic protons of pyrene), 5.327 (s, H6 of cholesterol), 4.45 (s, 1H, H_3 of cholesterol), 4.125 (m, 1H, H_2 of lysine), 3.68 (m, $\underline{CH_2}$NHCOO), 3.40 (m, $\underline{CH_2}$NHCONH), 3.33-3.10 (m, H_6 of lysine and 1,4-CH_2 of pyrene), 2.005-1.061 (m, H_3-H_5 of lysine, H of cholesterol and 2,3-CH_2 of pyrene), 1.40 (s, CH_3 of t-BOC), 0.636 (s, 18-CH_3 of cholesterol); IR (KBr, cm^{-1}): 3327 (NH), 2930, 2851 (CH), 1692, 1627, 1575 & 1535 (amide), 1438, 1312 (CH_3), 1245, 1179, 1088, (C-C-OCO), 892, 844, 642.

2. 2. 9. *Nε-t*-Boc-*Nα*-[6-(3β-cholesteryl)urethane]-1-hexylurea--*L*-lysine-*N*-[1-(1-naphthyl)ethyl]amide (4c) Compound 4c was obtained from 3C described previously (3.085 g, 7.72 mmol); ^1H NMR (CDCl3): 8.026-7.460 (m, 7H, aromatic proton of naphthalene), 5.845 (s, methine of naphthylethylene) 5.334 (s, H_6 of cholesterol), 4.35(s, 1H, H_3 of cholesterol), 4.108 (m, H_2 of lysine), 3.48 (m, $\underline{CH_2}$NHCOO) 3.33 ($\underline{CH_2}$NHCONH), 3.05 (m, H_6 of lysine), 2.33 (m, H_4 of cholesterol), 1.99-0.84 (m, H_3 - H_5 of lysine and H of cholesterol), 1.40 (s, t-BOC), 0.64 (18-CH_3 of cholesterol); FTIR

(KBr): 3330 (NH), 3053 (CH of aromatic), 2935, 2856 (CH of aliphatic), 1689, 1627 1535 (amide), 1465 1367, 1249, 1174, 799, 777 (naphthalene CH out of plane), 643.

2.2.10. *N*α-[6-(3β-cholesteryl)urethane]-1-hexylurea-*L*-lysine-[*N*-(1-pyrenyl)methyl]amide-ε-amine hydrochloride (5a) Trifluoroacetic acid (5 mL) was added to a solution of 4a (0.625 g, 0.066 mmol) in methylene chloride (10 mL). The reaction mixture was stirred at room temperature for 4 h. Removal of the solvent *in vacuo*, yielded an oil residue, which was dissolved in 30 mL of methylene chloride. The solution was washed with aqueous bicarbonate (5%), water and HCl (0.1 N). The residue obtained after evaporation of the solvent was recrystallized from methanol/petroleum ether (1/20, v/v); 0.28 g, 48% yield; mp 56°C isotropic mp 132°C[3]; ^{1}H NMR ($CDCl_3$) 7.92~8.29 (m, 9H, aromatic protons of pyrene), 5.32 (s, 1H, H_6 of Cholesterol), 5.01 (s, 2H, CH_2 of pyrenylmethylene), 4.40 (s, 1H, H_3 of cholesterol), 4.29 (m, H2 of lysine), 3.45 (m, $\underline{CH_2}$NHCOO), 3.37 (m, $\underline{CH_2}$NHCONH), 3.08 (m, H_6 of lysine), 2.29~0.84 (m, H_3-H_5 of lysine and H of cholesterol) 0.64 (18-CH_3 of cholesterol); IR (KBr, cm^{-1}): 3325 (NH), 2933, 2856 (CH of aliphatic), 1695, 1628, 1533 (amide) 1450, 1407 (CH_3), 1243, 1136 (ester of cholesterol), 846 (pyrene); UV (methanol, λ_{nm}, nm) : 342, 326, 312, 276, 266. ε_{342}: 4497 M^{-1}. cm^{-1}; MS/ES, *m/e*: 914 $(M-Cl)^+$, calcld. for $C_{58}H_{84}N_5O_4Cl$ 949.5.

2.2.11. *N*α-[6-(3β-cholesteryl)urethane]-1-hexylurea-*L*-lysine-*N*-[4-(1-pyrenyl)butyl]amide-ε-amine hydrochloride (5b) Compound 5b was prepared by the same procedure as 5a, starting from 4b (2.0 g, 1.90 mmol). Compound 5b was recrystallized from EtOAC/MeOH; yield: 55%; Mp 75°C, isotropic mp 133°C; ^{1}H NMR

($CDCl_3$, ppm): 7.96-8.13 (m, 9H aromatic protons of pyrene), 5.35 (s, 1H, H_6 of cholesterol), 4.46 (s, 1H, H_3 of cholesterol), 4.14 (m 1H, H_2 of lysine), 3.68 (m, $\underline{CH_2}$NHCOO), 3.40 (m, $\underline{CH_2}$NHCONH), 3.36-3.05 (m, H_6 of lysine and 1,4-CH_2 of pyrene), 2.33 (m, H_4 of cholesterol), 2.00-0.83 (m H_3-H_5 of lysine, 2,3-CH_2 of pyrene and H of cholesterol), 0.64 (s, 18-CH_3 of cholesterol); FTIR (KBr, cm^{-1}): 3413.8 (broad strong absorption resulting from NH_3^+ stretching band), 2935.6 & 2862.4 (stretching vibration of methyl and methylene groups), 1691.7 (amide I band), 1534.0 (The symmetry NH_3^+ bending), (the C=O amide II band), 1465.0 (the symmetry bending vibration of methyl groups), 1249.8, 1031.5 (C-C-OCO), 845 (out of aromatic ring C-H bending); UV (methanol, λ_{nm}, nm): 342, 326, 312, 276, 266; ε_{342}: 8557 $M^{-1}cm^{-1}$; MS/ES, *m/z* (%): 957 $(M\text{-}Cl)^+$, calcld. for $C_{61}H_{90}O_4N_5Cl$ 991.5.

2.2.12. *N*α-[6-(3β-cholesteryl)urethane]-1-hexylurea-*L*-lysine-{*N*-[1-(1-naphthyl)ethyl]}amide-ε-amine hydrochloride (compound 5c) Compound 5c was obtained from 4c (0.6 g, 0.067mmol) using the procedure described in the preparation of 5a. It was purified by recrystallization from the mixture solvent of ethyl acetate/methanol (1/20=v/v); 51% yield; mp 80°C, isotropic mp 199°C; ^1H NMR (CD_3OD): 8.08-7.44 (m, 7H, aromatic protons of naphthalene), 5.80 (m, 1H, $\underline{CH}CH_3$ph), 5.33 (s, 1H, H_6 of cholesterol), 4.56 (d, 1H, H_3 of cholesterol), 4.10 (m, 1H, H_2 of lysine), 3.1(m, 4H, $\underline{CH_2}$NHCOO + $\underline{CH_2}$NHCONH), 2.9(d, H_6 of lysine), 2.30-2.15 (m, H_4 of cholesterol), 2.02-1.06 (m, H_3-H_5 of lysine, H of cholesterol and CH_3 of naphthylethylene), 0.70 (s, 3H, 18-CH_3 of cholesterol); FTIR (KBr, cm^{-1}): 3346 (NH), 3328 (NH), 3127, 2934, 2852 (CH of aliphatic), 1692, 1626, 1572(amide) 1465, 1401, 1255, 1138, 800, 777

(naphthalene CH out of plane); UV (MeOH, λ_{max}, nm) 290, 282, 272, 226; ε_{290}: 3379 M^{-1}. cm^{-1}; MS/ES *m/e*: 854 $(M\text{-}Cl)^+$, calcld. for $C_{53}H_{84}O_4N_5Cl$: 889.5.

2.2.13. *N*ε-t-Boc-*N*α-CBZ-*L*-lysine-{[6-(3β-cholesteryl)urethane]-1-hexyl}amide (2e)

Nε-t-Boc-Nα-CBZ-L-lysinedicyclohexylammonium salt (7.0 g) was dissolved in methylene chloride, washed with HCl (0.1 N) and deionized water, white solid was obtained by the removal of solvent and dried over P_2O_5 *in vacuo*, yielding the lysine derivative with a free carboxylic acid (1e), 5.8 g. A mixed solution of 1e (4.0 g, 0.0116mmol) and 1-hexylisocyanato-6(3β-cholesteryl)-urethane (6.4226 g, 0.0116 mmol) in dry toluene was stirred 48 h at 70°C. Removal of the solvent in *vacuo* yielded crude product 2e, which was recrystallized from ethyl acetate; 7.64 g, 77% yield; ^{1}H NMR ($CDCl_3$, ppm): 7.308 (m, aromatic protons of $CH_2C_6H_5$), 5.526 (s, α-NH of lysine), 5.34 (s, H_6 of cholesterol), 5.085 (s, CH_2Ph), 4.67 (s, ε-NH of lysine), 4.59 (s, NH of urethane), 4.46 (s, H_3 of cholesterol), 4.34 (s, NH of hexanylamide), 4.09 (m, H_2 of lysine), 3.47 (m, $\underline{CH_2}NHCOO$), 3.33 (m, $\underline{CH_2}NHCO$), 3.073 (s, H_6 of lysine), 2.33-0.83 (m, H_3-H_5 of lysine and H of cholesterol), 1.40 (s, CH_3 of t-butyl), 0.65 (s, 18-CH_3 of cholesterol); FTIR (KBr, cm^{-1}): 3393, 3345 (NH), 2934, & 2859 (CH), 1704 (C=O of ester), 1693, 1627, 1530 (amide), 1465, 1455 & 1366 (CH3), 1250, 1176.

2.2.14. *N*ε-t-Boc-*N*α-amine-*L*-lysine-[6-(3β-cholesteryl)urethane]-1-hexylamide (3e)

Compound 3e was prepared by following the same procedure as 3a. Started with compound 2e (7.64 g, 8.92 mmol); 3.24 g, 50%; ^{1}H NMR ($CDCl_3$, ppm): 5.34 (s, 1H, H_6 of cholesterol), 4.55 (d, ε-NH), 4.46 (s, H_3 of cholesterol), 4.24 (m, H_2 of lysine), 3.47 (m,

$\underline{CH_2}$NHCOO), 3.33 (m, $\underline{CH_2}$NHCO), 3.07 (s, H_6 of lysine), 2.19-0.84 (m H_3-H_5 of lysine and H of cholesterol), 1.40 (s, CH_3 of t-butyl), 0.65 (s, 18-CH_3 of cholesterol); IR (KBr, cm^{-1}): 3375 (NH), 2934 & 2860 (CH), 1690, 1628, 1529 (amide), 1464, 1448 & 1366 (CH_3), 1251, 1177, 663; MS/ES, *m/e*: 757 (MH^+), calcld. for $C_{45}H_{80}O_5N_4$ 756.

2.2.15. *N*ε-*t*-Boc-*N*α-[4-(1-pyrenyl)butyl]amide-*L*-lysine-[6-(3β-cholesteryl)urethane]-1-hexylamide (4e) DCC (2.31 g) was added to a mixed solution of 3e (3.24 g, 4.5 mmol), NSI (0.522 g, 4.5 mmol) in methylene chloride (100 mL) and pyrenyl butyric acid (1.442 g, 0.5 mmol) in DMF (10 mL). The resulting mixture was stirred 2 days at room temperature. The work-up followed the same procedure as used for 2a. Crude product was applied on a silicon gel chromatography column and eluted with ethyl acetate/methyl chloride (3/2, v/v); 85% yield; ^{1}H NMR ($CDCl_3$, ppm): 8.26-786 (m, 9H, aromatic protons of pyrene), 6.38 (s, 1H α-NH), 5.789 (s, NH), 5.34 (s, H_6 of cholesterol), 4.64 (s, H_3 of cholesterol), 4.13 (m 1H, H_2 of lysine), 3.46 (m, $\underline{CH_2}$NHCOO and 2-CH_2 of pyrenyl butyric acid), 3.35 (m, $\underline{CH_2}$NHCO), 3.12 (s, H_6 of lysine), 2.29 (m, H_4 of cholesterol and 4-CH_2 of pyrenyl butyric acid), 2.00-0.84 (m H_3-H_5 of lysine, H of cholesterol and 3-CH_2 of pyrenyl butyric acid), 1.40 (s, CH_3 of t-butyl), 0.64 (s, 18-CH_3 of cholesterol); FTIR (KBr, cm^{-1}): 3402, 3332 (NH) 2931, 2853 (CH), 1692 (amide I), 1627, 1529 (amide II), 1443 & 1365 (CH_3), 1215, 1069, 843 (phenyl), 647.

2.2.16. *N*α-[4-(1-pyrenyl)butyl]amide-*L*-lysine-[6-(3β-cholesteryl)urethane]-1-hexylamide-ε-amine hydrochloride (5e) Compound 5e was prepared by following the

same procedure as used for 5a. The crude product was recrystallized from a mixture of ethyl acetate/methanol; 48% yield; Mp 76°C, isotropic mp 188°C. ^{1}H NMR (CDCl3, ppm): 8.261-7858 (m, 9H aromatic protons of pyrene), 5.341 (s, 1H, H_6 of cholesterol), 4.635 (s, H_3 of cholesterol), 4.06 (m, H_2 of lysine), 3.479 (bs, $\underline{CH_2}NHCO$, $\underline{CH_2}NHCOO$ and 2-CH_2 of pyrenyl acid), 3.128 (s, H_6 of lysine), 2.292 (m, H_4 of cholesterol and 4-CH_2 of pyrenyl butyric acid), 1.918-0.839 (m H_3-H_5 of lysine and H of cholesterol), 0.636 (s, 18-CH_3 of cholesterol); FTIR (KBr, cm^{-1}): 3436 (NH), 3332 (NH), 2932 & 2853 (CH of aliphatic), 1628, 1577, 1536 (amide band), 1450 & 1373 (CH3), 1312.5, 1245.0, 845 (phenyl), 653; UV (MeOH, λnm) 342, 336, 276, 264, 242; ε_{342}: 8876 M^{-1} cm^{-1}; MS/ES, m/e: 927 $(M\text{-}Cl)^+$, calcld. for $C_{60}H_{87}O_4N_4Cl$ 962.5.

2. 3. Results and Discussion

The parallel synthetic schemes were employed to prepare three fluorescent cholesterol-substituted lysine derivatives 5a, 5b, 5c (Scheme 2. 1) with similar structure but varying fluorescent groups. The starting materials were a protected lysine, *Nε-t*-Boc-Nα-CBZ-*L*-lysine dicyclohexylammonium salt (1), 1-hexylisocyanate-6-cholesterylurethane,[35] and three aminoalkyl-substituted fluorescent derivatives. The protected lysine derivative 1 was converted first to the fluorescent derivatives 2a, 2b, and 2c (Scheme 2. 2) by coupling free lysine carboxyl group to 1-pyrenylmethylamine, 4-(1-pyrenyl)-butylamine, and 1-(1-naphthyl)amine, respectively. The peptide bond was formed with dicyclohexylcarbodiimide (DCC) in the presence of *N*-hydroxylsuccinimide (NHS).[37] The N-α-CBZ group in compounds 2a, 2b, and 2c was removed by catalytic hydrogenation with Pd/C in the presence of 1,3-dicyclohexadiene to yield 3a, 3b, and 3c.

Scheme 2. 1. Chemical structure of prepared lysine derivatives (5a, 5b, 5c)

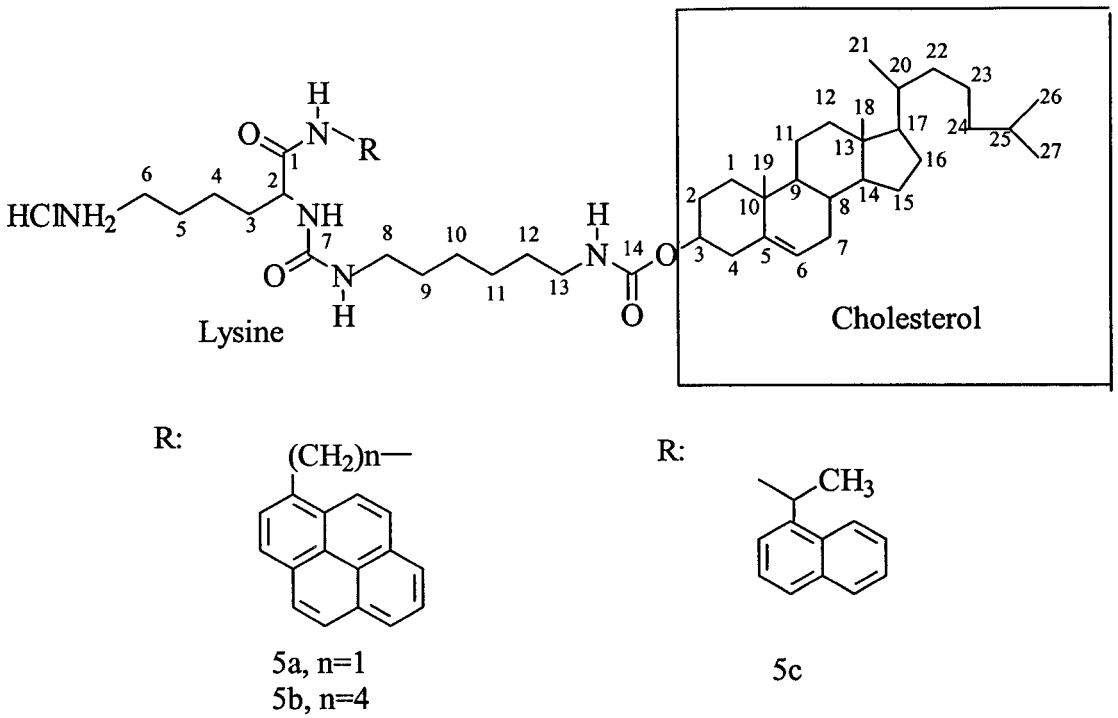

Subsequently, the free amine was linked to hexylisocyanato-6-(3β-cholesterol)-urethane forming an urea bond. The reaction proceeded readily in toluene. Deprotection of the N-ε-Boc functional group was achieved by treatment with trifluoroacetic acid (30% in CH_2Cl_2).[38] Under these mild conditions only the Boc group was removed. Competing cleavage of the urethane bond between cholesterol and the hexyl chain took place at higher trifluoroacetic acid concentrations. Recrystallization from the appropriate solvents gave analytically pure samples 5a, 5b, and 5c.

Compounds 5a, 5b, and 5c possess four nitrogen functionalities: a primary amine (ε-NH_2 of lysine), a secondary amide, a secondary urea, and a secondary urethane. Their conformation in solution is directed primarily by the formation of intramolecular amide-urea, amide urethane, or urea-urethane hydrogen bonds. The ^1H NMR spectrum of the

Scheme 2. 2. Synthesis of *N*α-[6-(3β-cholesteryl)urethane]-1-hexylurea-*L*-lysine-*N*-[fluorescent substituent]amide-ε-amine hydrochloride (5a, 5b, 5c); reagents: (i) RNH_2, HCl (R = (1-pyrenyl)methyl, 4-(1-pyrenyl)butyl, 1-naphthylethyl, see Scheme 2.1), NSI, DCC, CH_2Cl_2/DMF; (ii) Pd/C, 1,3-cyclohexadiene, EtOH, RT; (iii) 1-hexylisocyanate-6-(3β-cholesteryl)-urethane, toluene, 40°C; (iv) CF_3COOH, CH_2Cl_2, RT, then HCl.

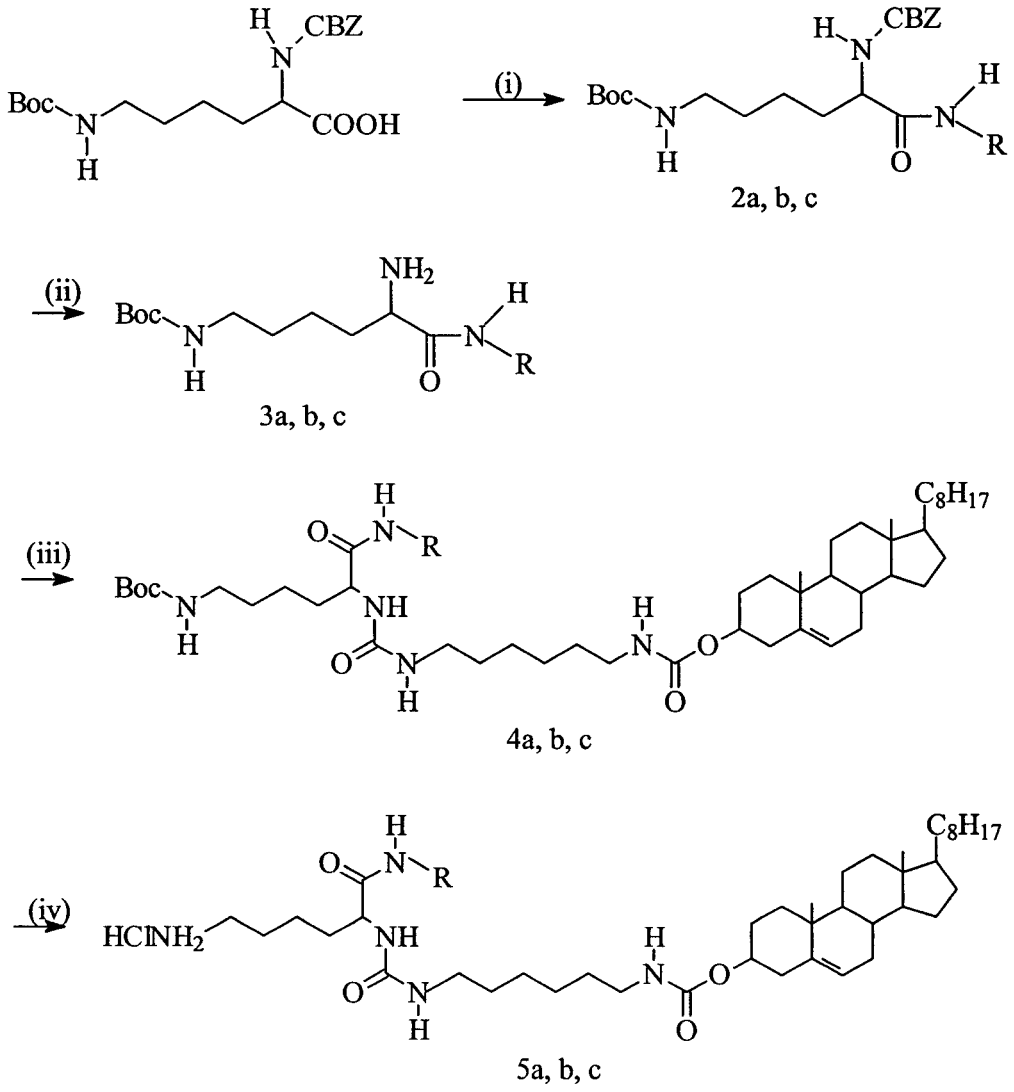

naphthalene derivative 5c dissolved in DMSO-d_6 or CD_3OH exhibited distinct signals assigned to nitrogen functionality on the basis of COSY and ROESY experiments described below. In the ROESY spectrum of 5c in CD_3OD, we only observed proton interaction within naphthalene (methine 5.8 ppm, methyl group 1.6 ppm and aromatic ring 7.8-8.2 ppm) and within cholesterol (H7 at 1.3 ppm and H4 at 2.3ppm and 1.7ppm interaction) respectively.

Figure 2. 1. COSY spectrum of 5c in CD_3OH.

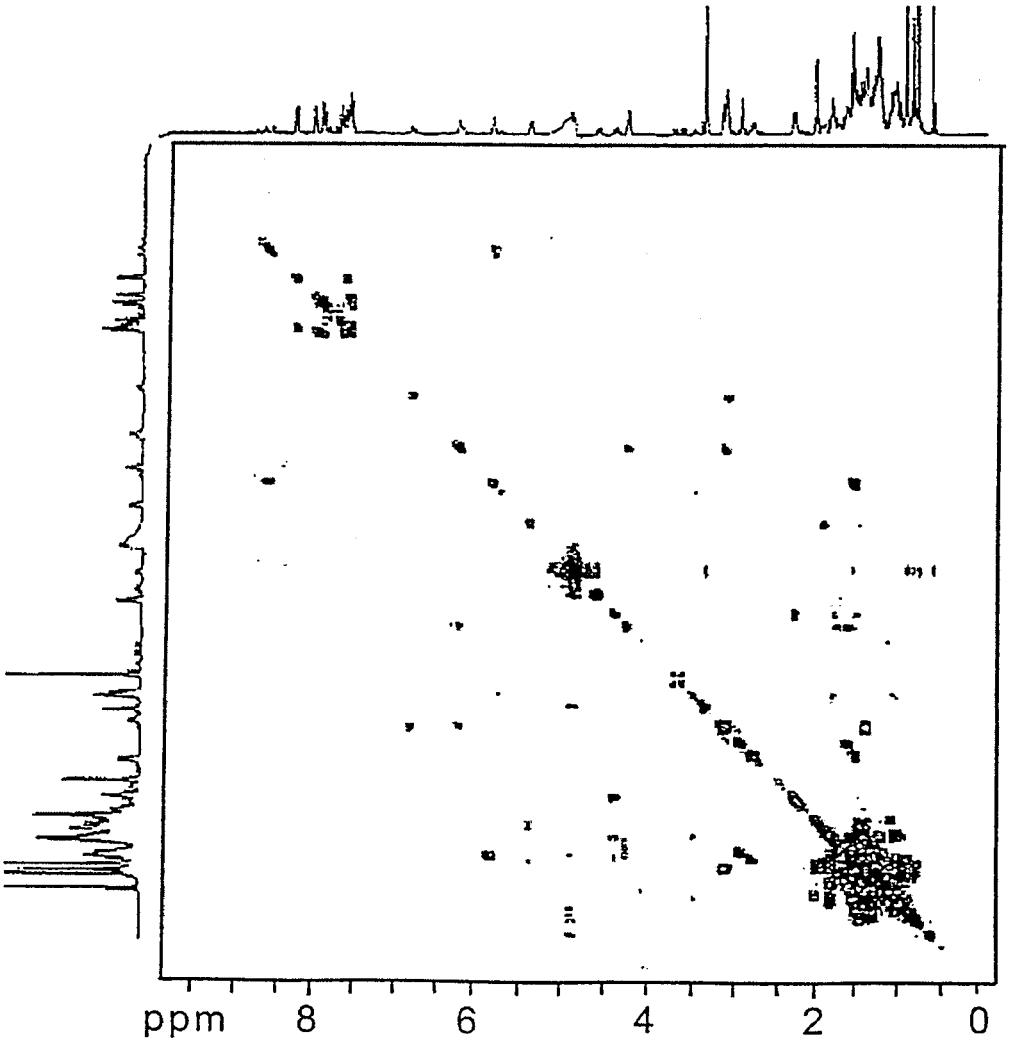

The COSY spectrum of 5c in CD_3OH (Figure 2.1) presents evidence of interactions between the aromatic protons of the naphthyl group with resonances at 7.45 and 8.05 ppm. Interactions between cholesterol protons are also observed for the protons H6 and H7, with resonances at 5.3 and 2.0 ppm, respectively and the protons H3 and H4, with resonances at 4.3 and 2.2 ppm, respectively. However, no interactions are detected between the cholesterol and the naphthyl protons, suggesting that theses two moieties are not in close proximity. The constraints brought about by the formation of the seven membered ring and the occurrence of interactions between the methine proton linked to C15 (δ 5.8) and both the C1 amide proton (δ 8,4) and the methyl protons of C6 (δ 1.6) suggest a Y-shaped structure where the lysine side chain would be the truck and the cholesterol and naphthyl groups the two arms. The interaction detected between the urea protons resonating at 6.2 ppm and the methylene protons of C2 of lysine bring evidence for the formation of a quasi-planar structure comprising the 7-membered ring, the cholesteryl and the naphthyl moieties. As the extended 9-unit chain carrying the cholesteryl group is much longer than the naphthyl group, the two groups are not expected to be in close proximity when compound 5c adopts the conformation depicted in Scheme 2.3. This is confirmed by the absence of interactions between naphthyl and cholesteryl protons. From qualitative deuterium exchange measurements (Table 2.1), we determined that the C7 urea and C14 urethane functionalities undergo hydrogen bonding with solvent molecules, while the C1 amide group N-H, which underwent very slow deuterium exchange, is involved in intramolecular hydrogen bonding. This observation is consistent with the chemical shift of this proton (8.5 ppm). Typical chemical shifts of H-bonded amide proton lie in this range, while free N-H protons resonate at ca. 6 ppm.[39]

Moreover, the chemical shift of the amide NH proton of 5c was insensitive to changes in solution concentration, again suggesting a seven-member ring created by the H-bond between the amide proton and the carbonyl C7 (Scheme 2.3).

Scheme 2. 3. Proposed conformation of 5c in solution.

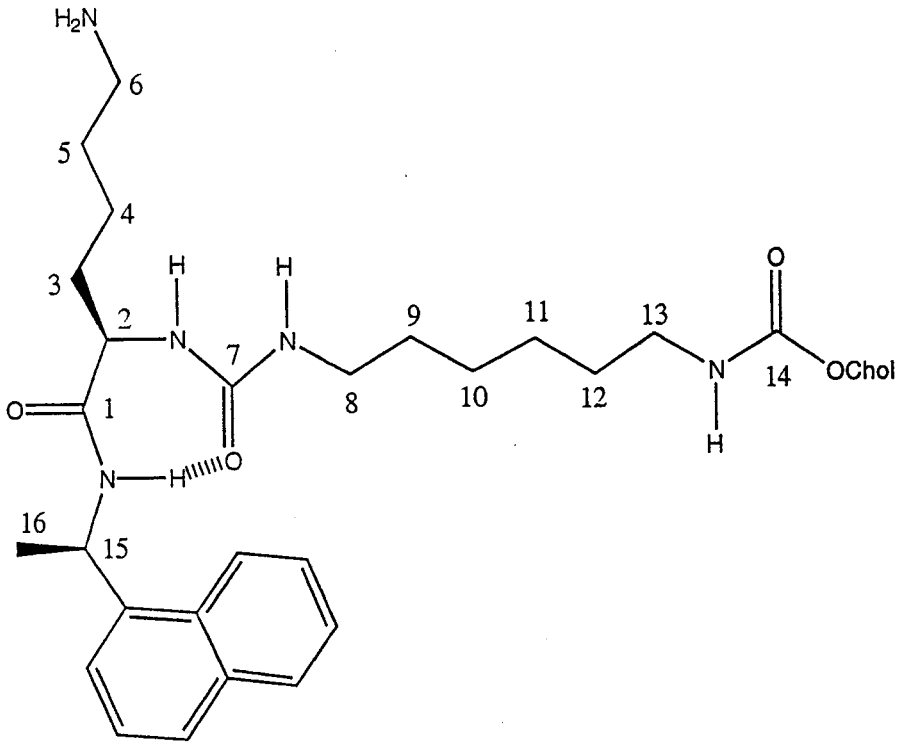

The temperature-dependence of the amide proton chemical shift has been widely used as a tool for studying intramolecular hydrogen bonding in peptides.[40] Figure 2.2 shows the NMR spectra of compound 5c in DMSO-d_6 at three different temperatures. The reduced temperature coefficient ($\Delta\delta/\Delta T$) derived from this experiment for the C1 amide proton was –5.4 ppb/K. This coefficient has become a standard parameter in the characterization of peptide behavior in solution.[41] In general, a large temperature dependence, such as observed here, is indicative of the formation, via H-bonding, of 5 to

7-membered rings.[42] Figure 2.2 also shows large temperature dependence for the C14 2° urethane proton (-5.0 ppb/K), suggesting the formation of an intramolecular hydrogen bond in 5c, which, however, was not detected by the deuterium exchange measurement presented in Table 2.1.

Table 2.1. ^{1}H NMR Chemical Shifts of N-H Protons of Compound 5c

Functional group	CD_3OH	DMSO-d_6	DMSO-d_6 + D_2O
C1 2°amide	8.5	8.64	Slow exchange
C14 2°urethane	6.7	7.0	Fast exchange
C7 2°urea	6.2	6.2	Fast exchange
C1 1°amine	-	8.15	Fast exchange

The overall NMR data lead us to propose that the C1 2° amide proton in 5c undergoes intramolecular hydrogen bonding with the C7 urea carbonyl group, and the planar structure thus formed prevents interactions between the cholesteryl and naphthyl moieties. We expect the other derivatives to adopt the same configuration in solution, since the most important features that keep the cholesteryl and the naphthyl moieties apart are the length of the linker to the cholesteryl and the H-bonded seven-member ring structure, which were the same in all the synthesis.

Figure 2. 2. NMR spectra of 5c at variable temperature in DMSO-d_6.

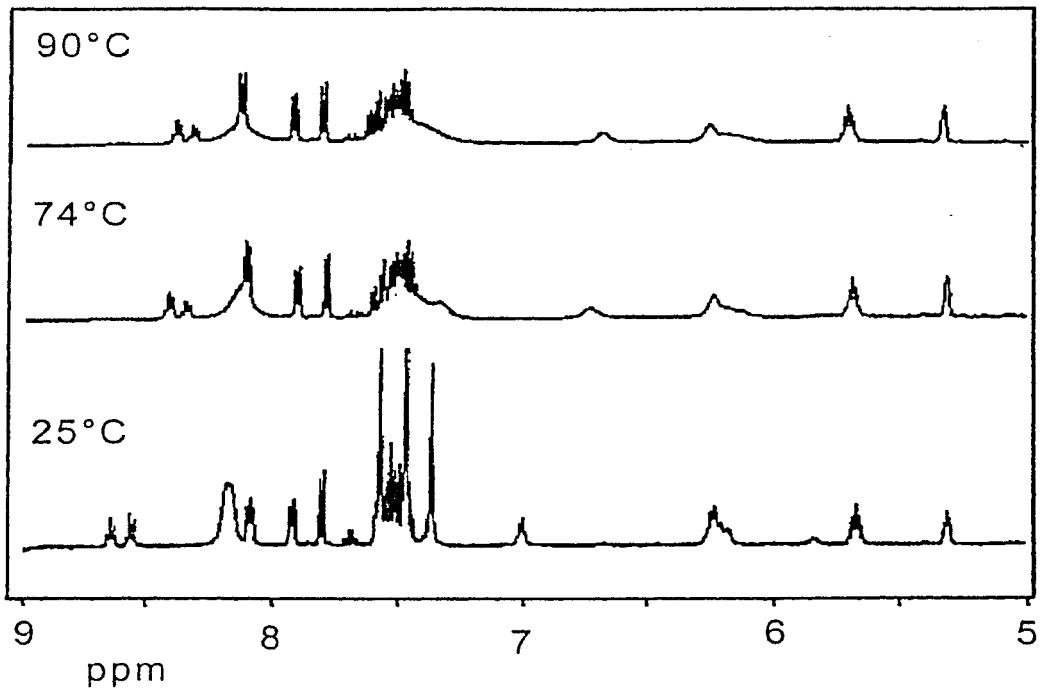

In order to shorten the reaction steps but keep the long alkyl pyrene substituents, we further designed *N*α-[4-(1-pyrenyl)butylamide]-*L*-lysine-{[6-(3β-cholesteryl)urethane]-1-hexylamide}-ε-amine hydrochloride (5e), which was prepared with a commercial available compound, pyrenyl butyric acid rather than pyrenylbutylamine (Scheme 2.4). This procedure removes 4 preparation steps from the overall process and provides a more efficient route to prepare pyrenylbutyl substituent cholesteryl lysine derivative.

Scheme 2. 4. Synthesis of *N*α-[4-(1-pyrenyl)butylamide]-*L*-lysine-[6-(3β cholesteryl)urethane]-1-hexylamide-ε-amine hydrochloride (5e).

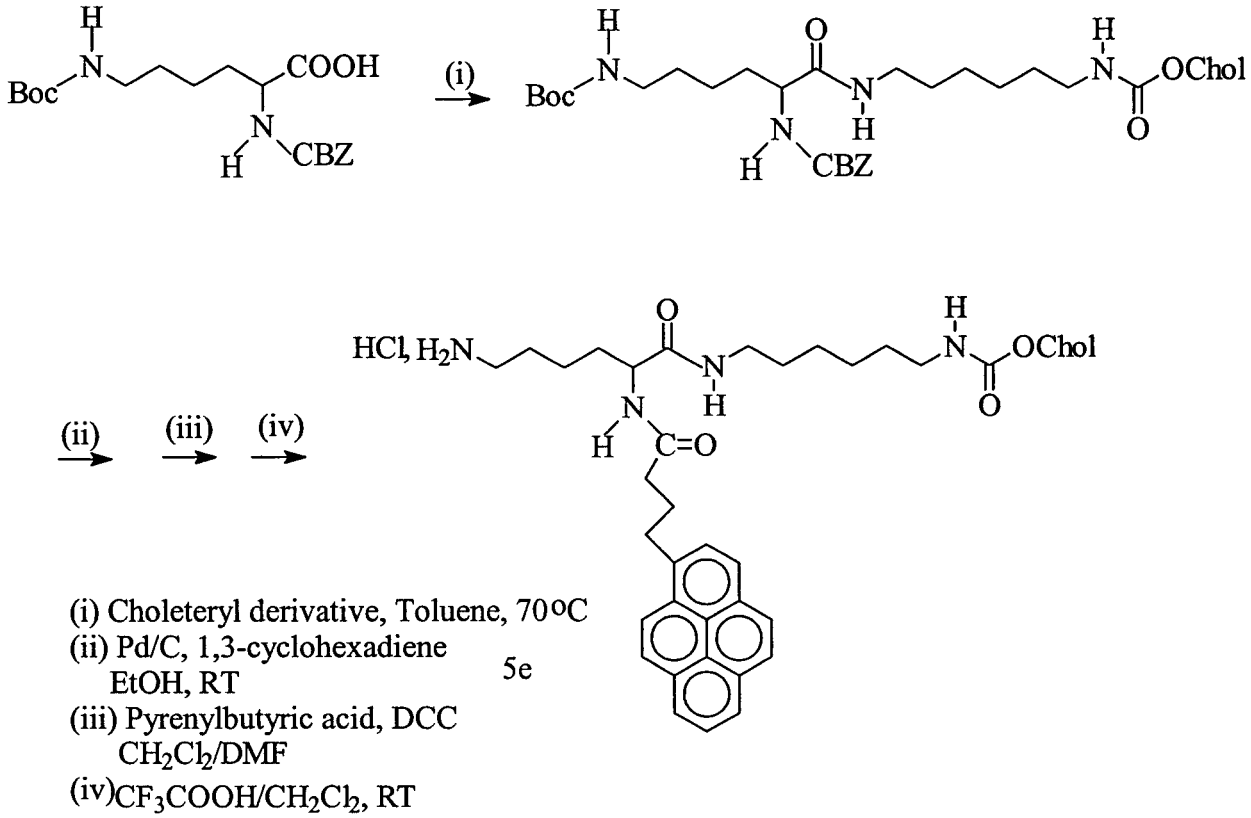

The key step is the preparation of the compound 2e. Compound 2e was prepared by reacting the isocyanate group of 1-hexylisocyanato-6-(3β-cholesteryl)-urethane with the carboxyl group of the lysine derivative (1e). The mechanism involves the formation of an intermediate carbamylcarboxylate. The intermediate is unstable and rapidly loses carbon dioxide with the formation of amide.[43] Additional sequences may involve the formation of disubstituted urea and normal acid anhydrides, which in turn interact to form 2 moles of amide and one mole of CO_2. The band at 2257 cm^{-1} disappeared in the FTIR spectrum of compound 15, indicating that the isocyanate group was completely converted. Neither the species of disubstituted urea (672 g/mol) nor the normal acid anhydrides (1081.6 g/mol) were observed in the electron spray mass spectrum, which indicates that the conversion into amide was complete. The subsequent steps, such as deprotection and coupling, were followed the same procedure as previously described. The major structural differences of between the compound 5e and the compound 5b is the linkage position of the pyrenylbutyl and cholesteryl substituents to the functional groups of lysine: in 5e the α-amino group of lysine is linked with pyrenyl butyric acid and the carboxylic group of lysine is linked to the rigid hydrophobic cholesteryl group. The linkages are opposite in 5b. However, they are expected to have the same functionalities, such as a higher affinity anchor to lipid bilayers compared to octadecyl group.

Chapter 3

Synthesis and Characterization of Poly(*N*-isopropylacrylamide) Bearing Cholesteryl and Fluorophore Groups

Abstract

Poly(*N*-isopropylacrylamide) bearing *N*α-[6-(3β-cholesteryl)urethane]-1-hexylurea-*L*-lysine-[*N*-(1-pyrenyl)methyl]amide (PNIPAM-Pymecho), *N*α-[6-(3β-cholesteryl)urethane]-1-hexylurea-*L*-lysine-*N*-[4-(1-pyrenyl)butyl] amide (PNIPAM-Pybucho), and *N*α-[6-(3β-cholesteryl)urethane]-1-hexylurea-*L*-lysine-*N*-[1-(1-naphthyl)ethyl]amide was developed by post-modification of poly(*N*-isopropylacryamide-co-*N*-acryloxylsuccinimide). In the modified copolymers, both the cholesteryl group and the chromophores were linked to lysine, which in turn was incorporated into the copolymer backbone through ε–amino of lysine by an amide bond. The copolymers were sequentially characterized by ^{1}H NMR, FTIR, UV spectroscopy and viscosity measurements. The solution properties were further investigated by dynamic light scattering (DLS), static, and time-resolved fluorescence spectroscopy. In aqueous solutions, the polymers can form micellar aggregates ranging in the size from 46 to 120 nm (25°C), as determined by DLS. The micellar size was affected by hydrophobic domain and the polymer architecture. No larger pyrene excimer was observed over the entire concentration range studied and the ratio of excimer to monomer emission intensities had no significant change as a function of concentration. The distance of chromophores located in hydrophobic microdomains was estimated by nonradiative energy transfer (NRET).

3.1. Introduction

Hydrophobically modified poly(*N*-isoproylacrylamide) (HM-PNIPAM) has attracted much attention because of their unique properties and potential applications.[44] Specifically, the use of hydrophobically substituted water-soluble polymers to modify liposomes[45] is a promising approach for developing highly efficient drug delivery systems with increased circulation time[46] and responsiveness to external stimuli.[4a] Hydrophobically modified water-soluble polymers consist of a water-soluble backbone which carries a small number of hydrophobic groups, such as long single alkyl chains, double alkyl chains or cholesteryl groups, acting as anchors inserted into the lipid bilayers. The performance of polymer-modified liposomes as drug delivery systems depends on the affinity of the anchoring groups within the lipid bilayers.[6b] A study of liposomes coated with octadecane-bearing PNIPAM was initiated by Ringsdorf and Winnik;[4a] the polymers were incorporated into liposomes via octadecyl anchor and remained incorporation during thermal-induced collapse of PNIPAM chains. However, Polozova and Winnik[6b] found that the octadecane-substituted polymer chains bound to the fluid bilayer were in dynamic exchange with unbound polymers, which caused that the majority of liposomes to be lost their surface coated polymers and unprotected. One approach to overcome this problem is to use an anchor group with a higher affinity for the lipid bilayer compared with the octadecyl group.

Cholesterol is well known as a high affinity group for the bilayer membranes[47] and as a versatile building block for the formation of liquid crystals.[48] However, only a few cases of cholesterol as a hydrophobic group incorporated into water-soluble polymers have been reported.[49] Cholesterol-bearing polysaccharide coated liposomes have shown that

cholesterol has a higher affinity for lipid bilayers than O-palmitoyl groups, especially at a low level of hydrophobic substitution in each polymeric chain.[53c, 53d]

In this study, synthesis, characterization, and the fundamental solution properties of the polymers bearing these fluorescent cholesterol groups, compound 5a, 5b, and 5c, were described. Fluorescence spectroscopy, DLS, and TEM were used to study the polymer behavior in solutions.

3. 2. Experimental

3. 2.1. Materials *N*-isopropylacrylamide (Acros) was recrystallized twice from toluene/hexane (1/1, v/v). Azobisisobutyronitrile (AIBN, Spectrum) was recrystallized from methanol. *N*-acryloxysuccinimide (Acros) and *N*-isopropylamine (Aldrich) were used without further purification. All solvents were obtained as previously described.

3.2.2. Synthesis of Reactive Copolymer (PNIPAM/NASI) A series of PNIPAM/NASI with different molecular weights were synthesized by adjusting the ratio of initiator to monomers (Table 3.1). *N*-isopropylacrylamide (NIPAM, 10 g, 88.03 mmol), and *N*-acryloxysuccinimide (NASI, 74.7 mg, 0.44 mmol) were dissolved in 120 mL of dry dioxane over molecular sieves. AIBN (62.5 mg, 0.38 mmol), was dissolved in 5 mL of dioxane and injected into the solution preheated to 60 °C. The mixture was stirred for 24 hrs and cooled to room temperature. The polymers was isolated by precipitation into anhydrous diethyl ether and reprecipitated once from tetrahydrofuran (THF) into anhydrous diethyl ether, the yielding 7.34 g. The molecular weight of copolymers was estimated by viscosity measurement as described in 3. 2. 4.

Table 3. 1. Molecular Weight of Copolymers

Copolymers	NIPAM (mmol)	NASI (mmol)	Molar ratio of AIBN to Monomers (% mol)	Solvent	M_v (Da)*.
L-PNIPAM/NASI 200/1	53.0	0.27	1.5	THF	$2{,}0 \times 10^4$
M-PNIPAM/NASI 200/1	88.5	0.44	0.43	dioxane	4.0×10^5
M2-PNIPAM/NASI 50/1	88.5	1.76	0.43	dioxane	2.4×10^5

*$[\eta] = 9.59 \times 10^{-3} M_v^{0.65}$, 27 °C, THF as solvent.

3. 2. 3. Synthesis of Chromophore Labeled Cholesterol-Bearing PNIPAMs

Typical procedure for preparation of singly labeled PNIPAMs incorporating compound 5a (Pymecho), compound 5b (Pybucho), and compound 5c (Npcho) is described as following: Triethylamine (0.5 mL) and compound 5a were added to a solution of the reactive copolymer (1.0 g, 8.85 mmol) in freshly dried THF (50 mL). The mixture was stirred for 3 days at room temperature in the dark and then quenched with *N*-isopropylamine (1 mL). The polymer was isolated by precipitation into anhydrous diethyl ether and reprecipitated from THF into diethyl ether. It was further purified by dialysis against methanol/water (9/1, v/v) for 3 days and water for 2 days using dialysis tubes with molecular weight cut-offs of either 6,000-8,000 or 12,000-14,000 Dalton. The polymer was finally isolated by freeze-drying. ^{1}H NMR and FTIR were used to confirm the chemical structures of the modified polymer. UV(methanol λ, nm): 342, 326, 312, 276, 264. All of the singly labeled polymers were prepared by the same procedure as described above. The components of each copolymer are listed in Table 3.2.

Table 3. 2. Recipes for Modification of Copolymers*

Copolymers	PNIPAM /NASI (mmol)	Cholesterol Fluorescence groups (mmol)	Solvent (THF, mL)
L-PNIPAM-Pymecho (20K-P_M88)**	1.7	0.087	15
L-PNIPAM-Pybucho (20K-P_B85)	8.85	0.178	50
L-PNIPAM-Npcho (20K-N45)	8.85	0.178	50
M2-PNIPAM-Pybucho3 (240K-P_B177)	17.6	0.176	60
M2-PNIPAM-Npcho (240K-N74)	8.8	0.044	50
M2-PNIPAM-Pybucho-Npcho (240K-P_B325-N72)	8.85	0.044(Npcho) 0.02 (Pybucho)	50
M-PNIPAM-Pymecho (400K-P_M225)	4.42	0.022	20
M-PNIPAM-Pybucho2 400K-P_B157	8.85	0.088	50
M-PNIPAM-Pybucho (400K-P_B439)	8.85	0.044	50

*All reactions were carried out at room temperature.
**20K: molecular weight of the polymer; 88: the number of NIPAM units per chromophore determined by UV; PM: Pymecho; PB: Pybucho; N: Npcho.

3. 2. 4. Molecular Weight of Copolymers The molecular weight of chromophore labeled cholesterol-bearing PNIPAM was evaluated from the viscosity of precursor PNIPAM, which were prepared by quenching the reactive polymer PNIPAM/NASI with *N*-isopropylamine. The measurement was carried out in THF at 27°C and the concentration of polymer is in the range of 20 g/L. Mark-Houwink-Sakurada equation[50] was used to calculate the viscosity average molecular weight of the polymers, M_v.

$[\eta] = 9.59 \times 10^{-3} M_v^{0.65}$

where $[\eta]$ is intrinsic viscosity of a polymer solution at the given solvent and temperature.

3. 2. 5. Fluorescence and Sample Preparation Fluorescence spectra were recorded on a SPEX Fluorolog 212 spectrometer equipped with a GRAM/32 dada system. The temperature of the water-jacketed cell holder was controlled with a Neslab circulating bath. The temperature of the sample fluid was measured with a thermocouple immersed in a water-filled cuvette placed in one of the four cell holders. Emission spectra were not corrected and excitation spectra were measured in the ratio mode. They were recorded with an excitation wavelength of 346 nm (pyrene) and 290 nm (naphthalene). Emission and excitation slit widths were set at 0.5 and 2.0 mm, respectively. Time-resolved fluorescence spectra were recorded in PTI LS-100 luminescence system. Lifetime of pyrene monomer emission and excimer emission were monitored at 395 nm and 474 nm, respectively. Concentration of polymer solution was 0.2 g/L. Solutions in water were not degassed. Solutions in methanol were degassed by vigorously bubbling methanol saturated argon for 1 min through the solutions. Samples for spectroscopic analysis were prepared from stock aqueous solutions of the polymers (0.5 to 5 g/L) and were kept at 5 ° C for at least 24 hrs to ensure complete dissolution. To obtain the desired concentrations, the stock solutions were further diluted by deionized water. These solutions were kept at room temperature for at least 2 hrs, except for the poly(*N*-isopropylacrylamide) bearing *N* α-[6-(3β-cholesteryl)urethane]-1-hexylurea-*L*-lysine-*N*-[1-(1-naphthyl)ethyl]amide

(240K-N74) solution, which was kept at room temperature at least 1 day before measurements.

3. 2. 6. LCST Determination. The lower critical solution temperatures (LCST) of the polymers were determined using UV spectrophotometer. The changes in the turbidity of the solutions were recorded as a function of temperature. The samples were heated at a constant rate of 0.3°C/min in a magnetically stirred UV cell in the temperature range of 20 to 50 °C. The turbidity of the solutions was monitored at 500 nm. The solution concentration ranged from 0.5 to 1.0 g/L.

3. 2. 7. Determination of Chromophore Content by UV Absorbance. Compound 5a, 5b, 5c were used as model compounds to calculate pyrene and naphthalene content in the polymers, and their molar extinction coefficients (ε) in methanol were 4497 for compound 5a at 342 nm, 8557 for compound 5b at 342 nm, and 3379 for compound 5c at 290 nm, respectively. The absorbance of the polymers in dilute methanol solution was measured at 342 nm. Beer's Law ($A = \varepsilon L C$) was applied to calculate the chromophore concentration in the solutions, the chromophore content in the polymers can be evaluated from the chromophore concentration in the solutions and is listed in Table 3.3.

3. 2. 8. Dynamic Light Scattering DLS measurements were conducted with a Brookhaven Instrument Corp. Model BI-9000AT digital correlator equipped with a Lexel Laser ($\lambda = 514$ nm) with the scattering angle at 90°. The temperature was set at 25 °C. The sample concentration ranged from 2.5 to 0.1 g/L. The solutions were clarified

by filtering through Millipore Membrane with 0.45 μm pore size. The CONTI program was used to calculate a mean diameter.

3. 3. Results and Discussion

3. 3. 1. Synthesis and Characterization Cholesterol-bearing PNIPAMs (Scheme 3.1) were prepared by post-modification of reactive copolymer PNIPAM/NASI to ensure the hydrophobic groups to be randomly distributed along the polymer backbone.[51]

Scheme 3. 1. Synthesis scheme of cholesterol bearing poly(*N*-isopropylacrylamide)

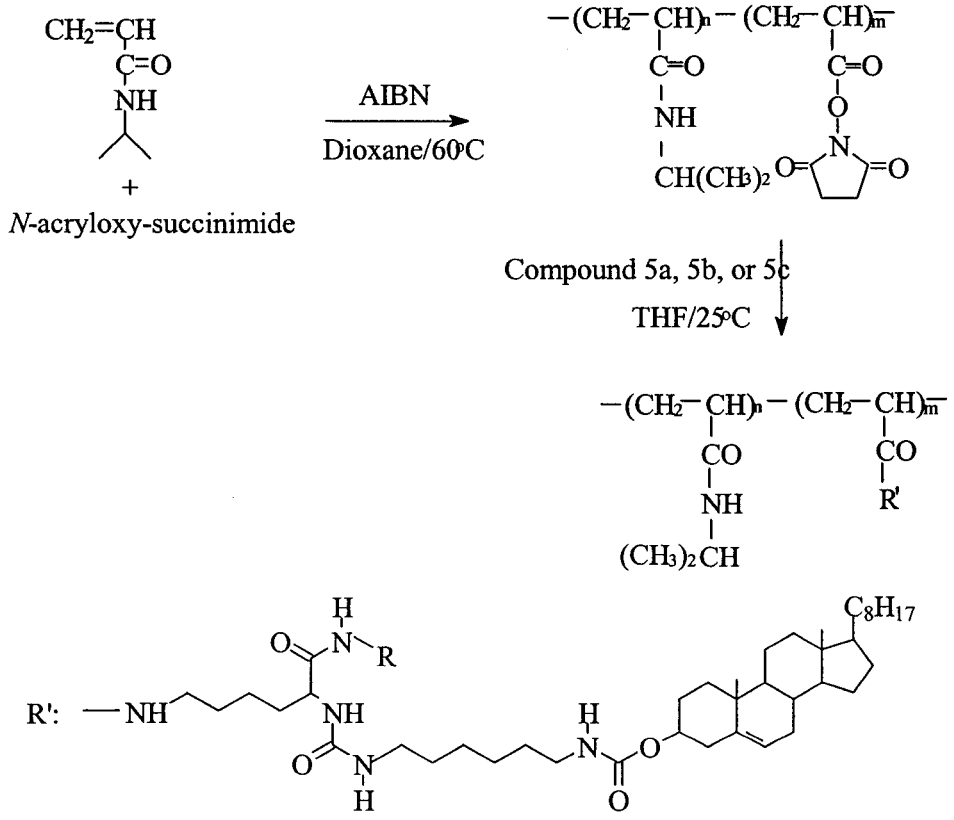

R: varied from pyrenylmethyl (5a), pyrenylbutyl (5b) to naphthalyene (5c).

The chemical structure of copolymers was investigated by FTIR and ^{1}H NMR. The proton signals of pyrene and cholesteryl groups could be observed at a high degree of substitution (Figure 3.1). The molecular weight of the copolymers was estimated by measuring the corresponding viscosity of reactive polymer after being quenched with isopropylamine. The viscosity average molecular weight of copolymer was 20,000 for L-PNIPAM, 240,000 for M-PNIPAM and 400,000 for M2-PNIPAM, respectively. Pyrene content was determined by UV as listed in Table 3. 3.

Figure 3. 1. ^{1}H NMR spectrum of cholesterol bearing poly(*N*-isopropylacrylamide) in $CDCl_3$.

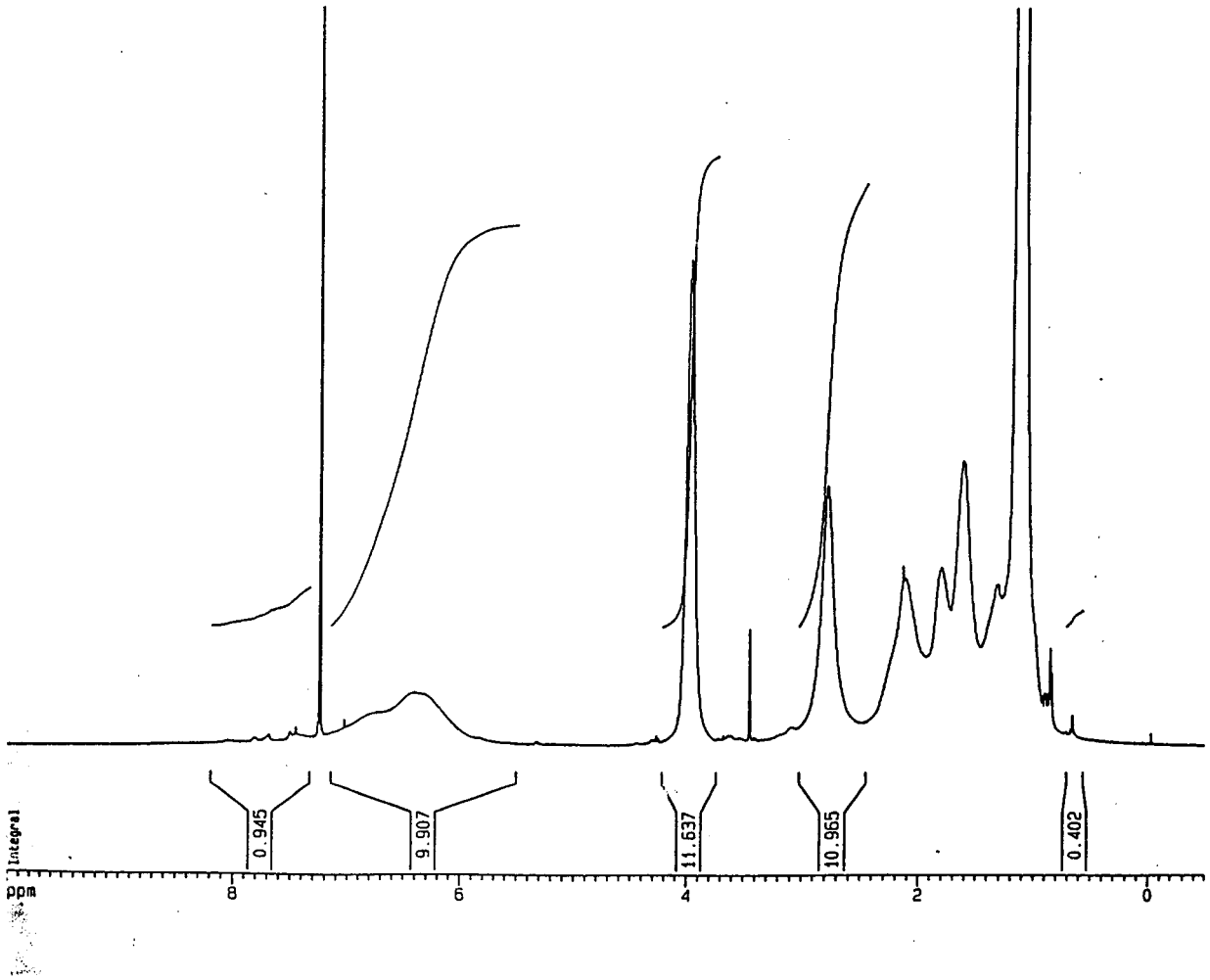

Table 3. 3. Label Contents of Copolymers

Copolymer	MW_v (Dalton)	Label content (mol/g)	Number of NIPAM units per chromophore		
			NIPAM/ Py-Me	NIPAM/ Py-Bu	NIPAM/ Np
L-PNIPAM	20,000	-	-	-	-
20K-P_M88 *	20,000	1.00×10^{-4}	88	-	-
20K-P_B85	20,000	1.33×10^{-4}	-	85	-
20K-N45	20,000	2.57×10^{-4}	-	-	45
M-PNIPAM	240,000	-	-	-	-
240K-P_B177	240,000	5.00×10^{-5}	-	177	-
240K-N74	240,000	1.19×10^{-4}	-	-	74
240K-P_B325-N72	240,000	1.23×10^{-4} (Np) 2.72×10^{-5} (Py)	-	325	72
M2-PNIPAM	400,000	-	-	-	-
400K-P_B439	400,000	2.01×10^{-5}	-	439	-
400K-P_B157	400,000	5.63×10^{-5}	-	157	-
400K-P_M225	400,000	3.93×10^{-5}	225	-	-

* code listed in Table 3.2.

3. 3. 2. Solution Properties

3. 3. 2. 1. Lower Critical Solution Temperature (LCST) The cholesterol-modified PNIPAM was soluble in water below the LCST, but its aqueous solution became turbid above its LCST. The LCST values of the polymers are listed in the Table 3.4. They are close to 31.5 °C and slightly lower than that of unmodified PNIPAM (32.5°C) as expected.[52] Exception was cholesterol-bearing poly(*N*-isopropylacrylamide) with low molecular weight (e.g. 20K-P_M88), which exhibited a much higher LCST (36°C) than that of modified PNIPAM with higher molecular weight (31.5°C), but the LCST is still lower than that of unlabeled polymer with the same molecular weight (L-PNIPAM, 37.5 °C). Microcalorimetric results for the PNIPAM samples were examined and each of polymers yielded well-defined endothermic peak at the LCST, which will be discussed in chapter 5.

Table 3. 4. LCST of Polymers

Polymers	LCST (°C)
L-PNIPAM	37.5
20K-P_M88	36.0
20K-N45	36.0
20K-P_B85	36.0
M-PNIPAM	32.5
240K-P_B177	31.5
240K-N74	31.5
240K-N72-P_B 325	31.5
M2-PNIPAM	32.5
400K-P_B439	31.5
400K-P_B157	31.5
400K-P_M225	31.5

3. 3. 2. 2. Micellar Aggregation The cholesterol-modified polymers can form polymeric aggregates or micelles in aqueous solutions as detected by DLS. The diameters of the micelles were determined by a cumulate analysis of the data as listed in Table 3.5.

Table 3.5. Mean Diameter of Polymeric Aggregations in Aqueous Solutions

Polymers	Mean Diameter[53] (± 5 nm)	Polydispersity
240K-P_B177 2.5 g/L 1.0 g/L 0.5 g/L	 60 64 61	 0.26 ± 0.06 0.26 ±0.07 0.25 ± 0.03
240K-N74, 0.57 g/L	122	0.15 ± 0.1
240K-P_B325-N72, 0.5 g/L	91	0.30 ± 0.10
400K-P_M225, 2.5 g/L	46	0.24 ± 0.06
20K-P_M88, 0.3g/L	126	0.26 ± 0.11

The attractive force among polymeric chains was induced by hydrophobic interaction of cholesterol and aromatic substituents in aqueous solutions. The substitution degree of the polymers can influence the size of polymer aggregates formed in water, that is larger aggregates were formed by the polymers with a higher hydrophobic substitution content. For instance, the mean of aggregates from 240K-N74 was measured as diameter of 122 nm. The polymer architecture and type of hydrophobic groups also affected the aggregate size and behavior. The compound 5a, 400K-P_M225 which was modified by poly(*N*-isopropylacrylamide) with higher molecular weight 400,000 and average 225 NIPAM units per pyrene, can generate the smallest aggregate among all the polymers. However, compound, 20K-P_M88 was modified with low molecular weight 20,000 and average 88 NIPAM units per pyrene can only form larger micellar aggregates. The polymer carried only two cholesteryl fluorescent groups per polymeric chain averagely, which were distributed randomly along the polymeric backbone and acted as if they were the hydrophobic heads of surfactants. It can be expected that the hydrophobic groups will consist of a core of the multimolecular aggregates with the polymeric chains as the shell. The size of aggregates may be controlled by interor or intramolecular association and fluorescence experiments will be further conducted to confirm this hypothesis. Nevertheless, no aggregates were observed in the methanol solution of the polymers.

3. 3. 2. 3. Static and time-resolved fluorescence spectra

Fluorescence spectra The emission spectra of the solutions with the pyrene labeled cholesterol-bearing PNIPAM were measured at 25°C in both water and methanol. In

general, all emission spectra exhibited a large pyrene monomer emission ranged from 360 to 460 nm and a smaller pyrene excimer emission can be found at 475 nm as evidenced by the band shift of excimer and monomer in excitation spectra with excitation at 346 nm in aqueous solution (Figure 3.3).

Figure 3. 2. Fluorescence emission spectra of 240K-P_B177 (Polymer concentration: (0.05 g/L); λ_{ext} = 346 nm in water; λ_{ext} = 342 nm in methanol; 25 °C).

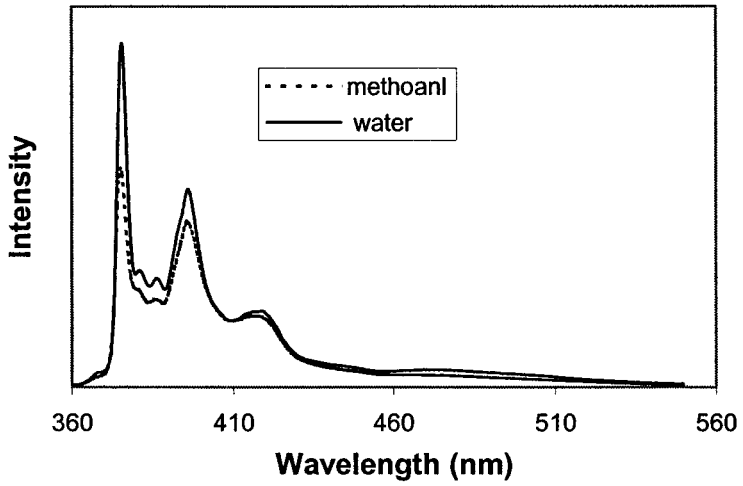

The excitation spectra were monitored at 392 nm for the monomer emission and 474 nm for excimer emission (Figure 3.3). From excitation spectra, we can determine the formation mechanism of pyrene excimer. In the dynamic mechanism, spectra monitored at the monomer and excimer emission wavelengths will be superimposable, indicating they originated from the same excited species. In the static case, the spectra will not be superimposible. The spectra monitored at excimer emission wavelength will be red-shifted by 1 to 4 nm and the bands will be broadened when compared with that of the monomer emission. The results indicate the pyrene moieties from two different absorbing species that is, preassociated pyrene and isolated pyrene with excited status [11b]. Although the general features of the excitation spectra were similar, the monomer

excitation spectra were slightly blue-shifted in water when compared with the excimer excitation spectra (Table 3.6). The bands monitored for the excimer were broader, as indicated by the peak-to-valley ratios of monomer (P_M) and excimer (P_E) in the excitation spectrum (Figure 3.3). Since P_E is smaller than P_M in all cases as listed in Table 3.6, pyrene can be preassociated in the solutions.

Table 3. 6. Photophysical Parameters of Cholesterol-bearing PNIPAM

Parameters	400K-P_B439		240K-P_B177		400K- P_M225		20K-P_M88	
	H_2O 0.1 (g/L)	MeOH 1.0 (g/L)	H_2O 0.5 (g/L)	MeOH 0.47 (g/L)	H_2O 0.5 (g/L)	MeOH 0.5 (g/L)	H_2O 0.57 (g/L)	MeOH 0.5 (g/L)
I_E/I_M	0.048	0.049	0.048	0.05	0.11	0.09	0.21	0.13
λ_E, nm	474	474	474	474	474	474	471	474
P_M	2.2	2.2	2.0	2.2	2.2	2.5	2.2	2.2
P_E	1.9	1.8	1.7	1.9	1.6	1.8	1.8	1.6
$\Delta\lambda$*, nm	0.5	0	0.5	0	1.5	1.0	1.5	1.0
P_A**	1.7	1.5	1.6	1.7	1.6	2.4	1.2	1.7

*$\Delta\lambda = \lambda P_E - \lambda P_M$

** Peak to valley ratio for the (0, 0) transition in absorption.

Figure 3. 3. Fluorescence excitation spectra of 240K-P_B177 in water and methanol (0.05 g/L, 25°C).

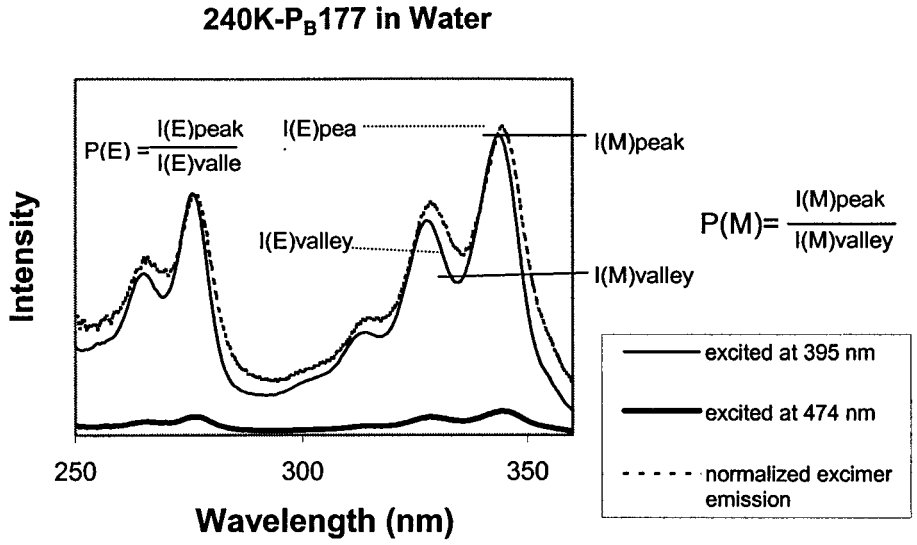

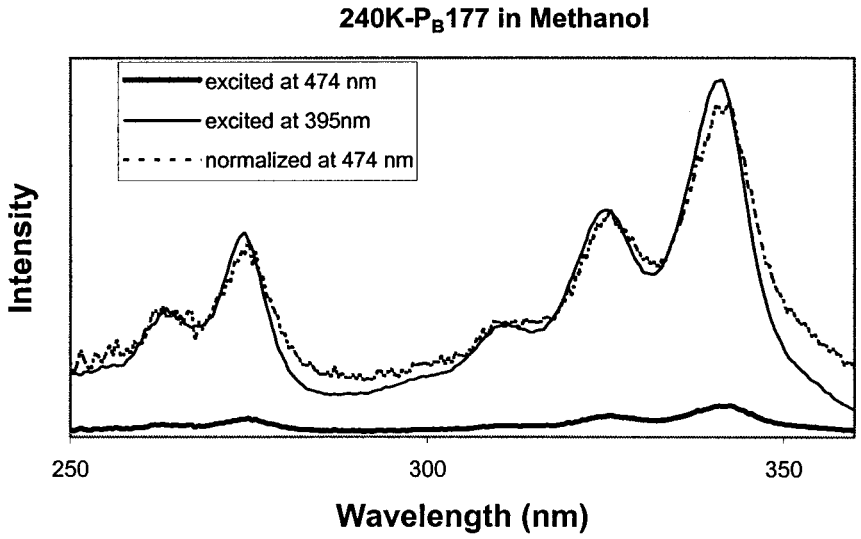

Effect of Concentration on Spectra Fluorescence properties of hydrophobically modified polymers in water provide an alternative evidence for polymer micellar aggregates. Usually, a critical aggregation concentration can be determined by Fluorescence. Spectra of the pyrene labeled cholesterol-bearing PNIPAM in aqueous solutions were investigated over a polymer concentration range as wide as possible. The solution with a lowest concentration should still give a spectrum with good signal and noise ratio, and the solution with a highest concentration should still be optically clear. In polymer solutions, the interpolymeric association occurs when pyrene excimer intensity increases as polymer concentration increases. The ratio of excimer emission intensity (I_E at 480 nm) to monomer emission intensity (I_M at 375 nm) was monitored in the pyrene labeled cholesterol-bearing PNIPAM. In all cases, the fluorescent spectra demonstrated similar features in aqueous and methanol solutions, i.e., a large monomer emission and smaller excimer emission (Figure 3.4). In the case of 400K-P_M225, the value of I_E/I_M was between 0.090 and 0.120 (± 0.005). The value of I_E/I_M was constant for the polymer concentration ranging from 10^{-3} to 2.12 g/L. The I_E/I_M value of 240K-P_B177 has no significant change from 0.051 to 0.071 (± 0.006) with the polymer concentration ranging from 0.05 to 5.63 g/L. The I_E/I_M value of 400K-P_B439 was slightly lower in aqueous solutions and showed the same trend as the polymer concentration increased. In the case of a high degree of the hydrophobic substituents 20K-P_M88, the I_E/I_M value increased from 0.160 to 0.210 (± 0.007) in the polymer concentration range from 5×10^{-5} to 0.54 g/L.

Figure 3. 4. Ratio of pyrene excimer emission to pyrene monomer emission (I_E/I_M) in polymer aqueous solutions as a function of polymer concentration (25°C, λ_{ext} = 346 nm).

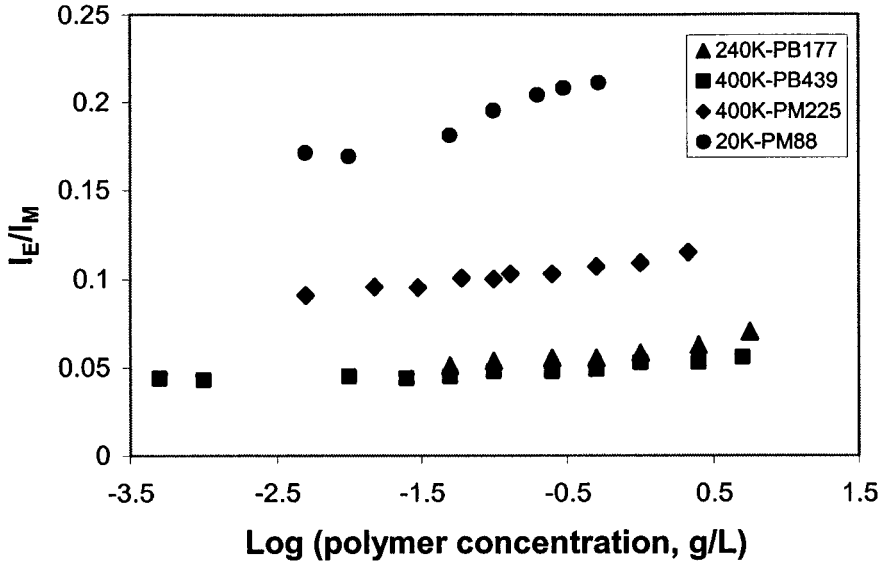

The ratio of I_E/I_M in all cases, except 20K-P_M88, was insensitive to the changes of polymer concentration, suggesting the hydrophobic aggregation formed at a low polymer concentration depends on the degree of substitution and is insensitive to concentration. In the solution of 20K-P_M88, it showed an inflection point for interpolymeric aggregation as the polymer concentration increased.

Figure 3. 5. Ratio of I_E/I_M in 240K-P_B177 methanol solutions as a function of polymer concentration (25°C, λ_{ext} = 342 nm).

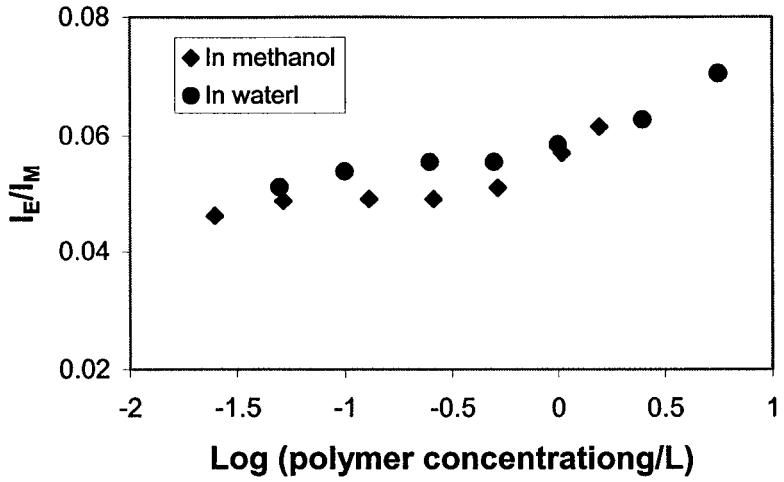

The fluorescence spectra of 240K-P_B177 in methanol were also studied as a function of concentration. The value of I_E/I_M was in the same range (from 0.045 to 0.070 ± 0.007) as that in the aqueous solutions and did not significantly change with concentration (Figure 3. 5), indicating pyrene moieties were not in close contact in both water and methanol.

Effect of Temperature on Spectra Aqueous solutions of the pyrene labeled cholesterol-bearing PNIPAM were heated from 20 to 65°C (Figure 3. 6). The pyrene fluorescence spectra underwent remarkable changes as the solution temperature reached the LCST. The pyrene monomer emission increased at the expense of the pyrene excimer emission. The overall fluorescence intensity remained approximately constant. I_E/I_M did not significantly increase as the temperature increased from 20 to 28 °C for either

compound 5a or compound 5b modified PNIPAM, then decreased rapidly with increasing temperature and reached a plateau above the LCST. The change of I_E/I_M with temperature depended on the actual LCST value. The lower the LCST of the polymer solutions, the higher the slopes of the I_E/I_M curve. Therefore, the aggregation of hydrophobic pyrene groups was disrupted near or/and above LCST.

Figure 3. 6. Ratio of I_E/I_M for pyrene in polymer aqueous solutions as a function of temperature (0.05 g/L, λ_{ext} = 346 nm).

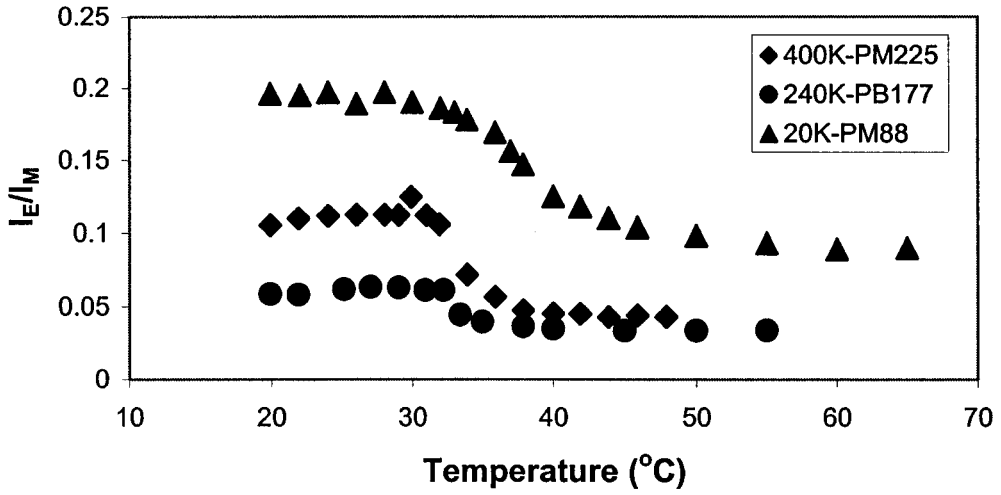

Micropolarity In order to detect the polarity and rigidity of the hydrophobic microdomains in aqueous solutions, the ratio of I_1/I_3 defined as the intensity of the (0, 0)[54] band (I_1) to that of the (0, 2) band (I_3) in the fluorescence monomer emission was measured. Because pyrene monomer emission is sensitive to the changes in its environments,[55] the solvent interaction can perturb the relative intensities of the weak electronic transitions from the forbidden vibration of fine structures in the pyrene fluorescence spectra.[56] Consequently, a mixed polarization can be observed due to the vibration coupling between the first (S_1) and second (S_2) singlet excited states.

Therefore, the ratio of I1/I3 can be used to evaluate micellar structures in an aqueous solution. It is clear that the ratios of I1/I3 have a higher value in polar media and a low one in less polar media. A low value of I1/I3 for pyrene probe entrapped in surfactant micelles was observed, for instance, 1.14 for sodium dodecyl sulfate (SDS) and 1.3 for cetyltrimethylammonium bromide (CAB). [14] However, pyrene probe gives a high ratio of I_1/I_3 as1.80 in water.[53a] There is a controversy about I_1/I_3 of pyrene label as polarity indicator of its microenvironment same as pyrene probe. It is certain that the value of I_1/I_3 for pyrene label will not be the same as that of pyrene probe, but it may reflect the trend of polarity change. Studies have shown that pyrenylmethyl label (not pyrenylbutyl) still exist polarity sensitivity of pyrene probe since a ratio I_1/I_3 of pyrenylmethyl labeled PNIPAM was 1.72 but a ratio I_1/I_3 of 20K-P_M88, pyrenylmethyl cholesterol labeled PNIPAM, was 1.38(± 0.03) in the absence of a surfactant and 1.22 (± 0.01) in the presence of SDS (16 mM). In the aqueous solutions of 400K-P_M225 with amphiphilic characteristics, the I_1/I_3 ratio of pyrenylmethyl was 1.45 (± 0.03) and kept almost unchanged as a function of polymer concentration (Figure 3.7).

Figure 3.7. Ratio of I_1/I_3 for pyrene in PNIPAM-Pymecho aqueous solution as a function of polymer concentration (25°C, λ_{ext} = 346 nm).

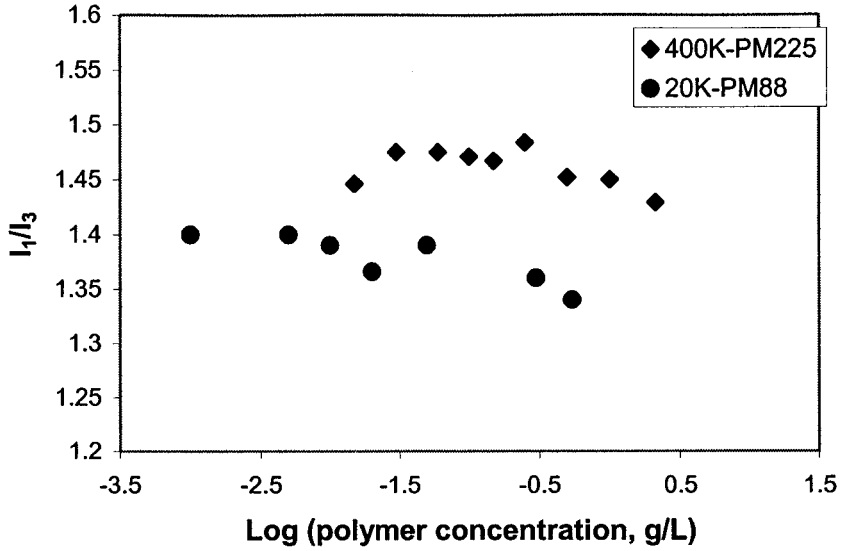

This value was lower than that of pyrene in PNIPAM solution, suggesting pyrene moieties were incorporated into hydrophobic microdomains and the increasing of polymer concentration has no effect on the polarity of hydrophobic microdomains. However, value of I_1/I_3 decreased slightly with increasing temperature (Figure 3.8), particularly in the case of 20K-P_M88. It means that pyrene moieties were inserted into the hydrophobic microdomains, but the polarity of pyrene microdomains reduced when the polymer chains collapsed above LCST.

Figure 3. 8. Ratio of I_1/I_3 for pyrene in polymer aqueous solution as a function of temperature (0.05 g/L. λ_{ext} = 346 nm).

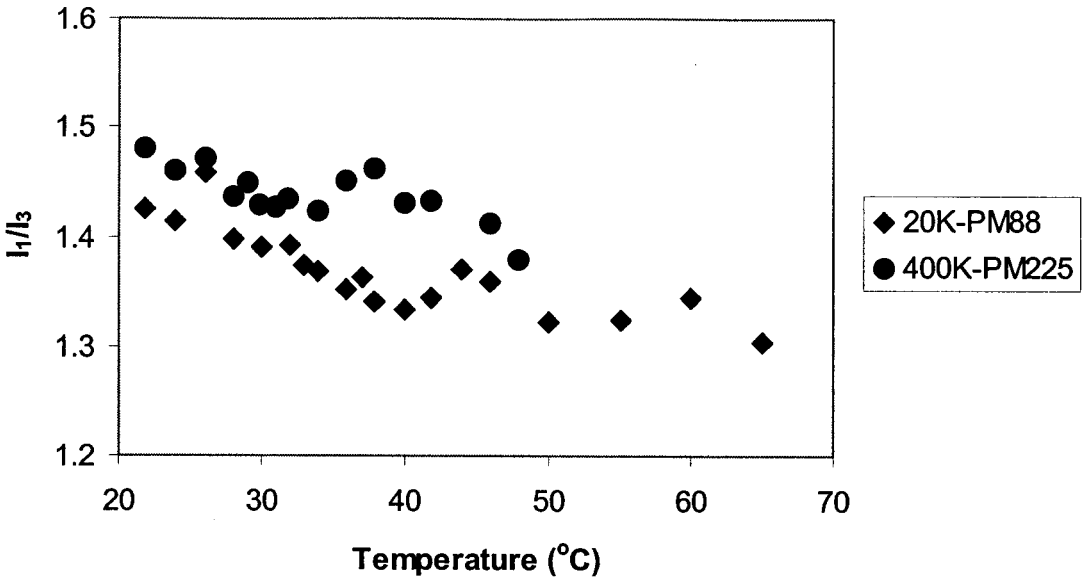

On the other hand, the polarity of microenvironments of pyrene labels is also reflected in the fluorescence lifetime. Time-resolved spectra of the polymer solutions were measured in water and the fluorescence decay profiles were monitored at 395 nm for pyrene monomer and 485 nm for pyrene excimer, respectively. Fluorescence decays of the pyrene-labeled polymers were best fitted to a double-exponential function. The values of the preexponential factors a_i and the lifetimes τ_i are listed in Table 3.7 together with the average lifetime $<\tau>$, defined by

$$<\tau> = \sum a_i \ \tau_i^2 / \sum a_i \ \tau i$$

A good agreement between the experimental decay curves and the double exponential function was achieved in all cases ($0.92 < \chi^2 < 1.29$).

Table 3. 7. Fluorescence Decay Parameters of Copolymers in Water at 25.0 ± 0.3°C

Polymer	Lifetime τ (ns) for pyrene excimer at 474 nm*, χ^2, average <τ>	Lifetime τ (ns) monomer emission at 395 nm for Py*, χ^2, average <τ>
20K-P_M88	0-250 ns 28.89 (0.36) 85.5 (0.64) 1.05 <τ> = 76.6 0-100 ns 11.07 (0.38) 66.38 (0.62) 0.93 <τ> = 61.2	149.4 (0.55) 24.28 (0.45) 1.05 <τ> = 134.6
400K-P_M225	-	23.53 (0.38), 169.6 (0.62) 1.12 <τ> = 158.4
240K-P_B177	-	145.8 (0.71), 40.73 (0.29) 1.053 <τ> = 135.0
240K-N72-P_B325	-	Py: direct 88.0 (0.48), 276.3 (0.52), <τ> = 226.2 χ^2 = 1.14 Py: NRET 96.8 (0.54), 276.3 (0.46) <τ> = 223.5 χ^2 = 1.12

*pyrene excitation at 346 nm.

The fact that the fluorescence decay profiles are not single exponentials indicates some degree of heterogeneity exists in the hydrophobic microdomains. There were two states of pyrene labels with respect to the extent of the incorporation of each label into a hydrophobic microdomains, i.e., incorporated and nonincorporated or only partially incorporated. The former may be responsible for the slower decay and the latter for the

faster one. These data agree with previous reports[57] on the copolymers of octadecane-bearing PNIPAM (PNIPAM-C18Py/200). There were two lifetimes of pyrenylmethylamine in the copolymer PAMS/CholMa/Py with up to 5% mol of cholesterol substituents.[15] One is much longer (346 ns), which suggests that a fraction of the pyrene labels is incorporated in hydrophobic microdomains formed by cholesteryl groups. The other fraction of pyrene is outside of the cholesteryl group microdomains. In our case, we did not observe such longer lifetimes for pyrene, which may be due to low degree of hydrophobic substitution (0.02-1.1% mol) or to the mobility of pyrene label being constrained by its linking group.

Meanwhile, the lifetime of pyrene excimer exhibited also two distributions as that of pyrene monomer and it was further measured in a short scale (0-100 ns). However, the growth of excimer emission cannot be observed, therefore the pyrene excimer was formed from preassociation. The observed phenomenon in this study is in agreement with the conclusion obtained from excitation and absorption spectra.

3. 3. 2. 4. Nonradiative Energy Transfer The study of DLS suggested that polymeric aggregations can be formed in aqueous solutions of the cholesterol-modified PNIPAM. However, the formation of micelles cannot enhance the pyrene excimer emission as anticipated. It is unclear why pyrene moieties cannot be close enough to each other (5Å) to form excimer in the hydrophobic microdomains as pyrene labeled PNIPAM-C18 and how far the chromophore groups could be separated as well as the micellar structures are unimolecular or multimolecular. To clarify these questions, NRET between two chromophores was carried out. The photophysical process of NRET originates in dipole-

dipole interactions between an energy donor in its excited state and an energy acceptor in its ground state.[10] The probability of energy transfer between two chromophores depends to a larger extent on their separation distance and to a less extent on their relative orientation. The pyrene-naphthalene pair of chromophores is well known to interact as energy donor (naphthalene) and energy acceptor (pyrene) by NRET with a characteristic distance, 29 Å.[58] Therefore, the extent of energy transfer between the two labels can be related to the extent of interpolymeric association in the mixed solutions of polymers carried either donor or acceptor chromophore.

The structure of labeled polymers had to be specifically designed to probe the composition of hydrophobic microdomains. It was critical to attach the chromophore in close spatial proximity to a hydrophobic substitutent. The design was also guided by other factors such as the spectral characteristics of the donor and acceptor as well as the amount of label incorporation. Based on the previous experience with octadecane-modified PNIPAM, we synthesized the naphthalene labeled polymer that has the spatial arrangement of naphthalene and cholesterol as pyrene labeled cholesterol-bearing polymers shown in Scheme 3.1. The difference of copolymers 240K-N74 and 240K-P_B177 is only in the chemical structure of the fluorescent labels.

The spectrum observed from the mixed stock aqueous solution of 240K-N74/240K-P_B177 upon excitation at 290 nm is displayed in Figure 3. 9, together with emission spectra of 240K-P_B177 and 240K-N74 recorded under the identical conditions. A weak monomer emission from isolated excited naphthalene (ranging from 300 to 400 nm) and a relatively strong monomer emission from isolated excited pyrene (360 to 450 nm) indicate that energy transfer between naphthalene and pyrene occurred. The extent

of energy transfer was estimated by the ratio of the intensity of the pyrene emission at 395 nm (I_{Py}) to the intensity of the naphthalene emission (I_{Np}) at 340 nm (I_{Py}/I_{Np} =1.9). Suggesting the intermolecular association existed in the solution of cholesterol-bearing PNIPAM with a molecular weight of 240,000. The fact that the ratio of I_E/I_M is insensitive to the change of polymer concentration may reflect the limitation of the excimer method.

Figure 3. 9. Fluorescence spectra of mixed singly labeled PNIPAM in water (25°C, λ_{ext} = 290 nm).

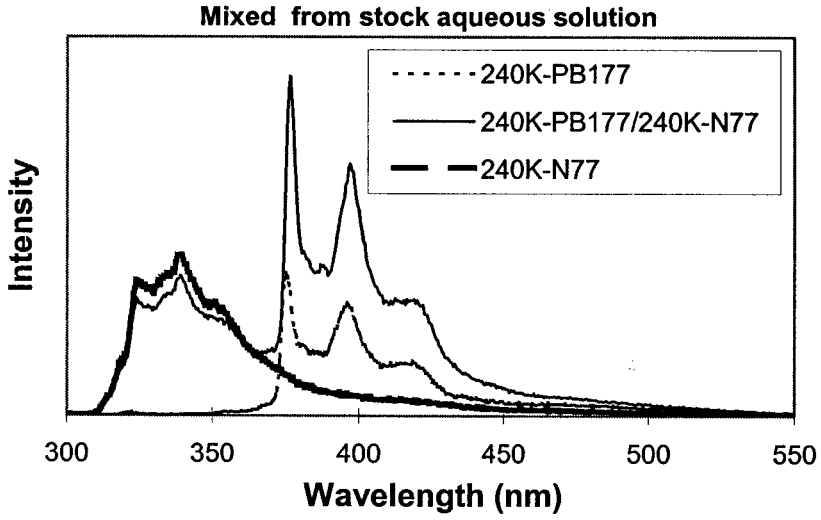

Table 3. 8. Np/Py Concentration Ratio Effect on NRET

Polymer solution	C_{Np}/C_{Py} Molar concentration ratio of Np/Py	I_{Py}/I_{Np} ($\leq \pm 0.1$) 25°C	35°C
PN/240K-P_B177 from stock solutions	1	3.4	3.8
	2.7	1.9	2.1
	4.5	1.1	1.6

Emission of pyrene excited at 346 nm should not be perturbed by the presence of naphthalene from the photophysical point of view since naphthalene is transparent at this wavelength. However, the pyrene emission was affected in mixed stock solutions. I_E/I_M decreased significantly as compared with a solution of 240K-P_B177 (400K-P_B439, 240K-P_B157) with the same chromophore concentration in the absence of 240K-N74, which indicated a local concentration of pyrene groups in the hydrophobic core of the polymeric micelles decreased.

Most pyrene molecules of the cholesterol-bearing polymers cannot move closely enough to form excimer as pyrene concentration increased, however, a large pyrene excimer emission was observed when pyrene linked next to octadecane, then incorporated into PNIPAM.[6a, 4a, 59] In case the polymer incorporated pyrene with 3.74×10^{-4} mol/g, I_E/I_M could be as high as 1.5[6a]. When pyrene and cholesterol were separately attached to PNIPAM, I_E/I_M was dropped to 0.18 while the polymer incorporated pyrene with 5.5×10^{-5} mol/g.[60] The ratio of I_E/I_M is still much higher than that of pyrene and cholesterol linked together, then incorporated into PNIPAM with the same magnitude of pyrene content (400K-P_M225, 240K-P_B157, and 240K-P_B177). The results could be attributed to two factors which limited pyrene excimer formation: (1) the existing of bulky cholesteryl group may shield pyrene moieties from each other and prevent them forming dimers, (2) the linkage of pyrene to the bulky cholesterol may limit pyrene mobility. The extent of NRET from two singly labeled cholesterol bearing PNIPAM (I_{Py}/I_{Np} = 1.9) is slight higher than that of octadecane bearing PNIAPM (I_{Py}/I_{Np} = 1.1),[52] which shows that interpolymeric association of cholesterol bearing PNIPAM is not weak although no large excimer emission was observed. A pyrene excimer can form only if

two molecules of the chromophore are in close enough proximity (< 5 Å) during the lifetime of excited pyrene[11a] and NRET between pyrene and naphthalene occurred in the 29 Å range. The pyrene and naphthalene groups were in close enough proximity to satisfy the NRET requirements for mixed aqueous solution. Hence, it can be concluded that the distance between two chromophores is larger than 5 Å and less than 29 Å (assuming efficiency of energy transfer is higher than 50%) in aqueous solutions.

3. 4. Conclusion

PNIPAM bearing cholesteryl fluorescent groups was prepared by post-modification of reactive copolymers. These copolymers exhibited a low critical solution temperature and formed micellar aggregates in aqueous solutions. The sizes of micellar aggregates ranged from 46 to 120 nm, depending on the degree of hydrophobic substitutents and the polymer architecture. The hydrophobic cholesteryl and pyrene groups formed the core of the micellar aggregates and were shelled by amphiphilic polymeric chains, but pyrene and cholesteryl moiety could be separated in the hydrophobic microdomain, as evidenced by fluorescence decay. Intermolecular association of the polymers in aqueous solutions was weak. The distance between the two chromophores in the micelles was larger than 5 Å and less than 29 Å in aqueous solutions.

Chapter 4

Competition of Inter and Intrapolymeric Associations of Amphiphilic Polymer Bearing Cholesteryl and Fluorophore Groups

Abstract

Poly (*N*-isopropylacrylamide) bearing cholesteryl and fluorophore groups can form micellar aggregates in water by inter and intrapolymeric associations. The competition of inter and intrapolymeric associations of the copolymers in aqueous solutions was investigated by nonradiative energy transfer (NRET). The results indicate that the associations depend on the polymer architecture, methods of sample preparation and thermal history of prepared samples. The intrapolymeric association of copolymers with the viscosity molecular weight of 240,000 (e.g. 240K-P_B177) played a key role when temperature of copolymer solutions was below the low critical solution temperature (LCST), as estimated by NRET. However, the interpolymeric association of the coplymers became dominant while the temperature of solutions was above the LCST. The interpolymeric association was much stronger while the copolymer aqueous solutions were prepared from stock THF solution than that in copolymer aqueous solutions prepared either from the mixed stock aqueous solutions or codissolution of the two types of the polymers (240K-P_B177 and 240K-N74) into water. We found that the intrapolymeric association was extremely strong and the interpolymeric association was weak in the solution of polymer with relatively high molecular weight (400K-P_M225, M_v = 400,000). In contrast, the intrapolymeric association was weak and the interpolymeric association was extremely strong in the solutions of polymer with low molecular weight (20K-PM88, M_v = 20,000).

4. 1. Introduction

Many efforts have been involved to develop hydrophobically modified poly(*N*-isoproylacrylamide) (HM-PNIPAM) as the drug delivery systems with unique properties and special applications.[43] It had been found that the liposomes can be modified by water-soluble polymers with hydrophobic domains and this promising strategy offers a new method to develop highly efficient drug delivery systems with the characteristics of extended circulation time and fast response to external stimuli. Usually, this kind of a water-soluble polymers modified by hydrophobic domains contains water-soluble backbone and a small number of hydrophobic alkyl side chains acting as anchors into the lipid bilayers. The performance of polymer-modified liposomes as drug delivery systems depends on the affinity of anchoring groups to the lipid bilayers.[6b]

Thermally sensitive liposomes prepared by octadecane-bearing PNIPAM coated liposomes were extensively studied in the past decade.[4a, 82] The polymers interacted with liposomes via octadecyl anchors and remained on the surfaces of liposomes during the thermally-induced collapse of the PNIPAM chains when the polymers contained high degree of hydrophobic substitutents. Polozova and Winnik[6b] found that the octadecane substituted polymer chains bound to the fluid bilayers were in dynamic exchange with unbound polymers, which caused a majority of liposomes to lose the coated polymers and become unprotected. One of the approaches to overcome this problem is to use an anchor with a higher affinity for lipid bilayers compared with the octadecyl group.

Cholesterol-bearing polysaccharide coated liposomes have shown that cholesterol had a higher affinity for lipid bilayers than O-palmitoyl groups, especially, in a low incorporation level of hydrophobic substituents in each polymeric chain.[61] In this

dissertation cholesterol was chosen as hydrophobic group and a new family of anchors has been successfully prepared and were attached to amphiphilic PNIPAM as described in the Chapter 2 and the solution properties of the copolymers were investigated as discussed in the Chapter 3. Because only a few cholesterols as a hydrophobic group incorporated in water-soluble polymers has been studied[62] and the behaviors of modified polymers were still unclear, further experiments should be carried out on this field. A doubly labeled copolymer bearing both pyrene cholesteryl group and naphthalene cholesteryl group was prepared for this purpose. We used NRET to investigate the competition of inter and intrapolymeric associations of PNIPAM bearing the cholesteryl and fluorophore groups in aqueous solutions. The effects of methods of sample preparation, thermal history, and polymer molecular weight on the polymer associations had been also studied. The results were compared with octadecane-substituted PNIPAM (PNIPAM-C18Py). The fluorescence spectrum of PNIPAM-C18Py in water was characterized by a very large pyrene excimer emission and the ratio of excimer emission intensity to monomer emission intensity (I_E/I_M). The pyrene groups remained in close proximity in the hydrophobic microdomains, as confirmed by the strong contribution of excimer emission to the overall pyrene fluorescence. The energy transfer occurred in both aqueous and methanol solutions for doubly labeled octadecane-substituted PNIPAM (PNIPAM-C18Np/360-C18Py/2000)[63] with a high concentration ratio of naphthalene to pyrene ([Np]:[Py] = 5.6),. However, NRET was observed only in water, but not in methanol for doubly labeled PNIPAM-C18Np/600-C18Py/1700 with a low chromophore concentration ratio (Np]: [Py] = 2.5). Although, the exchange of the polymeric chains among individual polymeric micelles was slow below the LCST in the mixtures of the

singly labeled PNIPAM-C18Py and PNIPAM-C18Np, the efficient and rapid intermixing of the polymeric chains occurred above the LCST.[64]

4. 2. Experimental

4. 2. 1 Materials *N*-isopropylacrylamide (Acros) was recrystallized twice from toluene/hexane (1/1, v/v). Azobisisobutyronitrile (AIBN, Spectrum) was recrystallized from methanol. *N*-acryloxysuccinimide (NASI, Acros) and *N*-isopropylamine (Aldrich) was used without further purification. The solvents were used as received unless stated otherwise.

4. 2. 2. Instrumentation UV-spectra were measured with a Hewlett Packard 8452A photodiode array spectrometer equipped with a Hewlett-Packard 89090A temperature controller. Steady-state fluorescent spectra were recorded on a SPEX fluorolog 212 spectrometer operated by a GRAM/32 data system. Temperature control of the samples was achieved by using a water-jacketed cell holder connected to a Neslab circulating bath. The temperature of the sample fluid was measured with a thermocouple immersed in a water-filled cuvette placed in one of the four cell holders. Emission spectra without correction were recorded with an excitation wavelength of 346 nm (pyrene) and 290 nm (naphthalene). The slit widths of emission and excitation were set at 0.5 and 2.0 mm, respectively. Time-resolved fluorescence spectra were recorded by PTI LS-100 luminescence system.

4. 2. 3. Preparation of doubly Labeled Cholesterol-bearing PNIPAM The reactive copolymer (PNIPAM/NASI, 1.0 g, 8.8 mmol) was dissolved in 50 mL of freshly distilled tetrahydrofuran (THF). Triethylamine and compound 5b were added to the above solution. The mixture was stirred for 1 day at room temperature under dark, then compound 5c was added into the above mixture and stirred for another 2 days. The mixture was quenched with 1mL of *N*-isopropylamine. The purification procedure of the doubly labeled polymer was same as described in Chapter 2. UV (methanol λ, nm): 342, 326, 312, 290, 276.

4. 2. 4. Determination of the Spectroscopic Parameters P as the fraction of total light absorbed by naphthalene in the presence of pyrene at the excitation wavelength of 290 nm was calculated by the following formula.

$$P = [1-10^{-An\,(\lambda 1)}] / [2 - 10^{-An(\lambda 1)} - 10^{-Ap\,(\lambda 1)}]$$

where λ_1 is 290 nm, An (λ_1) and Ap (λ_1) are the absorbance of naphthalene and pyrene at λ_1, respectively.[65] In the doubly labeled PNIPAM aqueous solution, P was calculated as 0.62 i.e. 62% of incident light was absorbed by naphthalene. The ratios of pyrene excimer to monomer intensities (I_E/I_M) were determined by taking the ratio of the excimer intensity at 480 nm to the monomer intensity at 375 nm.

4. 2. 5. Fluorescence Sample Preparation Samples for spectroscopic analysis were prepared from stock polymer aqueous solutions (0.5 to 5 g/L) and kept at 5°C for at least 24 hrs to ensure complete dissolution. To obtain desired concentrations, the stock solutions were further diluted by deionized water. These solutions were kept at room

temperature for at least 2 hrs before measurements, except for the 240K-N74 solution, which was kept at room temperature for at least 1 day. Mixed solutions: Three methods are used to prepare mixed solution. (1) From aqueous stock solutions: the stock solution of 240K-P_B177 and the stock solution of 240K-N74 were added to deionized water. (2) From stock solution in THF: 240K-P_B177 and 240K-N74 were dissolved together in THF, then the stock solution was added to deionized water (H_2O/THF: 50/1). The resulting solution was kept at 5°C for 2 days. (3) From codissolution into water: the two copolymer powders obtained from freeze-drying of their aqueous solutions were dissolved together in deionized water, and the solution was kept at room temperature for 2 hrs and at 5°C for 2 days. All solutions were allowed to stand at room temperature for 2 hrs before fluorescent measurement.

4. 3. Results and Discussion

4. 3. 1. Structure and composition of copolymers The chemical structure of the copolymers used in this study are shown in scheme 4.1. The doubly labeled polymer (240K-N72-P_B325) was prepared in order to investigate the occurrence of intrapolymeric association between pyrene and naphthalene by nonradiative energy transfer. The parameters of the copolymers are listed in the chapter 3.

Scheme 4. 1. Chemical structure of doubly polymers.

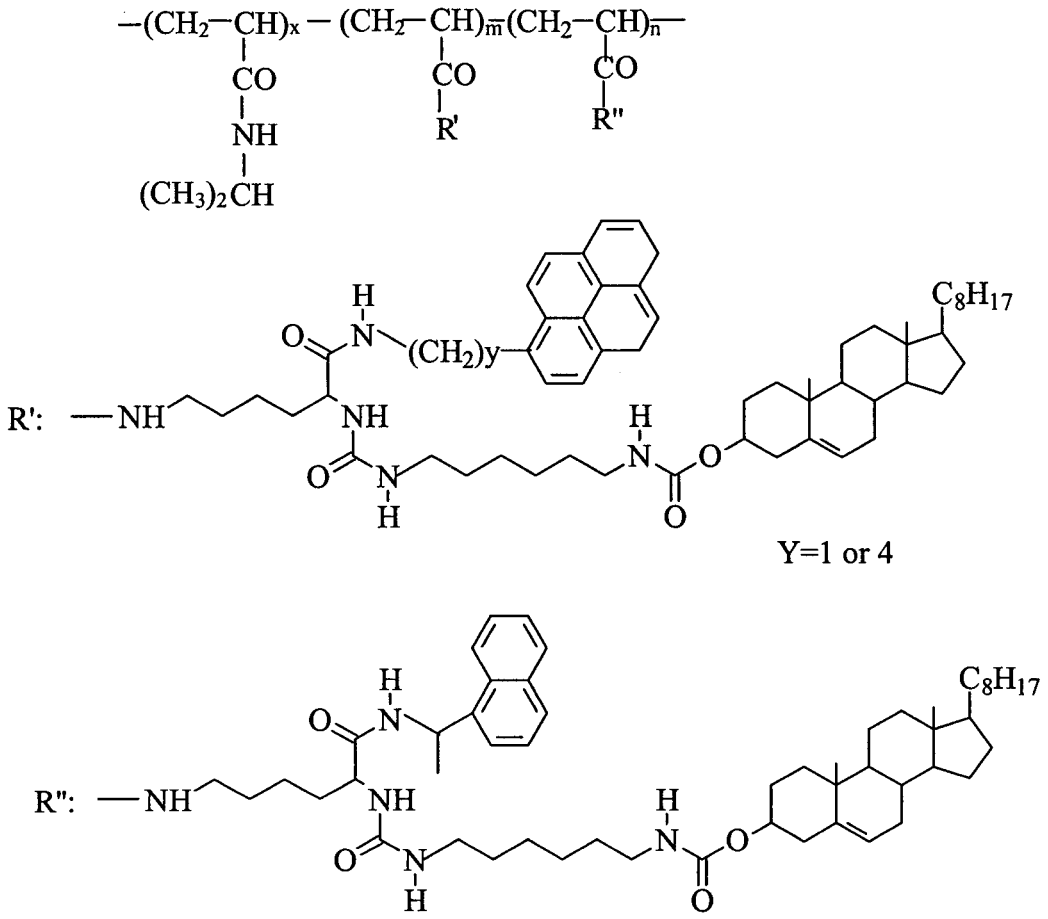

4. 3. 2. Spectroscopy of Copolymers The emission spectra of the pyrene labeled polymers were measured at 25°C in aqueous solutions. In general, all the spectra exhibited a large pyrene monomer emission and a smaller pyrene excimer emission with the excitation at 346 nm in aqueous solutions. The pyrene excimer was formed via static association. The general features of the excitation spectra of the pyrene labeled polymers were similar in both methanol and water, but the monomer excitation spectra were slightly blue-shifted compared with the excimer excitation spectra.

4. 3. 3. Intrapolymeric NRET The pyrene-naphthalene pair of chromophores is well known to interact as energy donor (naphthalene) and energy acceptor (pyrene) by NRET with a characteristic distance, 29 Å. Upon excitation at wavelength of 290 nm, most light (62%, calculated in the experiment section) was absorbed by naphthalene. Since the emission was detected from the direct emission of excited naphthalene and the emission of pyrene excited through NRET, the pyrene and naphthalene groups were in close enough to satisfy the requirements of NRET in solutions.

Figure 4. 1. Fluorescence spectra of doubly and singly labeled PNIPAM in water with identical pyrene concentration (25°C, λ_{ext} = 290 nm).

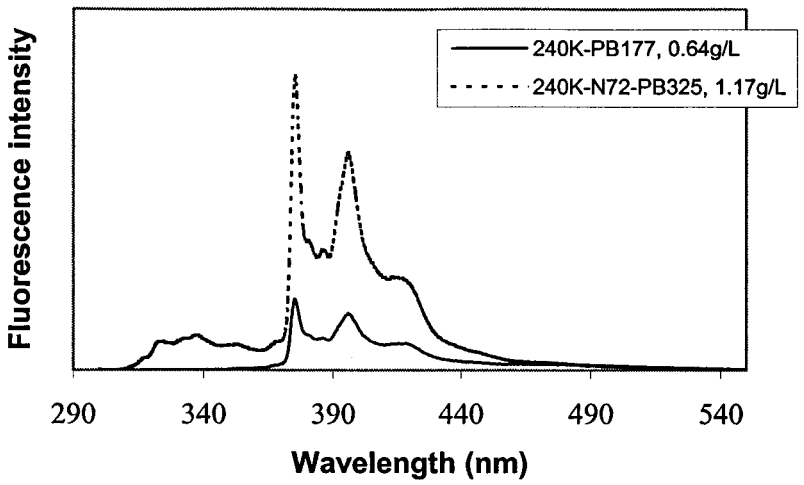

Upon excitation at 290 nm, the fluorescence spectrum of the doubly labeled PNIPAM (240K-N72-P_B325) exhibited a weak monomer emission in aqueous solution from isolated excited naphthalene ranging from 300 to 360 nm and a strong monomer emission from isolated excited pyrene ranging from 360 to 400 nm. No excimer emission from pyrene dimers can be observed (Figure 4.1). This result indicates there is a strong energy transfer between naphthalene and pyrene or a strong intrapolymeric interaction. In contrast, the fluorescence spectrum of 240K-N72-P_B325 in methanol demonstrated a strong naphthalene monomer emission and a weak pyrene monomer emission upon excitation at 290 nm (Figure 4.2). It can be concluded that no energy transfer occurred between naphthalene and pyrene in methanol when considering the contribution of direct pyrene emission. It should be noticed that another difference between the spectra recorded from water and from methanol with the identical concentration, that is the naphthalene emission spectrum from the aqueous solution was quenched considerably in comparison with the spectrum from methanol solution. This

phenomenon is similar to that observed in doubly labeled octadecane-substituted PNIPAM.[5]

Figure 4. 2. Fluorescence spectra of doubly labeled PNIPAM in water and methanol (25°C, λ_{ext} = 290 nm, 0.20 g/L).

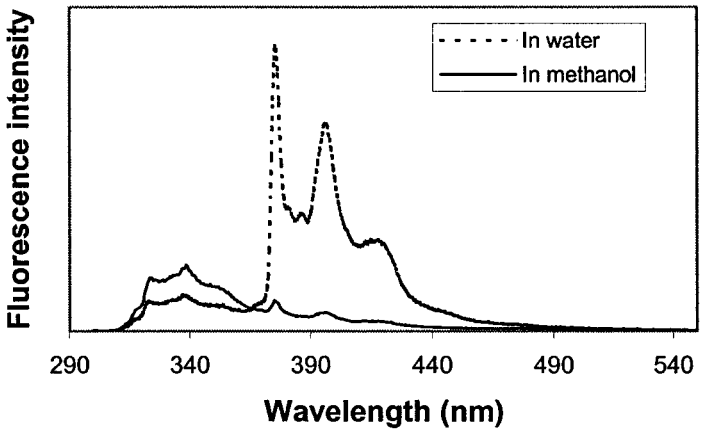

Effect of temperature In the 240K-N72-P_B325 solutions, the pyrene emission increased first with the increase of temperature close to the LCST, then decreased slightly with the increase of temperature above the LCST (Figure 4.3a); the naphthalene emission increased linearly with increasing temperature. Thus, the value of I_{Py}/I_{Np} kept constant when temperature was below the LCST, and sharply decreased when temperature was above the LCST. The same phenomena were observed by heating polymer solutions with different concentrations. In the cooling scan, the pyrene emission increased and the naphthalene emission decreased with decreasing temperature. The value of I_{Py}/I_{Np} followed a reverse trend in the cooling scan, as compared to that in the heating scan (Figure 4.3b).

Figure 4.3. Ration of Ipy/Inp due to NRET for doubly labeled PNIPAM in aqueous solutions as a function of temperature ((λ_{ext} = 290 nm; 0.25 g/L)

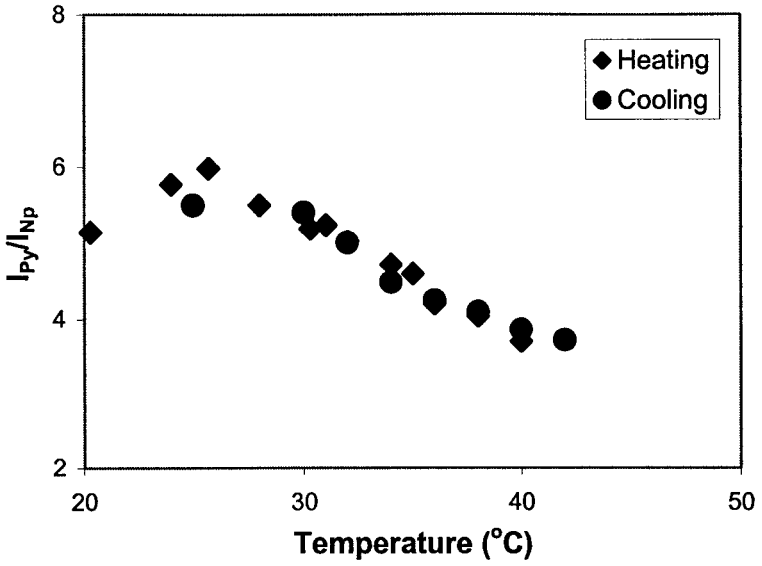

Fluorescence spectra of the 240K-N72-P_B325 were also monitored upon an excitation at 346 nm. In the heating scan, the ratio of I_E/I_M for 240K-N72-P_B325 with directly excited pyrene slightly decreased from in the temperature range of 28 to 32°C (Figure 4.4). In the cooling scan, I_E/I_M kept almost unchanged. The ratios of I_E/I_M for 240K-N72-P_B325 in the heating-cooling cycle were very close. But they were smaller than those of the mixtures of the two singly labeled polymer solutions, and much smaller than those of 240K-P_B177 solutions in the absence of naphthalene. These facts indicate that 240K-N72-P_B325 can form highly mixed micelles with the hydrophobic groups of naphthalene and pyrene. These aggregations were disturbed upon heating as the result of naphthalene and pyrene being separated from each other even in the "polymer rich" phase (in contrast to the solution of the mixed singly labeled polymers where naphthalene and pyrene from interpolymeric chains came into close proximity in the "polymer rich"

phase). This is the reason why the energy transfer efficiency between excited naphthalene to pyrene decreased with increasing temperature. This process was reversible and the intrapolymeric interaction may be less favorable in the "polymer rich" phase (above the LCST) than that in the isotropic liquid phase (below the LCST). The following experiments were designed to verify above hypothesis.

Figure 4. 4. Ratio of I_E/I_M in polymer solutions as a function of temperature (λ_{ext} = 346 nm).

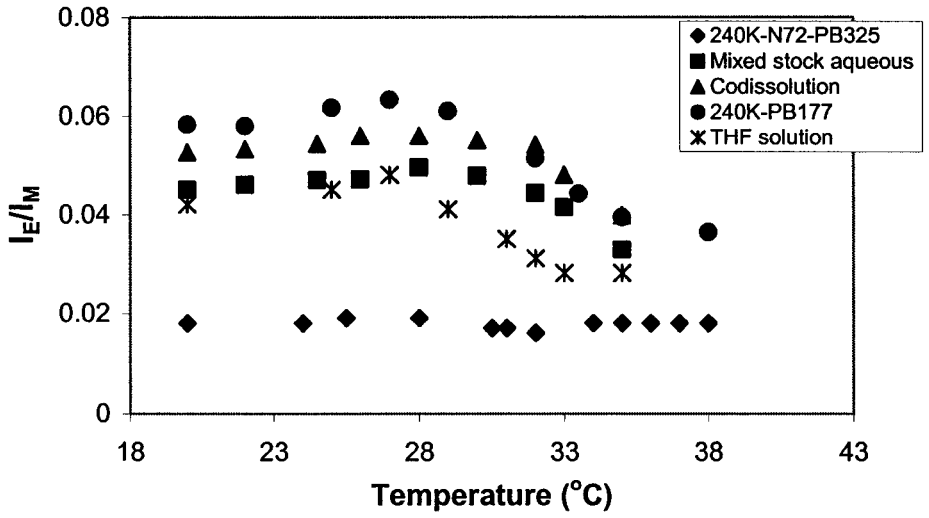

4. 3. 4. Interpolymeric NRET It was observed that the general feature of two spectra was identical when compared the spectrum from the mixed stock aqueous solution of 240K-P_B177/240K-N74 with that of 240K-N72-P_B325 in the aqueous solution. But the former showed much lower pyrene intensity upon the excitation at 290 nm (Table 4.1). The results indicate that the energy transfer efficiency of the mixed stock aqueous solution was much lower than that of the doubly labeled polymer in the aqueous solutions, i. e., interpolymeric association is less favorable than intrapolymeric association in the polymer solutions. In addition, one can observe a significant

quenching of the naphthalene emission and an enhancement of the pyrene monomer emission in the solutions containing an identical amount of each chromophore by comparing the emission of the solution of 240K-N72-P_B325 or the mixed stock aqueous solution of 240K-N74/240K-P_B177 with the spectra of the individual solution of 240K-P_B177 or 240K-N74.

4. 3. 4. 1. Effect of Concentration Ratio of Chromophores on NRET in Mixed Polymer Solutions A ratio of I_{Py}/I_{Np} as 3.4 was observed in the mixed stock aqueous solution of 240K-N74/240K-P_B177 when molar ratio of naphthalene to pyrene (C_{Np}/C_{Py}) was 1 while I_{Py}/I_{Np} of the doubly labeled PNIPAM was 6 with C_{Np}/C_{Py} of 4.5. Could the ratio of I_{Py}/I_{Np} from interpolymeric NRET have the same value as intrapolymeric NRET when the molar ratio of chromophore changed? The effect of molar ratio of naphthalene to pyrene on energy transfer was investigated in the mixed stock aqueous solution and the results are listed in Table 4.1. We found that the ratio of I_{Py}/I_{Np} decreased to 1.1 when molar ratio of naphthalene to pyrene increased to 4.5 (Table 4.2). The similar phenomenon was also observed from the mixed solutions of the polymers codissoluted into water (Table 4.1). This status even existed above the LCST, but the ratio of IPy/INP was close to the ratio of intarpolymeric NRET when C_{Np}/C_{Py} was 1. However, in octadecane-substituted PNIPAM solutions, energy transfer efficiency was increased with increasing molar concentration ratio of naphthalene to pyrene.[57]

Table 4. 1. The Effect of Np/Py Molar Concentration Ratio on NRET

Polymer solution	Concentration ratio of Np/Py (C_{Np}/C_{Py})	I_{Py}/I_{Np} (± 0.1)	
		25°C	35°C
240K-N72-P_B325	4.5	6.0	3.5
240K-P_B177/240K-N74 from mixed stock solution	1	3.4	3.8
	2.7	1.9	2.1
	4.5	1.1	1.6
240K-P_B177/240K-N74 from codissolution into water	1	2.8	3.3
	2.7	2.0	2.4
	4.5	1.3	1.9

The results may suggest the micellar aggregates formed by hydrophobic substituents could be very compact and stable in high polymer concentrations, and it should be difficult to form new micelles with the mixed hydrophobic groups. This also supports the conclusion that intrapolymeric association was more favorable than interpolymeric association at temperatures below the LCST. On the other hand, it was in agreement with the close values of the molar extinction coefficient for the cholesteryl naphthalene derivative and the cholesteryl pyrene derivatives; thus a relatively smaller amount of naphthalene was required. However, in the case of octadecane-substituted PNIPAM, the higher molar concentration ratio of naphthalene to pyrene was required in order to observe the same extent of energy transfer[5]. Since naphthalene has a much lower coefficient of molar extinction compared with pyrene, it is necessary to use naphthalene with higher concentration to ensure the occurrence of energy transfer from excited naphthalene to pyrene.

Table 4. 2. Composition of Solutions Used in NRET Experiment

Preparation method	Polymer concentration (g/L) 240K-N74	240K-P_B177	Total	Chromophore concentration (mol/L) Np (10^5)	Py (10^6)
From stock aqueous solutions	0.250	0.125	0.36	3.0	6.3
	0.125	0.110	0.235	1.5	5.5
	0.046	0.110	0.156	0.55	5.5
By codissolution Into water	0.270	0.140	0.410	3.2	7.0
	0.125	0.110	0.235	1.5	5.5
From THF stock solution	0.125	0.110	0.235	1.5	5.5

4. 3. 4. 2. Effect of Temperature on NRET The mixed solutions of 240K-N74 and 240K-P_B177 were prepared from the stock aqueous solutions of each polymer. The mixed solutions were heated from 20 to 40°C in the sample compartment of fluorescence spectrometer, then fluorescence spectra of the mixed solutions were recorded as a function of temperature. Upon excitation at 290 nm the emission intensity of pyrene monomer increased gradually with increasing temperature. The emission intensity of naphthalene also increased slightly and reached a plateau at the temperature corresponding to the macroscopic cloud point. The ratio of I_{Py}/I_{Np} was increased slightly with the increase of solution temperature as shown in Figure 4.5, which indicated that the hydrophobic groups can come into close proximity in the "polymer rich" phase above the LCST, i.e., the interpolymeric interaction is more favorable in the phase of separated mixtures (above the LCST) than that in the isotropic liquid phase (below the LCST).

Figure 4. 5. Ratio of I_{Py}/I_{Np} as a function of temperature (λ_{ext} = 290 nm) in mixed singly labeled PNIPAM solutions prepared from stock aqueous solutions.

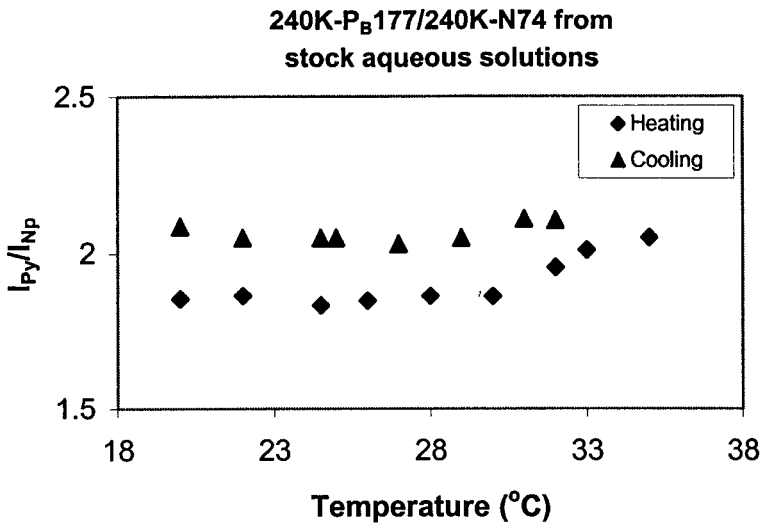

A comparison of spectra obtained from the mixed stock solutions at 20 and 35°C reveals that the emission of pyrene monomer is enhanced by a factor of ca. 1.2 in the solutions above the LCST. Since no excimer emission was observed in these cases, the monomer emission can be correlated to its total emission. In order to monitor the heat-induced changes in the emission of directly excited pyrene chromophore during the temperature change, the fluorescence spectra upon excitation at 346 nm were also recorded. The emission intensity of pyrene monomer increased at the expense of pyrene excimer emission, therefore the total emission intensity increased. Qualitatively, similar changes in pyrene fluorescence were also observed by heating the solution of 240K-P_B177 in the absence of 240K-N74 (Figure 4.4).

4. 3. 4. 3. Effects of Sample Preparations and Thermal History Three methods were used to prepare samples and detail compositions with different solutions were given in Table 4. 2. (1) the mixing of stock aqueous solutions of each polymer, (2) codissolution into water of the freeze-dried polymers, (3) dilution with water from the stock concentrated THF solution of the two polymers. The above solutions were matched as closely as possible, in terms of total polymer concentration, chromophore ratio and equilibrium time (Table 4.2). The mixed solutions were kept at 5°C for 24 hrs and at room temperature for 2 hrs before measurement. To investigate the effect of the preparation methods on the properties of mixed solutions, a series of fluorescence spectra were monitored at different temperatures.

When the mixed solutions were heated, the ratio of I_{Py}/I_{Np} for the polymer solution prepared from the stock THF decreased first until the temperature reached 27°C, then it increased to a maximum value with further increasing the temperature to 31°C and decreased slightly again with increasing temperature (Figure 4.6). In the cooling scan, the value of I_{Py}/I_{Np} followed the reverse trend, but the maximum value can shift slightly from 31 to 30°C. At 20°C, the same ratio of I_{Py}/I_{Np} was obtained with the sample before and after the heating-cooling cycle. The value of I_E/I_M upon the excitation at 346 nm increased slightly until the temperature reached to 27°C, and decreased abruptly with continuing increase of temperature (Figure 4.4). The photophysical properties of pyrene followed the same trend as in the 240K-P_B177 solution without 240K-N74.

Figure 4. 6. Ratio of I_{Py}/I_{Np} as a function of temperature in mixed singly labeled PNIPAM solutions prepared from THF concentrated solution (λ_{ext} = 290 nm).

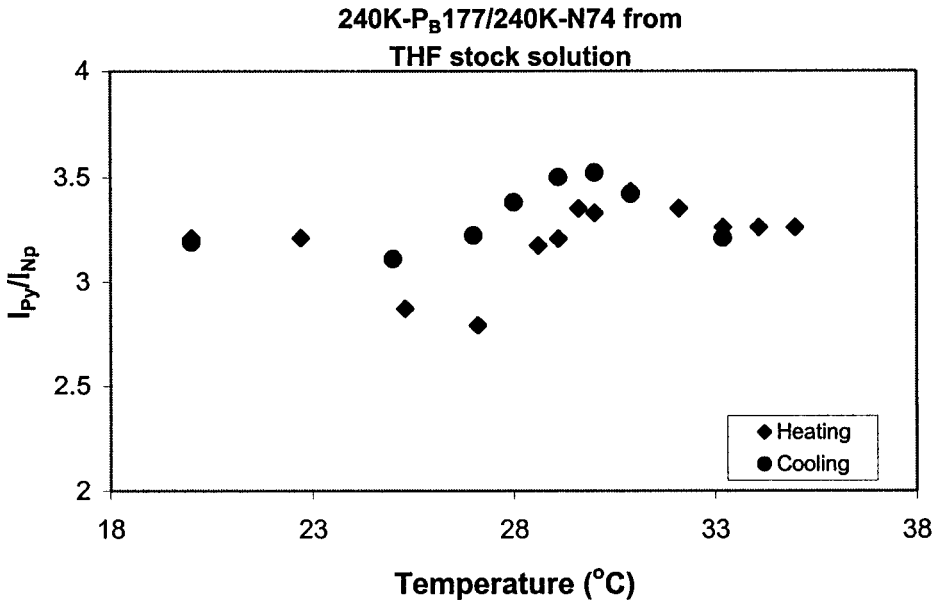

In the mixed solutions prepared by codissoluting polymers into water, the ratio of I_{Py}/I_{Np} increased with the increase of temperature during the heating scan, but the ratio of I_{Py}/I_{Np} enlarged abruptly as the temperature was changed from 28 to 32°C, (Figure 4.7). Clearly, there was higher energy transfer efficiency at 35°C than that at 20°C since the ratio I_{Py}/I_{Np} is 2.0 at 35°C *vs.* 1.2 at 20°C, indicating that the interpolymeric association becomes stronger above the LCST. As the solution was cooled to 20°C at a rate approximately identical to the heating rate, the spectra did not undergo the opposite changes as observed during the heating scan. The pyrene emission decreased slightly at first, then it increased slightly below the LCST. The ratio of I_{Py}/I_{Np} decreased slightly during the cooling scan, but it was always higher than that determined in the heating scan

at a given temperature during the cooling scan. At 20°C, the spectrum of the mixed solution that had been subjected to a heating-cooling cycle differed from that of the initial solution. It denotes that the efficiency of energy transfer of samples was higher after heating (I_{Py}/I_{Np} = 2.0) than that before heating (I_{Py}/I_{Np} = 1.2).

The solutions prepared by codissoluting polymers into water underwent the second heating scan and the ratio of I_{Py}/I_{Np} followed the exactly same trend as that observed in the first cooling scan (Figure 4.7).

Figure 4. 7. Ratio of I_{Py}/I_{Np} as a function of temperature in mixed singly labeled PNIPAM solutions prepared by codissoluting polymers into water (λ_{ext} = 290 nm).

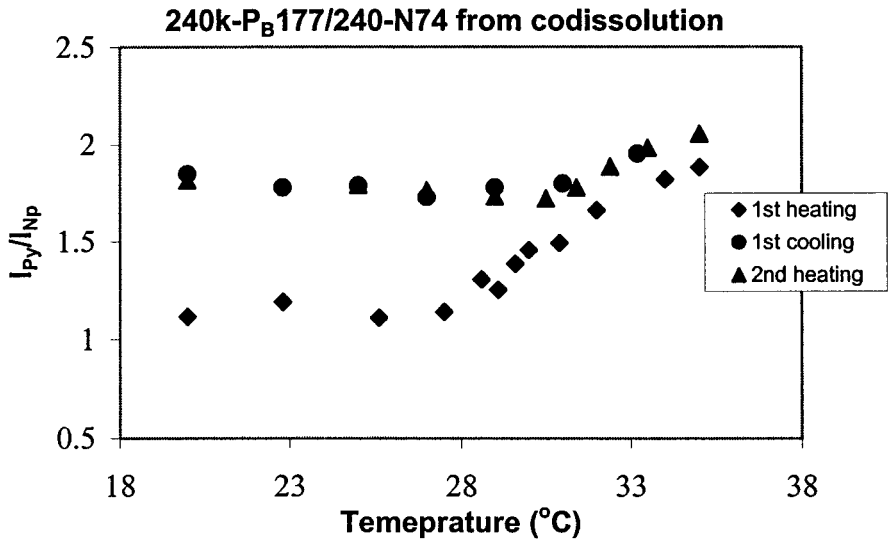

The ratios of I_{Py}/I_{Np} for the mixed solutions were larger than those equilibrated for 2 hrs, in which the mixed solutions were prepared either from the stock aqueous polymer solutions or by codissoluting polymers into water equilibrated for 2 days (Figure 4.8). It may be true that the cholesteryl and fluorophore groups move slowly due to their bulky

structure, and it requires a longer time to reassociate and reach a new equilibrium for mixed hydrophobic microdomains.

Figure 4. 8. I_{Py}/I_{Np} of polymer solutions prepared from different methods and thermal history (λ_{ext} = 290 nm).

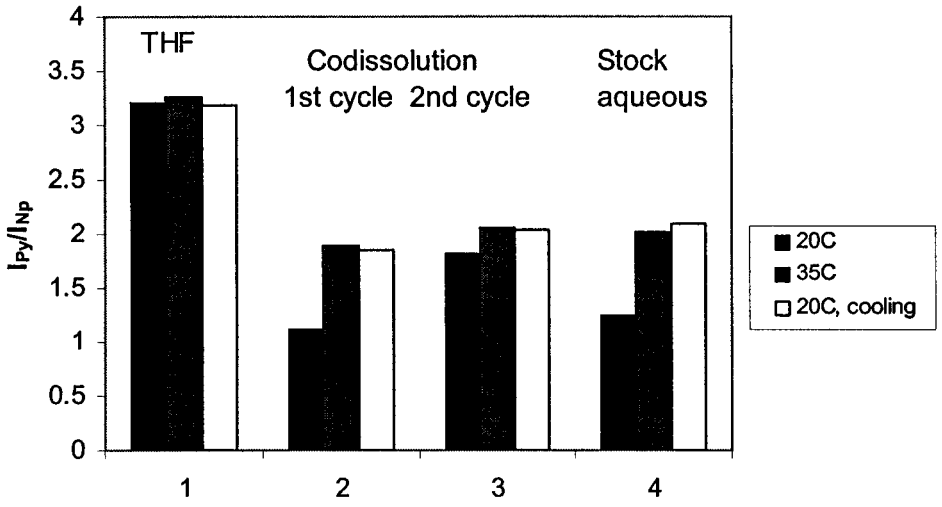

The higher ratio of I_{Py}/I_{Np}, the higher energy transfer extent from naphthalene to pyrene. Among the three samples (Figure 4.8), the ratio of I_{Py}/I_{Np} measured from THF stock solution exhibited the largest one at 20°C either before or after the heating-cooling cycle. A change of I_{Py}/I_{Np} was observed upon changing temperature, which indicates that strong interpolymeric interaction and weak intrapolymeric interaction occurred. In contrast, the interpolymeric interaction was weak and the intrapolymeric interaction was strong in the solutions prepared either from the stock aqueous solutions or by the codissolution of the polymers into water. Two types of the hydrophobic groups were initially well intermixed in the micelles by the interpolymeric association for the solutions prepared from the stock THF, but, two types of the chromophores were highly

separated within the micelles in the solutions prepared either from the stock aqueous solution or by the codissolution of the polymers into water because of strong intrapolymeric association and stability of the micelles.

It should be emphasized that the intrapolymeric association is more favorable in aqueous solutions below the LCST and the interpolymeric association is preferred in the solutions above the LCST, which was supported by the change of the energy transfer efficiency from excited naphthalene to pyrene upon changing temperature.

Figure 4. 9. Fluorescence spectra of mixed singly labeled PNIPAM with molecular weight 400,000 and 20, 000 Dalton, and identical concentration of pyrene and naphthalene (λ_{ext} = 290 nm, 25°C).

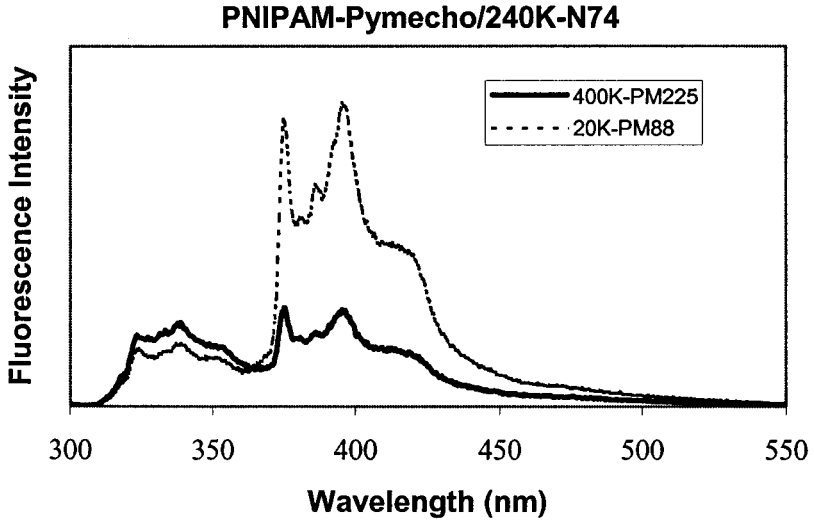

4. 3. 4. 4. Effect of Molecular Weight on NRET NRET experiments were also tested by Pymecho labeled PNIPAM with different molecular weights (Figure 4.9). The molecular weight of 240K-N74 was kept identical as 240,000 Dalton in all experiments. The mixed solutions were prepared from the stock aqueous solutions and equilibrated for 24 hrs at room temperature. It is clear that the efficiency of energy transfer from excited naphthalene to pyrene was strongly dependence on the polymer molecular weights and

the molar ratio of naphthalene to pyrene. By using the mixed polymers with low and high molecular weight, such as 20K-P_M88 and 240K-N74, the maximum value of I_{Py}/I_{Np} was obtained among all the polymers. The value of I_{Py}/I_{Np} increased upon increasing the temperature up to 35°C. It is possible that the interpolymeric association is favorable due to the high mobility of the short molecular chains, therefore the hydrophobic microdomains can be reorganized. In contrast, when the mixed polymer with high molecular weight such as 400K-P_M225 (400,000 Dalton) mixed with 240K-N74, the solution underwent very weak energy transfer (the lowest I_{Py}/I_{Np} value), and the value of I_{Py}/I_{Np} have no a noticeable change at 35°C (Table 4.3). It may suggest that the interpolymeric association is unfavorable due to the low mobility of long molecular chains and it is difficult to destroy the micelles and reorganize them under these experiment conditions.

Table 4. 4. Effect of Polymer Molecular Weight on NRET

Polymers	Concentration of the polymers (g/L)			Chromophore concentration (Mol/L)		I_{Py}/I_{Np} (± 0.1) 25°C	I_{Py}/I_{Np} (± 0.1) 35°C
	Np	Py	Total	Np	Py		
400K-P_M225/ 240K-N74	0.125	0.140	0.265	1.5×10^{-5}	5.5×10^{-6}	0.6	0.7
	0.046	0.140	0.186	5.5×10^{-6}	5.5×10^{-6}	1.1	1.3
20K-P_M88/ 240K-N74	0.125	0.055	0.180	1.5×10^{-5}	5.5×10^{-6}	2.3	2.9
	0.046	0.055	0.110	5.5×10^{-6}	5.5×10^{-6}	4.9	5.7

4. 3. 5. Discussion

The energy transfer can take place between chromophores attached by same or different polymeric chains. The energy transfer increases upon increasing temperature in the mixture of two singly labeled polymers with a molecular weight of 240,000 Dolton

and prepared either from codissolution or from stock solution. It suggests that the intermolecular association could be enhanced by increasing temperature. This phenomenon was also observed in the dodecyl (C12) or octadecyl (C18) substituted PNIPAM solution. In the mixed solution of PNIPAM-C12Py and PNIPAM-C12Np with molecular weight of 306,000 Dolton[66], the energy transfer increased upon increasing temperature above the LCST of the polymers. However, in the mixed solution of PNIPAM-C12Np and the pyrene labeled copolymer of sodium-2-(acrylamido)-2-methylpropanesulfonate and dodecylmethylacrylamides (PAMPS-C12PY), the energy transfer decreased upon increasing the temperature above the LCST of PNIPAM. The effect of temperature on intermolecular association will depend on composition of polymer. Furthermore, the intermolecular association of hydrophobically modified PNIPAM (C12, C18 or cholesterol) is enhanced by increasing temperature.

The interpolymeric association was obviously observed in the mixed solutions of two singly labeled polymers with a molecular weight of 240,000 Dolton as described above. However, the energy transfer extent of the doubly labeled PNIPAM with the same molecular weight in aqueous solutions exhibited much higher ratio (I_{Py}/I_{Np} = 6.0) than those of the mixed solution of the two singly labeled polymers (I_{Py}/I_{Np} = 1.9) at room temperature. Both inter and intrapolymeric associations can occur in the doubly labeled polymer solutions, although the concentration of polymer has no significantly affect the values of I_{Py}/I_{Np} in the equilibrium solutions. The energy transfer decreased and reached to 3.7 at 40°C when the solution of 240K-N72-P_B325 was above the LCST. However, it is still much higher than that from the mixture of two singly labeled polymer solutions and close to the ratio from concentrated THF solution. Therefore, the intermolecular

hydrophobic association is inhibited by collapsing of polymer chain. The observed energy transfer above the LCST may reflect the existence of intermolecular association. The results indicate that the intrapolymeric association plays a key role in the doubly labeled polymer solutions at room temperature. It can be concluded both inter and intrapolymeric associations coexisted in the solution of the fluorescence labeled cholesterol-bearing PNIPAM with molecular weight of 240,000 Dolton (Fig. 4.10).

Figure 4. 10. Proposed micellar aggregates of cholesterol-bearing PNIPAM.

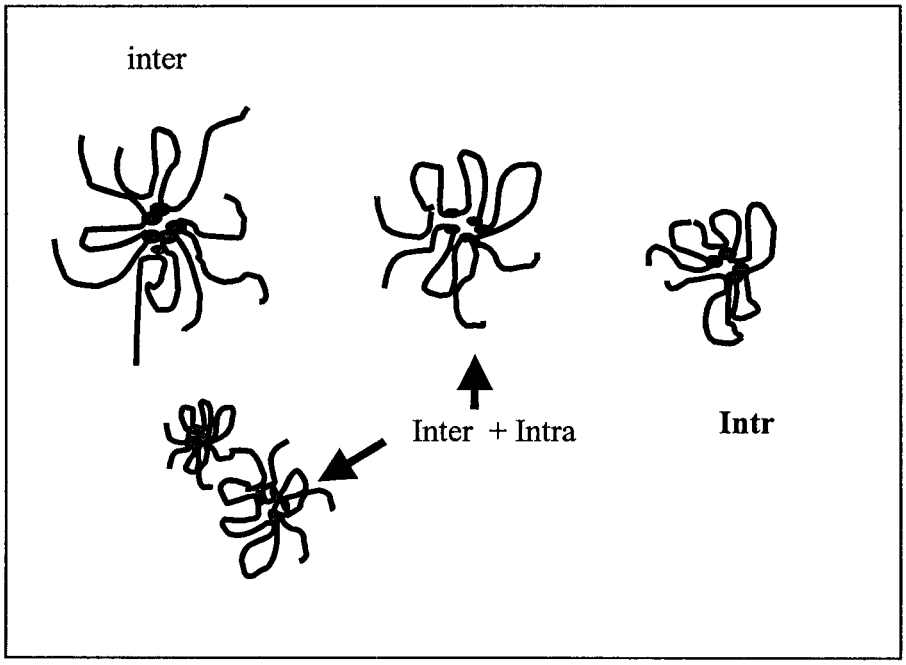

4.4. Conclusion

Both inter and intrapolymeric associations coexisted in the amphiphilic polymers with cholesteryl and fluorophore groups. The associations were related with polymer architecture, preparation methods and thermal history of polymer samples. There was a strong intrapolymeric association below the LCST and strong interpolymeric association above the LCST in the case of copolymer with relatively high molecular weight (400,000). There was always strong interpolymeric association with low molecular weight polymer due to the high mobility of the polymeric chains. Interpolymeric association became stronger when the copolymer solutions were prepared from the stock THF solution, but the intrapolymeric association was stronger in the solutions either from codissolution of two types of copolymers (240K-P_B177 and 240K-N74) into water or from stock aqueous solutions. The intramolecular association of polymer with a molecular weight of 240,000 Dolton is more favorable at room temperature and less favorable above the LCST of polymer. In contrast, the intermolecular association of the polymers with a molecular weight of 240,000 Dolton is more favorable above the LCST of polymer and less favorable at room temperature.

Chapter 5

Interaction of Phospholipid and Non-phospholipid liposomes with Cholesterol Bearing Thermal Sensitive Polymers

Abstract

The interaction of cholesterol bearing poly(*N*-isopropylacrylamide) (PNIPAM) with phospholipid and nonphospholipid liposomes was studied as a function of the type and concentration of lipid, temperature and polymer conformation. Fluorescence and non-radioactive energy transfer (NRET) were used to monitor the aggregation of polymeric micellar disrupted by liposomes. The experimental results indicate that cholesterol exhibited a great affinity for lipid bilayer and can be worked as a highly reliable anchor to maintain the polymers onto the liposome surfaces at the temperature either above the lower critical solution temperature (LCST) of polymer or in the fluid lipid bilayer. In addition, the results revealed that the cholesterol anchor did not diffuse laterally in the fluid membranes and the quenching experiments suggested that only cholesterol could be inserted into the lipid bilayer instead of pyrene chromophore. We conclude that pyrene and cholesterol can be separated apart when the polymers interact with the liposomes. The measurements of differential scanning microcalorlimetry (DSC) and fluorescence confirmed that the LCST of the polymers remained when the polymers coated onto the liposome surfaces. Gel-filtration chromatography revealed there was up to 65% of cholesterol-bearing PNIPAM bound into the lipid bilayer upon dilution through a column.

5. 1. Introduction

Liposomes are considered the most useful drug delivery systems because liposomes can carry not only hydrophilic drugs within inner pools but also hydrophobic ones inside the bilayer. Well-tailored liposomes can be used in the process to deliver highly toxic drugs and infectious disease drugs to specific target sites. By this way, it can be avoided to damage healthy tissues, organs and cells by the toxic chemicals. One of the promising approaches to prepare well-tailored liposomes used in *vivo* is to coat water-soluble polymers onto liposome surfaces. Stealth liposomes, temperature, pH, ionic strength and photon sensitive liposomes have been extensively studied over past decades in order to increase the lifespan of liposomes and control release of loaded chemical drugs. Currently, long alkyl chains are frequently used as a hydrophobic anchor attached to water-soluble polymers, then coated onto liposome surfaces. Winnik and her coworkers found that the alkyl chain bearing poly(*N*-isopropylacrylamide) can readily escape from the polymer modified liposomes when the liposome complexes were subjected to heat above the temperature of T_c or LCST, especially polymers had a low level of hydrophobic incorporation. In order to solve this problem, we synthesized a new type of anchor by using a cholesteryl group instead of alkyl chains, and examined the interaction of the cholesterol-bearing polymers with two types of liposomes (phospholipid and nonphospholipid liposomes).

We choose dimyristoylphosphatidylcholine (DMPC) to formulate phospholipid liposomes since the disaturated phosphatidylcholine was intensively used as model membranes and is easy to chemically synthesize and purify. It has been also found that DMPC is stable to oxidation, hydrates readily, and forms only lamellar phases in excess

water at physiological temperature.[67] Niosomes, or nonphospholipid liposomes (NPL), can be generated by the self-assembly of nonionic surfactants in aqueous suspension and have been used in the cosmetic industry.[68] The excellent chemical properties of NPL may lead to a potential application as drug delivery systems,[69] and the low cost of NPL compared with phospholipid vesicles is also an advantage.[70]

In this dissertation, we developed thermal sensitive liposomes based on cholesterol-bearing PNIPAMs coated phospholipid liposomes (DMPC) and n-octadecyldiethylene oxide surfactant vesicles (NPL). In this chapter, the interaction of the polymers with the liposomes was investigated by fluorescence, nonradiative energy transfer, microcalorimetry, and gel-filtration chromatography, respectively.

5. 2. Experimental

5. 2. 1. Materials Dimyristoylphosphatidylcholine (DMPC) was obtained from Avanti Polar Lipids. Brij72 [$C_{18}H_{37}$ $(EO)_2$], dimethyldioctadecylammonium bromide (DDAB), cetylpyridinum chloride monohydrate (CPC), and calcein were purchased from Aldrich. Sodium azide (NaN_3), sodium chloride (NaCl), ethylenediamine tetraacetate (EDTA), and Tris were purchased from BDH chemicals. The composition of the buffers used in this study is 10 mM Tris, 1mM EDTA, 140 mM NaCl, 0.02% NaN_3, and pH 7.2 for phospholipid liposomes; 150 mM NaCl, and 0.02% NaN_3 for nonphospholipid liposomes.

5.2.2. Preparation of Liposomes Liposomes were prepared as follows: a dry thin film of mixed lipids (100 mg, components listed in Table 5.1[71]) was dispersed in 5 mL of

buffer. The lipid suspension was mixed by vortex and extruded via a polycarbonate membrane (200 nm, Avanti Polar Lipids Inc.). The size of liposomes was measured by dynamic light scattering at 25°C with a fixed scattering angle 90°. The range of mean diameters of liposomes is from 195 to 225 nm.

Table 5. 1. Components of Liposomes

Liposome	Lipids (wt. %)		Cholesterol (wt. %)	DDAB (wt. %)	CPC (wt. %)
	Brij72	DMPC			
p-DMPC	-	100	0	0	0
DMPC5	-	75	20	5	0
DMPC5-CPC	-	73.5	20	5	1.5
DMPC10	-	70	20	10	0
DMPC10-CPC	-	68.5	20	10	1.5
NPL	75	-	20	5	0
NPL-CPC	73.5	-	20	5	1.5

5. 2. 3. Gel Filtration Chromatography (GFC) Gel filtration chromatography was carried out on a Gradfrac system (Pharmacia Biotech, Uppsala, Sweden) equipped with XK 16X70 mm column. The column with bed volume of 16X38 mm was packed with Sephacryl S-1000 SF (Pharmacia Biotech, Uppsala, Sweden) and equilibrated with the buffer solution as used for the sample preparation at 20°C. Typical procedure can de described as follows: a sample solution of 0.7 mL with 15 mg per mL of lipid and 1.5 mg per mL of polymer was injected in the column. The flow rate was 0.5 mL per min and the effluent was monitored at wavelength of 280 nm. Each fraction of sample (2 mL) was collected for further measurements.

5. 2. 4. Phosphate Assay The lipid concentration was determined by the phosphate assay. The concentrated sulphuric acid of 60 μL (99.99 wt.%) was added to different

Pyrex tubes filled with an aliquot (10 to 30 μL, containing up to 3mM of phosphate) of each fraction and followed by vortex mixing, then 10 μL of hydrogen peroxide (30 wt.%) followed by vortex mixing. The test tubes were placed in a preheated sand-bath (200°C) for 10 min and cooled at room temperature. To the solutions, doubly distilled water (670 to 650 μL) were added, then followed by vortex mixing. Finally, 20 μL of sodium sulphite solution was added and followed by vortex mixing again. The test tubes were placed in a preheated-sand bath (100°C) for 5 min. To the solutions, 200 μL of ammonium molybdate solution (kept in the dark, 20 mg/mL) were added and the solution was mixed by vortex mixing. Freshly prepared ascorbic acid (20 μL,100 mg/mL) was added in above solution and mixed by vortex. The test tubes were heated to 100 C at the preheated sand-bath for 10 min, then cooled to room temperature. The absorbance of each solution was measured by UV at the wavelength of 825 nm. The results were repeated three times and the average value was taken for evaluation. The absorbance of phosphate was calibrated at a series of known concentrations of KH_2PO_4 by the same procedure.

5. 2. 5. Quantitative Analysis of Hydrophobically Modified Polymers The copolymer concentration was analyzed by fluorescence intensity of pyrene attached to the polymer. To avoid self-quenching of the chromophore molecules due to inter- or intrapolymer interaction, all samples were standardized by solublization in an excess of sodium dodecyl sulfate (SDS). When the concentration of SDS is above its CMC, the excimer emission of pyrene (maximum emission centered at 480 nm) can be eliminated

because the pyrene groups can be isolated from each other in mixed polymer/SDS solutions.[6b] The concentration of SDS used in this study exceeded CMC of SDS by an order of magnitude, therefore all liposomes present in the solutions will be converted into mixed SDS/lipid micelles. It is reasonable there was no interactions between the polymer and liposome. The fluorescence intensity of the copolymer was calibrated by the polymer dissolved in a 16 mM of SDS solution with different known concentration. No excimer was detected at any polymer concentrations studied and there is a linear relationship between the emission intensity of pyrene monomer at 378 nm and the polymer concentrations over studied concentration range.

5. 2. 6. Calorimetry Differential scanning calorimetry (DSC, Microcal, Inc. Northampton, MA) was performed with a high sensitivity calorimeter. The samples were degassed first and analyzed at a heating rate of 1°C/min and 3 atmospheres. All thermographs were tested by using same volume of buffer as a reference and the equilibration time was set at 30 min and each sample was heated and cooled repeatedly at least 4 times within the temperature range from 0 to 85°C. Experimental conditions of liposome-polymer systems were chosen to allow monitoring of the polymers in the presence of excess liposomes.

5. 2.7. Lipid-polymer Mixture Polymer stock solutions (1- 6 g/L) were prepared in buffers. Liposome suspension and polymer solutions were mixed in the desired

proportion and the mixtures were allowed to equilibrate overnight at room temperature before measurement.

5. 3. Results and Discussion

5. 3. 1. Interaction of Liposomes and Polymers at Room Temperature

Fluorescence study The interaction among polymer-liposome was confirmed by fluorescence measurements. The polymers bearing cholesteryl substituents readily formed micellar aggregates in water. In fact, the polymer labeled as 20K-P_M88 showed a relative high ratio of pyrene excimer to monomer intensity (I_E/I_M) as discussed in Chapter 3 (Figure 5.1a). It is clear that the presence of liposomes can trigger a significant change in the emission of the pyrene labeled polymers, i.e., increased monomer emission I_M at the expense of excimer emission I_E.

Figure 5. 1. (a) Ratio of I_E/I_M for 20K-P_M88 with liposomes as a function of molar ratio of lipid to polymer (25°C; λ_{ex} = 346 nm) (b) Fluorescence spectra of 20K-P_M88 with and without NPL (25°C; λ_{ex} = 346 nm; polymer concentration: 0.05 g/L; lipid concentration: 0.5 g/L).

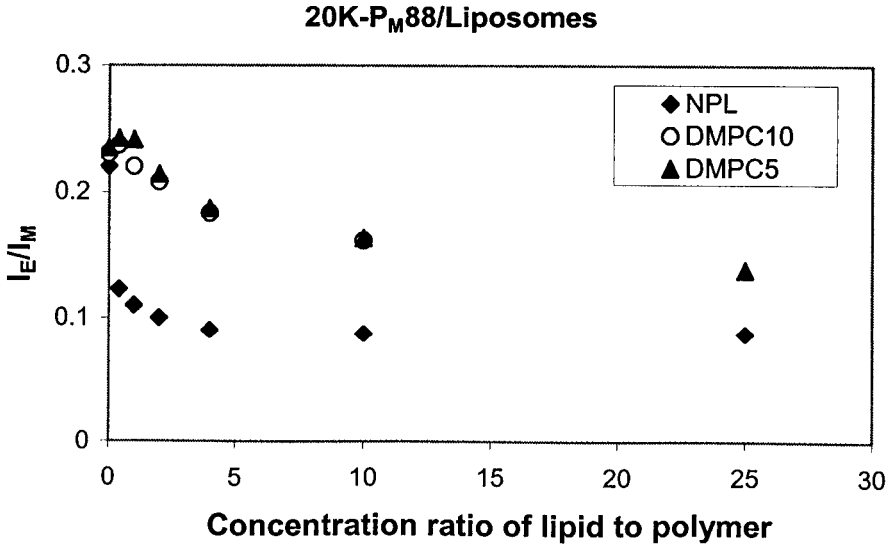

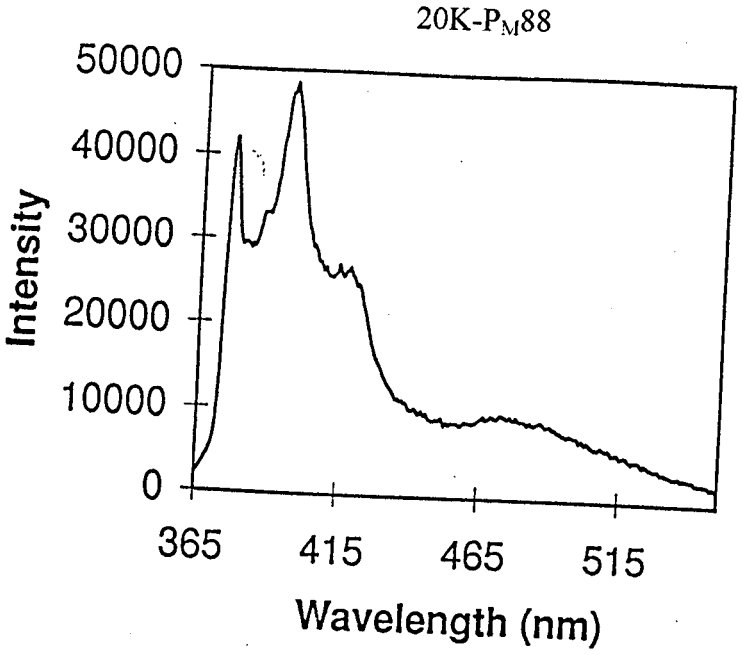
20K-P_M88
50000
40000
30000
20000
10000
0
Intensity
365
415
465
515
Wavelength (nm)

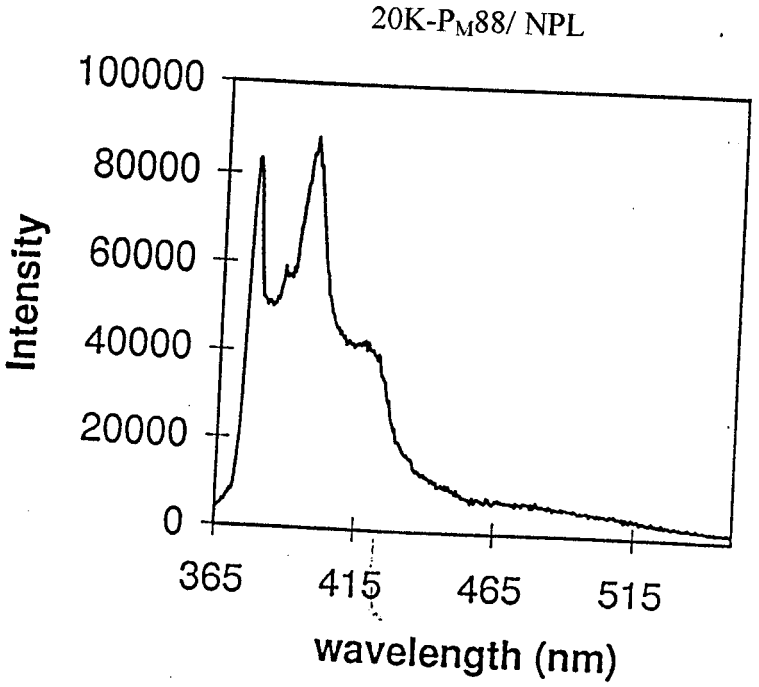
20K-P_M88/ NPL
100000
80000
60000
40000
20000
0
Intensity
365
415
465
515
wavelength (nm)

Figure 5.1 shows that the ratio of I_E/I_M for 20K-P_M88 decreased with an increase of ratio of lipid to polymer (R_c) in the presence of the liposomes, indicating the polymeric micelles was disrupted upon interaction with liposomes. The polymer chains were reorganized onto the surface of liposomes, which resulted in an increase of distance between the molecules of pyrene chromophores. The most noticeable difference between DMPC[72] liposomes and NPL was that the emission intensity ratio of I_E/I_M for the NPL/polymer system decreased dramatically at the same molar ratio of the polymer to lipid, indicating that the nonphospholipid liposomes (NPL) have a much stronger interaction with the polymers than the phospholipid liposomes (DMPC). The saturation molar ratio of lipid to polymer was 10 for both NPL and DMPC systems.

Figure 5.2. Ratio of I_{Py}/I_{Np} for doubly labeled PNIPAM with liposomes as a function of molar ratio of lipid to the polymer at 25°C, λ_{ex} = 290 nm. Fluorescence spectra of the doubly labeled PNIPAM in the absence (a) and presence (b) of NPL at 25°C, λ_{ex} = 290 nm, polymer concentration 0.05 g/L and lipid concentration 0.5 g/L.

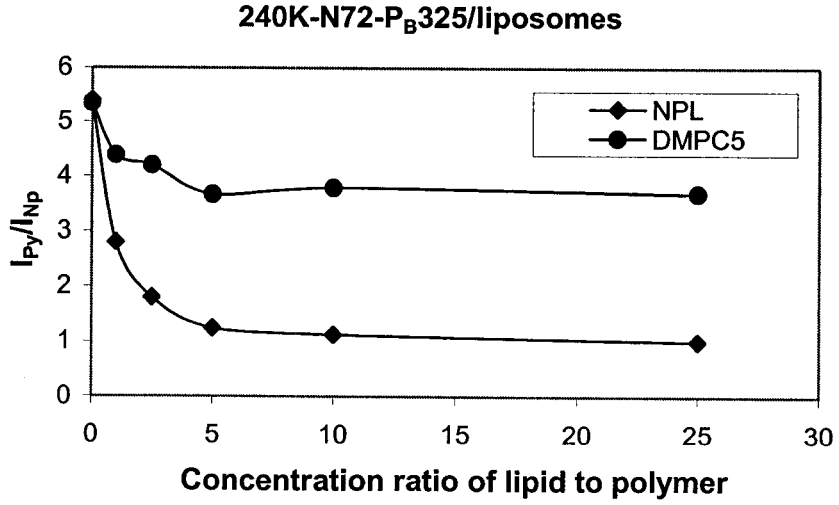

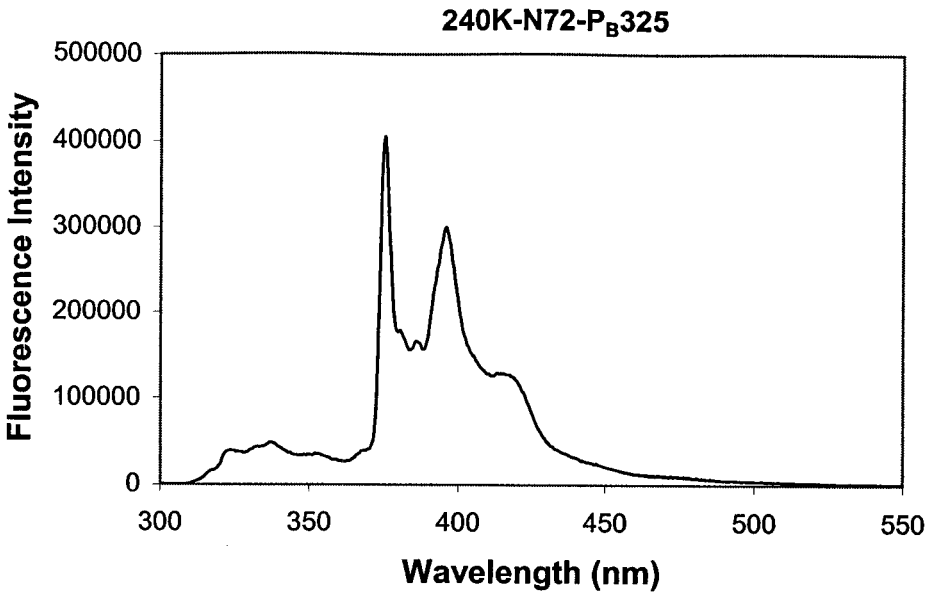
240K-N72-P$_B$325
Fluorescence Intensity
500000
400000
300000
200000
100000
0
300
350
400
450
500
550
Wavelength (nm)

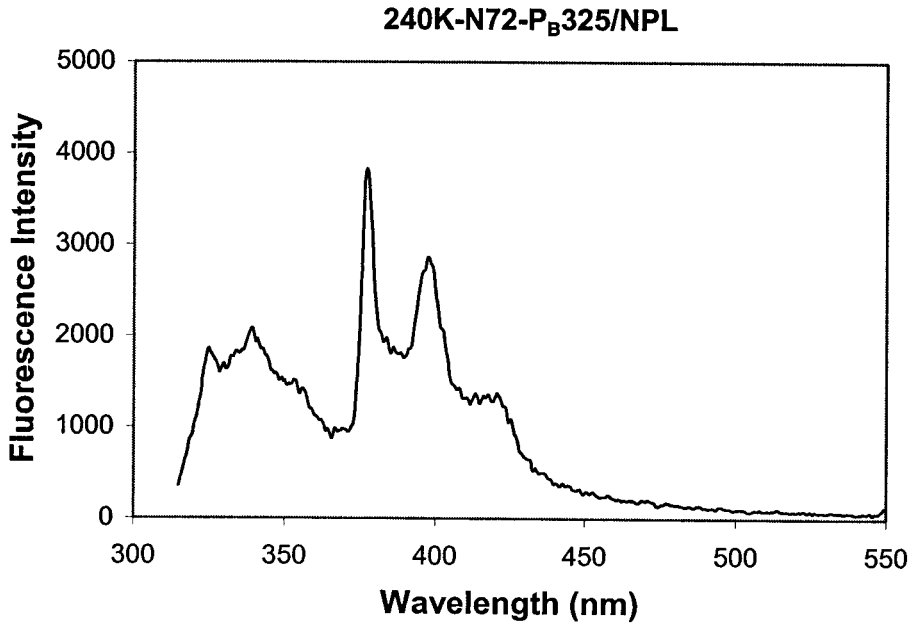
240K-N72-P$_B$325/NPL
Fluorescence Intensity
5000
4000
3000
2000
1000
0
300
350
400
450
500
550
Wavelength (nm)

Non-radioactive Energy Transfer Study The interaction of cholesterol-bearing PNIPAM with liposomes was also investigated in NRET study by using naphthalene and pyrene as donor-acceptor pairs.[61] Both singly labeled and doubly labeled polymers were used in this study. The doubly labeled PNIPAM (240K-N72-P_B325) showed a remarkable energy transfer indicated by a higher ratio of I_{Py}/I_{Np} in water; but the presence of liposomes produced a lower ratio of I_{Py}/I_{Np} with an increasing molar ratio of lipid to polymer (Figure 5.2). Similar phenomena were also observed in the case of a pair of singly labeled polymers, 20K-P_M88 and 240K-N74 (Figure 5.3). The decrease of energy transfer indicated the hydrophobic substituents were separated when the polymers interacted with liposomes. The pyrene and naphthalene chromophores in the NPL/polymer systems were separated much farther than those in the DMPC/polymer systems. The saturation molar ratio of lipid to polymer (20K-P_M88 and 240K-N72-P_B325) was 5 for both DMPC and NPL. The saturation molar ratio of lipid to polymer obtained from NRET was much lower than that obtained from excimer studies because of the difference on the distance between excited naphthalene and pyrene (29 Å) and the pyrene dimer (5 Å). Although the saturated molar ratios were constant for the same experiment with different liposomes, the saturated values of I_E/I_M or I_{Py}/I_{Np} for the two types of liposomes were quite different. The results suggest that the coating density of polymer on the surface of a NPL liposome is much higher than that on the surface of DMPC. It had been also found that the molecular weight of polymer had no effect on saturation molar ratio of lipid to polymer.

Figure 5. 3. Ratio of I_{Py}/I_{Np} for mixed singly labeled polymer: 20K-P_M88/240K-N74 with NPL as a function of lipid concentration, 25°C, λ_{ex} = 290 nm. Fluorescence spectra of mixed singly labeled polymer without (a) and with (b) of NPL at 25°C, λ_{ex} = 290 nm. Polymer concentration: [20K-P_M88] = 0.045 g/L, [240K-N74] = 0.055g/L, lipid concentration 1.0 g/L.

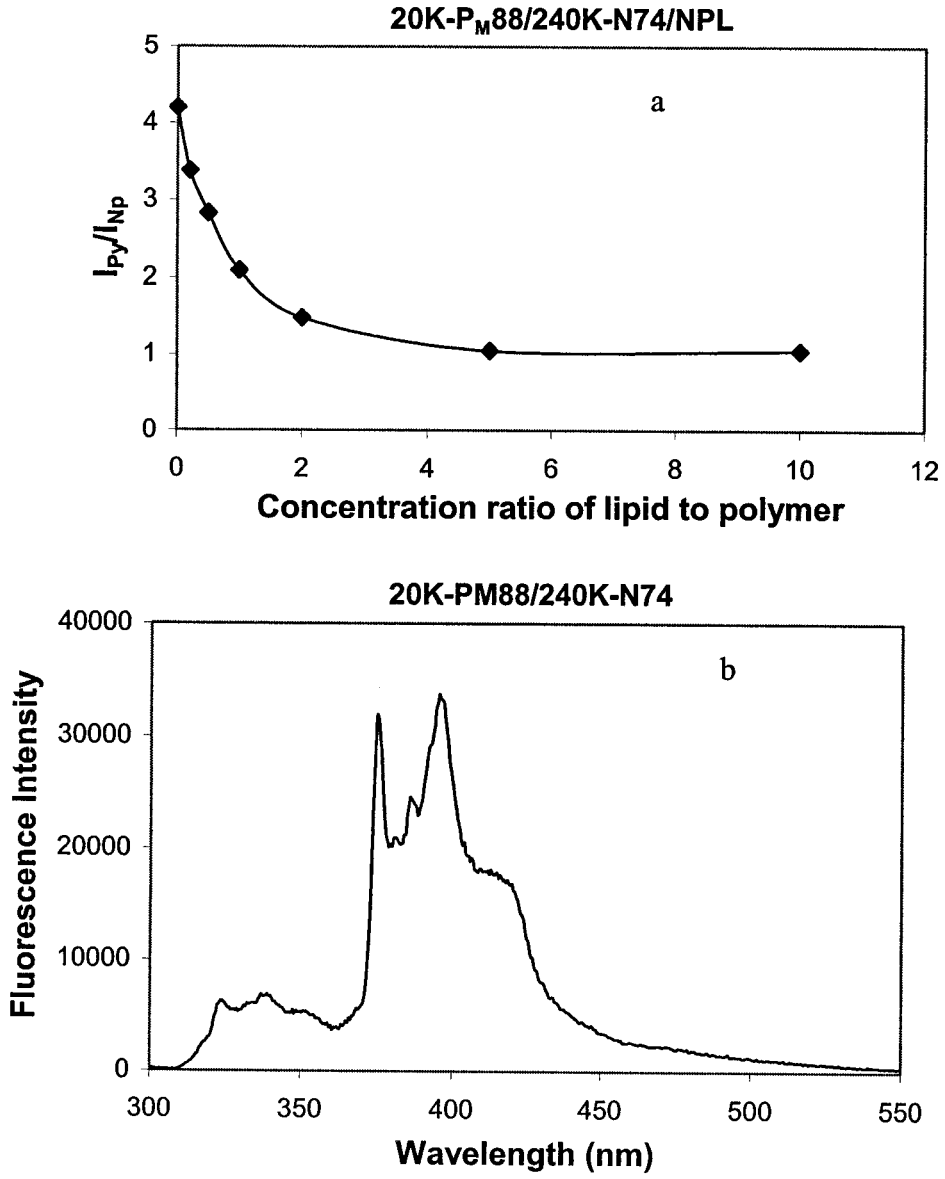

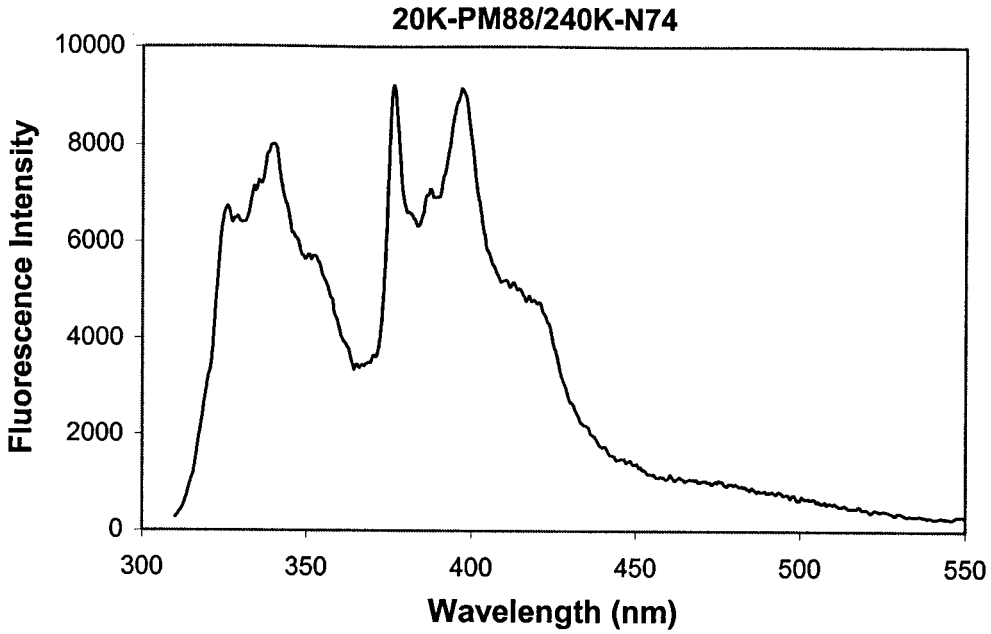

The grafting density of polymer for 240K-N72-P_B325 was the same as that of 20K-P_M88 when the same type of liposomes was used. This is because both of polymers has same saturated value of I_{Py}/I_{Np}. In summary, the interaction of the polymer with phosphatidylcholine membranes (DMPC) was much weaker than that with nonionic surfactant vesicles (NPL). The reason could be attributed by hydrogen bonding formed by the polyethylene oxide moiety in the surfactant and the amide moiety in the polymers.[4a] Meanwhile, the small size of head group in n-octadecyldiethylene oxide may be another reason.[73]

Quenching Study to Determine Pyrene Position As we known that pyrene moieties in the cholesterol-bearing polymers were separated apart by the presence of liposomes. Previous studies with PNIPAM-C18Py indicated that octadecane and pyrene moieties can be inserted into lipid bilayer together.[74] However, it was unclear whether the pyrene from the cholesterol-bearing polymers can be inserted into lipid bilayer with the

cholesterol moieties or will be still remained on the lipid surface. CPC carried liposomes were specifically prepared in order to clarify this issue. CPC and lipids were mixed in an organic solvent and the dried thin film of CPC and lipid was hydrated with buffers so that CPC can be randomly distributed in the lipid bilayer and generated CPC carried liposomes. The pyridinium ring of CPC is known as the ability of quenching pyrene fluorescence via diffusion-controlled quenching mechanism as described in Stern-Volmer model.[75] Of course, the fluorescence quenching may occur via a variety of processes such as collision, energy transfer, excitation-state reaction, or complex formation. If the entire hydrophobic substituents of the polymers could be inserted into lipid bilayer, the pyrene monomer intensity should be decreased due to the presence of CPC. Especially, it is true for the polymers such as 400K-P_B439, 400-P_B157 and 240K-P_B177 because no excimer emission of pyrene can be detected in water. Quenching data were plotted in terms of the Stern-Volmer equation.[10]

$$I_0/I = 1 + K_{sv}[Q]$$

where K_{sv} is the Stern-Volmer quenching constant; I_0 and I are the emission intensities at 377 nm with and without the quencher, respectively; Q is the quencher concentration.

Figure 5. 4. Lipid concentration ratio with the ratio I_{Mo}/I_M of PNIPAM-Pybucho in absence (I_{Mo}) and presence (I_M) of CPC bearing liposomes at 25°C, λ_{ex} = 346 nm, polymer concentration 0.05 g/L. (a) NPL, (b) DMPC.

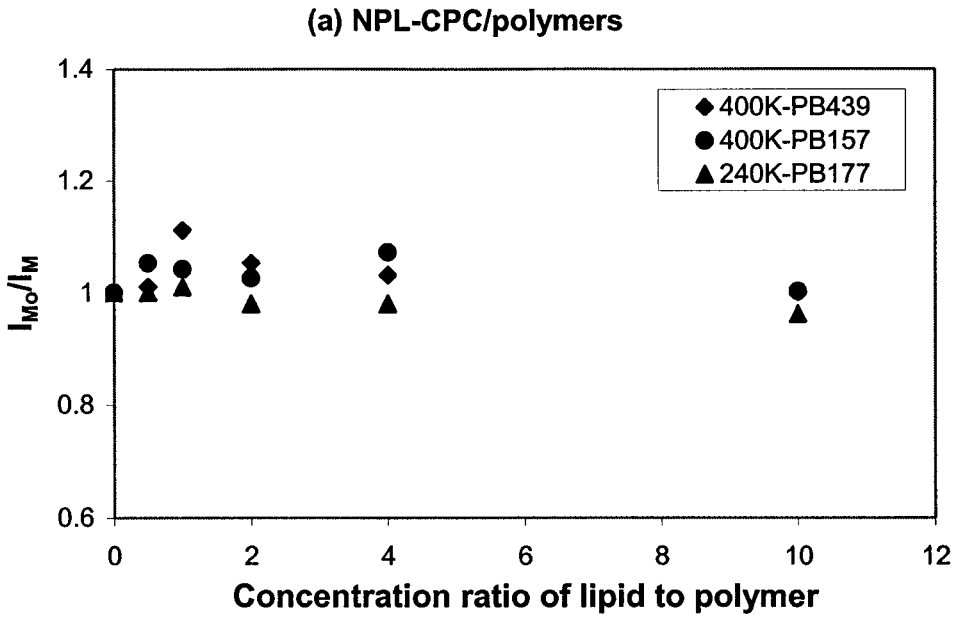

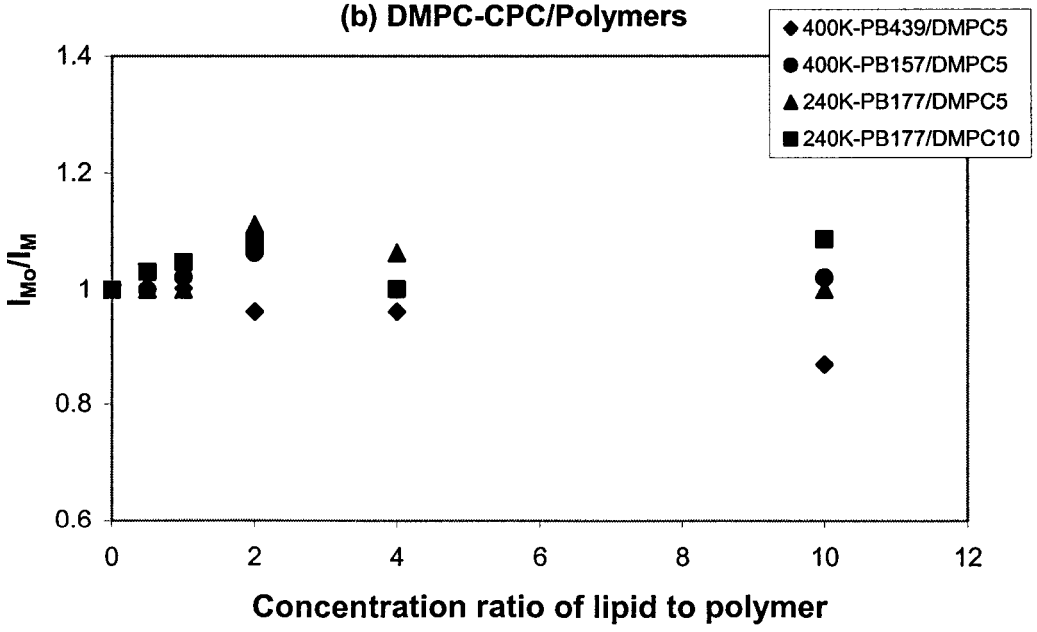

Figure 5.4 shows the ratio of pyrene monomer emission intensity of the polymers in the presence (I_M) and absence (I_{Mo}) of CPC liposomes as a function of lipid concentration ratio since the quencher concentration was proportional to lipid concentration. The ratios of I_{Mo}/I_M for 400K-P_B439, 400K-P_B157, and 240K-P_B177 remained as constant over the concentration range studied, indicating there is no quenching in the viscous lipid bilayer with all types of the studied liposomes. This result suggests that pyrene cannot be inserted into lipid bilayer instead of remaining on the lipid surfaces, which will further investigated below.

Figure 5. 5. Ratio of I_1/I_3 for 20K-P_M88 with liposomes as a function of molar ratio of lipid to polymer (25°C, λ_{ex} = 346 nm, polymer concentration: 0.05 g/L).

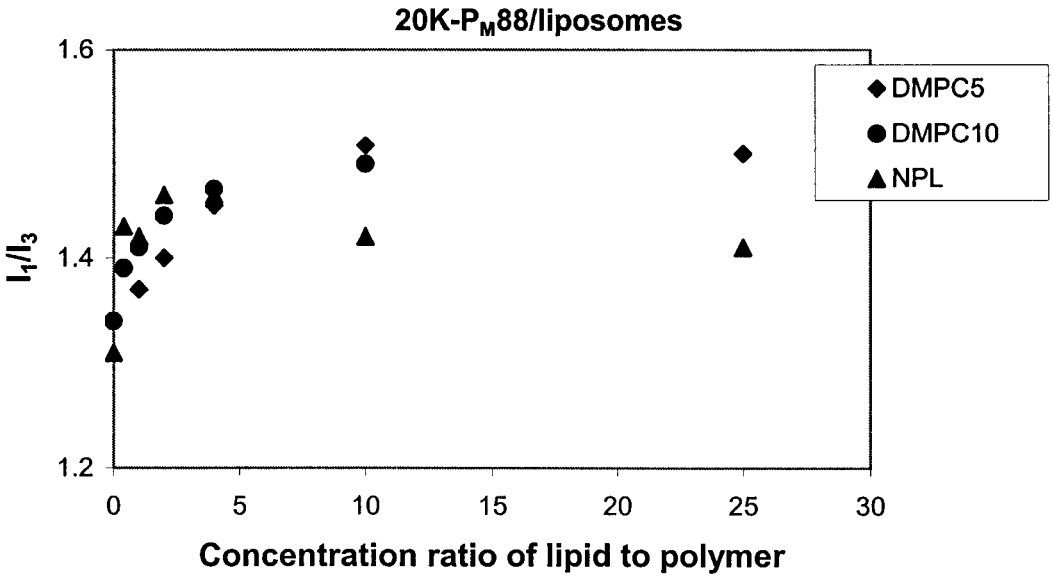

As previously discussed, the ratio of I_1/I_3 for pyrene represented the polarity of pyrene. If the environment around pyrene becomes less polar, a lower value of I_1/I_3 will be generated, otherwise a higher value of I_1/I_3 can be observed. It can be expected that

the ratio of I_1/I_3 for pyrenylmethyl labeled cholesterol-bearing PNIPAM would be decreased with an addition of liposomes, if pyrene together with cholesterol was inserted into lipid bilayer. The ratios of I_1/I_3 for 20K-P_M88/NPL and 20K-P_M88/DMPC5 complexes were given in Figure 5.5 as a function of lipid concentration. It can be seen from Figure 5.5 that the ratios of I_1/I_3 for both systems increased as when the molar ratio of lipid to polymer increased and a maximum value of I1/I3 as 1.5 can be measured for DMPC system and 1.45 for NPL system at the saturated ratio. These data were much higher than those for 20K-P_M88 in water. Together with the result of the quenching experiments, we suggest that pyrene was remained on the surface of lipid bilayer instead of inserting into lipid bilayer when the polymeric micelles were completely destroyed with liposomes.

5. 3. 2. Effects of Temperature on Interaction of Liposomes and Polymers The interaction of the polymers and liposomes was further evaluated by changing of temperature, especially, the LCST of the polymer or membrane phase transition (T_c). The liposome membrane exists in crystalline phase as gel at temperatures below T_c. The alkyl chains in an all-trans conformation are closely packed and the lateral diffusion coefficient of lipids as $10^{-11}cm^2\ s^{-1}$ was measured. Above T_c, the lipid bilayer transfers from gel to a liquid crystalline phase (L_a), i.e., the alkyl chains are in a state of chaos. Void volumes are created within the membrane so that the rotational and lateral diffusion was enhanced within the plane of the membrane. The lateral diffusion coefficient of lipids can increase by four orders of magnitude ($10^{-7}\ cm^2\ s^{-1}$) as compared to that of lipids in gel. Can cholesterol anchor moiety diffuse inside fluid membrane above T_c and act as

alkyl chain? The microcalorimetry was employed to evaluate the effect of temperature on the fluorescence in the liposome/polymer complex systems,.

Microcalorimetry Differential Scanning Microcalorimetry (DSC) is a useful tool to study the lipid phase transition in lipid membranes. The variation of excess specific heat with temperature for gel-to-liquid crystalline phase transition exhibits a first-order endothermic process. Microcalorimetric traces of the DMPC/polymer complexes with an excess of the liposomes are shown in Figure 5. 6. The main signal shown at 24°C was assigned to the DMPC gel-liquid crystal phase transition and the minor signal shown at 14.8°C was assigned to the pretransition of the lipid bilayer. Both main transition and pretransition temperatures of the DMPC membrane were independence with polymers, and the pretransition can be clearly observed in all the cases[76](Table 5. 2).

Figure 5.6. DSC traces of p-DMPC liposomes and p-DMPC/polymer mixtures, polymer concentration 0.1 g/L, ratio of lipid to polymer from top to bottom: 10, 20, 30. (a) 240K-P_B177/p-DMPC, (b) 240K-N72-P_B325/p-DMPC, (3) 20K-P_M88/p-DMPC (10, 30).

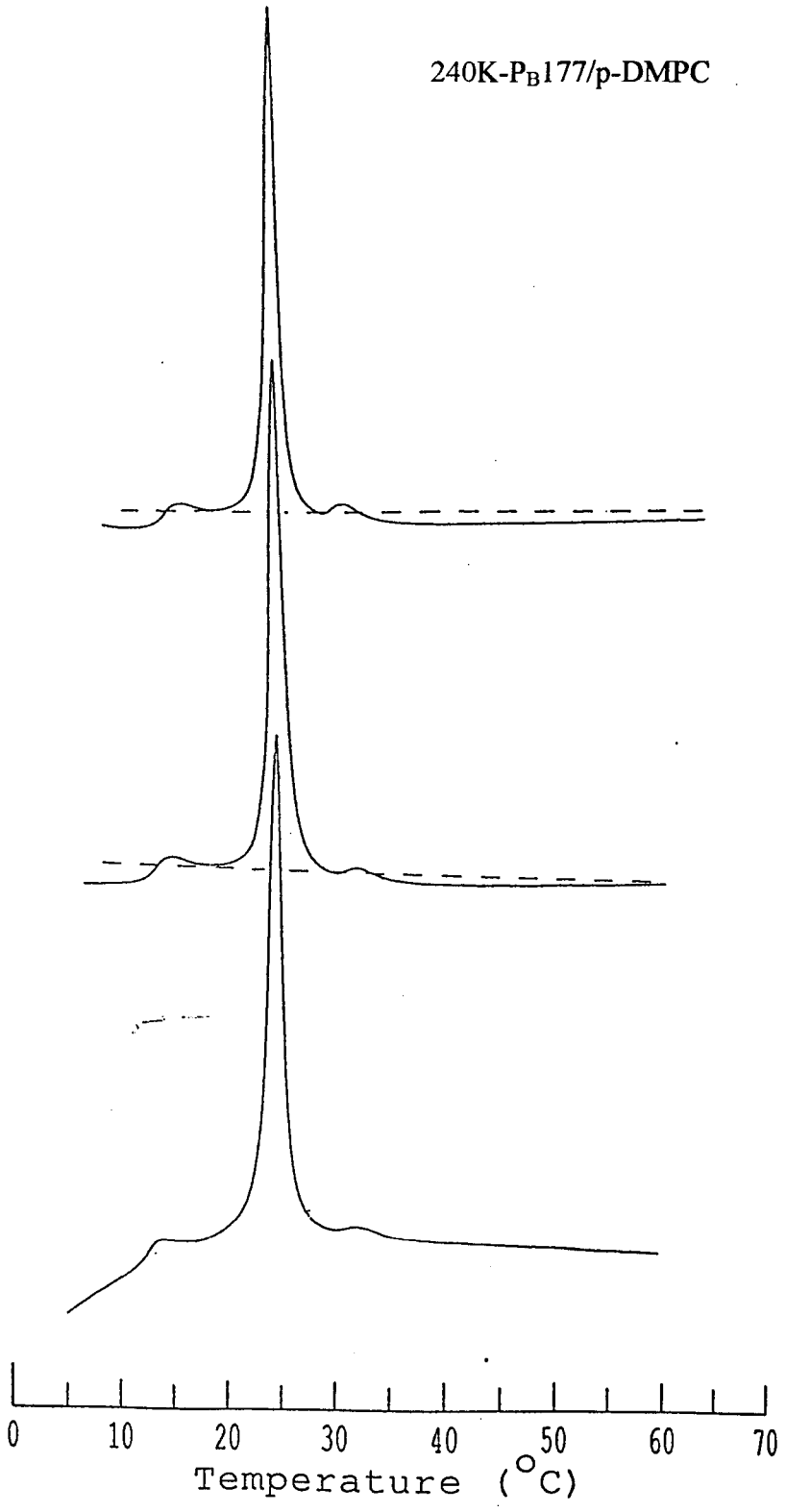

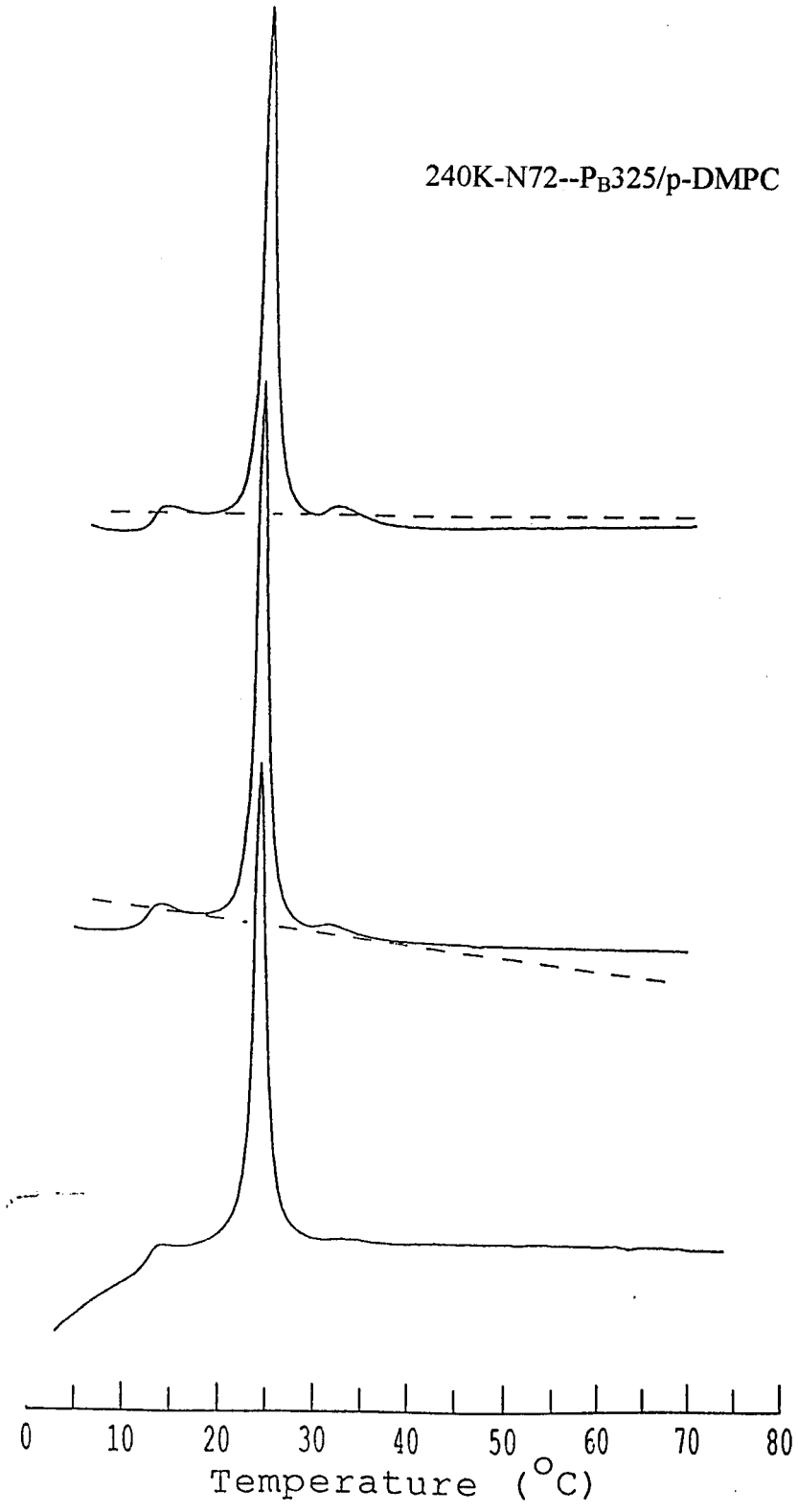
240K-N72--PB325/p-DMPC
0
10
20
30
40
50
60
70
80
Temperature (°C)

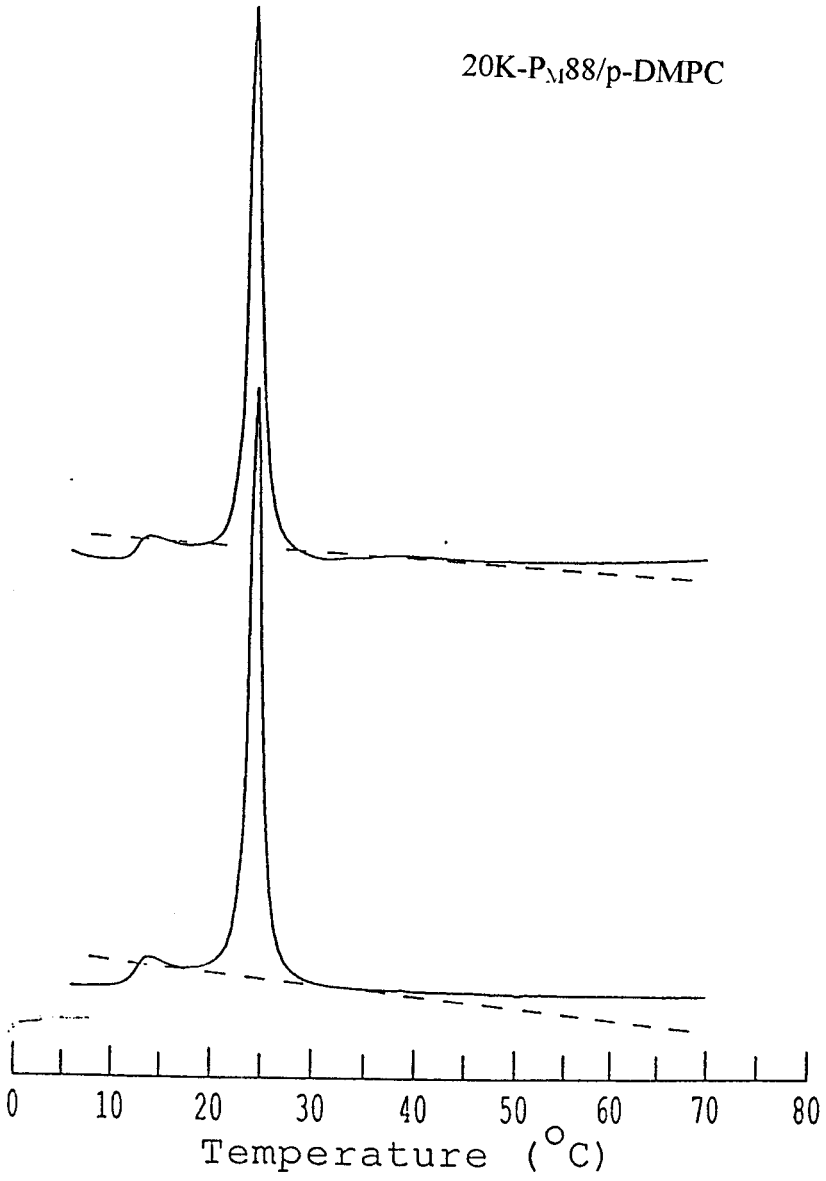
20K-P$_M$88/p-DMPC
0
10
20
30
40
50
60
70
80
Temperature (°C)

The LCST of 240K-P_B177 in the 240K-P_B177/DMPC complexes was clearly shown in both heating and cooling traces as a molar ratio of lipid to polymer (R_c) increased to 30. The LCST of 240K-N72-P_B325 in the 240K-N72-P_B325/DMPC complexes was much obvious in the cooling scan than that in the heating scan with R_c as 30 and in whole range of Rc form 10 to 20. In all cases, the polymers exhibited smaller and broad peaks compared with the polymers alone, and the enthalpies of the phase transition of the polymers were much lower than those obtained in buffer. The LCST of 20K-P_M88 in 20K-P_M88/DMPC complexes was undetectable in either heating or cooling scan when a molar ratio of lipid to polymer was equal or higher than 20. Thus, except for 20K-P_M88, the characteristics of the polymer thermal phase transition in DMPC/polymer complexes kept unchanged even in the case with an excess of lipids (assuming that all the polymers grafted onto liposome surfaces).

Table 5. 2. Phase Transition Temperature of DMPC/Polymer Complexes.

Complex	**LCST**	**Ratio of lipid to polymer**	**1st Heating**	**1st Cooling**	**2nd Heating**
			T_c (°C)	T_c (°C)	T_c (°C)
p-DMPC	-	-	24.3	-	-
DMPC5	-	-	Broad	-	-
p-DMPC/ 20K-P_M88	No LCST detected as $R_c \geq 20$	10	24.2	23.9	
		20	24.2	24.0	
		30	24.3	24.1	24.2
		40	24.2	24.2	
p-DMPC/ 240K-N72-P_B325	Detectable in all ratios	10	24.1	23.9	
		20	24.3	24.0	
		30	24.3	24.0	24.3
p-DMPC/ 240K-P_B177	Detectable in all ratios	10	24.3	23.9	
		20	24.3	24.0	
		30	24.3	24.1	24.3

Error range: $\leq \pm 0.2$

Figure 5. 7. DSC traces of NPL and NPL/polymer mixtures, polymer concentration 0.3 g/L, ratio of lipid to polymer from top to bottom in order of increasing: (a) 240K-P_B177/NPl, 10, 20, 30. (b) 240K-N72-P_B325/NPL, 10, 20. (C) 20K-P_M88/NPL, 10, 30.

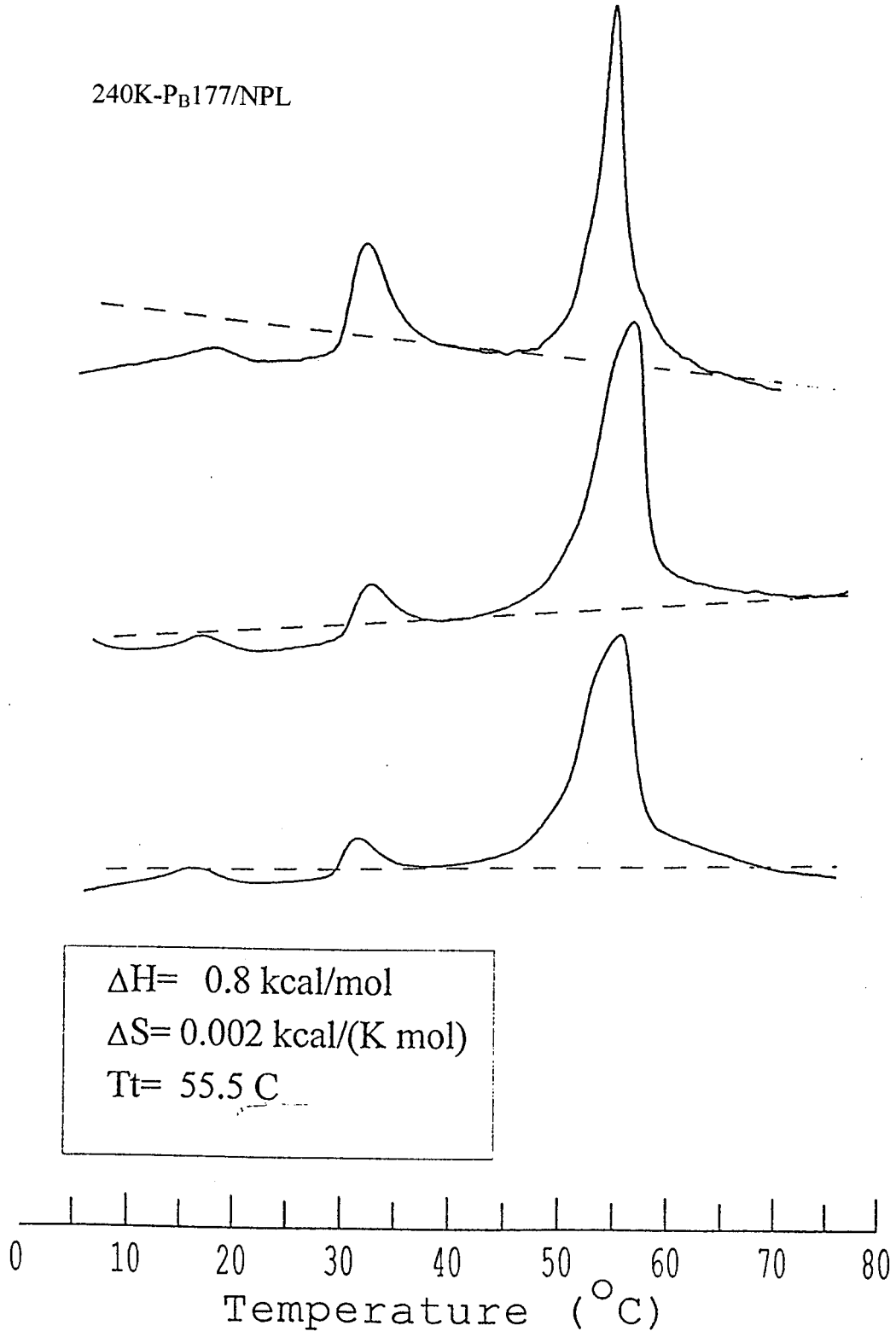

240K-N72--P_B325/ NPL

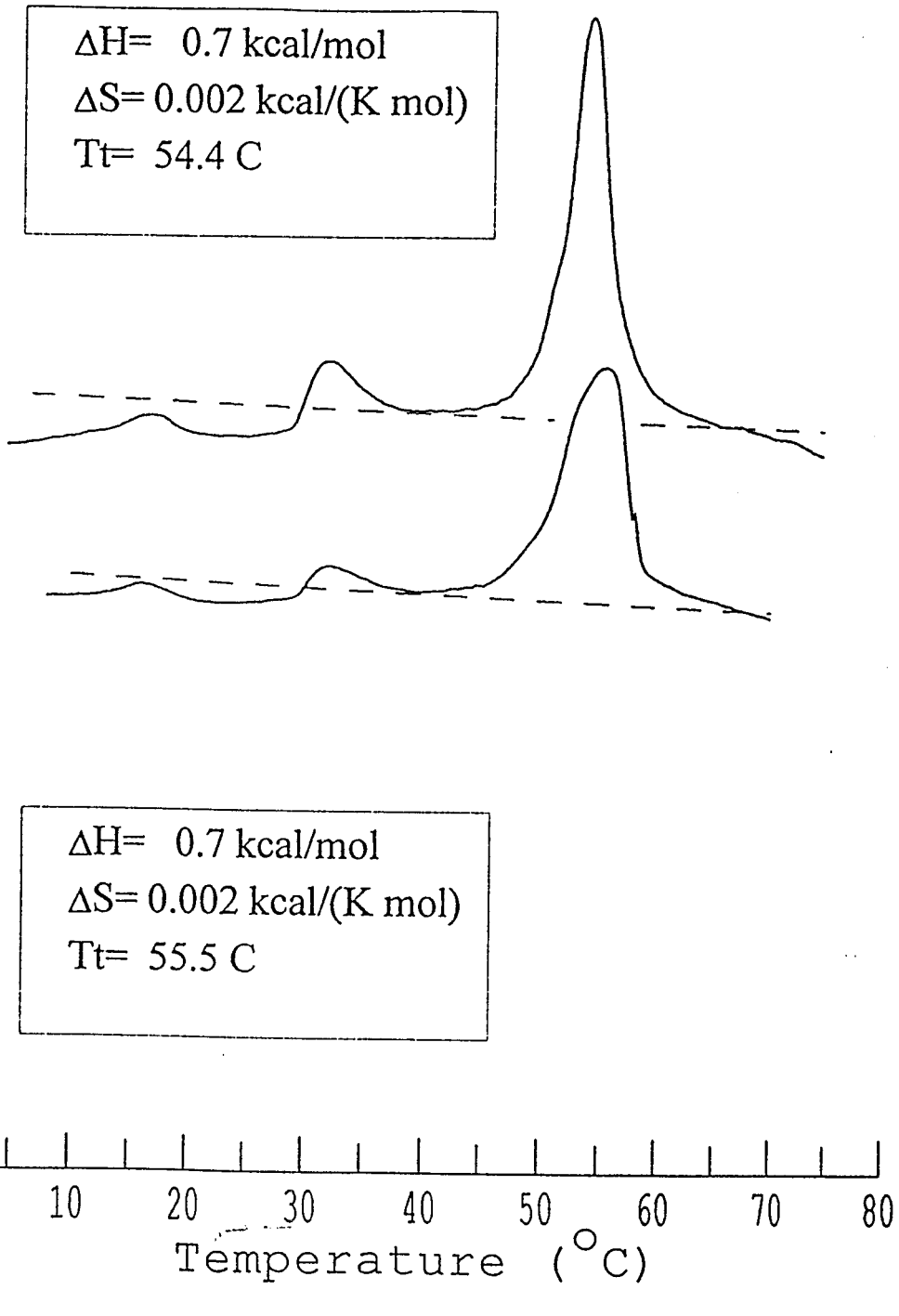

20K-P_M88/ NPL

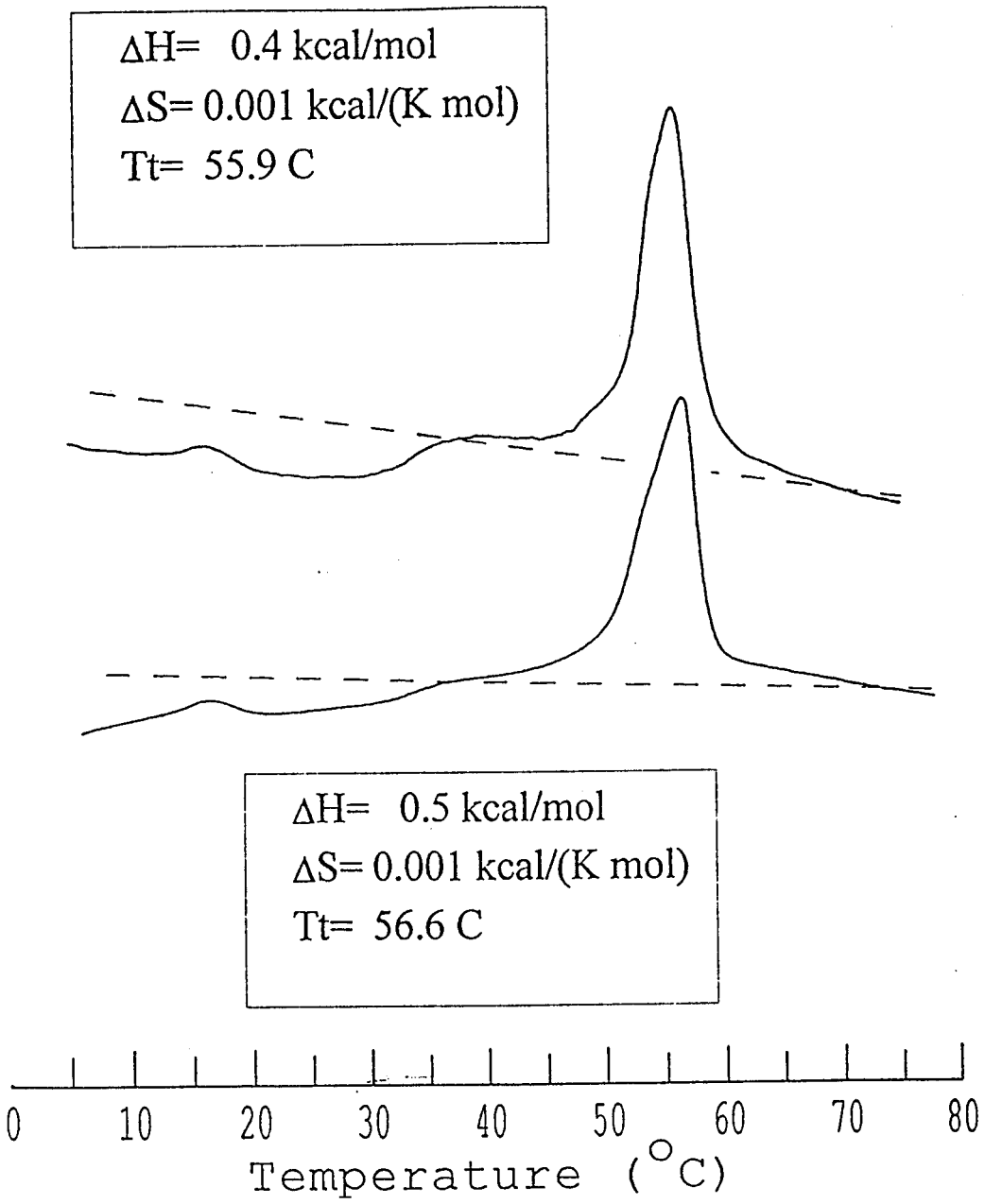
ΔH= 0.4 kcal/mol
ΔS= 0.001 kcal/(K mol)
Tt= 55.9 C
ΔH= 0.5 kcal/mol
ΔS= 0.001 kcal/(K mol)
Tt= 56.6 C
0
10
20
30
40
50
60
70
80
Temperature (°C)

In the NPL/polymer complexes with an excess amount of NPL, the main phase transition of NPL significantly decreased in the presence of the polymers when R_c varied from 10 to 30 (Table 5. 3). On the other hand, the phase transition of all polymers (240K-P_B177, 240K-N72-P_B325 and 20K-P_M88) was readily observed in all the cases at temperatures close to the LCST in the presence of an excess amount of liposomes (Figure 5. 7). The more lipids existed in the system, the less sharp the polymer phase transition.

The thermal behavior of NPL was readily affected by the polymer coated onto liposome surfaces and the hydrophobic groups anchored into lipid bilayers, but the thermal properties of DMPC liposomes were insensitive to the presence of the polymers. The polymers (except for 20K-PM88 in DMPC liposomes) can undergo the phase transition at temperature consistent with the LCST.

In conclusion, the interaction become more strongly with increasing amount of hydrophobic domain incorporated in the polymers.

Table 5. 3. Phase Transition Temperature of NPL/Polymer Complexes.*

Complexes/Rc	1st Heating T_c (°C)	1st Cooling T_c (°C)	2nd Heating T_c (°C)	2nd Cooling T_c (°C)
NPL	58.1	57.1	56.1	55.9
NPL/240K-P_B177				
10	53.9	53.0	54.1	53.1
20	55.0	53.0		
30	55.0	53.4		
NPL/240K-N72-P_B325				
10	54.4	53.2	54.3	53.2
20	55.5	54.4	54.8	54.7
30	57.0	54.8		
NPL/20K-P_M88				
10	55.9	53.5	54.5	53.2
15	55.4	53.6		
30	56.6	54.5	56.7	56.1

* LCST of the polymers was detectable in all ratios and all complexes.
Error range: ≤± 0.4

Figure 5. 8. Ratio of I_E/I_M for 20K-PM88 as a function of temperature with liposomes (λ_{ex} = 346 nm; polymer concentration: 0.05 g/L; full signals: heating scan; empty signals: cooling scan).

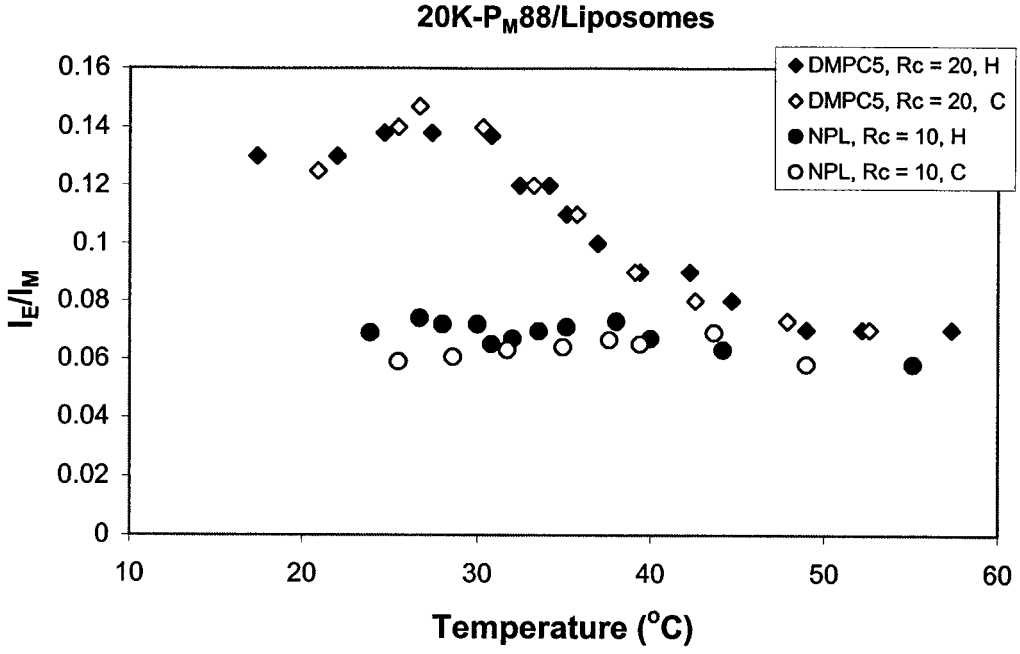

The effect of temperature on fluorescence of polymer/liposome complexes Mixtures of hydrophobically modified polymers and DMPC or NPL liposomes were subjected to heating-cooling cycles in the temperature range from 20 to 60°C. The temperature range covered phase transitions of the polymers and the liposomes. As previously studied, the temperature can induce the changes of fluorescence emission and energy transfer from excited naphthalene to pyrene in the polymer solutions. The pyrene emission in the NPL/20K-P_M88 system ($R_c \geq 10$) was hardly affected by increasing temperature of the mixtures above either the LCST of the polymers or the T_c of the liposomes (Figure 5.8). Namely, the ratio of I_E/I_M remained constant with increasing temperature above either the LCST or the T_c. The ratio of I_E/I_M showed the same trend in the cooling scan as that in the heating scan. This behavior is clearly different from the effect of temperature on the

intensity ratio of pyrene excimer to monomer emission in the water/polymer systems. In the aqueous solutions, the excimer emission decreased as the solutions were heated above the LCST, indicating that the polymeric micelles were disrupted. This difference suggests that the polymer can be stabilized on the liposome surfaces even above the LCST and the T_c. In the DMPC/20K-P_M88 system ($R_c \geq 20$), the ratio of I_E/I_M started to decrease from 0.13 to 0.07 with increasing temperature up to 30°C and it reached the same plateau at 40°C as that of the NPL/20K-P_M88 system ($R_c \geq 10$) (Figure 5.8). The ratio I_E/I_M followed the reverse trend iIn the cooling scan when compared with that in the heating scan. The ratio of I_E/I_M for 20K-P_M88 in water decreased at a temperature near 36°C in the heating scan and followed the reverse trend in the cooling scan (Figure 5.9). It is very interesting that the onset temperature of I_E/I_M was affected by the presence of the DMPC5 liposomes.

Figure 5. 9. Ratio of I_E/I_M for 20K-P_M88 as a function of temperature without liposomes (λ_{ex} = 346 nm; polymer concentration: 0.05 and 0,1 g/L; full signals: heating scan; empty signals: cooling scan).

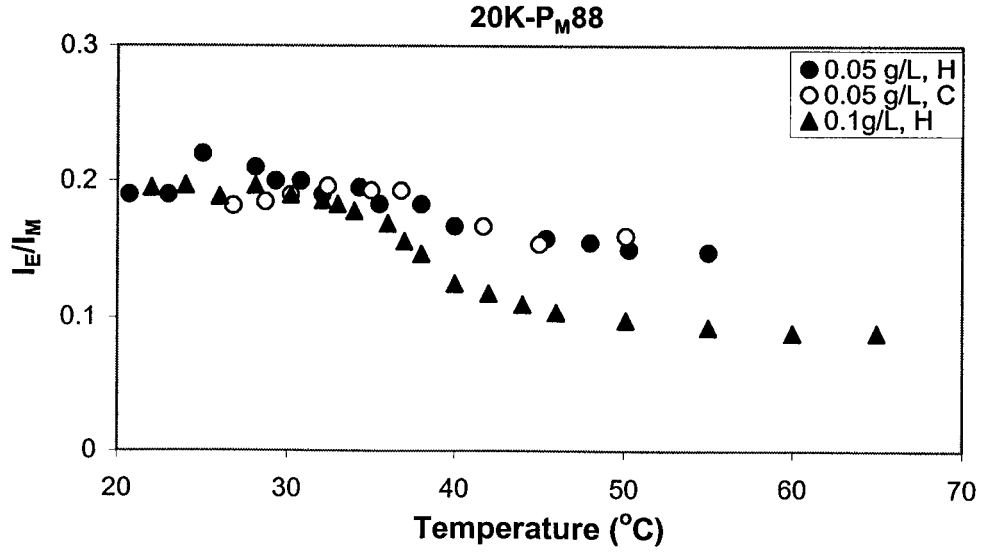

Figure 5. 10. DSC traces of 20K-P_M88 in water, polymer concentration 0.92 g/L,from bottom to top: 1st heating, 1st cooling, 2nd heating and 2nd cooling.

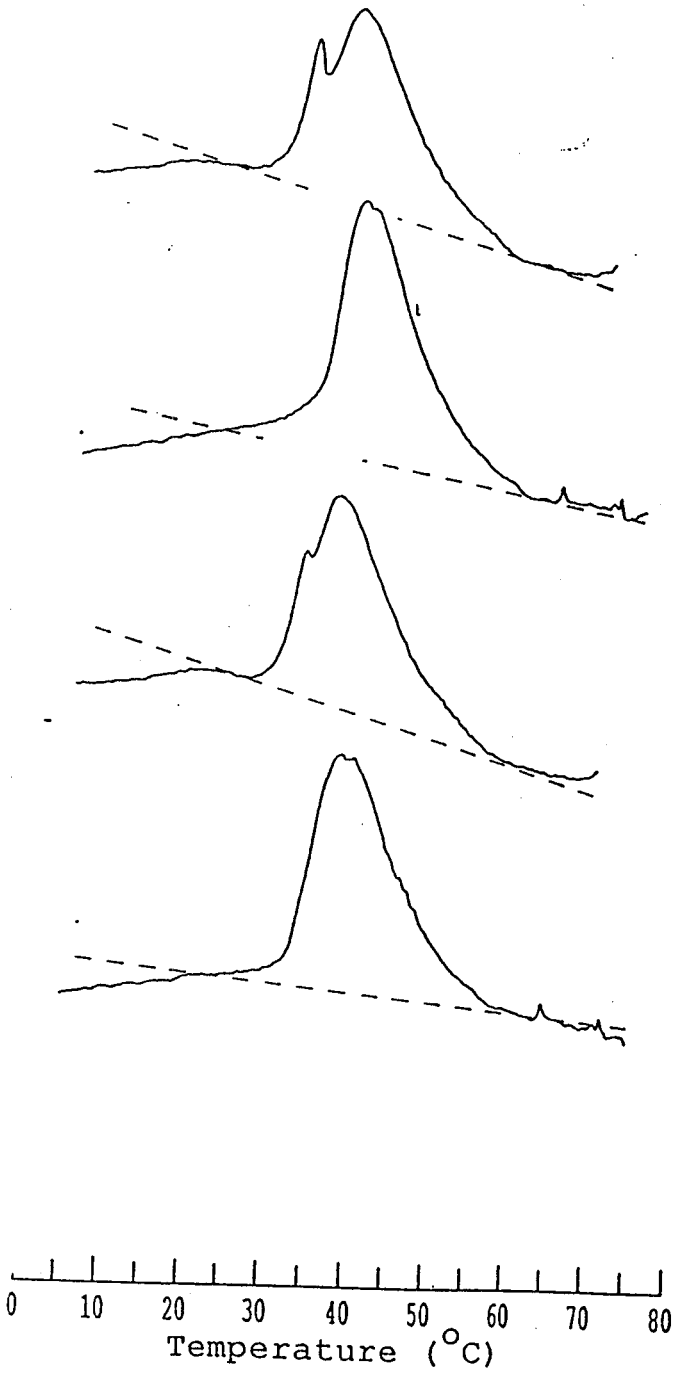

The LCST of 20K-P_M88 as 36.5°C was also observed by UV. However, DSC traces of 20K-P_M88 in water showed two transitions (Figure 5.10), one located around 32 °C and the other at 40°C. Two peaks were partially overlapped and the peak at 32°C was more obvious in the cooling scan. The phenomena can be reproduced in subsequent heating-cooling cycles at various concentrations of the polymer (Fig. 5.10). The LCST of 20K-P_M88 near 32°C cannot be detected by UV in an aqueous solution but discovered by DSC measurement. The LCST was also observed with DMPC5 in the fluorescence measurement. The peak around 40°C in the DSC trace of 20K-P_M88 aqueous solution was completely disappeared in the presence of DMPC and partially disappeared in the presence of NPL. It is clear that both fluorescence and DSC have special advantages to examine polymer/liposome complexes and reliable results can be obtained by combination them together.

It is important to recall that the ratio of I_E/I_M for octadecyl (C18Py) end-modified PNIPAM and DMPC system increased with increasing temperatures above the LCST,[6a] indicating that the polymers escaped from the liposome surfaces by the driving force of the polymer chain collapse. The difference between cholesterol modified PNIPAM and octadecyl chain modified PNIPAM demonstrates that the cholesterol chain has a higher affinity anchor as the bilayers than the octadecyl chain.

Effect of temperature on I_1/I_3 of polymer/liposome complexes The ratio of I_1/I_3 for 20K-P_M88/liposome system remained constant with increasing temperature up to 30°C, then decreased with increasing temperature continuously and reached to a plateau at 55°C in

Figure 5. 11. Ratio of I_1/I_3 for 20K-P_M88 as a function of temperature with liposomes (λ_{ex} = 346 nm; polymer concentration: 0.05 g/L, lipid to polymer concentration ratios were 10, 20, respectively. Full signals: heating scan; empty signals: cooling scan).

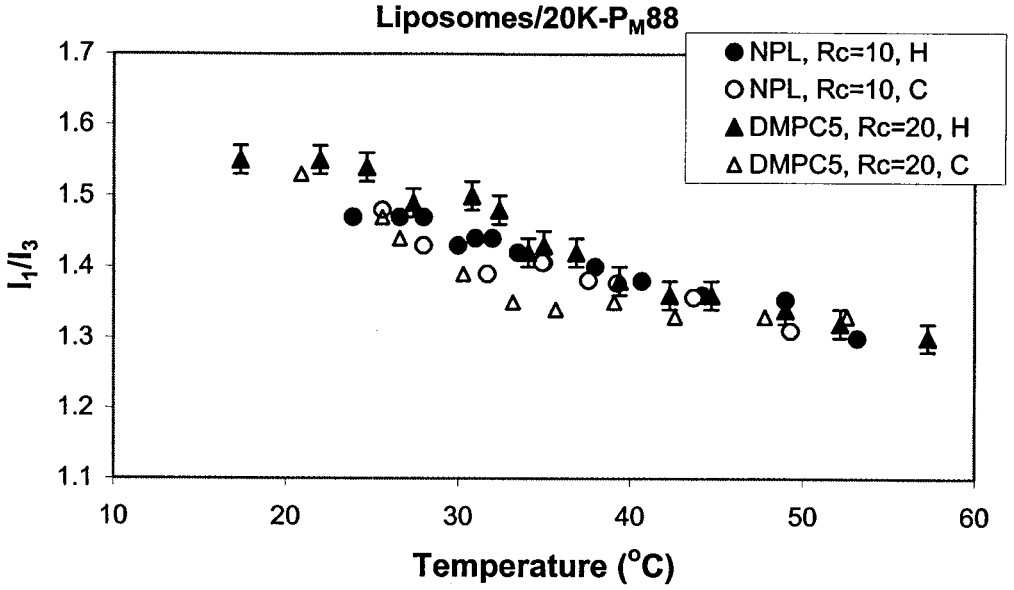

both liposome systems (Figure 5.11) finally. The ratio of I_1/I_3 for the 20K-P_M88/NPL complex systems followed the same trend in the heating-cooling cycle. The ratio of I_1/I_3 for 20K-P_M88/DMPC5 systems in the cooling scan was lower than that in the heating scan. The ratio of I_1/I_3 for 20K-P_M88/liposomes as a function of temperature has same behavior as that of 20K-P_M88 in water. The lower values of I_1/I_3 obtained at high temperatures can be attributed the effect of a more hydrophobic microenvironment from dehydrated polymeric chains, and the higher values of I_1/I_3 at low temperature is the reason of a more hydrophilic microenvironment from hydrated polymeric chains.

Effect of temperature on NRET of polymer/liposome systems Both pyrene emission intensity (Figure 5.12) and I_{Py}/I_{Np} remained constant with increasing temperature up to 40 °C in either the doubly labeled polymer solution or liposome complex systems with at the saturation solution of polymer (240K-N72-P_B325/NPL, $R_c \geq 5$). The ratio of I_{Py}/I_{Np}

decreased at the inception of gel-liquid crystal transition near 40°C and leveled off at lipid phase transition near 52°C. The LCST of 240K-N72-P_B325 has no significant effect on the ratio of I_{Py}/I_{Np} although the LCST can be clearly observed in DSC trace. However, the starting decrease point of I_{Py}/I_{Np} in 240K-N72-P_B325/DMPC5 ($R_c = 20$) system moved toward the LCST of the polymer near 30°C. Ratio of I_{Py}/I_{Np} remained constant with increasing temperature until 30°C and then decreased with continuing increase of temperature and reached a plateau near 58°C. The change of I_{Py}/I_{Np} in a cooling scan followed the same trend as the heating scan. This result is the same as the case of the polymer 240K-N72-P_B325 in water as a function of temperature. Therefore, the LCST of 240K-N72-P_B325 in the presence of DMPC5 can be clearly observed in fluorescence and DSC measurements, but the LCST of 240K-N72-P_B325 in the presence of NPL can only be detected in DSC traces.

Figure 5. 12. Ratio of I_{Py}/I_{Np} for doubly labeled polymer as a function of temperature with liposomes (λ_{ex} = 290 nm, lipid to polymer molar ratio was 10, 20, respectively, full signals are heating scan and empty signals are cooling scan). (a) Fluorescence emission intensities of 240K-N72-P_B325/NPL mixtures as a function of temperature, I_{Np}: naphthalene emission intensity, I_{Py}: pyrene emission intensity, concentration ratio of lipid to polymer: 10 or 20.

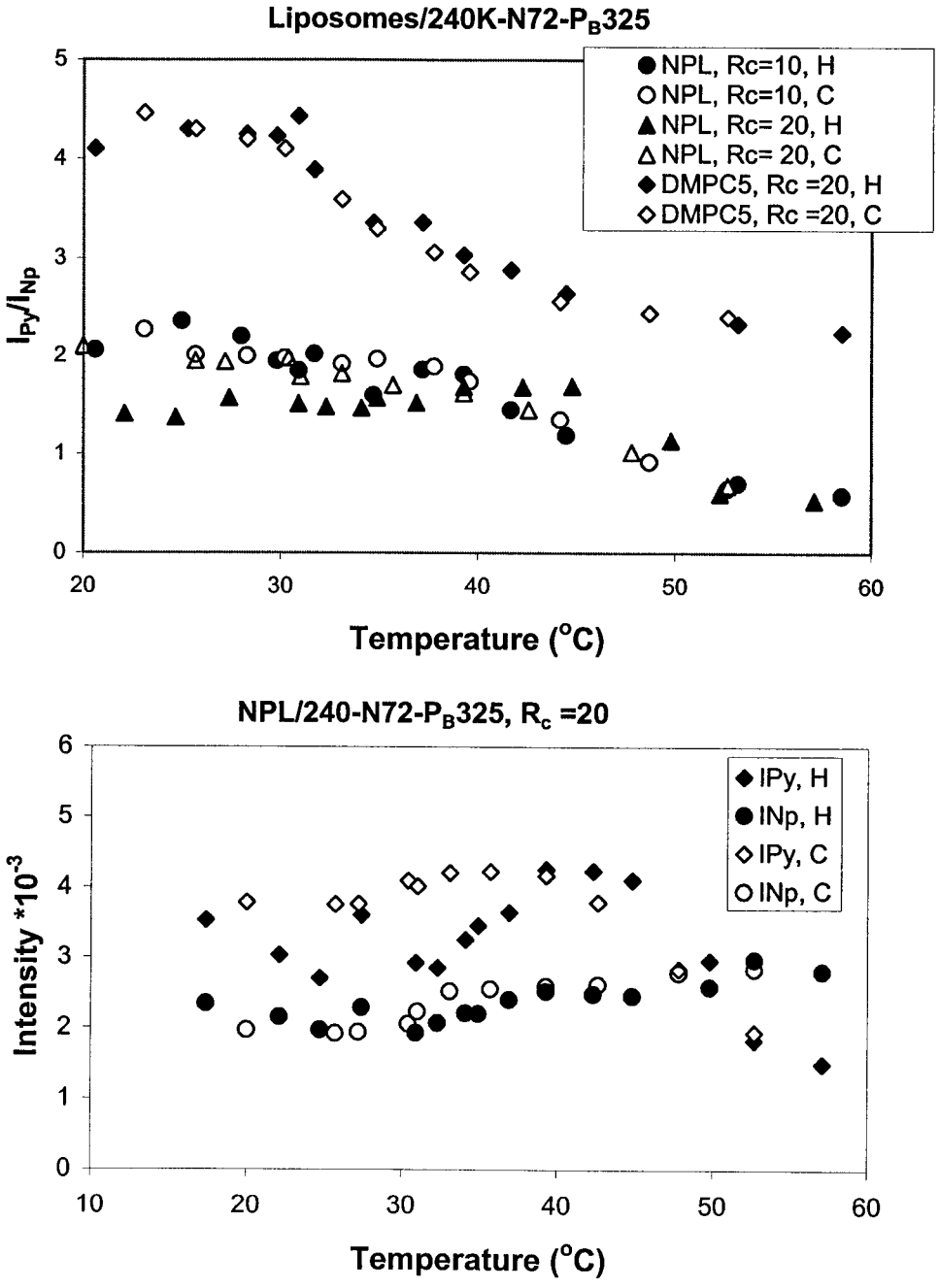

Figure 5. 13. Ratio of I_{Py}/I_{Np} for mixed singly labeled polymers 20K-P_M88/240K-N74 as a function of temperature with NPL (λ_{ex} = 290 nm, [20K-P_M88] = 0.045 g/L, [240K-N74] = 0.055 g/L. lipid to polymer ratios were 10 and 20, respectively. Full signals are heating scan and empty signals are cooling scan). (a) The emission intensity of pyrene and naphthalene of the 20K-P_M88/240K-N74/NPL complex as a function of temperature.

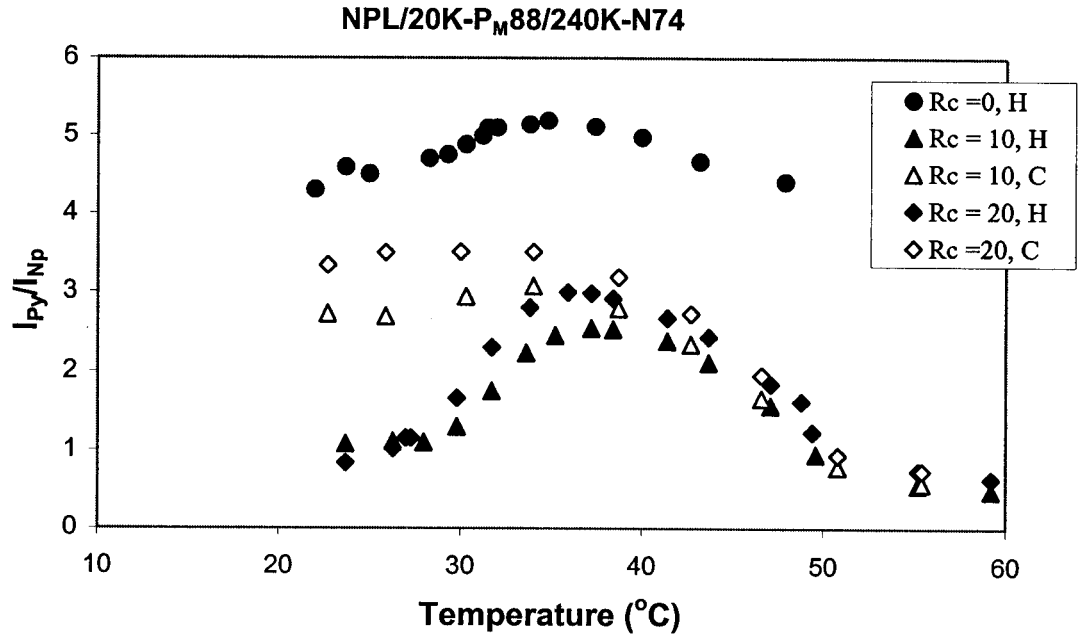

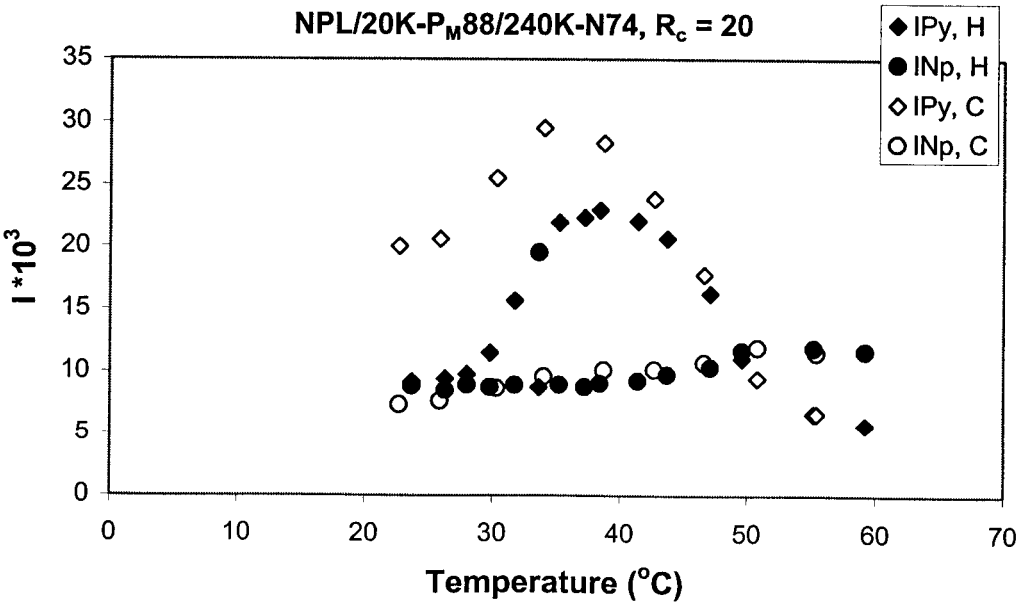

The liposome complexes (20K-P_M88/240K-N74/NPL) from mixture of singly labeled polymer revealed different results as shown in Figure 5.13 as compared with the liposome complexes from the doubly labeled polymer. Both pyrene emission intensity I_{Py} and the ratio of I_{Py}/I_{Np} kept constant below the LCST, then increased with increasing temperatures above the LCST until close to 40°C decreased further with increasing temperature. The ratio of I_{Py}/I_{Np} followed the reverse trend with decreasing temperature near 40°C in the cooling scan. After that, the ratio kept unchanged and was much higher than the initial value. However, pyrene emission intensity I_{Py} increased with decreasing temperatures to 30°C, then decreased with decreasing temperature. The increase of I_{Py}/I_{Np} indicates that the interpolymeric chains can shrink above the LCST and two chromophores with the structure of more compact will anchored on the lipid surfaces. The decreased region of I_{Py}/I_{Np} may present the chromophores separated from contracted interpolymeric chains. Further investigation will be performed by exploring the driving force of the separation. However, it is certain that there is no lateral diffusion of cholesterol acted by the driving force of the collapsed polymeric chains. The ratio of I_{Py}/I_{Np} for mixture of singly labeled C_{18} and modified PNIPAM slightly increased with increasing temperature above the LCST in the presence of distearoylphosphatidylcholine (DSPC) liposomes, but a dramatic increase can be observed when temperature increased close to T_c.[71] This is because that the hydrophobic substituents, pyrene and $C_{18}H_{37}$, were jointly inserted into lipid bilayer and moved towards close by lateral diffusion. Hence, the energy transfer extent was always increased throughout the all phase transition temperatures.[4a]

In the cooling scan, the value of I_{Py}/I_{Np} increased first, then kept constant after the temperature was lower than 40°C. This phenomenon was similar as $C_{18}H_{37}$ bearing PNIPAM and the reason may be due to the "frozen" cholesterol inside bilayer by the temperature of frozen membrane.

By comparing two anchors (cholesterol and $C_{18}H_{37}$), we can conclude that cholesterol cannot simply move together by lateral diffusion in the fluid membrane (I_{Py}/I_{Np} decreased around T_c) as the alkyl chain $C_{18}H_{37}$ did but there will exist a complex movement of cholesterol. The high lateral diffusion coefficient of lipids in fluid bilayer is only suitable for alkyl chains.

5. 3. 3. Gel-filtration Chromatography

Gel filtration of the cholesterol modified PNIPAM and DMPC5 liposome complexes was carried out on Sephacryl S-1000. This method gave a great recovery of DMPC liposomes and was suitable for spherical particles with sizes up to 400 nm. The DMPC5 liposomes used here contained 20% cholesterol and 5% DDAB, thus sharp phase transition T_c was vanished and a broad peak over a temperature range from 5 to 60 °C was observed. The 240K-P_B177 and 240K-N72-P_B325 polymers were applied to interact with DMPC5 liposomes, in which both polymers possessed the same molecular weight but a different level of hydrophobic substituents. The suspensions of DMPC5 liposome and the solutions of polymer 240K-P_B177 were first passed through the column respectively to ensure no overlap for each profiles.

Figures 15a and 15c show the elution profiles of liposome suspension and polymer solution. After the solution of the polymer/liposome complexes (240K-

P_B177/DMPC5) was injected to the column, the eluted fractions were collected to analyze the polymer content by a fluorescence assay and the lipid content by phosphate analysis. Two elution profiles were observed for the polymer/liposome complex: one from the liposomes as shown in Figure 5. 14b and another from the polymers as shown in Figure 5. 14d. Figure 5. 14b shows that the lipid distribution in the polymer/liposome complex was slightly left-shifted if compared with the elution profile of DMPC5 liposome suspension, which indicates the amount of larger liposomes was increased by coating polymer onto liposome surfaces.

Figure 5. 14. Elution profiles from Sephacryl S1000 at 20°C. Volume of all samples applied to the column was 0.70 mL, lipid concentration: 15 g/L, polymer concentration: 1.5 g/L. (a)DMPC5, (b)240K-P_B177, (c)lipid from DMPC5/240K-P_B177 complexes, (d)polymer from DMPC5/240K-P_B177 complexes.

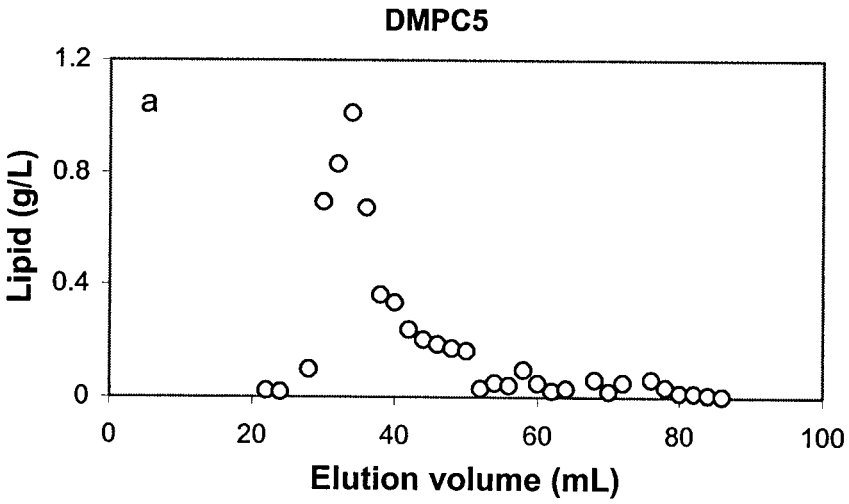

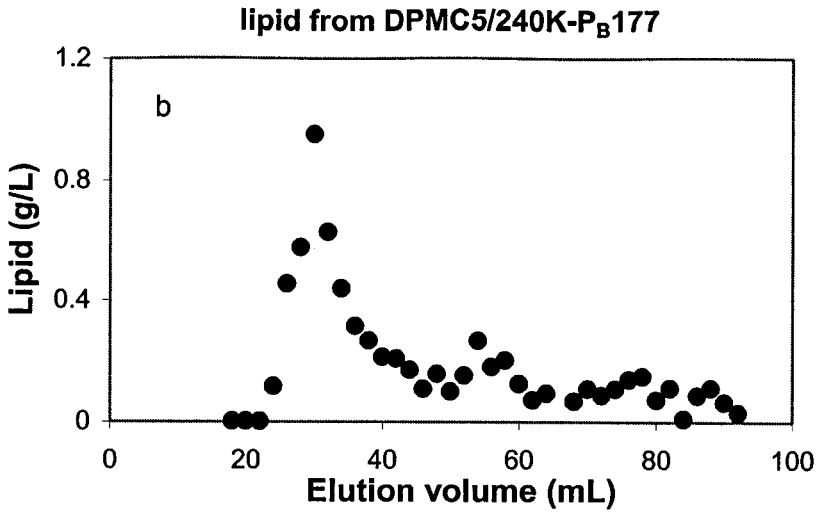
lipid from DPMC5/240K-PB177
b
Lipid (g/L)
1.2
0.8
0.4
0
0
20
40
60
80
100
Elution volume (mL)

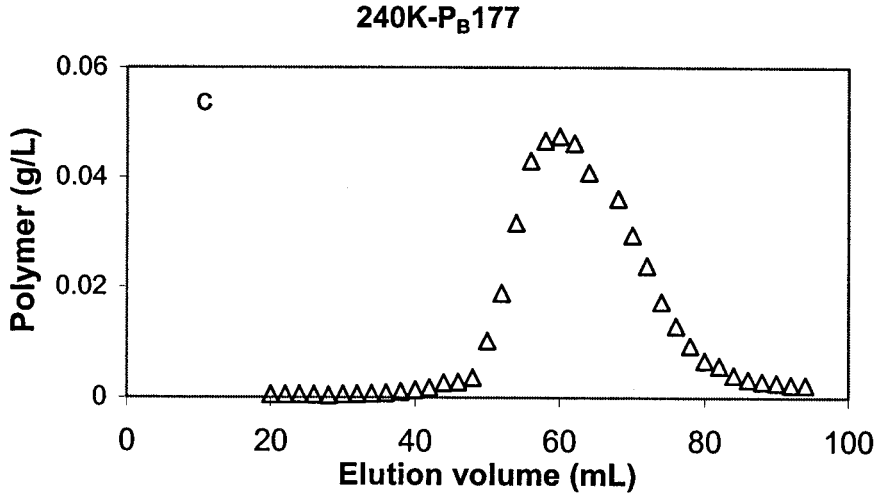
240K-PB177
c
Polymer (g/L)
0.06
0.04
0.02
0
0
20
40
60
80
100
Elution volume (mL)

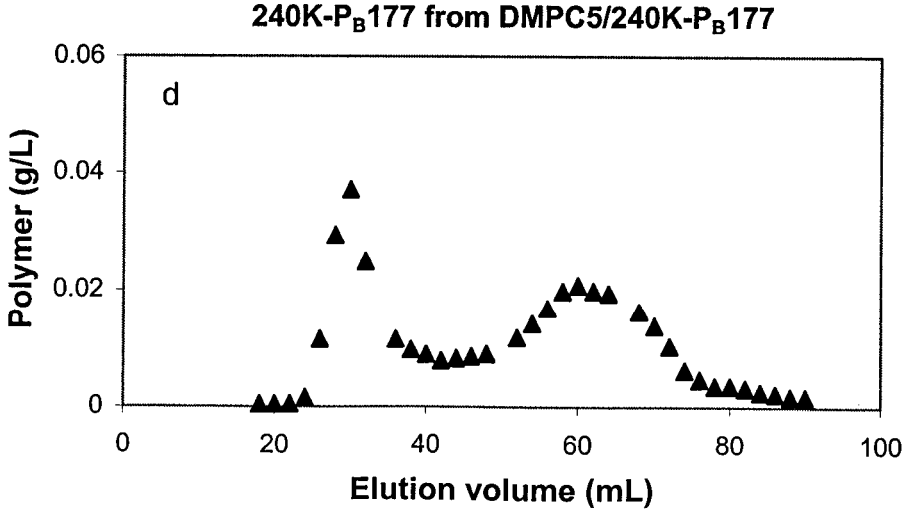
240K-PB177 from DMPC5/240K-PB177
d
Polymer (g/L)
0.06
0.04
0.02
0
0
20
40
60
80
100
Elution volume (mL)

The elution profile of the polymer from liposome complexes displayed a significant difference as compared with that of the polymer solution. Figure 5.14d shows that two distributions exist in the elution profile of the polymer from liposome complexes. One corresponded to the elution fractions of liposomes (centered approximately on 30 mL), and another corresponded to the elution profile of polymer solution (centered approximately on 60 mL). A superposition of two profiles of the polymer and liposomes from polymer/liposome complexes indicates co-elution of the polymer and liposomes. It can be taken as strong evidence that the polymers still remain on the liposome surfaces as they move throughout the column. All results strongly supported the conclusion confirm that the polymer remains onto the liposome surfaces although an elution buffer gradually diluted the polymer/liposome complexes passed through the column. The same result can be also observed in the mixtures of 240K-N72-P_B325/DMPC5 as shown in Figure 5. 15.

It was estimated that 65% of the co-eluted polymer of 240K-N72-P_B325 with a higher level of hydrophobic incorporation, was still remained onto the liposome surfaces upon dilution elution by the integral area of the elution profiles. This value was much higher than that of the co-eluted polymer 240K-P_B177 with a lower level of hydrophobic incorporation, 43% of the co-eluted polymer 240K-P_B177 can be still detected in the elution. Hence, cholesterol chain can be efficiently anchored on the surface of liposomes as compared with octadecyl chain. This is because one cholesterol chain with average 177 units of NIPAM has a ability to bound a certain amount of the polymer onto the liposome surfaces in elution. Similar result can be found by one octadecyl chain with average 20 units of NIPAM.[77]

Figure 5. 15. Elution profiles of 240K-N72-P_B325/DMPC5 from Sephacryl S1000 at 20°C (condition same as Fig. 14).

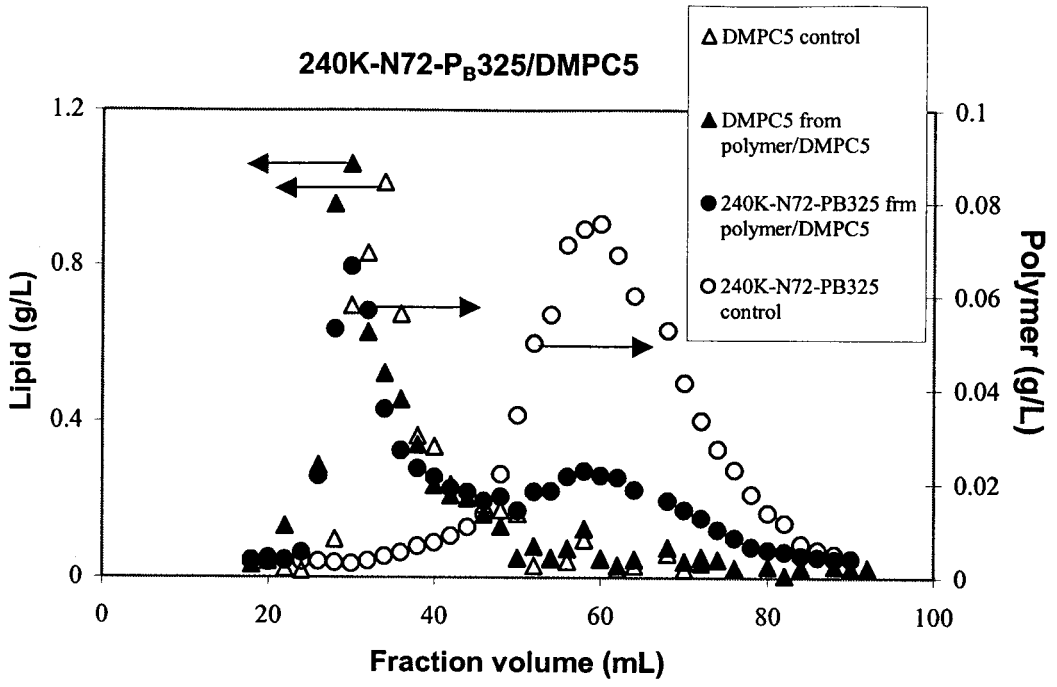

As we know that the saturation molar ratio of the DMPC5 lipid to polymer was 10 by fluorescence measurement. Generally, all polymers should be bound to the liposomes at or beyond saturation and there should be no free polymer left in the solution. However, The result from Gel Filtration showed that the polymers bound and unbound to the liposome bilayer (two distributions) can co-exist at saturation upon dilution and there was an equilibrium with a slow exchange rate between bound polymer and unbound polymer in the dilution. The equilibrium is more favor toward the side of the polymer bound to the liposomes.

5. 4. Conclusion

The cholesterol modified poly(*N*-isopropylacrylamide) can intimately interact with both nonphospholipid liposomes (NPL) and phospholipid liposomes (DMPC). It

was found that the conformation of the coating polymers has a significantly effect on the interaction that can be enhanced by increasing temperature to above the LCST of the polymers. The interaction can also be influenced by the lipid conformation and dramatically enhanced in the region of gel-liquid crystalline transition of the liposomes as evidenced by low energy transfer efficiency. The interactions with NPL were much stronger than those with DMPC because of small size of head group of the lipid, hydrogen bonding between amide moiety of NIPAM and polyethylene oxide moiety. Main phase transition and enthalpy of NPL were largely deceased by introducing the polymers. The reversible phase transition of the polymers is actively remained when the polymers are coated onto liposome surfaces. Thus, the polymer coated liposomes (NPL and DMPC) demonstrate a characteristics of thermal sensitivity. There is an equilibrium between the polymer and liposomes in a solution and the equilibrium was more favor to shift toward the side of the polymer anchored into the lipid bilayer. Cholesterol is a highly efficient and reliable anchor for liposome bilayer, which enables the polymers to be bound onto the liposome surfaces up to 60°C

Chapter 6

Temperature Controlled Release and Target Fusion of Novel Liposomes Coated with Cholesterol Bearing Poly(*N*-isopropylacrylamide)

Abstract

Non-phospholipid liposomes (NPL) were modified by cholesterol-bearing poly(*N*-isopropylacrylamide) (PNIPAM) and the calcein release from the polymers coated liposomes was investigated. Meanwhile, phospholipid liposomes (POPC/POPS and p-DMPC) were used as targeting liposomes and the targeting fusion was studied by high Sensitive Differential Scanning Microcalorimetry (DSC) with the method of dequenching high concentration dye incorporated into lipid bilayer. Either release or fusion from the polymer-coated liposomes can be promoted above the low critical solution temperature (LCST) of the polymers and be extremely enhanced at the temperature near the phase transition of the membrane.

Introduction

Research on responsive liposomes to various physical or chemical stimuli has been mainly conducted on phospholipid liposomes.[78] However, based on our knowledge, a little research was involved in non-phospholipid liposomes (NPL) formed by the self-assembly of nonionic surfactants in aqueous suspension and used in the cosmetic industry.[65] The excellent properties of NPL along with economic feature makes it possible to be used in drug delivery systems.[79]

In this dissertation thermal sensitive NPL has been investigated, in which NPL was prepared from non-ionic surfactant $(EO)_2C_{18}H_{37}$ surfactant (75%), cholesterol (20%) and cationic surfactant, dimethyldioctadecylammonium bromide (DDAB, 5%). Compared with phospholipid liposomes, NPL vesicles possess several advantages as high encapsulation capacity and chemical stability.[67] In addition, since the surfaces of liposomes are covered by ethylene oxide units (EO) with characteristics similar to polyethylene glycol derivatives used in stealth liposomes, it can be expected that NPL liposomes will demonstrate an extremely stability in blood circulation.[68]
With coating of cholesterol-bearing PNIPAM onto the liposome surfaces, the characteristics of temperature sensitivity can be introduced to the liposomes. Aqueous solutions of poly(*N*-isopropylacrylamide) (PNIPAM) demonstrate a lower solution critical temperature (LCST) around 32°C. The PNIPAM exists an extended water-soluble coil below the LCST and collapses into a water-insoluble globule above the LCST. Thus, the collapsed polymeric chains may trigger the release or fusion from PNIPAM coated liposomes by a control of temperature.[80] However, the extent of the

release or fusion was limited for the membrane without phase transition from gel to liquid crystal.[81]

The process of release can be monitored by a fluorescence assay. A hydrophilic dye is entrapped in the inner pool of liposomes, the fluorescence emission of the dye will be enhanced upon dilution when release of the dye from inner pool into the solution occurs. The process of fusion can also be studied by the fluorescence assay based on the recovery of the emission of a probe incorporated into the bilayer of non-phospholipid liposomes upon contacting with unlabeled liposomes. The calorimetric measurement was also used to examine the fusion process by the change of thermal phase transition of polymer. In the fluorescent assay, the increase of fluorescence reflects the relief of the self-quenching experienced by the concentrated probes in the non-phospholipid bilayers upon dilution with lipids from unlabeled liposomes as the fusion of the two vesicles occurs. In calorimetric measurement, two types of liposomes with different phase transition temperatures (T_c) incubated together at a given temperature. The T_c of parental membranes may disappear at its original position depending on the degree of vesicle fusing and a new endothermic peak may appear at a position between two parenting T_c.[82] Thermal sensitive NPL was not only able to release the entrapped dye but also able to fuse efficiently with target phospholipid liposomes as increasing temperature, such as 50% of palmitoyloleoylglycerophosphocholine and 50% of palmitoyloleoylglycerophosphoserine (negative-charged POPC/POPS)[83] or Dimyristoylphosphatidylcholine (neutral p-DMPC).

6.2. Experimental Section

6.2.1. Materials Dimyristoylphosphatidylcholine (DMPC) was obtained from Avanti Polar Lipids. Brij72 [$C_{18}H_{37}$ $(EO)_2$] and calcein were purchased from Aldrich. Sodium azide (NaN_3), sodium chloride (NaCl), ethylenediamine tetracetate (EDTA), and Tris were purchased from BDH chemicals. Buffer used for phospholipid liposomes was prepared by 10 mM of Tris, 1mM of EDTA, 140 mM of NaCl, and 0.02% of NaN_3. The value of pH was adjusted to 7.2. Buffer used for nonphospholipid liposomes was prepared by 150 mM of NaCl, and 0.02% of NaN_3.

6.2.2. Preparation of Liposomes Liposomes were prepared by following procedure: a dry thin film of the mixed lipids (100 mg, 75% lipid, 20% cholesterol and 5 % DDAB) was dispersed in 5 mL buffer. The lipid suspension was mixed by vortex and extruded via polycarbonate membrane (200 nm, Avanti Polar Lipids Inc.). The dry thin film was dispersed in calcein solution of 78 mM (pH = 7.2). In the case of liposomes loaded with calcein (Scheme. 6.1). Free calcein was removed by passing the solution through a sephacryl S-75 column (15 × 300 mm) with corresponding buffer as an eluant. The size of the liposomes without calcein was measured by dynamic light scattering at 25°C with a fixed 90 scattering angle. The mean diameters of the liposomes were in the range from 195 to 225 nm.

6.2.3. Calcein Release from Liposomes The release of calcein from liposomes were performed by the following procedure. A dispersion of liposomes encapsulated 78 mM of calcein was diluted to the desired concentration (0.01g/L of lipids) with a buffer at a

given temperature. A spectrophotofluorimeter was used to monitor the fluorescence intensity of the solution. The excitation and emission wavelengths were set at 450 and 515 nm, respectively. The monitoring time was 18 min and the ratio of the lipids to polymers was 1:1 in order to ensure all the liposomes in the mixtures were coated by the polymers. The release percentage of calcein from the liposomes was defined as[84]:

$$\% \text{ Release} = (F_t - F_i)/(F_f - F_i)$$

where F_i and F_t are the initial and intermediate fluorescence intensities of the liposomes suspension, respectively. F_f is the fluorescence intensity of the liposomes after adding SDS (16%, W/W).

Scheme 6.1. Chemical Structure of Calcein and BODIPY-PC.

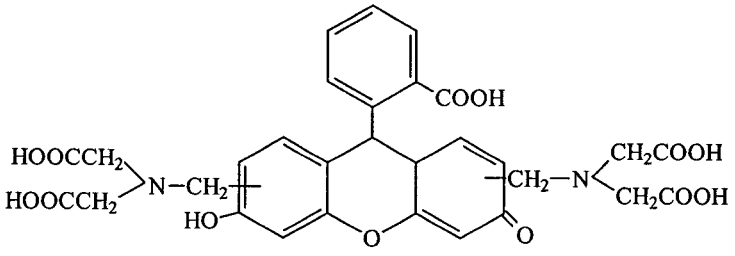

Calcein

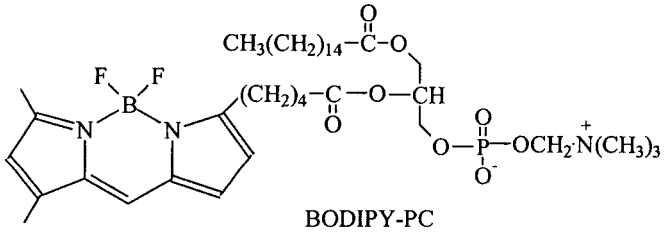

BODIPY-PC

6.2.4. Fusion Assay Fusion of liposomes can be monitored by measuring the increase of fluorescence in the lipophilic probe BODIPY-PC (Molecular probes, Eugene, OR. Fig.6.1) upon dilution. Specifically, the fluorescence quantum yield of BODIPY-PC became very low, when liposome was labeled with 2% (mole/mole) of BODIPY-PC.[85] The labeled liposomes were mixed with unlabeled liposomes in the proportion of 1 to10. Fusion of the labeled and the unlabeled liposomes results in the dilution of BODIPY-PC in the bilayer, therefore the fluorescence quantum yield increases. When the excitation wavelength was set at 504 nm and the emission wavelength was monitored at 518 nm, the extent of fusion F, can be calculated as the increase of fluorescence intensity in BODIPY-PC, by following the equation:[88b]

$$F\,\% = 100 \times (I - I_0)/(I_\infty - I_0)$$

where I, I_0 and I_∞ are the current, initial and final fluorescence intensities. To obtain the final intensity, corresponding to 100% BODIPY dequenching, the liposomes were solubilized into lubrol (25%, W/W).

6.2.5. Calorimetry Measurement High Differential Scanning Microcalorimetry (DSC, Microcal, Inc. Northampton, MA) was used as a sensitive calorimeter. In a typical protocol, samples were in the chamber cooled down to –5 or 2°C at a normal rate of 20 ° C/min, then equilibrated for 30 minutes until no further heat flow occurred. The samples were heated to 85°C at a scan rate of 1 °C/min. The same volume of buffer was used as a reference. In some cases, the samples were subjected to a cooling scan at the same rate as the heating scan. The second heating scan was used to check the hysteresis of the transition and the effect of heating-cooling history on the transitions. Samples from

NPL/PNIPAM/POPC/POPS and NPL/PNIPAM/p-DMPC were prepared by heating in a preheated water-bath with 45 °C for 30 min and cooled to room temperature, then transferred to the sample chamber. Duplicate samples were freshly prepared and scanned at the same condition.

6.2.6. Lipid-polymer Mixtures Polymer stock solutions with concentration from 1 to 4 g/L were prepared in buffers. Liposome suspensions and polymer stock solutions were mixed in the desired proportion and the mixture was allowed to incubate overnight at room temperature before measurement.

6.3. Results and Discussion

6.3.1. Release Properties of Thermosensitive Polymer Coated Liposomes

It is reasonable that liposome surfaces coated by temperature-sensitive polymers will demonstrate the characteristic of thermal sensitivity. Below the phase transition temperature of the polymers, the highly hydrated polymer chains will effectively covered up the liposome surfaces. However, above the phase transition temperature of the polymers, the hydrophobic polymer chains can absorbe onto the liposome surfaces tightly, therefore the liposome become more hydrophobic. The exchange of hydrophobic and hydrophilic chains will induce the defects in the membranes, consequently the membrane is unstable.

In this study, the polymer-coated liposomes were prepared by incubating the calcein loaded NPL with cholesterol-bearing PNIPAM overnight at room

Figure 6.1. Release profiles of calcein from NPL/ PNIPAM complexes (150 mM NaCl, pH = 7.2, λ_{ex} = 450 nm, [NPL/PNIPAM] = 0.01g/L) (a) NPL/ 20K-P_M88, (b) NPL/ 240K-N72-P_B325, (c) NPL/ 240K-P_B177, (d) NPL.

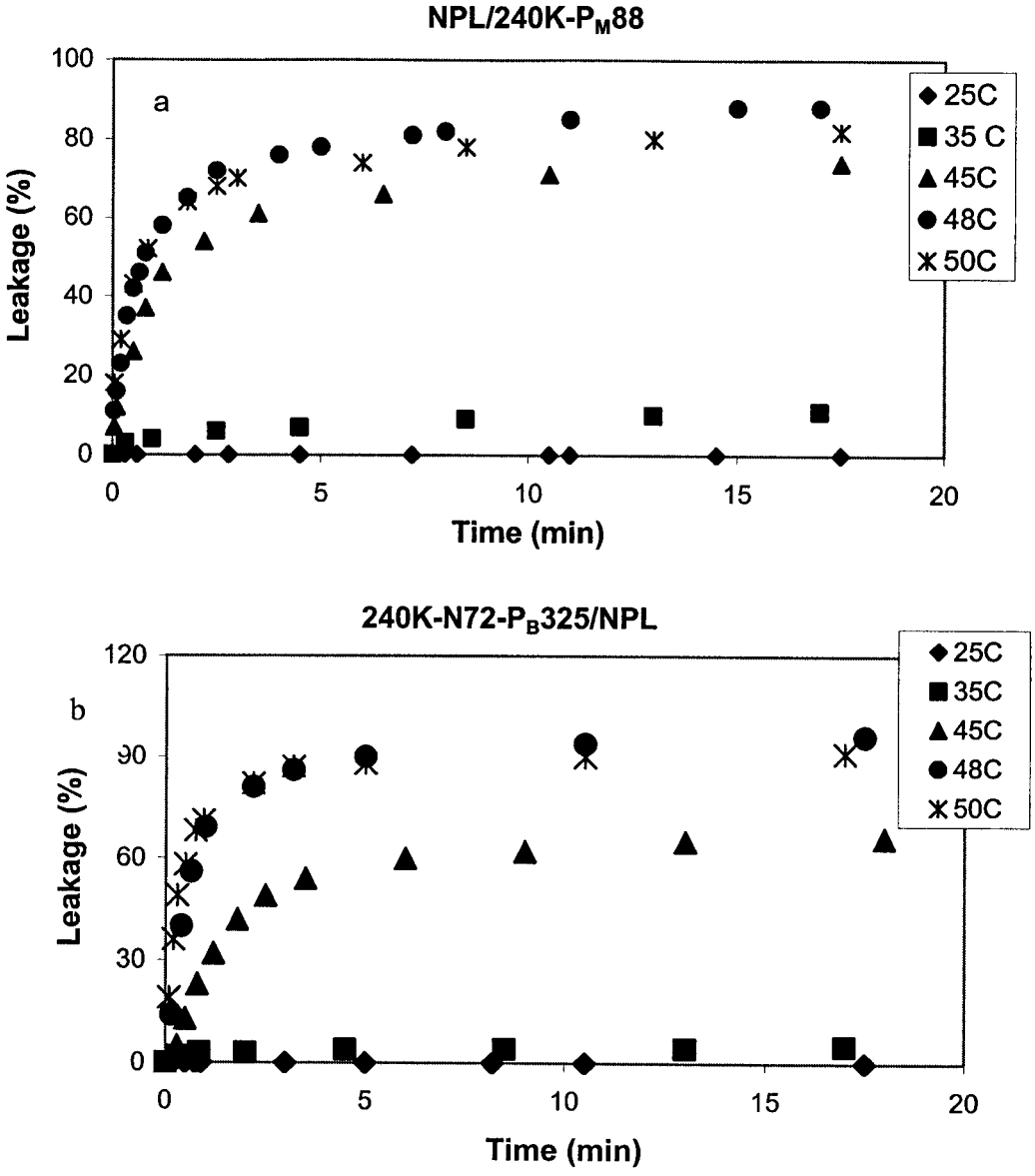

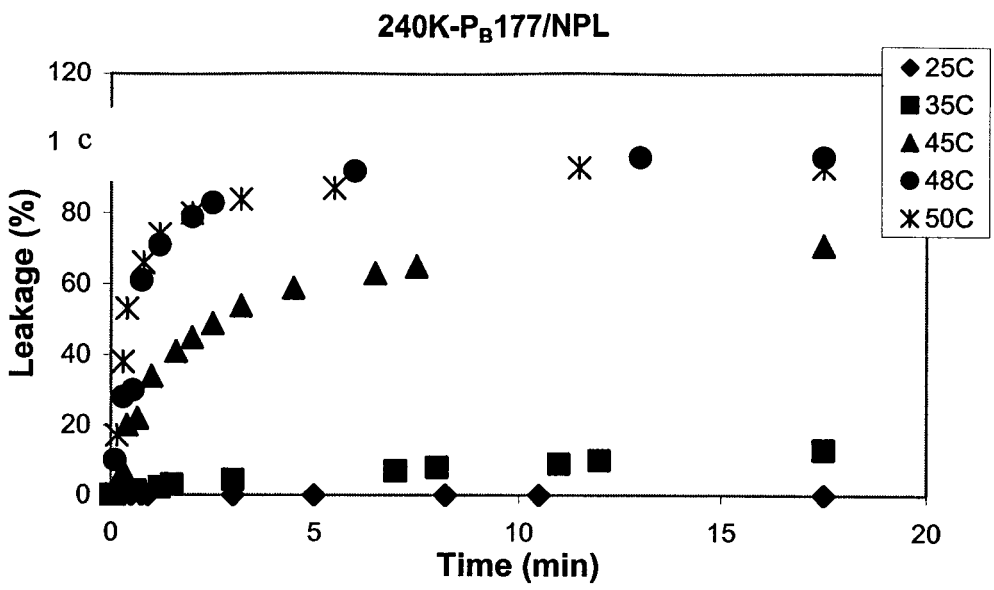
240K-P$_B$177/NPL
120
1 c
80
60
40
20
0
Leakage (%)
0
5
10
15
20
Time (min)
25C
35C
45C
48C
50C

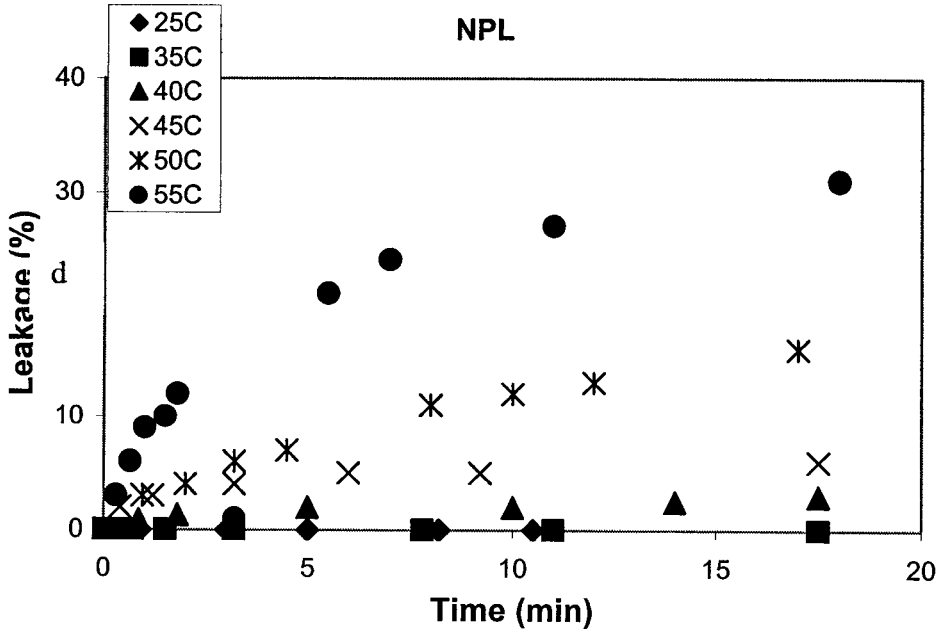
NPL
40
30
d
10
0
Leakage (%)
0
5
10
15
20
Time (min)
25C
35C
40C
45C
50C
55C

temperature. The liposomes with the polymers coated onto the surfaces were confirmed by the fluorescence assays and gel filtration chromatography as described in chapter 5. The release of calcein from liposomes was monitored as the increase of calcein emission intensity when the defects in the liposomes were created. The emission wavelength of calcein was taken at 515 nm upon an excitation at 450 nm. Figure 6.1 shows typical profiles of the calcein released from the liposomes coated with cholesterol-bearing PNIPAM as a function of time at various temperatures. The release percentage can be calculated as described in the experimental section. The polymers 240K-P_B177, 240K-N72-P_B325 and 20K-P_M88 were used for evaluating of release property, in which 240K-P_B177 and 240K-N72-P_B325 have the same molecular weight but a different hydrophobic domain, 240K-N72-P_B325 and 20K-P_M88 have different molecular weight but the same level of hydrophobic domain.

Figure 6.2. Release percentage of calcein from NPL/PNIPAM complexes as function of temperature after 17 min incubation in 150 mM of NaCl, pH = 7.2, λ_{ex} = 450nm, [NPL/PNIPAM complexes] = 0.01g/L.

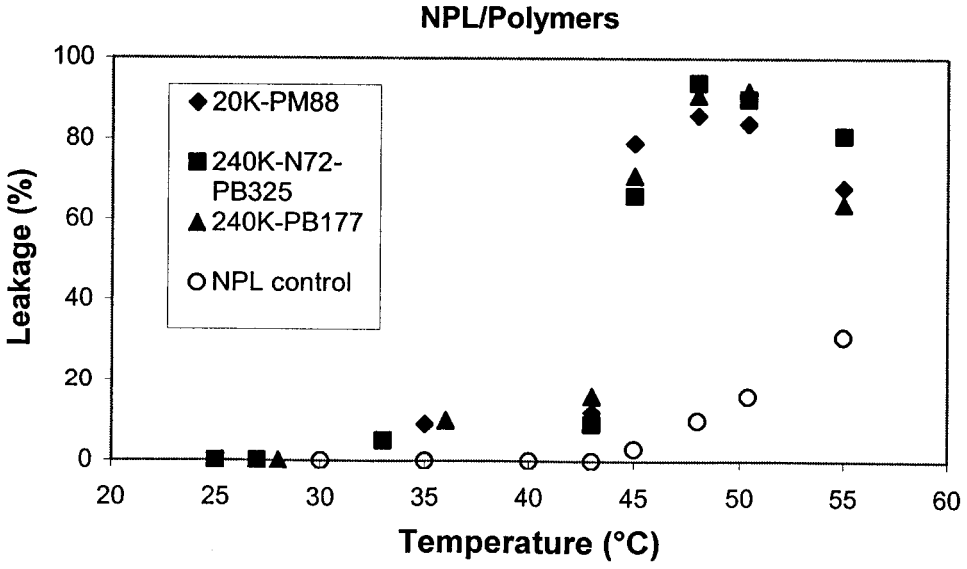

In all the cases of the polymer/liposome complex systems, the entrapped calcein in liposome complexes hardly released below 30°C, but the release was promoted above ca. 32°C. Since the LCSTs of discussed PNIPAMs were ca. 31.5°C, the release of calcein around 32°C can be attributed to the transition of the PNIPAM chains grafted onto the liposome surfaces. Calcein release became more obvious and 80% of calcein was released within 2 minutes as the temperature continuously increased up to 50°C. Since bare NPL only slightly released calcein near 50°C, the difference of calcein release between the polymer coated liposomes and the bare liposomes must be the reason of the presence of PNIPAM.

Figure 6.2 shows the release of calcine as a function of temperature. It is clear there are four steps on release process. (1) no release of calcine was observed at a temperature range of 20 to 30°C; (2) only about 15% of calcine was released from a temperature of 32 to 42°C; (3) release of calcein sharply increased up to 95% from 42 to 50°C for 240K-P_B177/NPL, and 240K-N72-P_B325/NPL complexes and 85% for 20K-P_M88/NPL complex. (4) release of calcein from the polymer coated liposomes decreased slightly above 50°C and a remarkable release from bare NPL was observed at 55°C. The third step started at the temperature near the gel-liquid crystalline transition of NPL membrane. According to the DSC results, the gel-liquid crystalline transition of NPL started around 40°C and continued until ca. 65°C. During this period, the gel and liquid crystalline phases coexisted in the membrane with structural defects and irregular microdomains. In addition, DSC measurement indicated that dehydration of the polymer chains still proceeded above the LCST (32 °C). It is likely that polymeric chains become

more hydrophobic as temperature increased much higher than the LCST and destabilized the liposome membrane more significantly. Thus, the liposomes were strongly destabilized by interaction with the dehydrated polymers. Two factors can affect the calcein release, i.e. the LCST of the polymers and the membrane phase transition temperature. The bilayer may become more orderly when phase transition occurred into liquid crystal at this temperature and lesser defects in the membrane can be expected, although this temperature is still below the T_c of the bare liposomes (58°C). Similar phenomena were also observed in dilauroylphosphatidylcholine (DLPC) liposomes coated with octadecane substituted PNIPAM.[86]

Because of no difference of released calcein from 240K-N72-P_B325/NPL and 240K-P_B177/NPL complexes, the hydrophobic incorporation level of the polymers should be no significant effect on the release properties of the lipid/polymer complexes (240K-P_B177 and 240K-N72-P_B325). The release of calcein from 20K-P_M88/NPL complexes was relatively lower compared with that from 240K-N72-P_B325/NPL complexes. It seems that molecular weight of the polymers could affect the release of the 20K-P_M88/NPL and 240K-N72-P_B325 complexes. In summary, two critical factors, i.e. the conformation of the polymeric chains coated onto the liposome surfaces and the membrane phase transition, can strongly enhance the release performance of the liposomes.

6.3.2. Target Fusion of Thermal Sensitive Non-phospholipid Liposomes with Phospholipid Liposomes

Figure 6.3 shows the fusion profile of NPL modified by cholesterol-bearing PNIPAM in the presence of fully hydrated POPC/POPS at various temperatures.

Apparently, the fusion of the copolymer-modified liposomes depends on temperature. The liposomes were hardly fused below 30°C, whereas the intensive fusion takes place around 41°C. The fusion of the liposomes was completed within 15 min and was relatively slow process in comparison with leakage process of liposomes. Figure 6.4 shows the percentage fusion of PNIPAM/NPL/POPC/POPS complex systems as a function of temperature. The maximum fusion was achieved at ca. 41°C. In comparing three modified NPL (240K-P_B177, 240K-N72-P_B325, and 20K-P_M88), the molecular weight of the polymers has no significantly effect on the fusion of liposomes but the amount of hydrophobic group incorporated in the polymers does. The maximum fusion of liposomes can be observed by copolymer with higher molecular weight and less hydrophobic group, or by copolymer with a longer loop chains surrounded the bilayer surfaces. However, the percentage of fusion for all modified NPL reached a same value. The temperature while the maximum fusion occurred was close to the beginning temperature of the NPL phase transition in the NPL/PNIPAM complex systems and it was 15°C lower than the main phase transition of NPL in the same complex systems. Since bare NPL in the presence of POPC/POPS exhibited a low percentage of fusion throughout the same experimental temperatures, the fusion property of the copolymer modified NPL liposomes can be enhanced and controlled by the copolymers.

Figure 6.3. Profiles of fusion between NPL/PNIPAM and POPC/POPS (150 mM NaCl, pH = 7.2, λ_{ex} = 504 nm, the concentration of NPL/PNIPAM was 0.01g/L). (a) NPL/ 20K-P_M88, (b) NPL/ 240K-N72-P_B325, (c) NPL/ 240K-P_B177, (d) NPL.

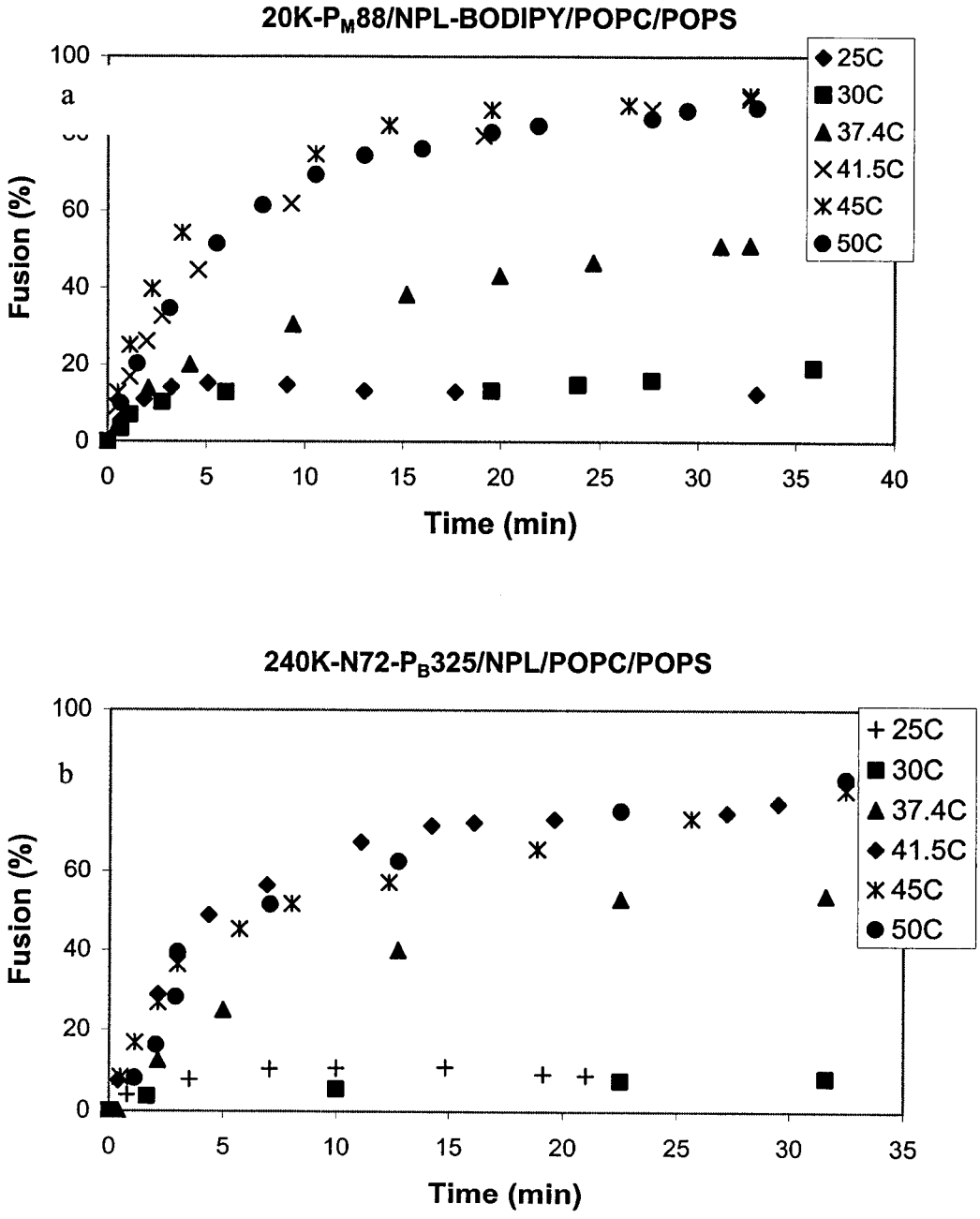

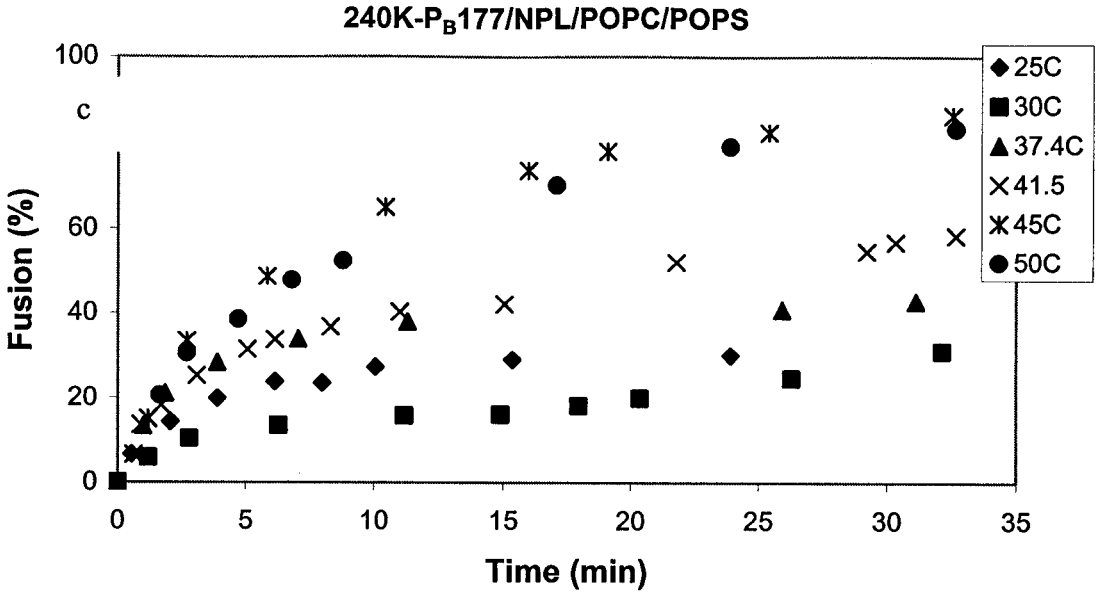

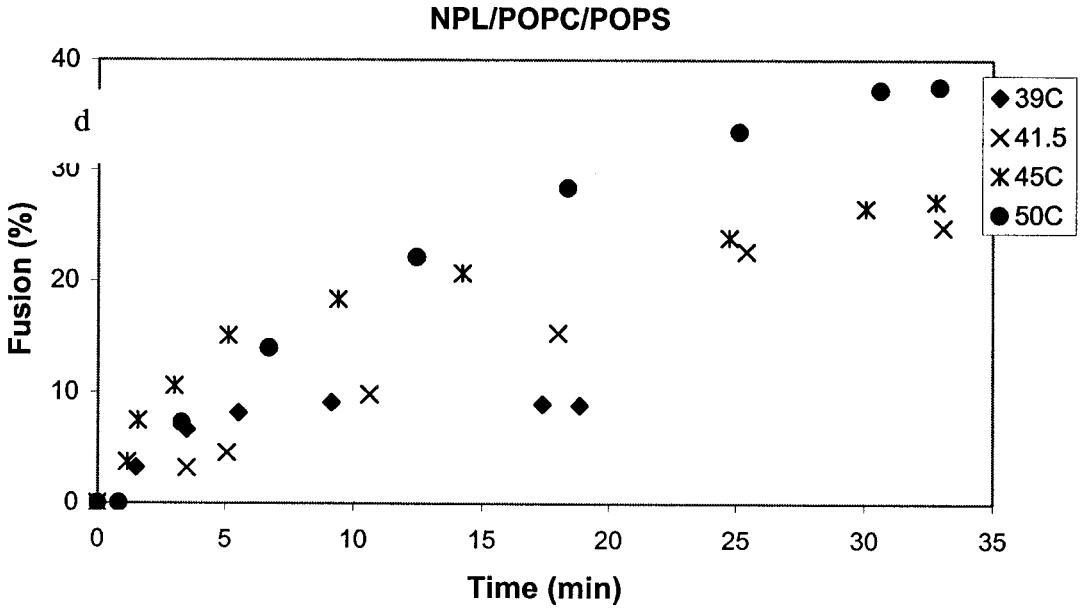

Similar results were found by Kono and his coworker,[82] in which the fusion between DPPC and DPPC with hydrophobically modified PNIPAM was increased at the temperature near the membrane phase transition. Ringsdorf[4a] et al also reported that hydrophobically modified PNIPAM shrank more efficiently on the surface of the

liposome with a liquid-crystalline membrane than that with a gel membrane because of the lateral diffusion of the hydrophobic groups inserted into the membrane.

Figure 6.4. Fusion between modified NPL and POPC/POPS as a function of temperature (150 mM NaCl; pH = 7.2; 32 incubation min; λ_{ex} = 504 nm; [NPL/PNIPAM] = 0.01g/L).

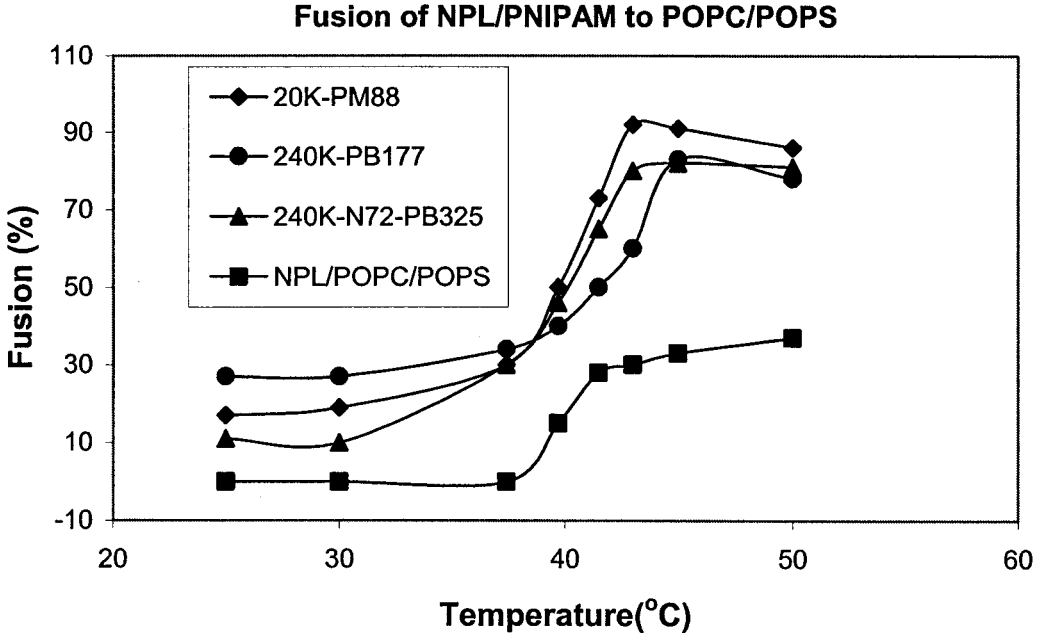

In summary, the liposomes become more obviously unstable by the interaction with the hydrophobic polymer when the defects of liposome membranes appear near the temperature of gel-liquid crystalline phase transition. Therefore, it is likely that the dehydrated copolymer and the presence of membrane defects together strongly promote the fusion of liposomes.

Figure 6.5. Profiles of fusion for NPL/PNIPAM and p-DMPC (150 mM of NaCl; pH = 7.2; 37.4°C; [NPL/PNIPAM] = 0.01g/L).

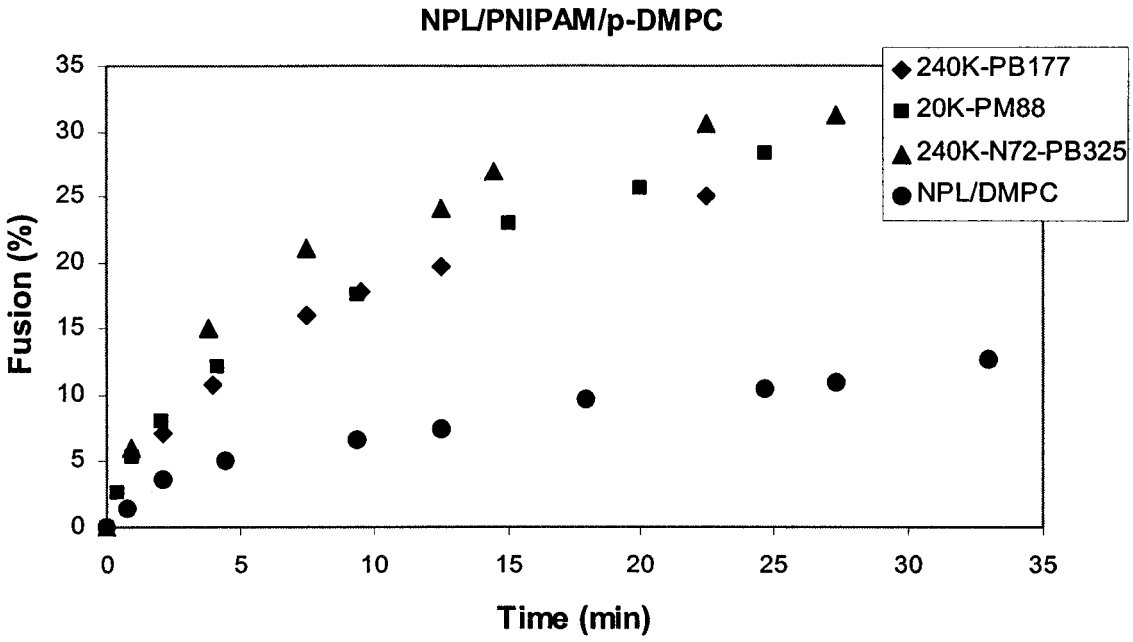

p-DMPC as neutral vesicles and targeting liposomes was also examined and the parallel experiments were conducted at 37.4°C. Fusion of liposomes occurred in the system of PNIPAM/NPL/p-DMPC as shown in the Figure 6.5. The results indicated that NPL/PNIPAM and phospholipid vesicles with a low phase transition temperature can fuse each other efficiently, and two critical factors will promote the membrane fusion, i.e. the LCST of PNIPAM and the temperature of membrane phase transition.

High sensitive differential scanning calorimetry (DSC) as an alternatively tool was used to evaluate the fusion process occurred in the vesicles since phase transition temperature of a membrane depends on the lipid composition and the lipid microdomain of each membrane.[87] The phase transition of NPL/240K-N72-P_B325/POPS/POPC and NPL/240K-N72-P_B325/p-DMPC complexes with varied ratio of composition was

investigated by DSC. Figure 6.6 shows the partial molar heat capacity of the polymer/liposome complexes (240K-N72-P_B325 and POPC/POPS) as function of temperature. There are two obvious endothermic phase transitions in each trace; one located near 30°C was attributed to the phase separation of PNIPAM. Another varied from 8 to 22°C was attributed by the phase transition of POPC/POPS lipid bilayers.[88] No phase transition of the POPC/POPS liposomes was detected in the absence of PNIPAM/NPL. This phase transition was calculated as 5°C from POPC (-2°C) and POPS (14°C).[89] It is clear that the phase transition of POPC/POPS can be shifted toward a high temperature with the addition of NPL/240K-N72-P_B325 complexes.

The T_c of NPL disappeared when the molar ratio of NPL/240K-N72-P_B325 to POPC/POPS was equal or above 1 (Figure 6.6). Therefore, we can conclude that a new

Figure 6.6. HSDSC traces of mixtures from NPL/240K-N72-P_B325 and POPC/POPS in varied molar ratios after incubation 30 min at 45°C. Ratios of POPC/POPS to NPL/240K-N72-P_B325 (w/w): (a) 0.1, (b) 1, (c) 2, (d) 3, and (e) 10.

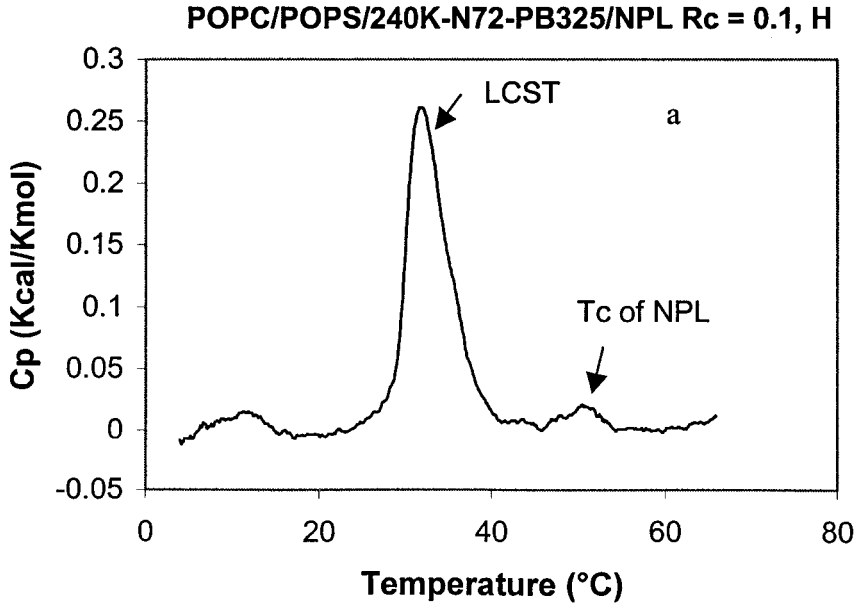

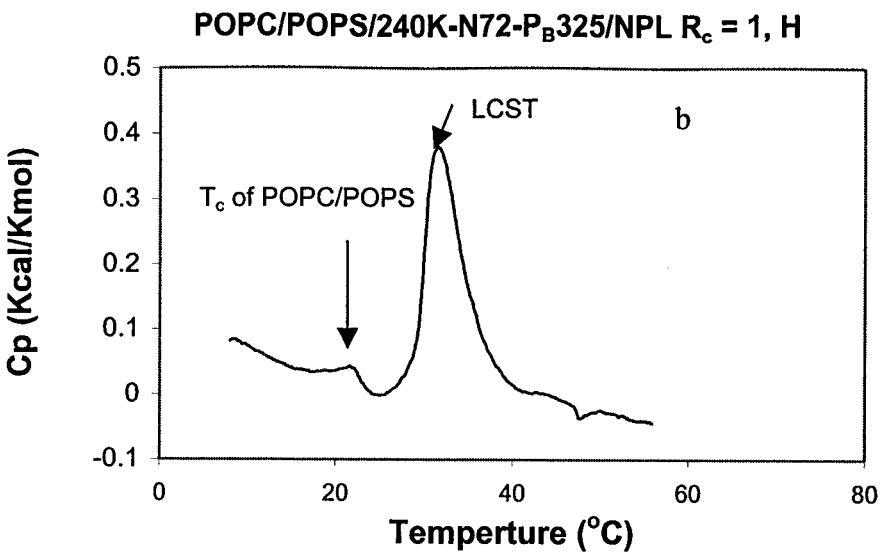
POPC/POPS/240K-N72-P$_B$325/NPL R$_c$ = 1, H
Cp (Kcal/Kmol)
0.5
0.4
0.3
0.2
0.1
0
-0.1
0
20
40
60
80
Temperture (°C)
LCST
b
T$_c$ of POPC/POPS

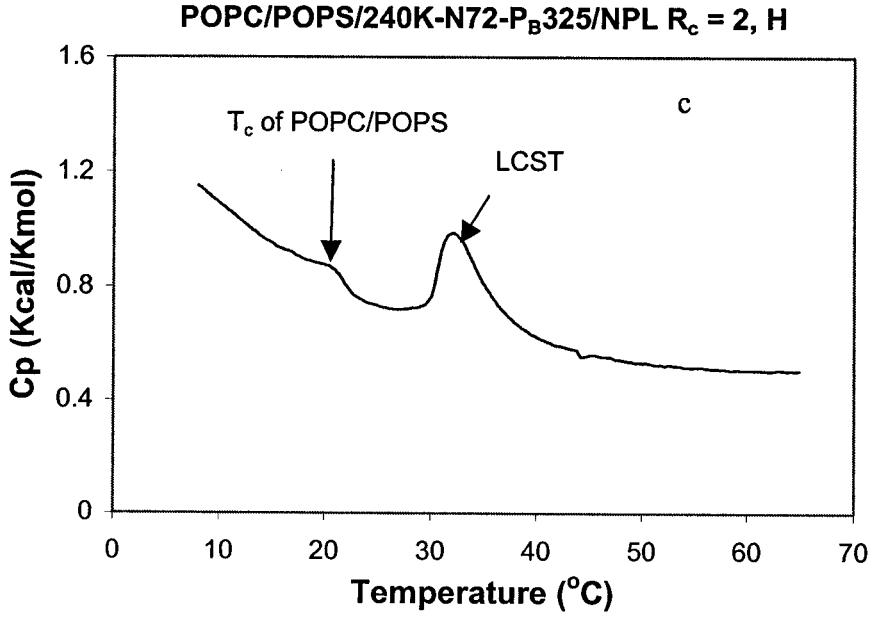
POPC/POPS/240K-N72-P$_B$325/NPL R$_c$ = 2, H
Cp (Kcal/Kmol)
1.6
1.2
0.8
0.4
0
0
10
20
30
40
50
60
70
Temperature (°C)
c
T$_c$ of POPC/POPS
LCST

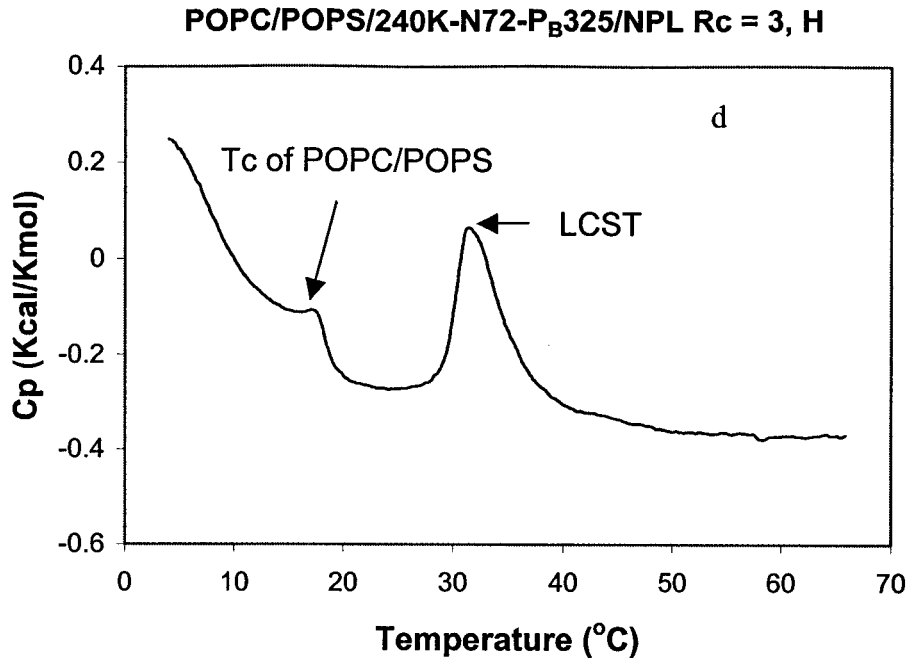
POPC/POPS/240K-N72-P$_B$325/NPL Rc = 3, H
d
Tc of POPC/POPS
LCST
Cp (Kcal/Kmol)
Temperature (°C)
0.4
0.2
0
-0.2
-0.4
-0.6
0
10
20
30
40
50
60
70

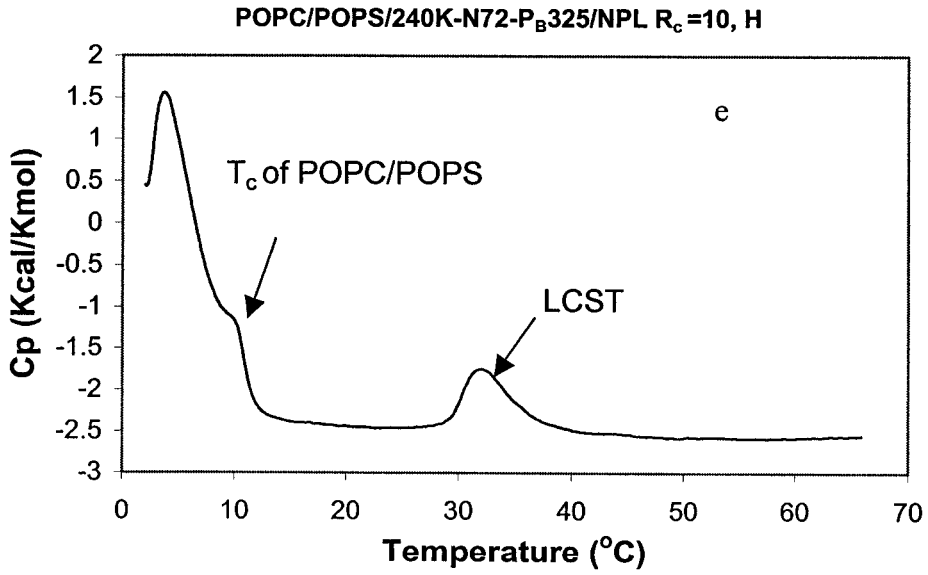
POPC/POPS/240K-N72-P$_B$325/NPL R$_c$ =10, H
e
T$_c$ of POPC/POPS
LCST
Cp (Kcal/Kmol)
Temperature (°C)
2
1.5
1
0.5
0
-0.5
-1
-1.5
-2
-2.5
-3
0
10
20
30
40
50
60
70

membrane POPC/POPS was generated due to the mixing of two parental vesicles, and the composition of new membrane can be changed by varying amount of NPL/240K-N72-P_B325. Papahadjopoulos suggested that the mixing degree of molecules observed from a new endothermic peak in the DSC trace could be taken as proportional to the fusion extent between separate vesicles. New peak shown in Figure 6.6 indicates that the fusion between NPL/PNIPAM and POPC/POPS was completely accomplished.

In the DSC traces of PNIPAM/NPL/DMPC complex systems (Figure 6.7), the phase transition of NPL disappeared when one portion of NPL/240K-N72-P_B325 (or NPL/240K-P_B177) mixed with one portion of p-DMPC or more. However, the main endothermic peak of p-DMPC was not significantly shifted, but the peak of the main phase transition became extremely broader. The pretransition of p-DMPC in 240K-P_B177/p-DMPC complexes as shown in Figure 6.8 cannot be observed in the presence of NPL. In this case, p-DMPC membrane became more orderly, therefore, its pretransition was disappeared.[90] It seems there is no new domain composition in the membrane due to no changing in the main phase transition temperature. How can we explain the conflicting results (T_c of DMPC) measured by DSC and fluorescence assay? Where is NPL? Similar conflicting results between DSC and vesicle permeability and monolayer expansion can be found in the interaction of phospholipids (DPPC and DPPG) with proteins.[91] Especially, the T_c remained almost unchanged (within 1°C) in the case of DPPC and myelin proteolipid apoprotein (N-2 apoprotein) although it became broader at high ratio of protein

Figure 6.7. DSC traces of the mixture of copolymer modified NPL and p-DMPC, (a) NPL/240K-N72-P_B325, (b) NPL/240K-P_B177, (150 mM NaCl, pH = 7.2, incubation 30 min, 45 °C, ratio of p-DMPC to NPL/PNIPAM: 2).

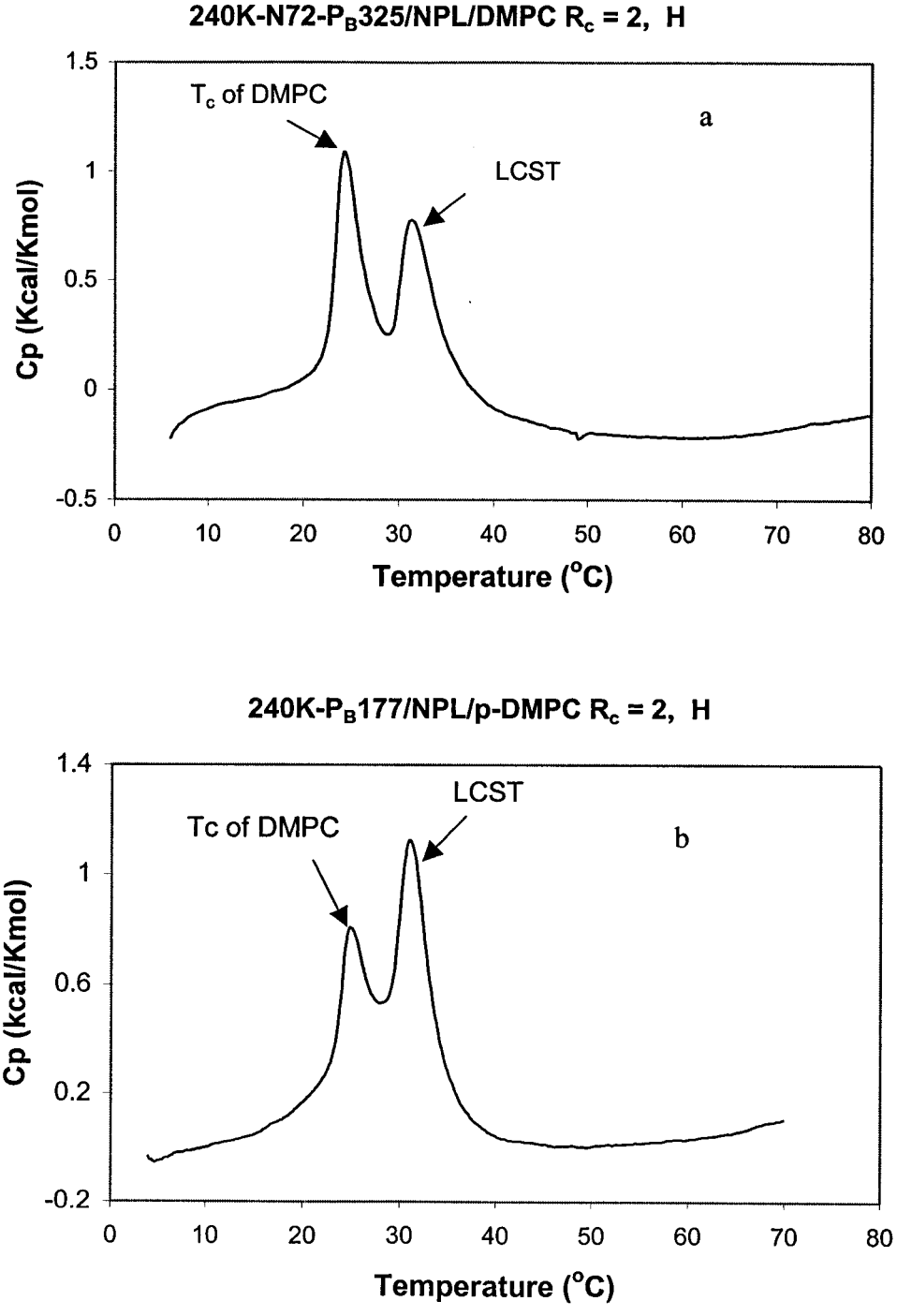

to lipid ratio. The pretransition was eliminated by samples with more than 20% of protein. It was unexpected that the N-2 apoprotein could increase the permeability of phospholipid vesicles and expanded the area of phospholipid monolayers at a constant pressure of 24 dynes/cm^2. Hence, N-2 apoprotein may only penetrate deeply into the bilayer. The N-2 apoprotein embedded in the bilayer cannot perturb the acyl chain packed in the bulk lipid due to no change of T_c. The phospholipid molecules around the embedded protein could be strongly bound with the protein by hydrophobic association or perhaps immobilized by the protein. Consequently, there is no participation in the cooperative melting of the bulk lipid. Thus, we suggest that NPL might have a minimal effect on acyl chain packed in the bulk lipids even though NPL exhibits strong interaction with phospholipid DMPC and can fuse (or penetrate) into bilayer.

Another example reported by Taylor et al[92] is that the pretransition of phospholipid DMPC was more sensitive than the main transition from the association of poloxamers with DMPC liposome bilayers. Poloxamers are non-ionic surface-active copolymers with two hydrophilic polyoxyethylene (EO) moieties. When the poloxamers penetrated into lipid bilayer, the enthalpy of the pretransition for DMPC can be reduced. NPL is a non-ionic surfactant with two hydrophilic poloxyethylene (EO) moieties and may play a similar role as poloxamers in the DMPC liposomes.

Figure 6.8. (a) DSC trace of p-DMPC/240K-P_B177 (R_c = 1) without NPL (b) DSC trace of p-DMPC/240K-P_B177/NPL (molar ratio of p-DMPC to NPL/ 240K-P_B: 177/ 1).

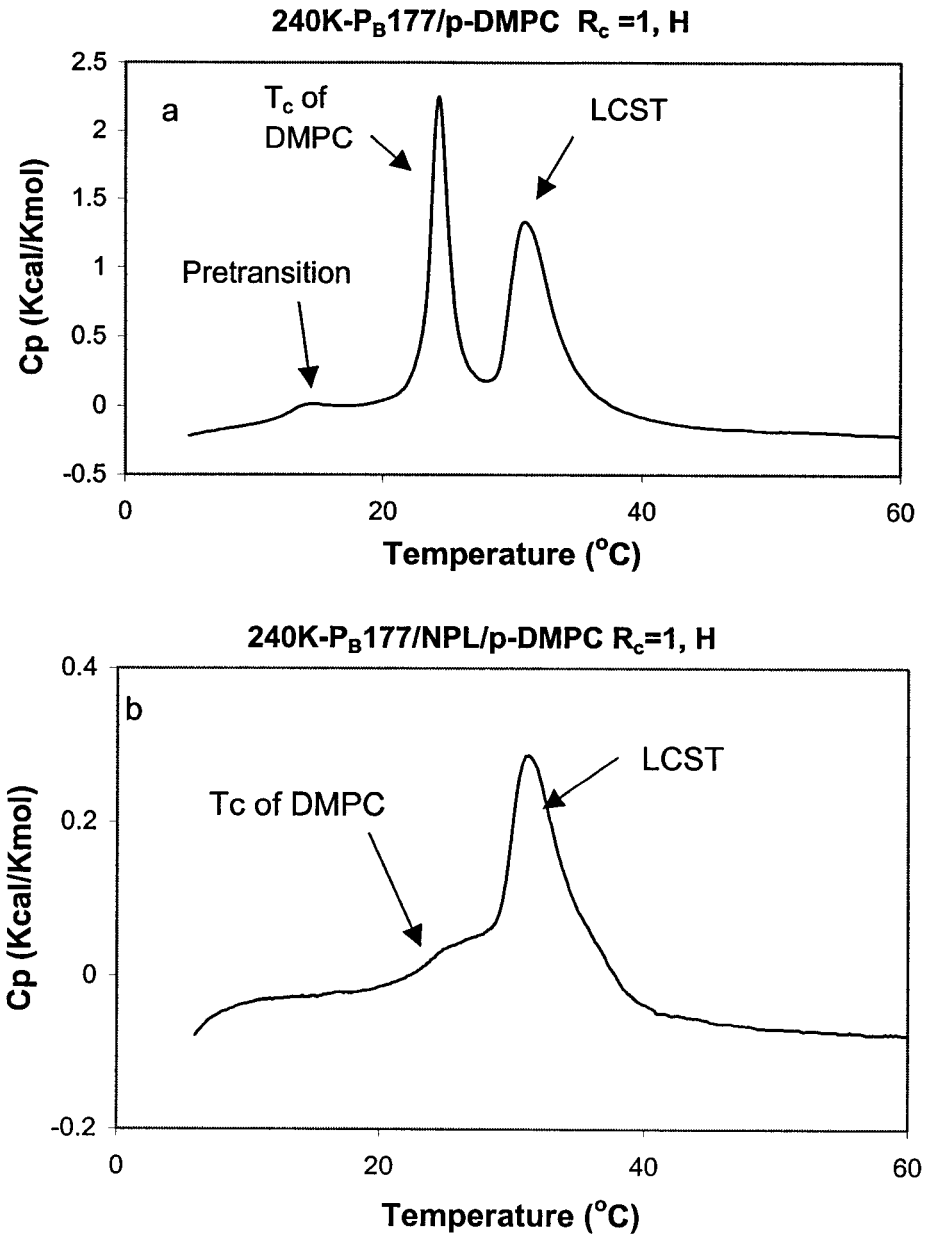

It is unclear the so minor effect of foreign hydrophobic chains embedded into parental bilayer on the main T_c of parental bilayer. Does T_c depend on the size of lipid microdomain? If so, the main phase transition may require rather smaller lipid microdomain as vesicle shown in Scheme 6.2 when the T_c of lipid bilayers was insensitive to the second hydrophobic chains embedded into the bilayers such as DMPC. Perhaps, T_c may require large lipid microdomain as vesicle c shown in Scheme 6.2 when the T_c of lipid membranes was sensitive to anything such as POPC/POPS inserted into lipid bilayers.

Scheme 6.2. Schematic structure of membrane fusion

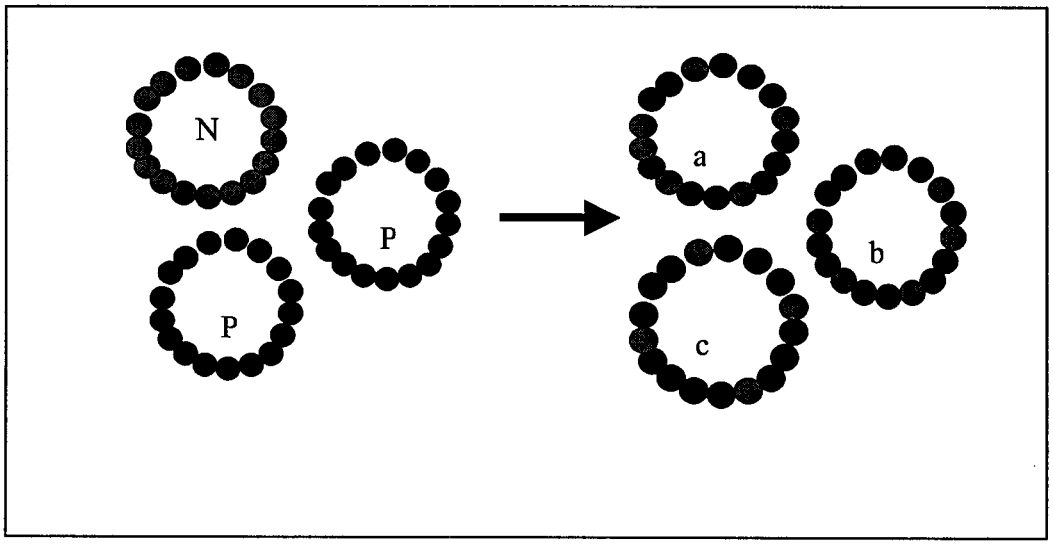

6.4. Conclusion

The cholesterol-bearing poly(*N*-isopropylacrylamide) can interact with nonphospholipid liposomes (NPL). The interaction can be controlled by the conformation of the polymers coated on liposomes and enhanced by increasing temperature above the LCST of the polymers. The interaction can also be affected by the lipid conformation and enhanced in the region of gel-liquid crystalline transition of the membrane. The interaction resulted in a high release of calcein (95%) from the polymer-modified NPL liposomes.

Targeting fusion efficiently occurred in the systems of NPL/PNIPAM /POPC/POPS and NPL/PNIPAM/p-DMPC as evidenced by the fluorescence assay and DSC. The fusion process can be strongly promoted by the factors of the LCST of the polymers and the temperature of membrane phase transition. The attraction of opposite charges may play a certain role in the case of POPC/POPS and NPL/PNIPAM systems.

Chapter 7

Thermosensitive Nanoparticles Prepared by Self-assembled Cholesterol-Bearing Pullulan and Poly(*N*-isopropylacrylamide)

Abstract

Thermosensitive hydrogel nanoparticles had been prepared by the self-assembly of two types of cholesterol modified water-soluble polymers, namely, cholesterol-bearing pullulan (CHP) and cholesterol bearing poly(*N*-isopropylacrylamide). The interaction between the modified polymers was investigated by fluorescence spectroscopy, dynamic light scattering, and differential scanning microcalorimetry. Fluorescence results show that the micellar aggregates generated from the cholesteryl and fluorophore groups bearing poly(*N*-isopropylacrylamide) were disrupted by adding CHP solution at 25°C and the hybrid nanoparticles were formed by an association of hydrophobic microdomains existed in the two polymers. The sizes of hybrid nanoparticles can be tailored by molecular weight of the cholesterol-bearing poly(*N*-isopropylacrylamide). Monodisperse nanoparticles with the average size of 60 nm can be obtained by mixing of CHP and cholesterol-bearing PNIPAM with a molecular weight of 240, 000 Dalton such as 240K-N72-P_B325 at 25°C. The average size of monodisperse particles can be reduced to 28 nm by using cholesterol-bearing PNIPAM with a molecular weight 20,000 Dalton such as 20K-P_M88. The size of nanoparticles was subjected to reversible change upon changing temperature. Above the lower critical solution temperature (LCST) of the cholesterol-bearing poly(*N*-isopropylacrylamide), the phase separation of 240K-N72-P_B325 can induce the aggregation of CHP/240K-N72-P_B325 nanoparticles, which suggests that PNIPAM chains were on the surfaces of the hybrid particles or/and partially mixed with pullulan chains.

7.1. Introduction

Functional nanoparticles prepared by self-assembly of amphiphilic molecules have been attracted much attention because of their unique properties and potential applications in biotechnological, pharmaceutical, painting electron and photon industries.[19a, 93, 94] Most studies focus on an association of one specific polymer in water, very few studies were concerned in the association based on two different chemical compositions.[101] In this chapter, we presented the associations between two different hydrophobically modified polymers, i.e. cholesterol-bearing pullulan (CHP) and cholesterol-bearing poly(*N*-isopropylacrylamide). The self-assembly of cholesterol-bearing pullulan (CHP) was extensively studied[37] and stable nanoparticles with monodisperse (20 - 30 nm) from CHP can be formed by intermolecular self-aggregations in dilute aqueous solutions. This kind of nanoparticles exhibits a hydrogel structure, in which the pullulan chains were noncovalently cross-linked by cholesterol moiety association. As the concentration of CHP increased, the hydrogel could be formed. The sizes and density of the nanoparticles can be controlled by changing the degree of hydrophobic substituents. The disassociation and association could be induced by adding a trigger, such as β-cyclodextrin and adamantaanecarboxylic acid. In addition, the CHP self-aggregates were capable of binding various hydrophobic substances and soluble proteins.[48c]

It was well known that the hydrophobically modified poly(*N*-isopropylacrylamide) can form inter and intrapolymeric micellar aggregates in cold water. The micellar aggregates consisted of hydrophobic cores (or microdomains) surrounded by hydrophilic polymer chains. The polymeric association depended on the

amount of hydrophobic incorporation and the polymer architecture. The micellar aggregates can be disrupted and precipitated from aqueous solutions above low critical solution temperature (LCST) of polymers. It is clear that the phase separation temperature of hydrophobically modified PNIPAM depended on the degree of hydrophobic substituents. The phase separation mechanism of PNIPAM can be elucidated in two steps: (1) collapsing of individual polymer chain from a highly extended coil into a globule; (2) aggregation of the globules.[54a] The cholesterol-bearing poly(*N*-isopropylacrylamide) carried fluorescence labels, such as pyrene or/and naphthalene was used to monitor the change of a micellar structure by the efficiency of nonradiative energy transfer or the relative intensity of pyrene excimer emission and pyrene monomer emission. The results show that the hybrid thermosensitive nanoparticles are formed by choleterol-bearing CHP and PNIPAM and the sizes of the nanoparticles can be altered by changing temperature of the solutions and the polymer architecture. It should be emphasized that the nanoparticles further proved that cholesterol is a reliable anchor when it is incorporated into hydrophobic microdomains and remained in the microdomains during the system heated above the LCST.

7.2. Experimental Section

7.2.1 Materials Water was purified with a Barnstead NANO-pure water purification system. Analytical grade solvents were used without further purification. Cholesterol-bearing pullulans (CHP-108-0.9 and CHP-108-1.2) were prepared from pullulan with molecular weight of 108, 000 by Akiyoshi'lab. We used CHPs with 0.9 or 1.2 cholesterol groups per 100 glucose units. Fluorescence cholesterol-bearing PNIPAM

(240K-N72-P_B325, 20K-P_M88, 20K-P_B85 and 20K-N45) were synthesized as described in previous chapters, in which 240K-N72-P_B325 show a viscosity molecular weight of 240, 000 and contained average 72 NIPAM units per naphthalene, while 20K-P_M88, 20K-P_B85, and 20K-N45 had a viscosity molecular weight of 20, 000 and 88, 85 or 45 NIPAM units per pyrene or naphthalene.

7.2.2. Characterization UV-spectra of samples were recorded with a Hewlett-Packard 8425A photodiode spectrometer equipped with a Hewlett Packard 89090A temperature controller. Cloud points of samples were determined by the change in turbidity of solutions heated at a constant rate (0.2 °C /min) in a magnetically stirred UV cell. Fluorescence spectra of samples were recorded on a Hitachi F-3010 fluorescence spectrometer. The sample compartment was equipped with a thermostat cell holder. The samples were heated stepwise from 20 to 50°C and equilibrated at a desired temperature for 30 min before measurement. The excitation wavelength was set at 345 nm for pyrene and the slits widths were set at 2.0 for excitation and 1.0 for emission. The ratio of the pyrene excimer emission intensity (I_E) to the pyrene monomer emission intensity (I_M) was taken as the ratio of the emission intensity at 480 nm to the emission intensity at 377 nm. The excitation wavelength was 290 for naphthalene in nonradiative energy transfer. The ratio of pyrene emission intensity (I_{Py}) to naphthalene emission intensity (I_{Np}) was taken as the ratio of emission intensity at 377 nm to the emission intensity at 337 nm. Measurements of dynamic light scattering were performed on a Brookhaven BI9000 instrument equipped with an argon laser (λ: 514 nm, scattering angle: 90°). The samples were kept in the cell compartment at 25.0 ± 0.2°C for 15 min prior to measurement. In

temperature–controlled experiments, the samples were heated stepwise from 25 to 40°C and equilibrated for 15 min at each desired temperature. Data were analyzed by CONTIN. The average diameter of the nanoparticles was calculated by using three closest values. Differential scanning microcalorimetry (DSC) was performed in a high sensitive calorimeter. In a typical procedure, samples were cooled to 10°C in the chamber at a rate of 20°C/min, then equilibrated at that temperature for 30 minutes until no further heat flow occurred. Finally, the samples were heated to 60°C at a scan rate of 1°C/min. Meanwhile, the same volume of buffer was used as a reference. The samples were subjected to the cooling scan at the same rate used as heating scan in order to examine the reversibility.

7.2.3. Sample preparation

CHP was dissolved in dimethyl sulfoxide (DMSO) and dialyzed against Tris sulfate buffer (50 mM, pH 7.5). After dialysis, the suspension was sonicated for 10 minutes (TOMY, UR-200P). The obtained suspension was passed through three types of membrane filters (Super Acrodisc 25, Gelman science) with pore size of 1.2, 0.45 and 0.2 μm, respectively until the clear suspension was obtained. The concentration of CHP was determined with a sulfuric acid method.[37] A stock solution of cholesterol-bearing PNIPAM was prepared by adding water to the polymers. The solution was kept at 4°C for 24 hrs to allow the polymers to be completely dissolved. Mixed solutions were prepared by adding aliquots of CHP stock solution to cholesterol-bearing PNIPAM stock solution with a desired ratio and diluted to desired concentration. The mixture was kept at 25°C for 24 hrs and further mixed by sonication for 5 min.

Scheme 7.1. Chemical structure of cholesterol bearing pullulan.

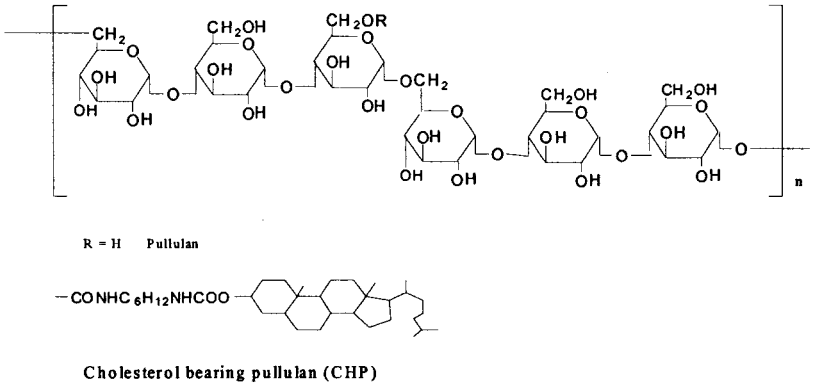

Cholesterol bearing pullulan (CHP)

7.3. Results and Discussion

7.3.1. Solution Properties of Mixed CHP/PNIPAM Systems at Room Temperature

The interaction of two hydrophobically modified water-soluble polymers was examined by fluorescence measurement. The photophysical properties of fluorescence labeled cholesterol-bearing PNIPAM have been studied in previous chapters. Upon the addition of CHP to a solution of pyrene labeled cholesterol-bearing PNIPAM, such as 20K-P_M88 and 20K-P_B85, the pyrene excimer emission decreased, while the pyrene monomer emission intensity increased significantly; thus, the ratio of I_E/I_M decreased dramatically as illustrated in Figure 7.1.

Figure 7.1. Ratio of I_E/I_M as a function of CHP concentration (25°C, λ_{ex} = 345 nm, PNIPAM concentration: 0.05 g/L).

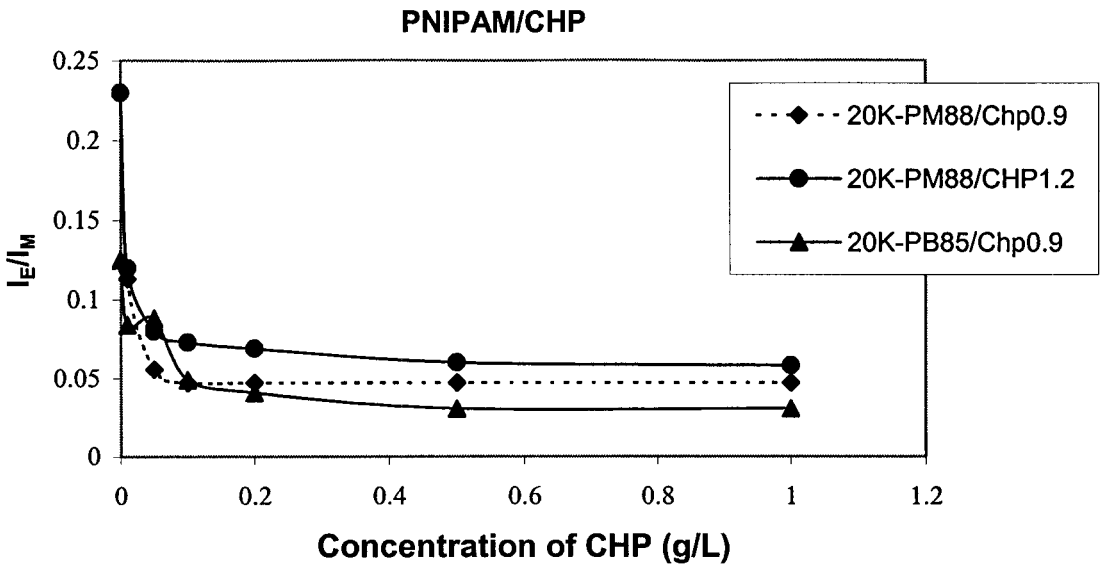

The ratio of I_E/I_M leveled off and remained constant while the concentration of CHP further increased. The decrease of I_E/I_M indicates that pyrene aggregation presented in 20K-P_M88 or 20K-P_B85 solutions was disrupted and pyrene molecules were separated each other. The hydrophobic pyrene molecule intended to aggregate in an aqueous solution in order to minimize the free energy, therefore pyrene molecules from the disrupted aggregation requests a new hydrophobic microdomain, in which to dwell, the ideal place could be the hydrophobic cores of CHP. The ratio of I_1/I_3 for pyrene essentially remained unchanged with a value of 1.28 (± 0.01) upon adding CHP to 20K-P_M88 solutions (Figure 7.2). This value was close to that of pyrene probe inside the CHP nanoparticles (1.25).[95]

Figure 7.2. Ratio of I_1/I_3 as a function of CHP concentration (25°C, λ_{ex} = 345 nm, [20K-P_M88]: 0.05 g/L).

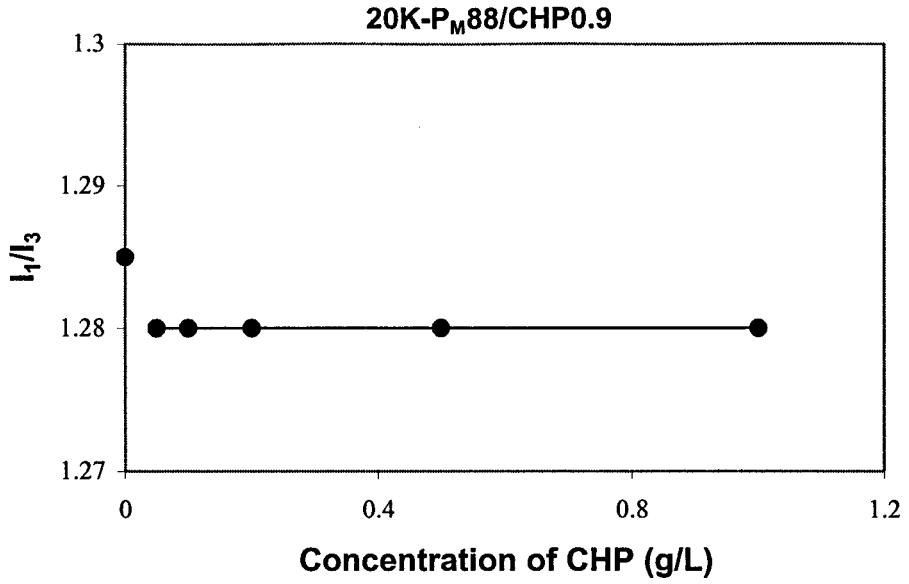

As we know, a low value of I_1/I_3 can be generated for pyrene probe entrapped in the surfactant micelles, such as 1.14 for sodium dodecyl sulfate (SDS), 1.30 for cetyltrimethylammonium bromide (CAB) and 1.31 for Triton X-100. A low ratio of I_1/I_3 as1.22 (± 0.01) was found in the SDS solutions of 20K-P_M88. Therefore, pyrene was certainly inserted into the hydrophobic microdomain with associated cholesteryl groups.

Figure 7.3. Ratio of I_{Py}/I_{Np} as a function of CHP concentration (25°C, λ_{ex} = 290 nm, [240K-N72-P_B325] = 0.05 g/L, [20K-P_B85]/[20K-N45] = 0.045/0.055 g/L).

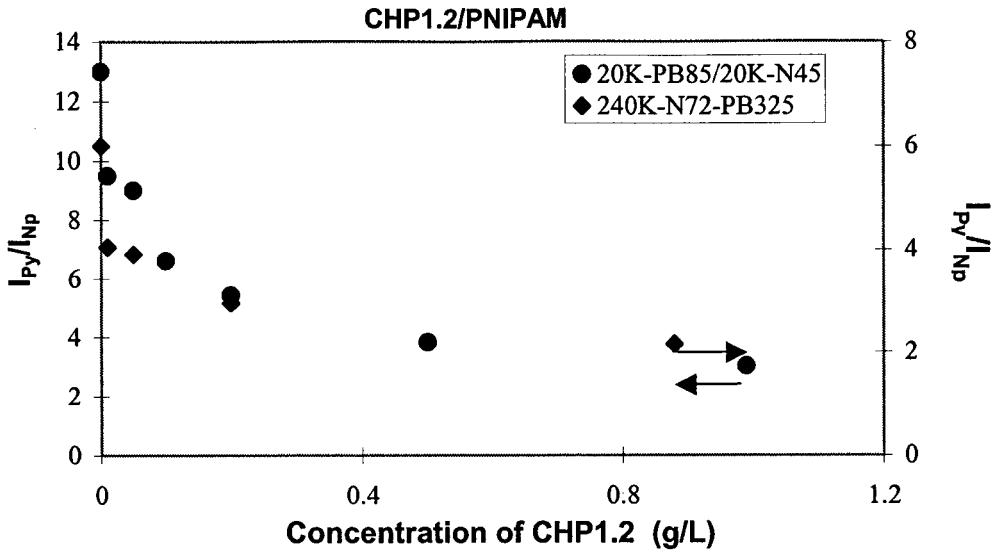

The nonradiative energy transfer was further conducted to examine the location of the hydrophobic chromophores in the hydrophobic cores of CHP nanoparticles. Upon excitation of naphthalene at 290 nm, the fluorescence spectra exhibited a strong pyrene monomer emission for the mixtures of CHP with either two singly labeled PNIPAM or doubly labeled PNIPAM due to nonradiative energy transfer, and the ratio I_{Py}/I_{Np} was taken as an extent of energy transfer. A high ratio of I_{Py}/I_{Np} indicates that the distance between pyrene and naphthalene molecule are close each other. Upon the addition of CHP to the mixture of two singly labeled 20K-P_B85/20K-N45 or solution of doubly labeled 240K-N72-P_B325, the emission intensity of pyrene monomer dramatically decreased. The ratio of I_{Py}/I_{Np} decreased from 14 without CHP to 3 with CHP (1 g/L) in the mixture of singly labeled 20K-P_B85/20K-N45 as indicated in Figure 7.4. Meanwhile, the ratio of I_{Py}/I_{Np} for 240K-N72-P_B325 dropped from 6 without CHP to 2 with CHP (1

g/L). The ratio of I_{Py}/I_{Np} was very sensitive to CHP, and kept unchanged with increasing further the concentration of CHP in both cases. The decrease of the pyrene emission intensity induced by CHP implies that the aggregation of chromophores formed in the PNIPAM solutions can be disrupted by introducing CHP. The more CHP, the more disrupted aggregates of the pyrene and naphthalene moieties. Therefore, we believe that pyrene and naphthalene was inserted into hydrophobic cores of CHP nanoparticles and separated from each other with a distance more than 29Å.

7.3.2. Dynamic Light Scattering (DLS)

It was found by DLS that CHP in aqueous solutions had a strong signal with a unimodal distribution and the uniform CHP nanoparticles showed an average diameter as 24 (± 2) nm. Such unimodal distribution signal was also detected in the mixture of CHP with cholesterol-bearing PNIPAM as a molar ratio of 10 (w/w). However, the average sizes of the colloidal nanoparticles depended on the molecular weight of PNIPAM. In the case of cholesterol-bearing PNIPAM with a relatively high molecular weight, such as 240K-N72-P_B325, the size of nanoparticles was largely increased to 60 (± 5) nm. In the case of cholesterol-bearing PNIPAM with low molecular weight, such as 20K-P_M88 and 20K-P_B85, the average size of the nanoparticles only slightly increased to 28 (± 2) nm. The results suggest that new nanoparticles can be formed by interaction of CHP and cholesterol-bearing PNIPAM. What is conformation of the hybrid nanoparticles? Three possibilities could be: (1) CHP was surrounded by PNIPAM as core but hydrophobic cholesteryl groups were entangled together; (2) PNIPAM was surrounded by CHP as core

and two polymers shared PNIPAM hydrophobic microdomains; (3) CHP and PNIPAM randomly distributed around hydrophobic cholesterol microdomains.

7.3.3 Temperature Effect

In order to investigate the formation mechanism and thermosensitivity of the hybrid nanoparticles, the mixture of CHP and cholesterol-bearing PNIPAM were heated from 22 to 50°C and monitored by fluorescence, dynamic light scattering, and difference scanning calorimetry, subsequently.

Figure 7.4. Ratio of of I_E/I_M for 20K-P_M88/CHP complex (0.05/0.5 g/L) as a function of temperature (λ_{ex} = 345 nm, H: heating scan, C: cooling scan).

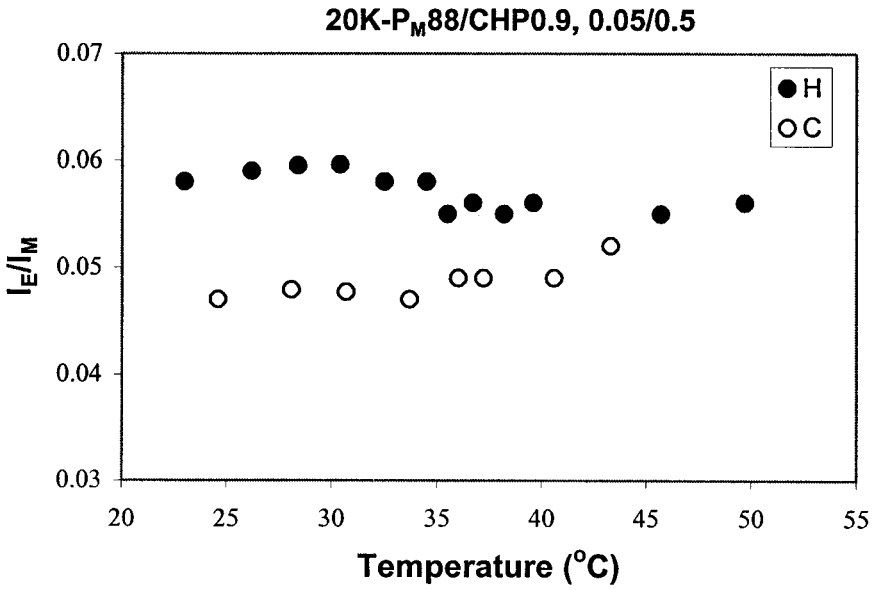

In the mixture of CHP and PNIPAM with low molecular weight, such as 20K-P_M88, the ratio of I_E/I_M for pyrene decreased slightly upon increasing the temperature up

to 32°C and leveled off at the temperature about 40°C as shown in Figure 7.4. The ratio of I_1/I_3 decreased also slightly upon increasing temperature up about 32°C and leveled off at the temperature around 40°C (Figure 7.5).

Recall the same experiment of hybrid nanoparticles formed by CHP and octadecane modified PNIPAM, I_E/I_M increased upon increasing temperature above the LCST, the different behavior of pyrene label suggests that cholesterol remains in the hydrophobic microdomains of CHP but octadecyl group escapes from the hydrophobic microdomains of CHP.

Figure 7. 5. Ratio of I_1/I_3 for 20K-P_M88/CHP complex (0.05/0.5 g/L) as a function of temperature (λ_{ex} = 345 nm, H: heating scan, C: cooling scan).

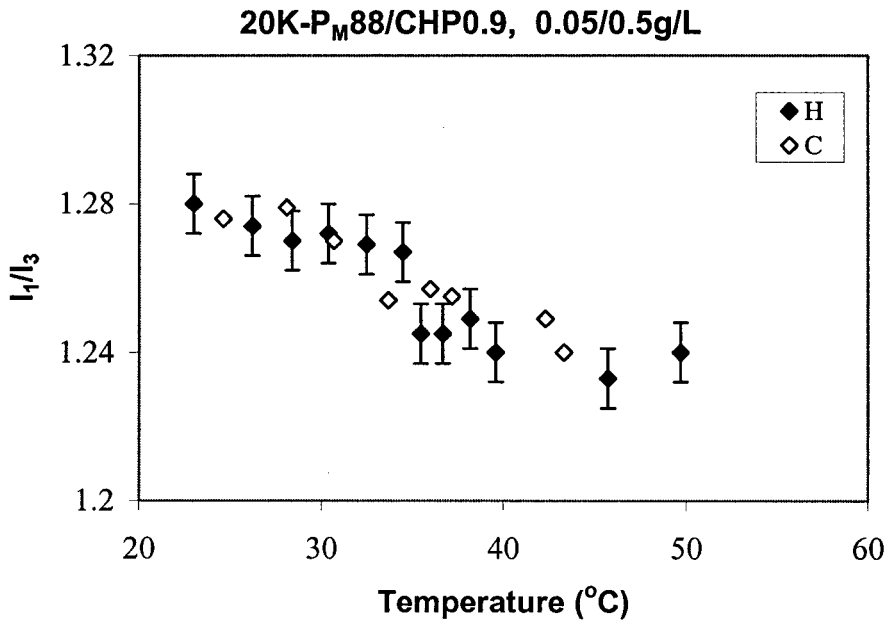

The nonradiative energy transfer was monitored for the mixture of CHP and PNIPAM with low molecular weight, such as 20K-P_B85/20K-N45 or medium molecular weight PNIPAM, such as 240K-N72-P_B325. In both cases, similar phenomena were

observed, namely the ratio of I_{Py}/I_{Np} slightly changed upon increasing the temperature up to 55°C as shown in Figure 7.6. The solution phase transition temperature of PNIPAM associated with CHP kept unchanged.

Figure 7.6. Ratio of I_{Py}/I_{Np} forCHP/PNIPAM complexes as a function of temperature (λ_{ex} = 290 nm): (a) 20K-P_B85/20K-N45/CHP complex (0.045/0.055/0.5 g/L), (b) 240K-N72-P_B325/CHP (0.05/0.5 g/L).

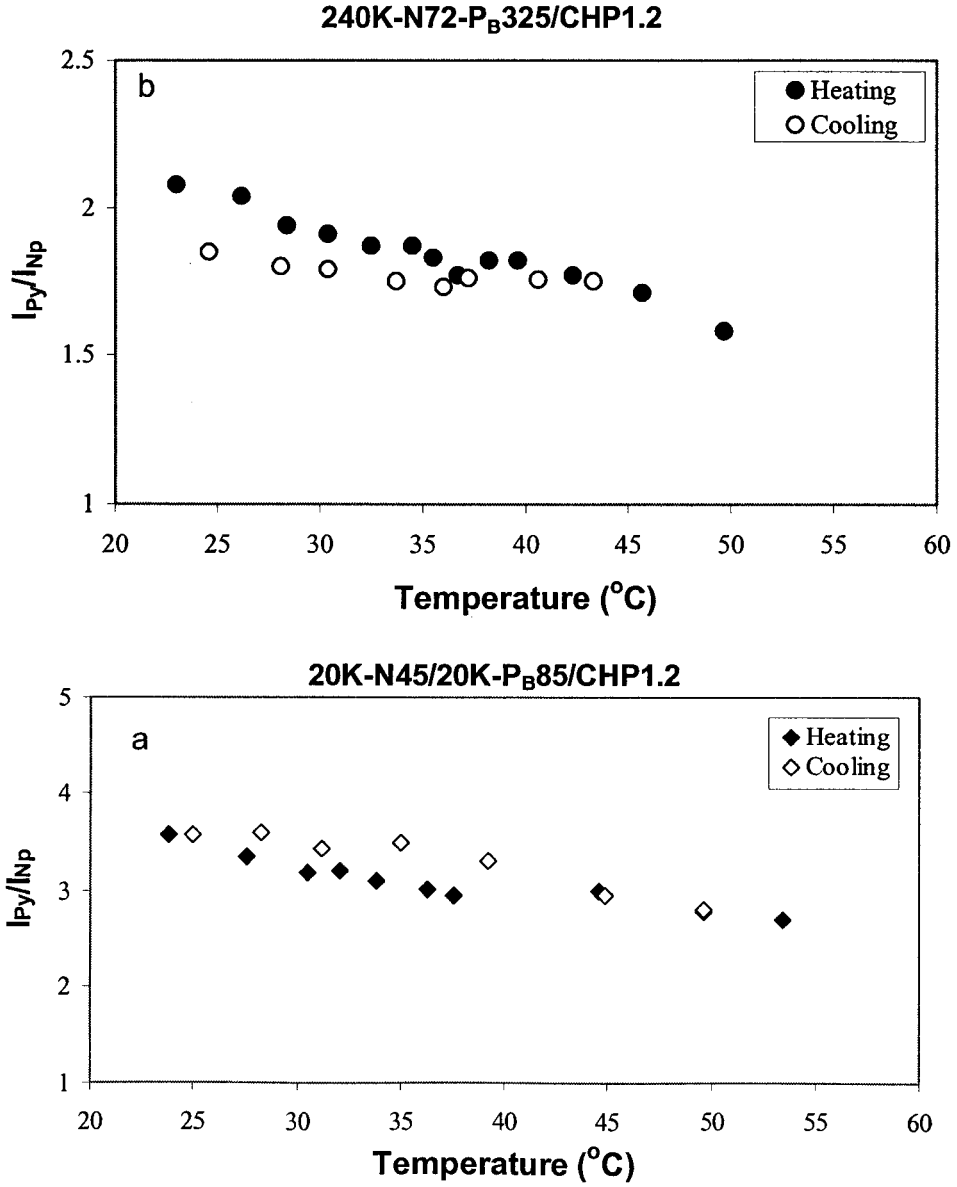

These results indicate that PNIPAM was incorporated to CHP nanoparticles beyond the LCST of PNIPAM. The thermosensitivity of the mixtures was further examined by DLS and the average diameter of 240K-N72-P_B325/CHP nanoparticles increased from 65 nm at room temperature to 250 nm at 45°C as shown in Figure 7.7a. The enlarged particles were shrunk to the original sizes upon decreasing the temperature to 25°C. This is because that PNIPAM can surround on the surfaces of nanoparticles or partially penetrate with CHP, therefore the sizes of the nanoparticles increased as the result of the hybrid particles entangled together and PNIPAM chains collapsed upon heating.

However, the average diameter of 20K-P_M88/CHP or 20K-P_B85/CHP nanoparticles only slightly increased upon increasing temperature as shown in Figure 7.7b. It should be mentioned that size of CHP nanoparticles kept unchanged under the same condition as given in Figure 8.7a.

The thermosensitivity of the hybrid nanoparticles was finally examined by DSC. A peak centered at 34.5°C was observed for mixture of 240K-N72-P_B325/CHP (0.3/1.5 g/L), which can be attributed to the thermal phase transition of 240K-N72-P_B325 (Figure 7.8a). In the cooling scan, the peak shifts to 32.5°C (Figure 7.8b). However, no peak was observed in both heating and cooling scans for the mixture of 20K-P_M88/CHP, (Figure 7.8c), although a peak around 40°C appeared in the heating scan of 20K-P_M88 solution (Figure 7.8d). A flat line was observed in CHP solution under the same experiment condition. Temperature has no significant effect on the size of nanoparticles (20K-P_M88/CHP and 20K-P_B85/CHP) as discussed in the DLS measurement.

Figure 7.7. Particle size of CHP/PNIPAM complexes as a function of temperature (a) CHP (0.5 g/L) and 240K-N72-P_B325/CHP (0.05/0.5 g/L), (b) 20K-P_M88/CHP (0.3/1.5 g/L).

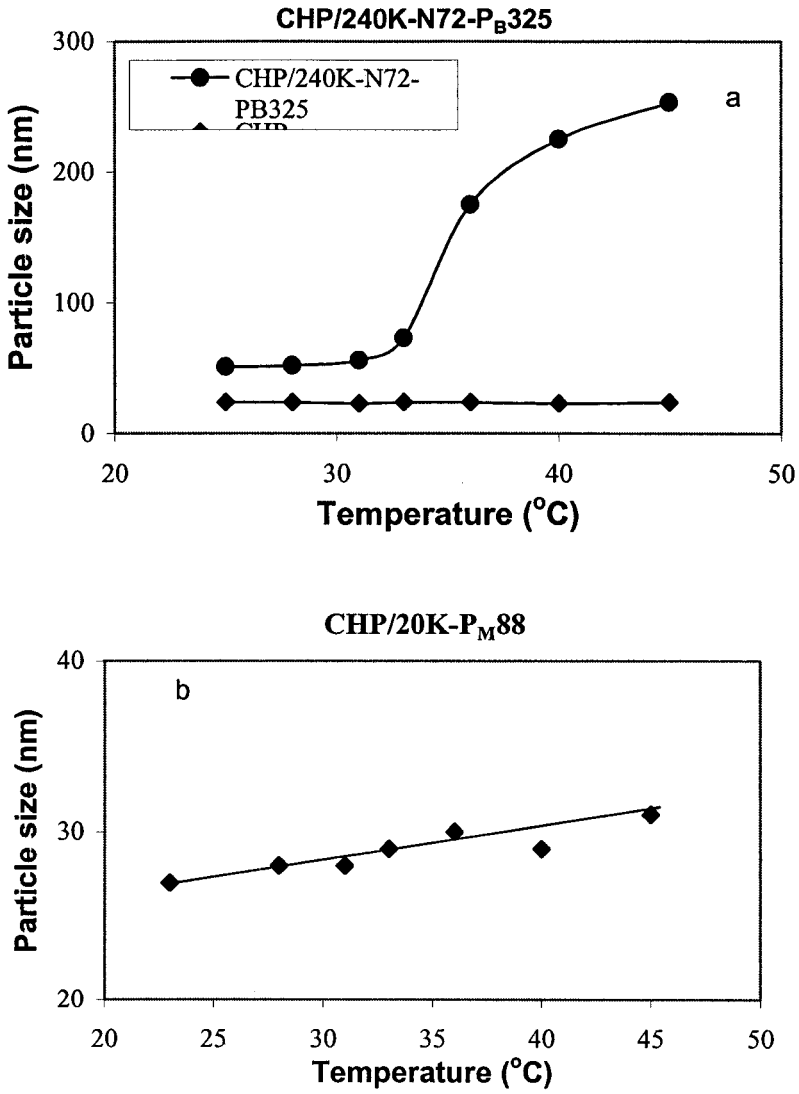

It is suitable to prepare thermosensitive hybrid nanoparticles with CHP and PNIPAM with medium molecular weight. Nanoparticles formed by CHP and PNIPAM with low molecular weight, such as 20K-P_M88 and 20K-P_B85 had no thermal sensitivity. This may be because of shorter polymer chains in 20K-P_M88.

Figure 7.8. DSC traces of CHP/PNIPAM complexes and PNIPAM (a) Heating scan of 240K-N72-P_B325/CHP (0.1/0.5 g/L), (b) cooling scan of 240K-N72-P_B325/CHP (0.1/0.5 g/L), (c) heating scan of 20K-P_M88/CHP (0.3/1.5 g/L), (d) heating scan of 20K-P_M88 (0.3 g/L) in water.

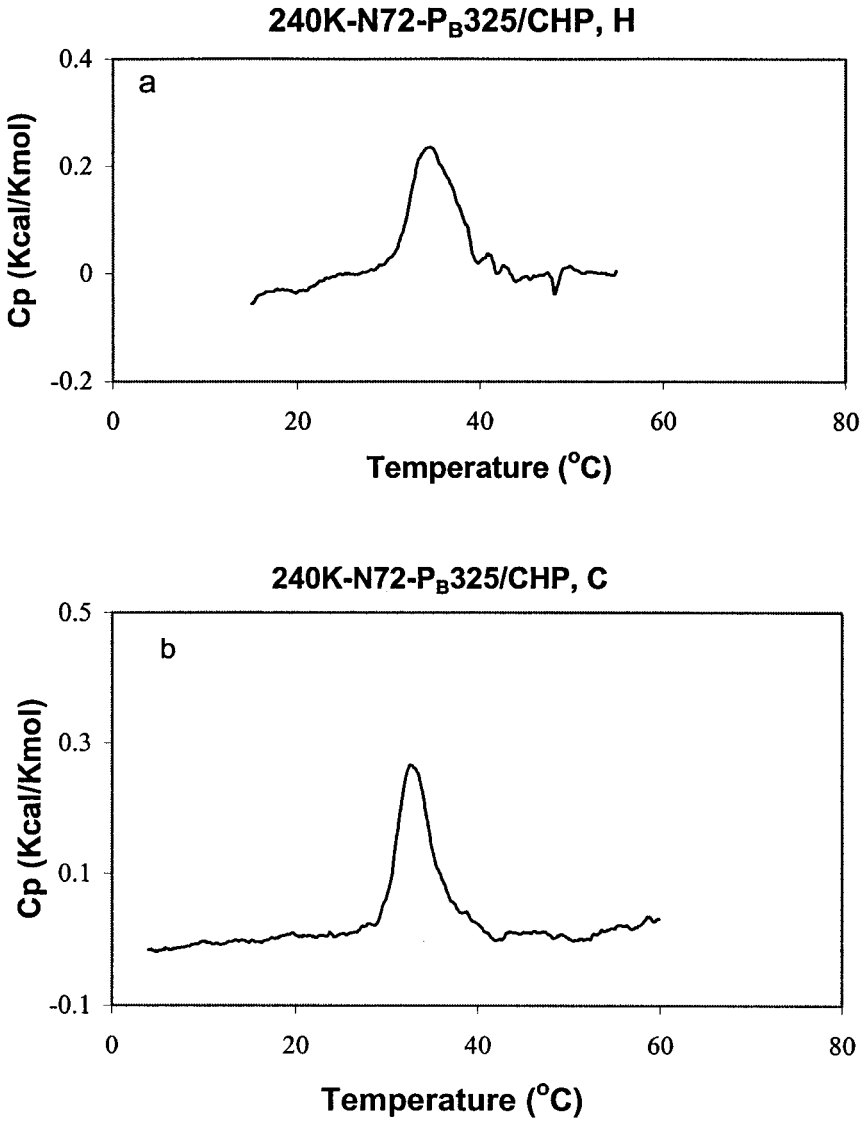

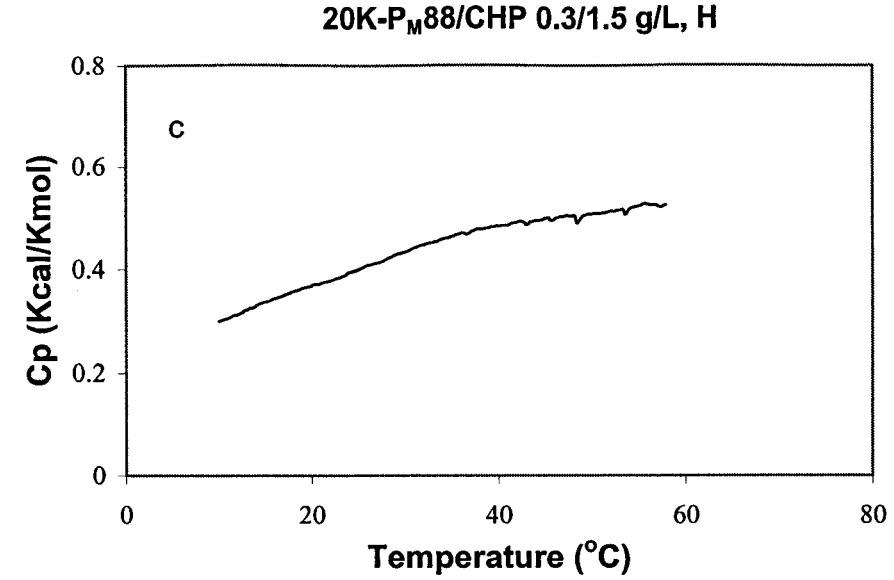

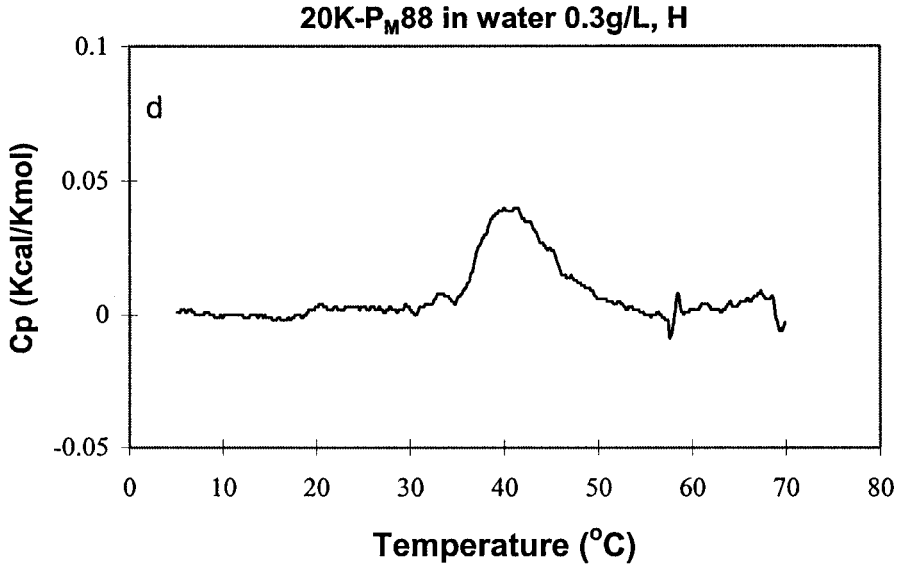

comparing to those in 240K-N72-P_B325. The collapse of the shorter polymer chains or/and the aggregation of the collapsed shorter polymer chains may be less sensitive than that of polymer with higher molecular weight such as 240K-N72-P_B325.

7. 4. Conclusion

The mixing of the two types of polymers by an association of hydrophobic groups represents a new preparation method for functional hydrogel nanoparticles. The thermosensitive hydrogel nanoparticles cab be prepared by the self-assembly of two different cholesterol-bearing polymers. In order to achieve an optimum thermosensitivity of the hybrid nanoparticles, the molecular weights of PNIPAM should be relatively high (e.g. 240, 000 Dalton). The thermal behavior of hybrid nanoparticles formed by CHP and cholesterol–bearing PNIAM indicates the strong association of the hydrophobic groups from the two polymers, the results suggest that cholesterol is a reliable anchor not only in ordered lipid bilayers but also in hydrophobic microdomains.

Chapter 8

Preparation and Characterization of Hyaluronan Bearing Cholesteryl and Fluorophore Groups

Abstract

Hyaluronic acid (HA) bearing cholesteryl and fluorophore groups had been synthesized and the solution properties and secondary structure of cholesterol-bearing HA were investigated by fluorescence, dynamic light scattering, and circular dichroism spectroscopy. The modified polymers can form micellar structure in aqueous solutions, which can be further aggregated in water. The aggregation can be reduced by either diluting the solution or adding counter ions. Rigid conformation of the modified polymers inherited from the parental HA although the modification can occasionally disturb its secondary structure, thereby occasionally disturbing hydrogen bonding in the intrapolymeric chains. The investigation of interaction from the cholesterol-bearing HA with cholesterol-bearing poly(*N*-isopropylacrylamide) disclosed that the neutral cholesterol-bearing poly(*N*-isopropylacrylamide) can also reduce the aggregation of the chemically modified HA in water and form hybrid nanoparticles with the hyaluranon. Finally, the interaction of the cholesterol-bearing HA with liposomes was studied and highly reliable liposomes in fetal bovine serum were developed by the cholesterol-bearing HA coated phospholipid liposomes.

8.1. Introduction

The glycosaminoglycan hyaluronic acid (HA) has a combination of unique physicochemistry properties and biological functions that allows it to serve as an important starting polymer for preparation of new biocompatible and biodegradable materials. The application of HA can be found in the fields of drug delivery, tissue engineering, medical imaging and ferrofluids.[96] Hualuronan can be served as lubricants in the synovial fluid of joints and as the vitreous humor of vertebrate eyes. Hualuronan as a central component of the extracellular matrix of cartilage and tendons makes special contributes to tensile strength and elasticity of materials.[97] In fact, HA is a linear polysaccharide with alternating units of D-glucuronic acid and N-acetylglucosamine as components of the extracellular matrix of animal tissues.[21a] The sugar rings are relatively fixed in their shapes by glycosidic links that consist of single oxygen atoms joining one sugar to the next. Each oxygen atoms in the sugar rings contributes two bonds that are directed like the arms of the letter V. The substitutents attached at the ends of these arms can rotate through 360 degrees. Hualuronan has a preferred conformation in water as shown in Scheme 8.1.[98]

Scheme 8.1 Secondary structure of HA in DMSO without water (top) and in DMSO with water (bottom) (adopted from Morris E., Rees D. and Welsh E. J. *J. Mol. Biol.* **1980**, 138, 383).

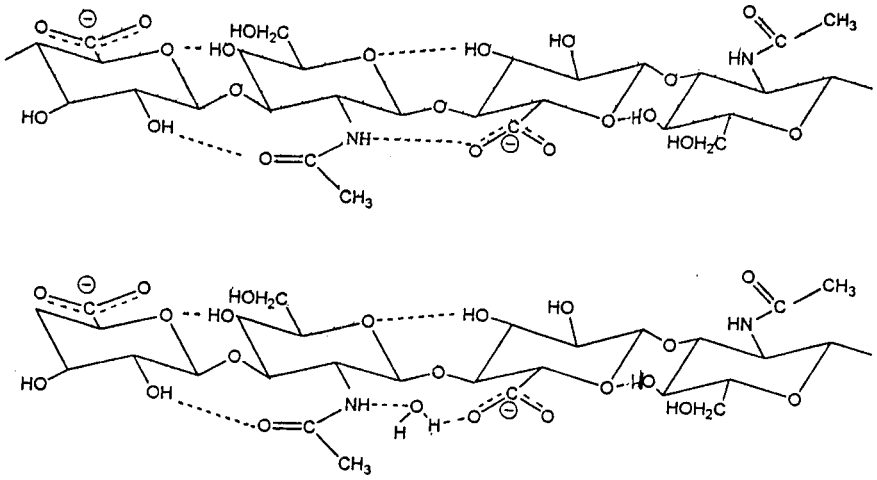

Molecular weight of HA can be higher than 1 million and the glycosidic linkages of HA can be hydrolyzed by hyaluronidase enzyme.[99] The pH of the carboxyl groups on the glucuronic acid residues is 3 to 4, which depends on ionic condition. At pH 7, these groups are predominantly ionized, therefore the polyanion hyaluronate molecule needs associated exchangeable counter ions to maintain its charge neutrality. The Measurement of dynamic light scattering in HA solutions revealed unspecific entanglements in combination with specific chain association.[100] There are some limitations on HA application due to its poor biomechanical properties in fabrication. Therefore, a variety of chemical modifications of HA have been developed to meet the requirements as biomaterials with excellent mechanical and chemical properties.[101] In this study, HA was modified by cholesteryl and fluorophore groups, in which cholesterol can be served as an anchor incorporated into lipid bilayers and fluorescent groups was used to monitor the conformation of the polymers. It can be expected that the cholesterol-bearing hyaluronans interact with phospholipid and nonphospholipid liposomes and form highly stable complexes. The results from leakage assay and cell culture studies indicate they could be used as promising carriers to deliver drugs or diagnostic agents into target sites with overexpressed CD44 or RHAMM, for instances, carrying diagnostic agents to breast tumor cells.

8.2. Experimental

8.2.1. Materials

Sodium hyaluronate was supplied by Hyal Pharmaceutical Corporation (Mississauga, ON) and was used without further purification. 1-Ethyl-3-(3-

dimethylaminopropyl)carbodiimide (EDC), Brij72, Cholesterol, Cetylpyridium Chloride (CPC) and calcein were purchased from Aldrich Chemical Co. Dimyristoylphosphatidylcholine (DMPC) and Dimethyl-di-n-octadecylammonium bromide (DDAB) was obtained from Avanti Polar Lipids. The composition of buffers used in this study was as followings: 10 mM Tris, 1mM EDTA, 140 mM NaCl, and 0.02% NaN_3, for phospholipid liposomes and 150 mM NaCl with 0.02% NaN_3 for nonphospholipid liposomes (NPL). pH was 7.2 unless stated.

8.2.2. Instrumentation

^1H NMR spectra were measured on a Brucker AC-200 or DRX-500 spectrometers. FTIR spectra were obtained with a Bio-Rad FTS-40 FTIR spectrometer (KBr pellets). UV-spectra were collected with a Hewlett Packard 8452A photodiode array spectrometer equipped with a Hewlett-Packard 89090A temperature controller. The measurement of dynamic light scattering was conducted with a Brookhaven Instrument Corp., Model BI-9000AT digital correlator equipped with a Lexel Argon Laser (λ = 514 nm). Steady-state fluorescent spectra were recorded on a SPEX fluorolog 212 spectrometer operated by a GRAM/32 data system. Temperature control of the samples was achieved by using a water-jacketed cell holder connected to a Neslab circulating bath. The temperature of the sample fluid was measured with a thermocouple immersed in a water-filled cuvette and placed in one of the four cell holders.

8.2.3. Preparation of *N*α-cholesterolhexanyl-*L*-lysine-pyrenylamide Derivatives Bearing HA (cholesterol-bearing HA)

HA (0.5 g) was dissolved in 200 mL of deionized water and the solution was stirred overnight. Compound 5a or compound 5b (Lypymecho or Lypybucho, 0.012 mmol) were dissolved into 20 mL of methanol, then added to the viscous HA solution. The pH of mixtures was adjusted to 4.75 with 0.1 N HCl. 1-(3-dimethylaminopropyl)-3-ethylcarbodine HCl salt (EDC, 0.015 mmol) was added into the above mixtures and the pH of mixtures was adjusted to 4.75 again. The mixtures were stirred for one week under dark condition. Ultrafiltration was applied to remove any molecules with molecular weight less than 31,000 Dalton. The residues were dialyzed against methanol/water (2/8, v/v) for 3 days and water 2 days at ambient temperature. The Modified HA was finally isolated by freeze-drying. ^{1}H NMR (DMSO-d6, ppm): 0.64 (s, cho 18-CH_3), 0.83-1.58 (m, proton of cho and lys), 1.77 (s, HA NHCOCH_3), 2.9-3.7 (b. H_2, H_3 and H_4 of N-ring, H_4 and H_5 of C-ring), 4.45-4.70 (b, H_1, H_2, H_3 of C-ring and H_1 of N-ring), 7.2-8.0 (b, aromatic proton of pyrene).

8.2.4. Determination of Pyrene Content

The dilute aqueous solutions of the modified HA were detected at 346 nm by UV measurement and the pyrene content was calculated based on Beer's law. *N*α-cholesterolhexanyl-*L*-lysine-pyrenylmethylamide and *N*α-cholesterolhexanyl-*L*-lysine-pyrenylbutylamide derivatives were used as corresponding model compounds and their extinction coefficient was 4497 and 8557 at 342 nm in methanol.

Table 8. 1. Pyrene Content of Cholesterol-Bearing HA

Polymer	Pyrene content /10^{-5} (mol/g)	Disaccharide units per pyrene
HA-Pymecho	17.0	14
HA-Pybucho1	3.73	64
HA-Pybucho2	5.24	46

8.2.5. Dynamic Light Scattering

The measurement of dynamic light scattering was conducted at 25°C in aqueous solutions or buffer solutions with 90° scattering angle. The sample concentration ranged from 0.1 to 1.0 g/L and the solutions were filtered through Millipore Membrane with pore size of 0.45 μm. CONTI program was used to calculate the average diameter of the micellar aggregates.

8.2.6. Preparation of Liposomes

Liposomes were prepared as follows: a dry thin film of mixed lipids[68] (100 mg, 75% of lipid, 20% of cholesterol and 5% of DDAB) was dispersed in 5 mL of buffer. The lipid suspension was mixed by vortex and extruded through a polycarbonate membrane with the pore size of 200 nm (Avanti Polar Lipids Inc.). In the case of calcein encapsulated liposomes, the dry thin film was dispersed in 78 mM of calcein solution (pH = 7.2). Free calcein was removed by passing the solution through a sephacryl S-75 column (1.5×30 cm) with a corresponding buffer as an eluant. The size of liposomes was measured by dynamic light scattering at 25°C with a fixed 90° scattering angle. The mean diameters of liposomes were located in the range from 195 to 225 nm.

8.2.7. Samples for Fluorescence Measurement

Samples for fluorescence analysis were prepared from stock aqueous solutions (0.5 to 5 g/L) and kept at room temperature for at least 24 hrs to ensure complete dissolution. In order to obtain the desired concentrations the stock solutions were further diluted by deionized water. The samples were further equilibrated at room temperature for at least 2 hrs before measurements. Excitation spectra were measured in the ratio mode. Emission spectra without correction were recorded with an excitation wavelength of 346 nm for pyrene and 290 nm for naphthalene. The slit widths of emission and excitation were set at 0.5 and 2.0 mm, respectively.

8.3. Results and Discussion

8.3.1. Synthesis and Characterization

Scheme 8.2 shows the procedure to modify HA by coupling carboimide-activated carboxyl groups with primary amine of cholesteryl and fluorophore lysine derivatives in a mixture of water and methanol. The modified HA was purified by ultrafiltration and dialysis, then isolated by freeze-drying. The attachment of cholesteryl and fluorophore groups to HA was ascertained by proton NMR. The aromatic protons appeared in the range of 7. 2 to 8.0 ppm and the 18-methyl group of cholesterol appeared at 0.62 ppm in DMSO-d_6.[37]

8.3.2. Solution Properties from Dynamic Light Scattering

The hydrophobically modified HA can form micellar aggregates in water as shown by two distributions of particle sizes. The larger size distribution (> 400 nm) would seldom be detected with the decrease of the polymer concentration (< 0.5 g/L), but the

smaller size distribution (130 nm for HA-Pymecho, 153 nm for HA-Pybucho) remained unchanged during the change of polymer concentration (Figure 3). Thus, it can be assumed the distribution of the larger sizes correspond to the aggregation of the smaller micelles structure. Once the polymers were dissolved in a salt solution (0.1 M NaCl, pH = 7.2), the size of micelles was shrunk to 56 nm for the HA-Pyme and 37 nm for HA-Pybu polymers, respectively (Table 8. 2). The micellar sizes can be also changed by dissolving the polymers in buffers with different values of pH. The micellar sizes increased with the decrease of pH at the solution with same ionic strength. The micellar sizes were slightly reduced by increasing ionic strength of solution with same pH. Two distributions remained in the buffer solutions at the concentration of 0.5 g/L. It was believed that eight CH groups attached on the alternate sides of the single HA helices as hydrophobic regions play a critical role in the aggregation of polymeric chains.[102] It is possible to tailor the size of micelles by adjusting the level substitution of cholesteryl and fluorophore groups and counterion condensation.

Scheme 8.2. Synthesis scheme of cholesterol-bearing HA

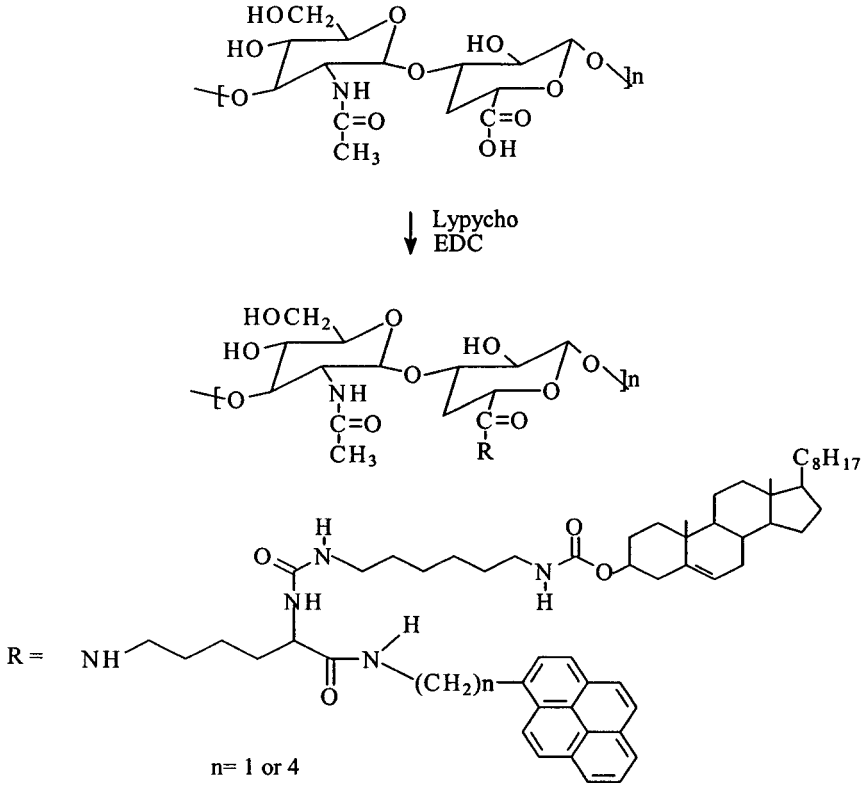

Figure 8.1. Dynamic light scattering profiles of cholesterol-bearing HA in water and buffer.

HA-Pymecho 1.0 g/L in water

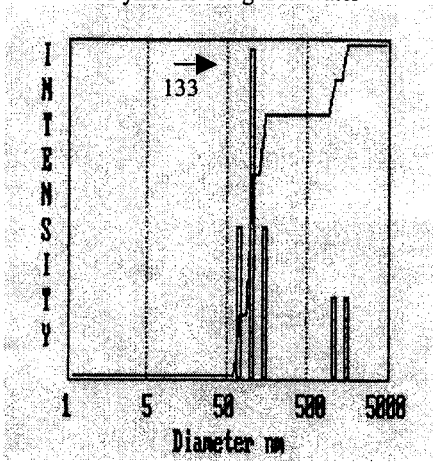

HA-Pymecho, 0.5 g/L in water

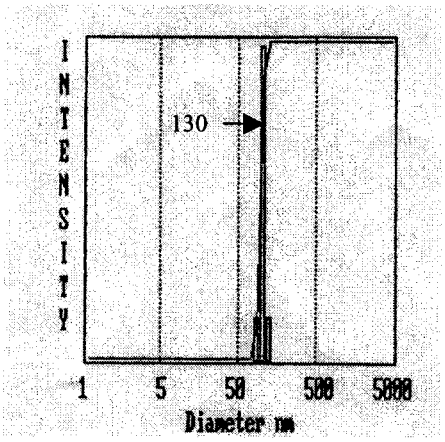

HA-Pymecho, 0.5g/L
pH=7.2, 0.1 M NaCl

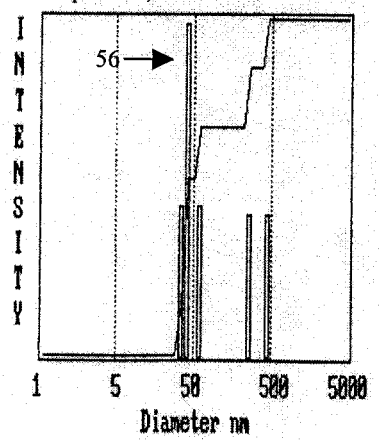

Table 8. 2. Effect of pH and Ionic Strength on Micellar Size

Polymer	pH	Concentration of NaCl (M)	Diameter (≤ ± 5 nm)
HA-Pymecho 0.5 g/L	3.0	0.1	87
	7.2	0.1	37
	9.1	0.1	52
		1.0	37
HA-Pybucho1 0.25 g/L	3.0	0.1	56
		1.0	37
	7.2	0.1	37
	9.1	0.1	37
		1.0	56

8.3.3. Solution Properties from Fluorescence

The fluorescence spectra of HA-Pymecho aqueous solutions exhibited a comparable excimer and monomer emission. The ratio of I_E/I_M for HA-Pymecho kept almost unchanged (0.27) in the range of polymer concentration from 0.005 to 1.0 g/L (Figure 8. 2a). The ratio of I_1/I_3 for HA-Pymecho had almost constant with increasing polymer concentration as shown in Figure 8. 2b. These results indicate that intrapolymeric chain association plays a major role rather than interpolymeric association. In the case of HA-Pybucho, a large monomer emission and very small excimer emission was observed. The ratio of I_E/I_M remained at a low value (0.085) over the studied concentration range from 0.005 to 2.5 g/L (Figure 8. 3).

The ratio of I_E/I_M for both HA-Pybucho and HA-Pymecho has no significant change with increasing pH from 2.5 to 9.0 in the buffer solution with 0.1 M ionic strength as shown in Figure 8. 4a.

Figure 8.2. (a) Ratio of pyrene excimer to monomer emission intensities (I_E/I_M) for HA-Pymecho in water as a function of polymer concentration; (b) ratio I_1/I_3 for HA-Pymecho in water as a function of polymer concentration (25°C, λ_{ex} = 45 nm).

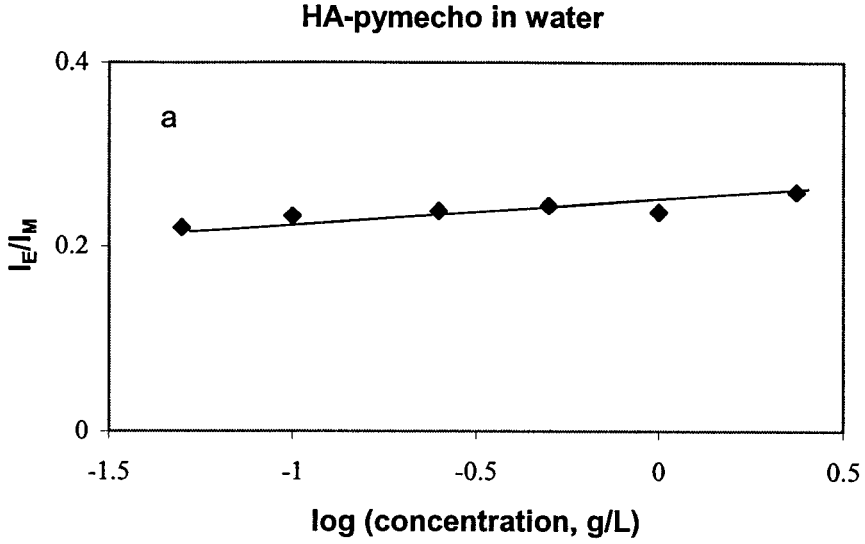

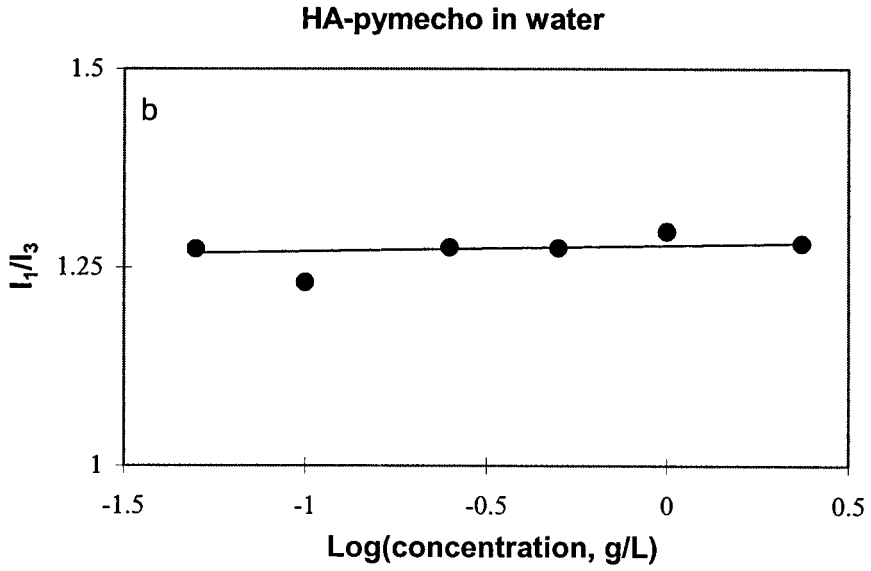

Meanwhile, the pH value of solution has no effect on the ratio I_1/I_3 of HA-Pymecho (Figure 8.4b). But the ratio I_E/I_M increased little upon increasing the ionic strength of solutions from 0 to 2.0 at the constant pH 3 or 9 (Figure 8.5a & 8.5b). The ratio I_1/I_3 of HA-Pymecho had little change from 1.22 to 1.27 with increasing ionic strength of solutions at the constant pH 3 or 9 (Figure 8.5c). The effect of ionic strength on the ratio I_1/I_3 was more significant when the ionic strength was below 0.5 M. The results indicate that cholesterol-bearing HA possesses rigid conformations in aqueous solutions and has a similar behavior to the parental HA.[103] One possible contribution to the polymeric chain stiffening could be the existence of hydrogen bonding as shown in Scheme 8.1.

Figure 8.3. Ratio of I_E/I_M for HA-Pybucho as a function of polymer concentration (25°C, λ_{ex} =345 nm).

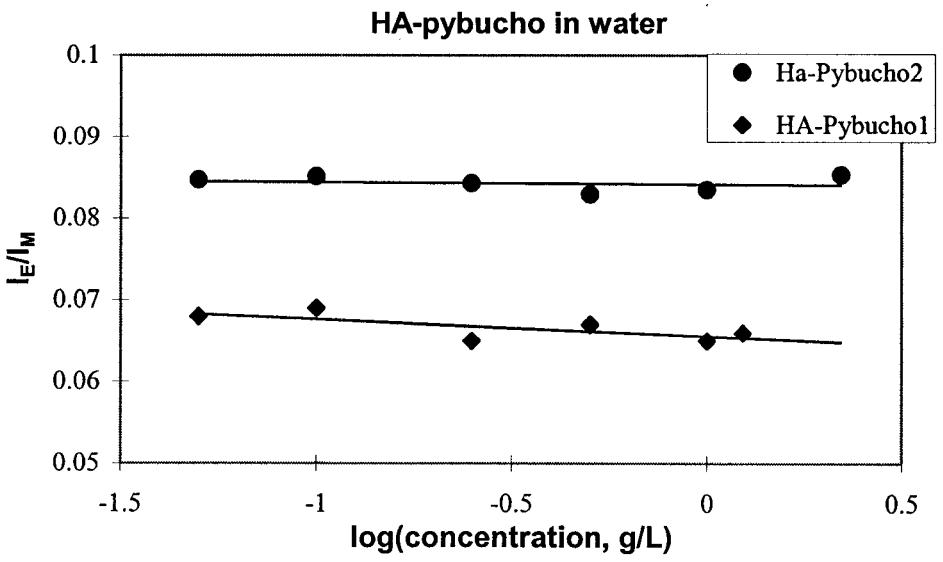

Figure 8.4. (a) I_E/I_M of HA-Pymecho and HA-Pybucho in buffer as a function of pH. (b) I_1/I_3 of HA-Pymecho in buffer as a function of pH (25°C, λ_{ex} = 345 nm, [NaCl] = 0.1 M).

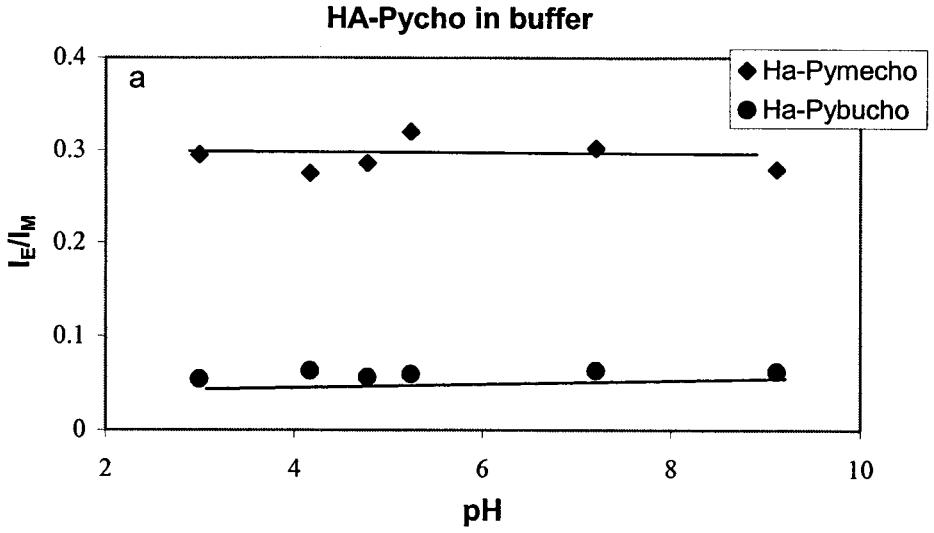

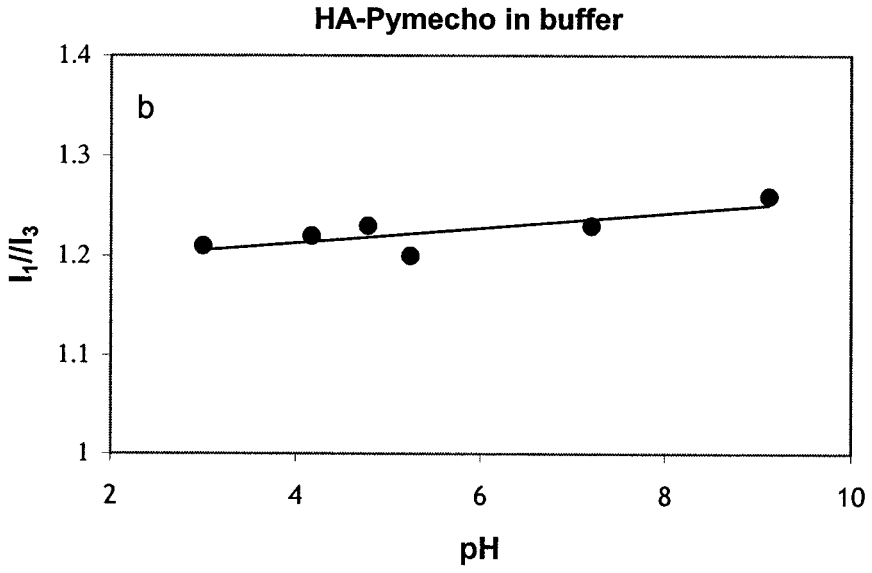

Effect of Temperature on Conformation of Cholesterol-Bearing HA.

The ratio of I_E/I_M remained as constant with increasing temperature up to 40°C, but the ratio of I_1/I_3 was decreased from 1.26 to 1.12 with the increase of temperature from 20 to 40°C as shown in Figure 8.6. It reached the limited value at 35°C, which indicates that the conformation of the polymer became more compact. A similar transition around 37°C was observed in an Arrhenius plot of HA periodate.[104] However, The transition was not observed in circular dichroism and a plot of viscosity vs. temperature.[105] Thus, it is only clear that the transition was not related with acetamido group and the solvent-draining properties of the polymer. Scott suggested that it may be caused by the rearrange of hydrogen bonding between the glucosamine C4 hydroxyl and the urinate ring oxygen.

Figure 8.5. (a) Ratio I_E/I_M of HA-Pymecho as a function of ionic strength; (b) I_E/I_M of HA-Pybucho as a function of ionic strength; (c) I_1/I_3 of HA-Pymecho as a function of ionic strength (25°C, λ_{ex} = 345 nm).

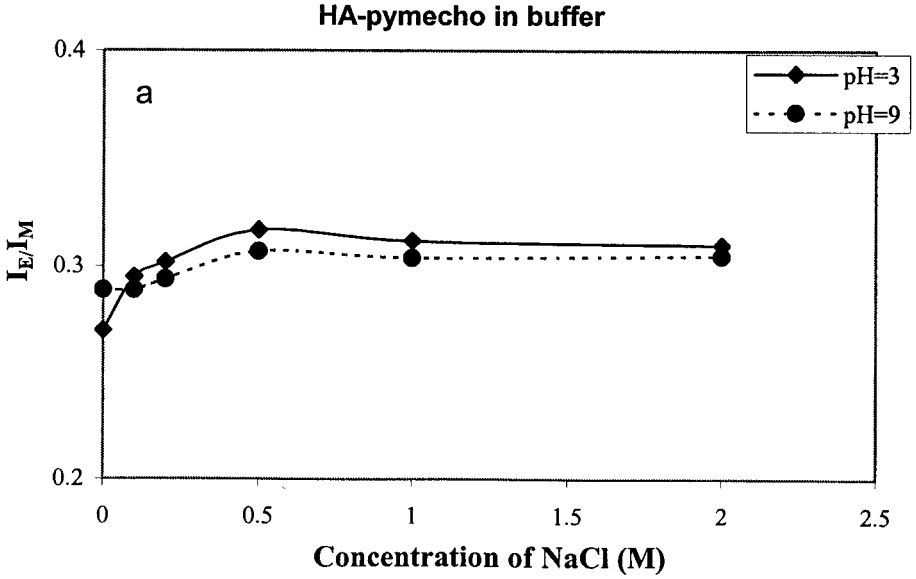

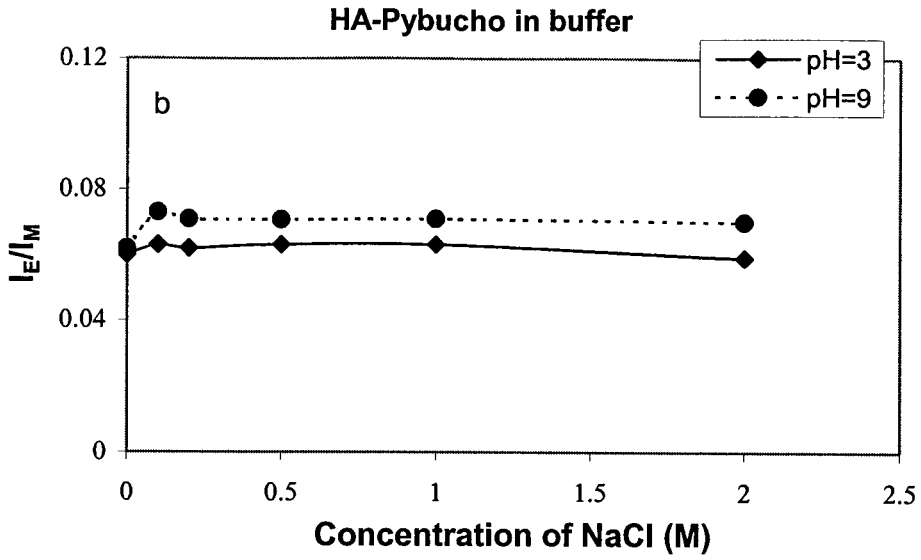

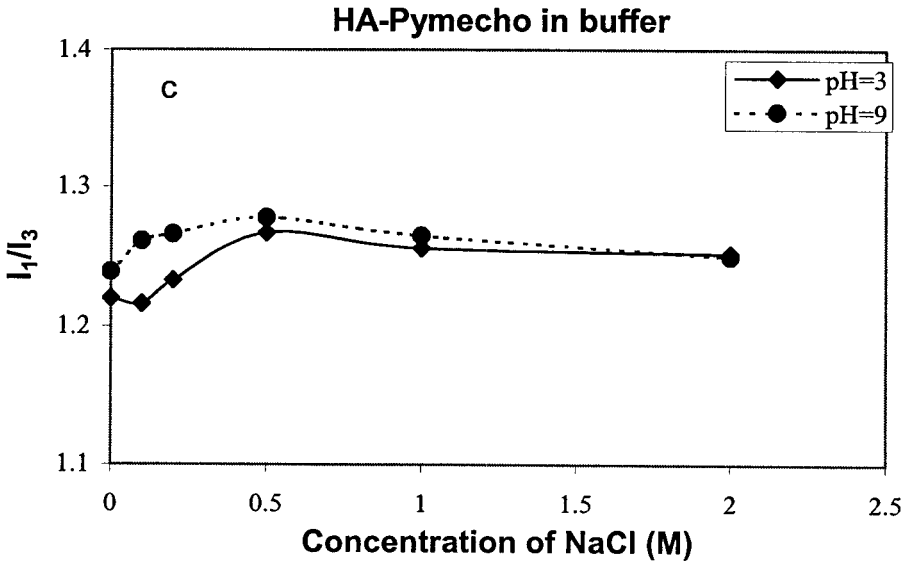

8.3.4. Secondary Structure of HA-Pycho

The Circular dichroism spectra (CD) of HA and HA-Pymecho were measured in aqueous solutions and the results were given in Figure 8.7. The negative band around 210 nm can be assigned to n-pi * transitions in acetamido chromophore of HA.[106] It was

observed that cholesterol-bearing HA had a lower CD intensity in this region than that of parental HA. The similar results were found as the CD intensity of HA enhanced when HA mixed with globular protein (lysozyme) and it was believed that the protein with a greater helical character could enhance the CD intensity of HA.[115] The disturbance of the secondary structure of HA by modified cholesterol and pyrene groups may reduce chiroptical activity since the mixture of Lypymecho, and unmodified HA solution has no effect on CD spectrum of HA, therefore it is certain that the conformation of HA-Pymecho was disturbed by the chemical modification of the cholesteryl and fluorophore groups. The disturbance of the secondary structure may cause a change in inter-residues hydrogen bonds, thus, the conformation of HA-Pycho in solution is determined by the balance of hydrophobic association, electrostatic repulsion and hydrogen bonding.

8.3.5. Interaction with Hydrophobically Modified Thermosensitive Amphiphilic Polymers

The association of two different hydrophobically modified polymers has been considered as an efficient strategy to prepare new functional nanoparticles.[107] The interaction between cholesterol-bearing HA and cholesterol-bearing poly(*N*-isopropylacrylamide) (e.g. 240K-N74) may form new functional nanoparticles, which was examined by nonradiative energy transfer.

Figure 8.6. (a) I_E/I_M of HA-Pymecho as a function of temperature; (b) I_1/I_3 of HA-Pymecho as a function of temperature ([HA-Pymecho] = 0.5g/L, λ_{ex} = 345 nm).

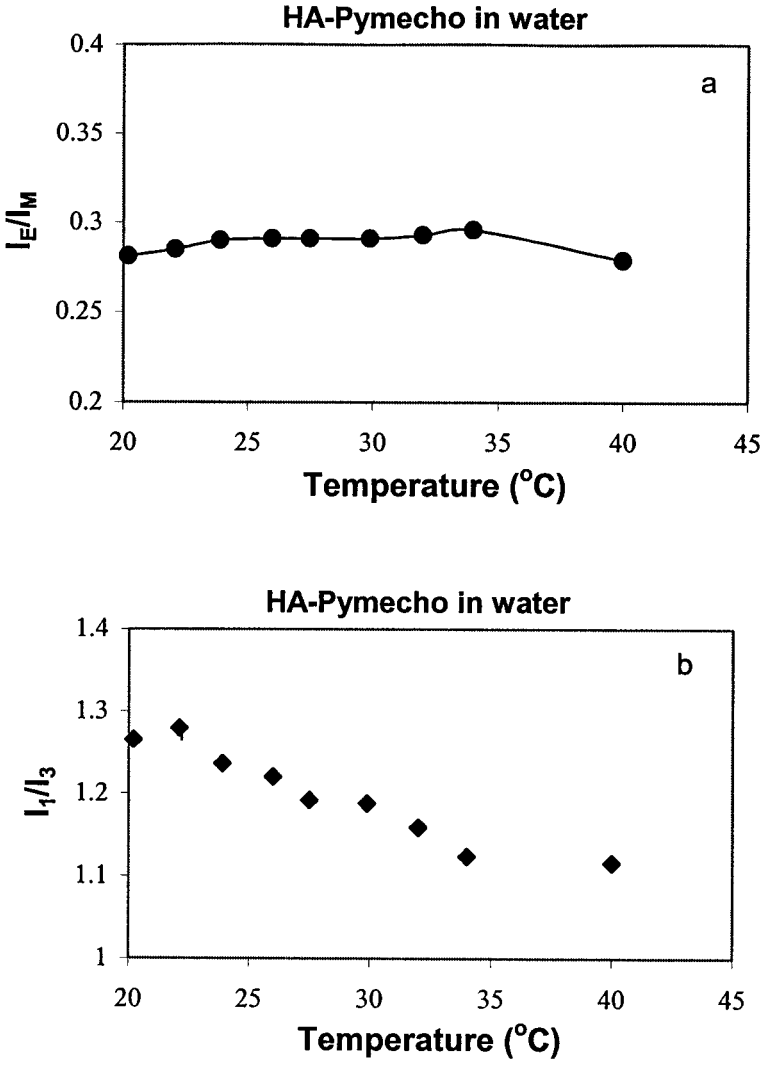

The mixed solutions with different ratios of HA-Pybucho to PNIPAM were excited at 290 nm (25 °C) and the larger pyrene monomer emission can be observed in the range from 375 nm to 450 nm as shown in Figure 8.8, comparing with the pyrene monomer emission from HA-Pybucho alone solution. The ratio I_{Py}/I_{Np} is taken as an extent of nonradiative energy transfer (NRET) from donor naphthalene to acceptor pyrene[10] and listed in Table 8.3. The large value indicates that the two chromophores are

approximately close to each other. The NRET study revealed that the hydrophobic groups attached on two different polymers were reorganized in microdomains.

Table 8.3. NRET between HA-Pycho and 240K-N74

Polymer pair	Polymer pair concentration (g/L)	Molar ratio of Np/Py	I_{Py}/I_{Np} ($\leq \pm 0.1$)
HA-Pymecho/ 240K-N74	0.032/0.11	2.4	0.3
	0.032/0.046	1.0	0.5
	0.10/0.11	0.8	0.7
	0.10/0.046	0.3	1.2
HA-pybucho2/ 240K-N74	0.102/0.11	2.4	3.2
	0.102/0.046	1.0	4.4

Figure 8.7 Circular dichroism spectra of HA and HA-Pymecho in water (25°C, [HA] = 0.5 g/L, [HA-Pymecho] = 0.5 g/L).

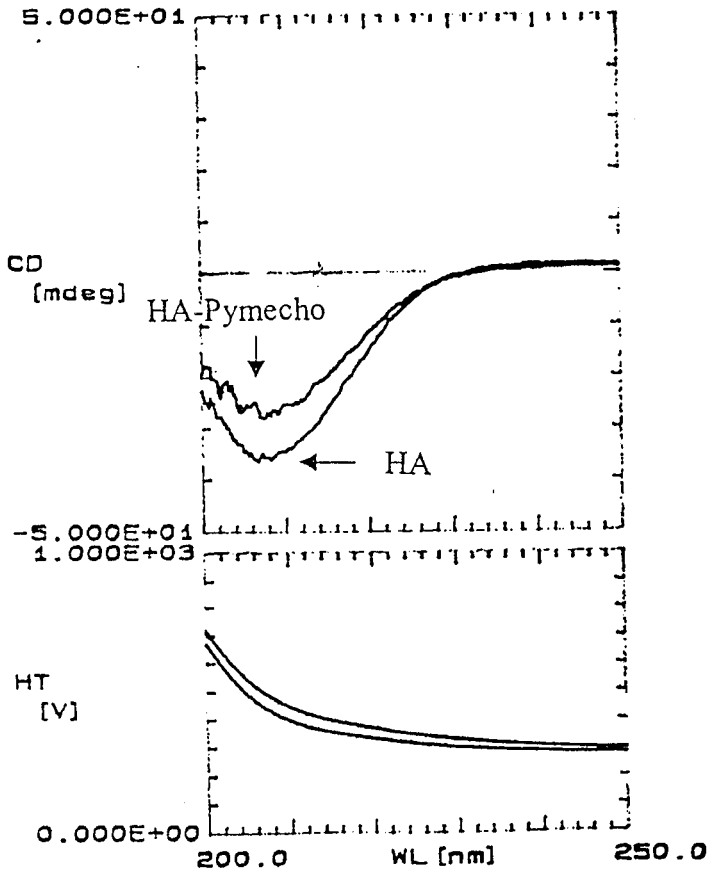

As discussed in the DLS section, the HA-Pycho micellar structure can aggregate in water and the addition of salts can prevent the aggregation. DLS results showed that the sizes of the cholesterol modified HA micellar structure significantly decreased upon adding 240K-N74 to the HA-Pycho solutions as shown in Table 8.4. This finding indicates that the aggregation of HA could be avoided by adding a neutral polymer on the surfaces of HA micelles and new hybrid nanoparticles can be generated from cholesterol-bearing HA and cholesterol-bearing poly(*N*-isopropylacrylamide).

Figure 8.8. Fluorescence spectra of HA-Pybucho/240K-N74 complexes at varied concentration ratio, 25 °C, λ_{ex} = 290 nm, [HA-Pybucho]/[240K-N74] =0.102/0.11 (top), [HA-Pybucho]/[240K-N74] = 0.102/0.046 (middle), [HA-Pybucho] = 0.102 g/L (bottom).

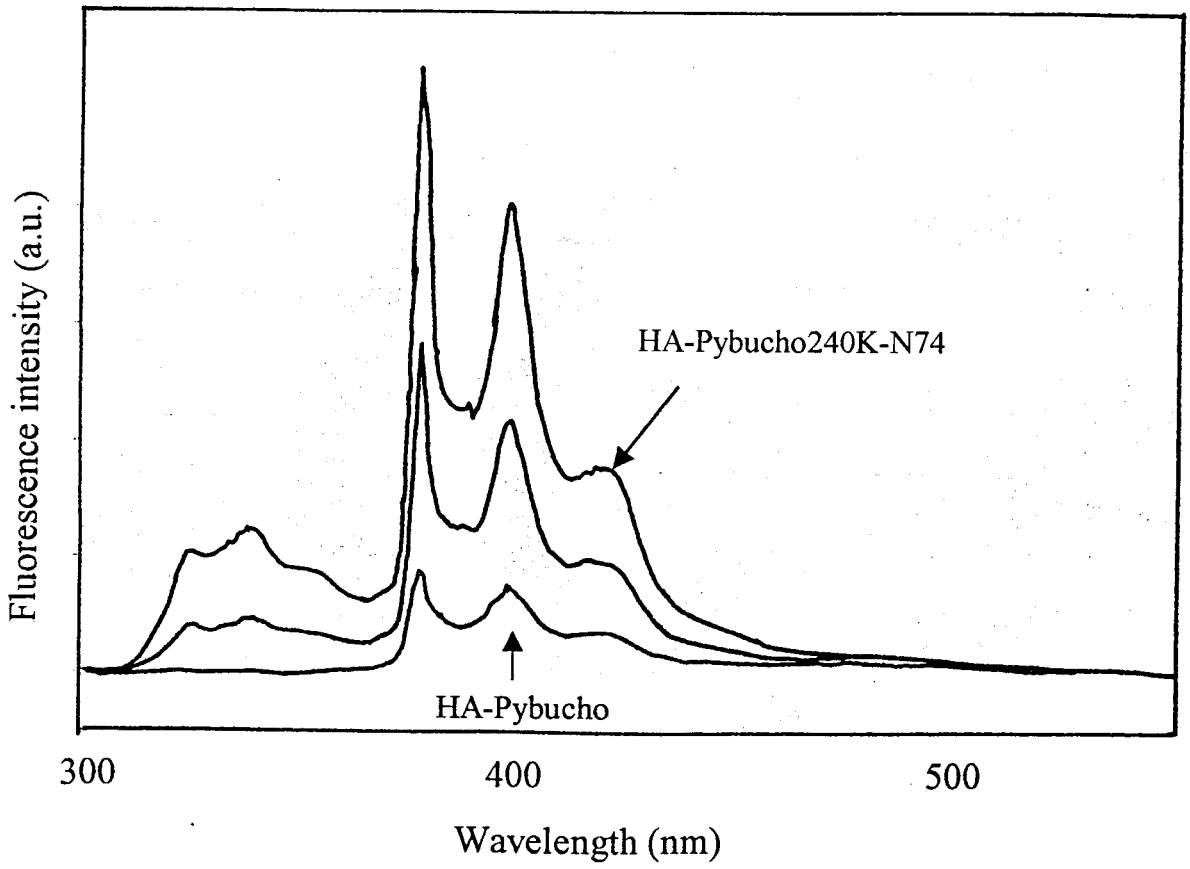

Table 8. 4. Association between cholesterol-bearing HA and cholesterol-bearing PNIPAM in water

Polymer pairs	Diameter (≤ ±6 nm)
HA-Pymecho 0.5 g/L	130
HA-Pybucho2 0.5g/L	153
HA-Pymecho/240K-N74 0.10/0.046 g/L	43
HA-Pymecho/240K-N74 0.10/0.11 g/L	32
HA-Pybucho2/240K-N74 0.105/0.046 g/L	58

8.3.6. Interaction of HA-Pymecho with Liposomes

Targeting liposomes has been developed rapidly in the past decade for controlled delivery of bioactive molecules in gene therapy and chemotherapy.[108] The most distinguished advantage of liposomes is the ability to carry a variety of highly toxic drugs within the aqueous compartment or in the lipid bilayers, and the damage on normal cells and side effects can be minimized. On the other hand, HA can bind specifically to proteins such as hyaladherins in the extracellular matrix and on the cell surface.[109] The protein-ligand interactions can stabilize the cartilage matrix and mediate signals for cell motility, cellular proliferation, morphogenesis, embryonic development, cancer metastasis and inflammation.[110] Liposomes coated with HA are naturally targeting liposomes for the cells with a high level of CD44 or RAHMM such as breast cancer cells. To develop this targeting liposomes, we studied the interaction of cholesterol-bearing HA with phospholipid (DMPC) and nonphospholipid liposomes (NPL) by fluorescence measurement and microcalorimetry. It was found that cholesterol-bearing HAs formed

micellar structure in water and exhibited relatively higher ratio of pyrene excimer emission to pyrene monomer emission (I_E/I_M). The ratio of I_E/I_M dropped slightly upon the addition of the liposomes to the polymer solutions and reached a constant value (Figure 8.9a).

Figure 8.9. (a) I_E/I_M of HA-Pymecho/liposome complexes in buffer as a function of lipid to polymer concentration ratio, (b) I_1/I_3 of HA-Pymecho/liposome complexes in buffer as a function of lipid to polymer concentration ratio (25°C, λ_{ex} = 345 nm).

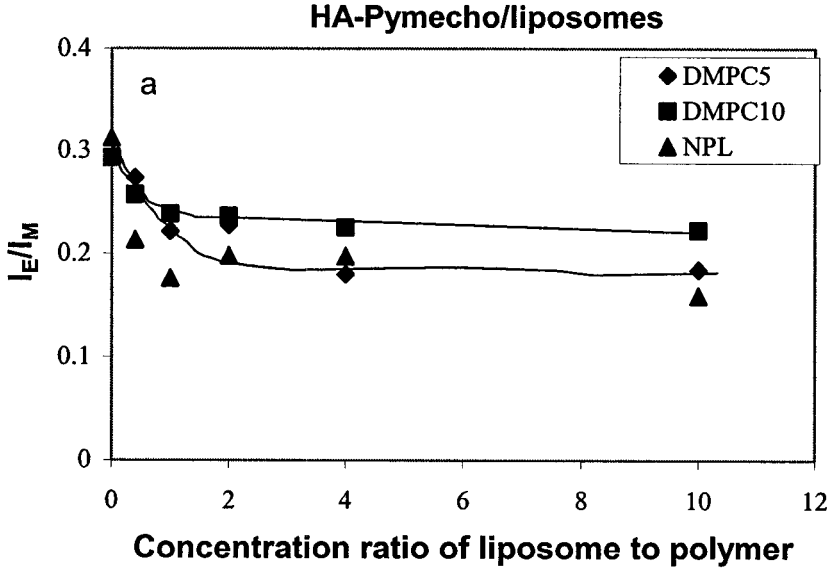

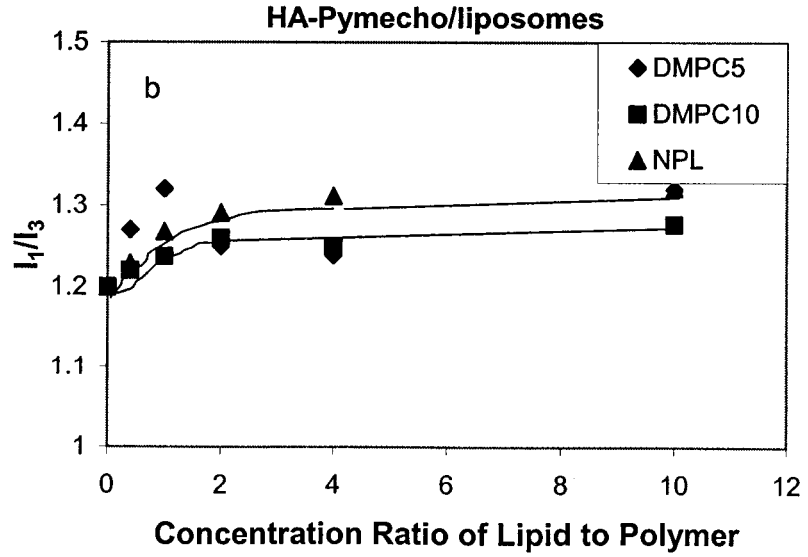

It means that the monomer emission increased at the expense of excimer emission. It can be induced that the micellar structure of cholesterol-bearing HA was disrupted in the presence of the liposomes, and the hydrophobic substituents inserted into the lipid bilayers and hydrophilic chains surround the liposome surfaces. However, the ratio of I_1/I_3 increased by the addition of the liposomes (Figure 8.9b), and no significant quenching of pyrene was observed when cetylpyridinum chloride (CPC)-carrying liposomes were applied. The results indicate that pyrene did not insert into the lipid bilayers together with cholesterol moieties as discussed before and only cholesterol hydrophobic substitutent of cholesterol-bearing PNIPAM inserted into lipid bilayers, so that cholesterol-bearing HA behaves the same as the cholesterol-bearing PNIPAM when it interacts with liposomes. Dynamic Light scattering shows that the size of liposomes only slightly changed after the surfaces of liposomes were coated by cholesterol-bearing HA (data not shown).

Figure 8.10. Fluorescence profiles of leakage extent of HA-Pymecho/liposome complexes monitored at 515 nm in fetal bovine serum at 37 °C, λ_{ex} =450 nm.

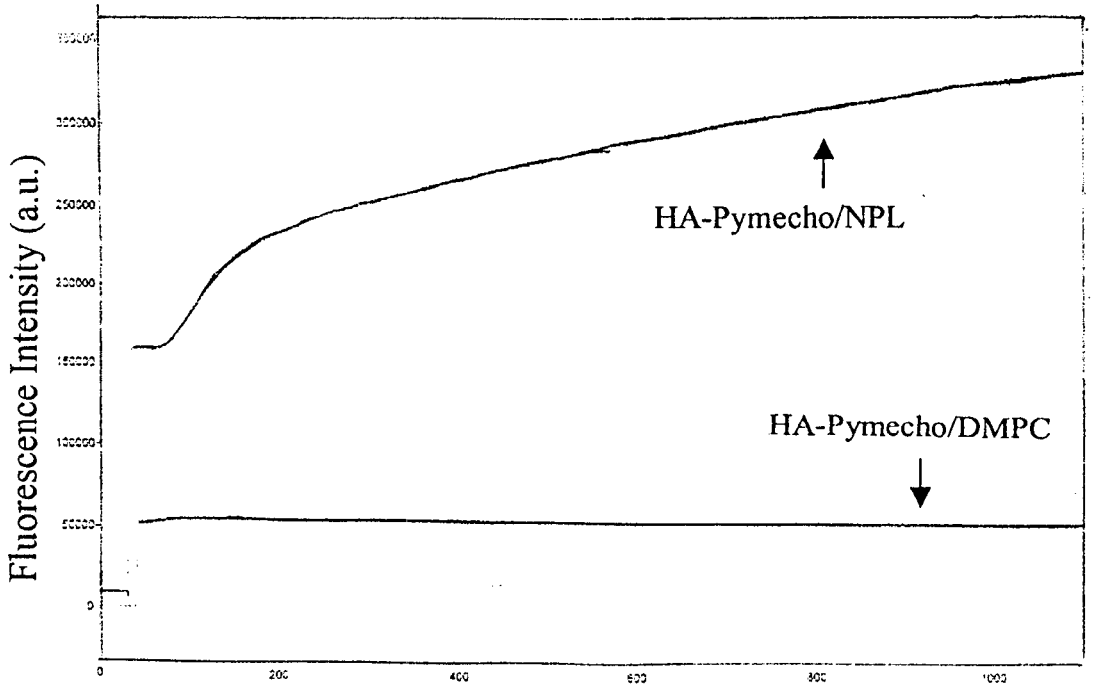

8.3.7. Leakage assay

Calcein loaded liposomes may release the entrapped dye by exterior triggers, such as pH and temperature.[111] This assay is considered as a standard assay for leakage study. The HA coated liposomes were obtained by incubating HA-Pycho with calcein loaded liposomes overnight at room temperature. Then the samples were diluted into a desired concentration, and the release extent was monitored as a function of pH at both 25 °C and 37.4 °C. No significant release was observed in either NPL/HA-Pymecho or DMPC5/HA-Pymecho complexes in the range of pH from 4 to 9 (data not shown). Once the complexes were placed into the fetal bovine serum (pH = 7.2) at 37.4 °C, a significant release (54%) was observed from NPL/HA-Pymecho complex, but no release was detected in the complexes of DMPC5/HA-Pymecho and DMPC5/HA-Pybucho (Figure 8.10). This indicates that the DMPC5/HA-Pycho complex systems were highly stable and they could be promising candidates for diagnostic agent carriers or gene therapy carriers.

Figure 8.11. Microcalorimetric endotherms for aqueous solutions of DMPC (1 g/l) and HA-Pymecho/DMPC complex (1/1 g/L).

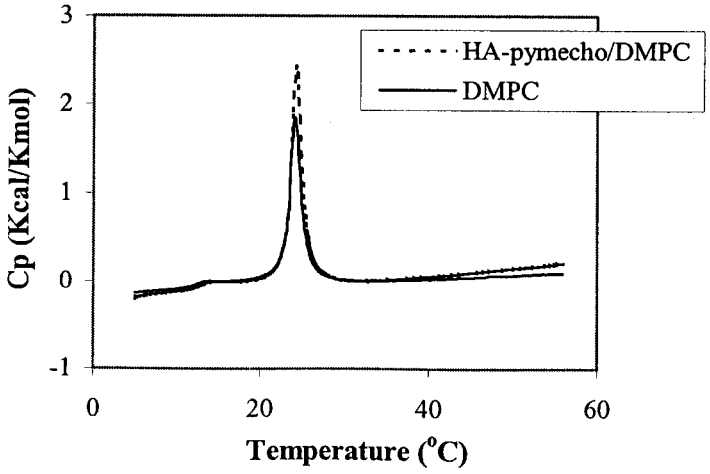

8.3.8. Microcalorimetry

A microcalorimetric trace of DMPC/HA-Pymecho with an excess of the polymer is shown in Figure 8.11. Since HA-Pymecho itself has no any visible phase transition in the examined temperature range, the main peak around 24.2 °C can be attributed to the gel-liquid crystal phase transition of DMPC and the minor peak around 13.8 °C is assigned to the pretransition of the lipid bilayers. The pretransition of DMPC solution appeared at 14.8 °C;[112] thus, the major effects of the polymer on the DMPC were the shift of the pretransition and the enthalpy of the main transition, which consist with that the interaction between cholesterol-bearing HA and DMPC liposomes.

8.4. Conclusion

HA can be covalently attached by cholesteryl and fluorophore groups and the modified HA can form micellar structure in aqueous solutions. The micellar size can be controlled by the level of hydrophobic incorporation and counterion condensation. The modified HA had a rigid conformation in aqueous solutions and were hardly affected by pH, ionic strength and concentration of the polymers. The aggregation of the micellar structure formed by the modified HA in water can be prevented by adding salt and PNIPAM. Hybrid nanoparticles can be obtained by an association of the modified HA and cholesterol-bearing PNIPAM. Highly reliable HA/DMPC complexes were developed by coating liposomes with cholesterol-bearing HA.

[1] (a) Lasic D. *Nature* **1997**, 387, 26; (b) Baldeschwieler J. D. and Schmidt P. G. *Chemtech*, **1997**, October, 33; (c) Lasic D. and Needham D. *Chem. Review* **1995**, 95, 2601; (d) Zignani M., Drummond D. C. Meyer O., Hong K., Leroux J. *Biochi Biophy Acta*, **2000**, 1463, 383.
[2] Ringsdorf H., Schlarb B. and Venzmer J. *Angew. Chem.* **1988**, 27, 113 and references therein.
[3] (a) Hirstova K. and Needham D. *Macromolecules*, **1995**, 28, 991; (b) Kenworthy A. K., Simon S. A. and Mcintosh T. J. *Biophy. J.* **1995**, 68, 1903.
[4] (a) Ringsdorf H., Venzmer J. and Winnik F. M. *Angew. Chem. Int. Ed. Engl.* **1991**, 30, 315; (b) Hayashi H. Kono K. and Takagishi T. *Bioconj. Chem.* **1999**, 10, 412.
[5] Takada M., Yuzuriha T., Katayama K., Iwamoto K., Sunamoto J. *Biochim. Biophys. Acta* **1984**, 802, 237.
[6] (a) Yamazaki. A. *Adsorption of Plasma Proteins to Liposome Surfaces*, McMaster University, **1997**; (b) Polozova A. and Winnik F. M. *Biochi. Biophy Acta*, **1997**, 1326, 213.
[7] Klok H. A., Hwang J., Iyer S., Tew G. N., Li L. and Stupp I. *Polym. Prepr.* **1998**, 166.
[8] Tsuchida E., Yamamoto K., Miyatake K. and Endo K. *Macromolecules* **1997**, 30, 4235.
[9] Turro N. J. (ed.) *Modern Molecular Photochemistry* The Benjamin/Cummings Publishing Co. Inc. **1978.**
[10] Lakowicz J. R. *Principle of Fluorescence Spectroscopy* Plenum Press, **1983.**
[11] (a) Birks J. B. (ed.) *Photophysics of Aromatic Molecules* Wiley-Interscience, **1970**; (b) Winnik F. M. *Chem Review* **1993**, 93, 587 and references therein.
[12] Becker R. S. *Theory and Interpretation of Fluorescence*, **1969**, Wiley Interscience.
[13] Winnik M. A. (ed.) *Photophysical and photochemical Tools in Polymer Science* Dordrecht Holland, **1986**.
[14] Förster T. *Discuss. Faraday Soc.* **1959**, 27, 7
[15] (a) Schild H. G. and Tirrell D. A. *Langmuir* **1991**, 7, 1319; (b) Ringsdorf H., Simon J. and Winnik F. M. *Macromolecules*, **1991**, 24, 1678; (c) Gutowska A., Bae Y. H, Feijen J., Feijen J. and Kim S. W. *J. Contr. Relea.* **1992**, 22, 95; (d) Casolaro M. *Macromolecules* **1995**, 28, 2351; (e) Nuniz E. C. and Geyskens G. *Macromolecules* **2001**, 34, 4480.
[16] (a) Smith G. L. and McCormick C. L. *Macromolecules*, **2001**, 34, 5579; (b) Anghel D. F., Alderson V., Winnik F. M., Mizusaki M., and Morishima Y. *Polymer* **1998**, 39, 3035.
[17] Liang D., Zhou S., Song L., Zaitsev V. S., and Chu B. *Macromolecules*, **1999**, 32, 6326.
[18] Hu Z. B., Chen Y. Y., Wang C. J., Zheng Y. D., and Li Y. *Nature*, **1998**, 393, 149.
[19] Jimenez-Regalado E., Selb J. and Candau F. *Langmuir*, **2000**, 16, 8611.
[20] (a) Shalaby S. W., McMormick C. L. and Butler G. B. (ed.) *Water-soluble Polymers: Synthesis, Solution Properties and Applications* ACS Symp Ser. 467. Washington DC, **1991**; (b) Glass J. E. (ed.) *Polymers in aqueous media: Performance through association* ACS Adv. Chem. Ser. 223, Wasington DC, **1989.**
[21] (a) Aspinall G. O. (ed.) *The Polysaccharides* vol. 1 Academic Press, **1982**; (b) Hayashi K., Tsutsumi K., Nakajima F., Norisage T. and Teramoto A. *Macromolecules*, **1995**, 28, 3824.
[22] (a) Laurent T. C. (ed.) *The Chemistry, Biology and Medical Applications of Hyaluronan and its derivatives* Portland Press **1998**; (b) Drobnik *Advanced Drug Delivery Review,* **1991**, 25, 295.
[23] (a) Peppas N. and Langer R. *Science*, **1994**, 263, 1715; (b) Freed L. E., Vunjak-Novakovic, G., Biron R. J., Eagles D., Lesnoy D., Barlow S. and Langer R. *Biotechnology*, **1994**, 12, 689.
[24] (a) Prestwich G. D., Marecak, D. M., Marecek J. F., Vercruysse K. P. and Ziebell M. R. *J Contr. Releas.* **1997**, 53, 99; (b) Luo Y., Kirker K. and Prestwich G. *J Contr. Releas.* **2000**, 69, 169.

[25] Cortivo E., Brun P., Rastrelli A. and Abatangelo G. *Biomaterials*, **1991**, 12, 727.
[26] (a) Pouyani T., Harbison G. S. and Prestwich G. D. *JACS*, **1994**, 116, 7515; (b) Glass J. R., Dickerson K. T., Stecker K., and Polarek J. W. *Biomaterials*, **1996**, 17, 1101.
[27]Lehninger A. L., Nelson D. L. and Cox M. M. *Principles of Biochemistry* Worth Publisher 2nd ed. **1993.**
[28] (a) Ahlers M., Muller W., Reichert A., Ringsdorf H. and Venzmer J. *Angew. Chem. Int. Ed. Engl.* **1990**, 26, 1269; (b) Kono K., Hayashi H. and Takagish T. *Bioconjugated Chem*, **1998**, 9, 382Whitesides G. M., Mathias J. P.and Seto C. T.; *Science*, **1991**, 254, 1312.
[29] See for example, Hydrophilic Polymers, Performance with Environmental Acceptability. Glass E. D. (ed.) *Advances in Chemistry Series 248*: ACS, Washington DC, **1991**.
[30] Stroeve P. and Balas A. C. (eds) *Macromolecular Assemblies in Polymeric Systems*, ACS Symposium Series 493, ACS, Washington DC, **1992.**
[31] Uhrich K. E., Cannizzaro S. M., Langer R. S. and Shakesheff K. M., *Chem Rev.* **1999**, 99, 3181 and reference therein.
[32] (a) Sunamoto J.; Sato T.; Taguchi T. and Hamazaki H. *Macromolecules* **1992**, 25, 5665; (b) Nishikawa T., Akiyoshi K. and Sunamoto J., *JACS*, **1996**, 118, 6110.
[33] Kang E. C., Akiyoshi K. and Sunamoto J. *Int. J. Biol. Macromol.* **1994**, 16, 348.
[34] Ringsdorf H., Simon J. and Winnik F. M. *Collod-Polymer Interactions* Dubin P. and Tong P. (ed.) ACS Symposium Series 532, Washington DC, **1993**, Chapter 16.
[35] Winnik F. M. *Macromolecules* **1990**, 23, 233.
[36] Akiyoshi K., Deguchi A., Moriguchi N., Yamaguchi S. and Sunamoto J. *Macromolecules*, **1993**, 26, 3062.
[37] Bodanszky M. (ed.) *Principles of Peptide Synthesis* Springer-Verlag, **1984.**
[38] (a) Kopple K. D., GO A., Logan G. H. and Savdra J. *JACS* **1972**, 94, 973; (b) Flex *J. Org. Chem.* **1978**, 43, 4194.
[39] Gung B. W., Zhu Z., Zou D., Everingham B., Oyeamalu A., Crist R. M. and Baudlier J. *JOC*, **1998**, 63, 5750.
[40] (a) Kessler H. *Angew. Chem. Int. Ed. Eng.* **1982**, 512; (b) Steven E. S., Sugawara N., Bonara G. M. and Toniolo C. *JACS* **1980**, 102, 7048.
[41] (a) Urry D. W. Ohnishi T. *Peptide, Polypeptides and Proteins,* Blout E. R., Bovey F. A., Goodman M. and Lotan N. (ed) Wiley Interscience, New York **1974**, 230-247; (b) Dado P. G., Gellman S. H. *JACS*, **1994**, 116, 1054; (c) Gung B. W. and Zhu Z. *JOC* **1997**, 62, 2324.
[42] (a) Clegg R. S., Reed S. M. and Hutchison J. E. *JACS*, **1998**, 129, 2486; (b) Junquera E. and Nowick J. S. *JOC*, **1999**, 64, 2527; (c) Dempsey C. E., *Biochemistry*, **1988**, 27, 6893; (d) Dixon D. A., Dobbs K. D. and Valentini J. J. *J. Phy. Chem* **1994**, 98, 13435; (e) Lee Y. *J. Raman, Spectra.* **1997**, 45.
[43] *Chemistry and Technology of isocyanates*, John Wiley & Sons Ltd, Chapter 1, **1996** and reference therein.
[44] (a) Schild H.G. and Tirrell D. A. *Macromolecules* **1992**, 25, 4553; (b) Schild H. G *Progress in Polymer Science* **1992**, 17, 163.
[45] Winnik F. M., Davidson A., R. Hamer G. K. and Kitano H. *Macromolecules* **1992**, 25, 1876.
[46] Oku N.and Namba Y. *Critical Review in Therapeutic Drug Carrier System* **1994**, 11, 231.
[47] Sunamoto J., Sato T., Taguchi T. and Hamazaki H. *Macromolecules* **1992**, 25, 5665.
[48] Brown G. H. and Wolken J. J. *Liquid crystals and Biological Structure* Academic Press, **1979.**
[49] (a) Tsuchida E., Yamamoto K., Miyatake K. and Endo K. *Macromolecules* **1997**, 30, 4235; (b) Akiyoshi K., Deguchi A., Moriguchi N., Yamaguchi S. and Sunamoto J. *Macromolecules* **1993**,

26, 3062; (c) Nishikawa T., Akiyoshi K. and Sunamoto J. *Macromolecules* **1994**, 27, 7645; (d) Tsuchida E., Yamamoto K., Miyatake K. and Endo K. *Macromolecules* **1997**, 30, 4235.
[50] Kubota K., Fujishige S., and Ando I. *Polym. J.* **1990,** 22, 15.
[51] Li M. *Synthesis and Chracterizationof Pyrene Labeled Poly(N-Isopropylacrylamide-co-N-Valine-Acrylamide) Copolymers,* McMaster University, **1997.**
[52] Fujishige S., Kubata K. and Ando I. *J. Phys. Chem.* **1989**, 93, 3311.
[53] Pecora R. (ed.) *Dynamic Light scattering- Applications of Photon Correlation Spectroscopy* Plenum Press, **1985.**
[54] (0, 0) band represented the emission from the lowest energy level of excited state to the lowest energy level of ground state.
[55] (a) Dong D., Winnik M. A. *Photochemistry and Photobiology* **1982**, 35, 17; (b) Thomas J. K *Chem. Rev.* **1980**, 80, 283.
[56] Kalyanasundaram K and Thomas J. K. *JACS,* **1977**, 2039.
[57] Ringsdorf H., Simon J. and Winnik F. M. *Macromolecules*, **1992**, 25, 5353.
[58] (a) Winnik F. M. *Polymer* **1990**; 31, 2125; (B) Kramer M. C. S., Steger J. R., Hu Y. and McCormick C. L. *Macromolecules* **1996**, 29, 1992.
[59] Barros T., Adronov A., Winnik F. M., and Bohne C. *Langmuir* **1997**, 13, 6089.
[60] Zhang J. *Syntheses, Chracterization and Solution Properties of Cholesterol Substituted Poly(N-Isopropylacrylamides)* McMaster University, **1999.**
[61] (a) Akiyoshi K., Deguchi A., Moriguchi N., Yamaguchi S. and Sunamoto J. *Macromolecules* **1993**, 26, 3062; (b) Nishikawa T., Akiyoshi K.and Sunamoto J. *Macromolecules* **1994**, 27, 7645.
[62] (a) Klok H.A., Hwang J. J., Iyer S., Tew G.N., Li. L. S. and Stupp I. *Polymer Preprint* **1998**, 166; (b) Tsuchida E.; Yamamoto K.; Miyatake K. and Endo K. *Macromolecules* **1997**, 30, 4235; (c) Akiyoshi K.; Deguchi A., Moriguchi N., Yamaguchi S. and Sunamoto J. *Macromolecules* **1993**, 26, 3062; (d) Nishikawa T., Akiyoshi K.and Sunamoto J. *Macromolecules* **1994**, 27, 7645; (d) Tsuchida E.; Yamamoto K.; Miyatake K. and Endo K. *Macromolecules* **1997**, 30, 4235.
[63] Ringsdorf H., Simon J. and Winnik F.M. *Macromolecules*, **1992**, 25, 5353.
[64] Ringsdorf H., Simon J. and Winnik F.M. *Macromolecules*, **1992**, 25, 7306.
[65] Lin G. and Guillet J. E. *Macromolecules* **1990**, 223, 1388.
[66] Mizusaki M. Kopek N. Morishima Y. Winnik F. *Langmuir* **1999,** 15, 8090.
[67] Yeagle P. (ed) *The Structure of Biological Membranes*, CRC Press, Chapter 2.
[68] Andrew S. (ed) Janoff *Liposomes Rational Design,* **1999**, Marcel Deker Inc., Chapter 1.
[69] Arunothayanun P., Turton J. A. and Florence A. T. *J. of Pharmaceutical Science* **1999**, 88, 34.
[70] Polozova A. and Winnik F. M. *Langmuir*, **1999**, 15, 4222 and references therein.
[71] Philippot J. R. and Schuber F. *Liposomes as Tools in Basic Reaserch and Industry* ***CRC press,*** **1995.**
[72] DMPC in general term, represented p-DMPC, DMPC5 or/and DMPC10.
[73] Gaidel P. and Blume A, *Biochimica et Biophysica Acta,* **1998**, 1371, 83.
[74] Ringsdorf H., Sackmann E., Simon J. and Winnik F. M. *BBA* **1993**, 1153, 335.
[75] Chu D. and Thomas J. K. *Macromolecules*, **1984,** 17, 2142.
[76] (a) Hinz H.J. and Sturtevant J. M. *J. of Biol. Chem.* **1972**, 247, 3697; (b) Savva M., Torchilin V. P. and Huang L. *J. of Coll. & Interf. Sci.* **1999**, 217, 166.
[77] Polozova A., Yamazaki A., Brash J. L. and Winnik F. M. *Colloids and Surfaces A: Physicochemical and Engineering Aspects*, **1999,** 147, 17.
[78] (a) Kono K., Zenitani K. and Takagishi, *Biochi. Biophy Acta* **1994**, 1193, 1; (b) Holland J., Hui C., Cullis P. and Madden T. *Biochem.* **1996**, 35, 2618; (c) Miller C., Bennet D., Chang D. and

O'Brien D. F. *Biochem.* **1996**, 35, 11782.
[79] Arunothayanun P., Turton J. A. and Florence A. T. *J. of Pharmaceutical Science* **1999**, 88, 34.
[80] Kono K., Nakai R., Morimoto K *Biochi. et Biophy. Acta*, **1999**, 1416, 239 and reference therein.
[81] Kono K., Hayashi H. and Takagishi T. *J. Contr. Release,* **1994**, 30, 69.
[82] (a) Hinz H.J. and Sturtevant J. M. *J. of Biol. Chem.* **1972**, 247, 3697; (b) Sava M., Torchilin V. P. and Huang L. *J. of Coll. & Interf. Sci.* **1999**, 217, 166.
[83] (a) Polozova A.; Winnik F. M. to be published; (b) Bailey A. and Cullis P. R. *Biochemistry* **1997**, 36, 1628.
[84] Kono K , Hayashi H. and Takagishi *J. contr. Rel.* **1994**, 30, 69; Kono K , Nakai R., Morimoto K. and Takagishi *Biochi. Biophys. Acta*, **1999**, 1416, 239.
[85] Hogland, R. P. *Handbook of Fluorescence Probes and research Chemicals*, Molecular Probes Inc.
[86] Kono K., Hayashi H. and Takagish T. *Bioconjugated Chem*, **1998**, 9, 382.
[87] (a) Papahadjopoulos D., Poste G.; Schseffer B. E. and Vail W. J. *Bioch. Et Bioph. Acta* **1974**, 352, 10.
(b) Papahadjopoulos D., Vail W. J., Schseffer B. E. and Poste G. *Bioch. Et Bioph. Acta* **1976**, 448, 265.
[88] Koster K. L., Webb M. S., Bryant G. and Lynch D. *Bioch et Bioph Acta* **1994**, 1193, 143.
[89] *Product Handbook Edition VI*, Avanti Polar Lipids, Inc.
[90] Yeagle P. (ed.) *The Structure of Biological Membranes* CRC Press, **1992**, chapter 2 and reference therein.
[91] Papahadjopopoulos D., Moscarello M., Eylar E. H. and Isac T. *Biochem. et Biophy. Acta*, **1975**, 401, 317 and reference therein.
[92] Castile J. D., Taylor K. M. G. and Buckton G. *International Journal of Pharmaceutics* **1999**, 182, 101.
[93] Moshishima Y.*Trends Polym. Sci.* **1994**, 2, 31.
[94] Dubin. P., Bock J., Davis R., Schulz, and Thies C. (Eds) *Macromolecular Complexes in Chemsitry and Biology*, Springer-Verlag, Berlin, **1994**.
[95] Akiyoshi K., Deguchi S., Tajima H., Nishikawa T. and Sunamoto J. *Macromolecules*, **1997**, 30, 857.
[96] (a) Drobnik *J. Advanced Drug Delivery Review* **1991**, 7, 295; (b) Turley E.A. *J. Advanced Drug Delivery Review* **1991**, 7; (b) Lapcik L. Jr. and Lapcik L. *Chem. Rew.* **1998**, 99, 2663; (c) Banerji S., Ni J., Wang S., Clasper S., Su J., Tammi R., Jones M. and Jacson D. *J Cell Biol* **1999**, 144, 789; (d) Winnik F. M. and Pillai V. *Round Table Series* **1996**, 37, 10.
[97] Denlinger J in *The Chemistry, Biology and Medical Application of Hyaluronan and its Derivatives.* Laurent T. C. (ed.) Portland Press, **1998,** Chapter 25.
[98] Morris E., Rees D. and Welsh E. *J. Mol. Biol.* **1980**, 138, 401.
[99] Darke A., Finer E.G., Moorhouse R. and Rees D. A. *J. Mol. Biol.* **1975**, 99, 477.
[100] Terbojevich M., Cosani A., Palumbo M. and Pregnolato F. *Carbohydrate. Res.* **1986**, 149, 363.
[101] (a) Kuo J., Swann D. A. and Prestwich G. D. *Bioconj. Chem.* **1991**, 2, 232; (b) Pouyani T. and Prestwich G. D. *Bioconj. Chem,* **1994**, 5, 339; (c) Asayama S., Nogawa M., Takei Y., Akaike Y., Akaike T. and Maruyama A. *Bioconj. Chem.* **1998**, 9, 476.
[102] (a) Scott J. E., Cummings C., Brass A. and Chen Y. *Biochem. J.* **1991**, 274, 699; (b) Scott J. E., Heatley F. and Hull W. E. *Biochem. J.* **1984**, 220, 197.
[103] Thom D. J., Grant G. T., Morris E. R., and Rees D. A. *Carbhy. Res.* **1982**, 100,26.

[104] Scott J.E. and Tigwell M.J. *J. Biochem.* **1978,** 173, 103.
[105] Scott J.E. *The Biology of Hyaluronan*, **1989**, p6, Wiley, Chichester.
[106] (a) Scott J. E., Cummings C., Brass A. and Chen Y. *Biochem. J.* **1991**, 274, 699; (b) Scott J. E. *FASEB J.* **1992**, 6, 2639.
[107] Akiyoshi K., Kang E., Kurumada S., Sunamoto J., Principi T. and Winnik F. M. *Macromolecles*, **2000**, 33, 3244.
[108] (a) Wright S. and Huang L. *Advanced Drug Delivery* **1989** 3, 343; (b) Calpen N. J., Alton E. W., Dorin J. R., Steven-son B. J., Gao X., Durban S. R., Jeffery P. K., Hodson M. E., Coutelle C., Huang L., Porteous D., J.Williamson R. and Geddes D. M. *Nat. Med.* **1995**, 1, 39.
[109] (a) Mauk M. R., Gamble R.C., and Baldeschwieler, J. D. *Proc. Natl. Acad. Sci.USA* **1980**, 77, 4430, (b) Leserman L. D., Weinstein J. N., Blumenthal R. and Terry W. D. *Proc. Natl. Acad. Sci.USA* **1980**, 77, 4089.
[110] Entwistle. J., Hall C. L. and Turley E. A. J. Cell. *Biochem.* **1996**, 61, 569.
[111] Hayashi H., Kono K. and Takagidhi T. *Bioconj. Chem.* **1998**, 9, 382.
[112] Papahadjopopoulos D., Moscarello M., Eylar E. H. and Isac T. *Biochem. Et Biophy. Acta*, **1975**, 401, 317 and reference therein.